

AVIONICS (R15A2121)

COURSE FILE

IV B. Tech I Semester

(2017-2018)

Prepared By

Prof. Ajai Kumar Rai

B.Tech. (IIT BHU), M.Tech.(IIT Madras), MIETE

Department of Aeronautical Engineering



**MALLA REDDY COLLEGE OF ENGINEERING &
TECHNOLOGY**

**(Autonomous Institution – UGC, Govt.
of India)**

Affiliated to JNTU, Hyderabad, Approved by AICTE - Accredited by NBA & NAAC – 'A' Grade - ISO 9001:2015

Certified)

Maisammaguda, Dhulapally (Post Via. Kompally), Secunderabad – 500100, Telangana State, India.

MRCET VISION

- To become a model institution in the fields of Engineering, Technology and Management.
- To have a perfect synchronization of the ideologies of MRCET with challenging demands of International Pioneering Organizations.

MRCET MISSION

To establish a pedestal for the integral innovation, team spirit, originality and competence in the students, expose them to face the global challenges and become pioneers of Indian vision of modern society.

MRCET QUALITY POLICY.

- To pursue continual improvement of teaching learning process of Undergraduate and Post Graduate programs in Engineering & Management vigorously.

To provide state of art infrastructure and expertise to impart the quality education.

PROGRAM OUTCOMES

(PO's)

Engineering Graduates will be able to:

1. **Engineering knowledge:** Apply the knowledge of mathematics, science, engineering fundamentals, and an engineering specialization to the solution of complex engineering problems.
2. **Problem analysis:** Identify, formulate, review research literature, and analyze complex engineering problems reaching substantiated conclusions using first principles of mathematics, natural sciences, and engineering sciences.
3. **Design / development of solutions:** Design solutions for complex engineering problems and design system components or processes that meet the specified needs with appropriate consideration for the public health and safety, and the cultural, societal, and environmental considerations.

4. **Conduct investigations of complex problems:** Use research-based knowledge and research methods including design of experiments, analysis and interpretation of data, and synthesis of the information to provide valid conclusions.
5. **Modern tool usage:** Create, select, and apply appropriate techniques, resources, and modern engineering and IT tools including prediction and modeling to complex engineering activities with an understanding of the limitations.
6. **The engineer and society:** Apply reasoning informed by the contextual knowledge to assess societal, health, safety, legal and cultural issues and the consequent responsibilities relevant to the professional engineering practice.
7. **Environment and sustainability:** Understand the impact of the professional engineering solutions in societal and environmental contexts, and demonstrate the knowledge of, and need for sustainable development.
8. **Ethics:** Apply ethical principles and commit to professional ethics and responsibilities and norms of the engineering practice.
9. **Individual and team work:** Function effectively as an individual, and as a member or leader in diverse teams, and in multidisciplinary settings.
10. **Communication:** Communicate effectively on complex engineering activities with the engineering community and with society at large, such as, being able to comprehend and write effective reports and design documentation, make effective presentations, and give and receive clear instructions.
11. **Project management and finance:** Demonstrate knowledge and understanding of the engineering and management principles and apply these to one's own work, as a member and leader in a team, to manage projects and in multi disciplinary environments.
12. **Life- long learning:** Recognize the need for, and have the preparation and ability to engage in independent and life-long learning in the broadest context of technological change.

EDUCATIONAL OBJECTIVES – Aeronautical Engineering

1. **PEO1 (PROFESSIONALISM & CITIZENSHIP):** To create and sustain a community of learning in which students acquire knowledge and learn to apply it professionally with due consideration for ethical, ecological and economic issues.
2. **PEO2 (TECHNICAL ACCOMPLISHMENTS):** To provide knowledge-based services to satisfy the needs of society and the industry by providing hands on experience in various technologies in core field.

3. **PEO3 (INVENTION, INNOVATION AND CREATIVITY):** To make the students to design, experiment, analyze, and interpret in the core field with the help of other multi disciplinary concepts wherever applicable.
4. **PEO4 (PROFESSIONAL DEVELOPMENT):** To educate the students to disseminate research findings with good soft skills and become a successful entrepreneur.
5. **PEO5 (HUMAN RESOURCE DEVELOPMENT):** To graduate the students in building national capabilities in technology, education and research

PROGRAM SPECIFIC OUTCOMES – Aeronautical Engineering

1. To mold students to become a professional with all necessary skills, personality and sound knowledge in basic and advance technological areas.
2. To promote understanding of concepts and develop ability in design manufacture and maintenance of aircraft, aerospace vehicles and associated equipment and develop application capability of the concepts sciences to engineering design and processes.
3. Understanding the current scenario in the field of aeronautics and acquire ability to apply knowledge of engineering, science and mathematics to design and conduct experiments in the field of Aeronautical Engineering.
4. To develop leadership skills in our students necessary to shape the social, intellectual, business and technical worlds.

MALLA REDDY COLLEGE OF ENGINEERING & TECHNOLOGY

IV Year B. Tech, ANE-I Sem

L T/P/D C

4 -/-/ 3

(R15A2121) AVIONICS

OBJECTIVES OF THE COURSE

To introduce the students with functioning and principle of operation of various avionics systems including sensors installed on a modern passenger and fighter aircraft.

UNIT I: INTRODUCTION TO AVIONICS

Importance and role of Avionics in modern aircraft-systems which interface directly with pilot-aircraft state sensor systems, outside world sensor systems, task automation systems. The avionics equipment and system requirement-environmental, weight, reliability. Standardization and specification of avionics equipment and systems- ARINC and MIL specification. Electrical and optical data bus systems. Integrated modular avionics architectures.

UNIT II: DISPLAY & MAN-MACHINE INTERACTION AND COMMUNICATION SYSTEM

Introduction to displays-head-up displays(HUD)-basic principles, Helmet mounted displays, Head tracking systems. Head down displays-Civil cockpit, Military cockpit, Solid state standby display systems, Data fusion in displays- Intelligent display systems. Introduction to voice and data communication systems- HF, VHF, UHF and Satellite communications, Flight data recorders.

UNIT III: INERTIAL SENSORS, ATTITUDE DERIVATION AND AIR DATA SYSTEMS

Basic principles of gyroscope and accelerometers. Introduction to optical gyroscope- ring laser gyros-principles. Stable platform system-strap down systems- error in inertial systems and corrections. Air data Information and its use, derivation of Air Data Laws and relationship- altitude-static pressure relationship, variation of ground pressure, Speed of sound, Mach Number, CAS, TAS, Pressure error. Air data sensors and computing

UNIT IV: NAVIGATION (INS AND GPS) AND LANDING SYSTEM

Principles of Navigation, Types of Navigation systems-. Inertial Navigation System- Initial alignment and Gyro compassing, Strap down INS computing. Landing System- localizer and glide-slope-marker systems. Categories of ILS. Global navigation satellite systems-GPS-description and basic principles. Integration of GPS and INS, Differential GPS.

UNIT V: SURVEILLANCE AND AUTO FLIGHT SYSTEMS

Traffic alert and collision avoidance systems(TCAS)-Enhanced ground proximity warning system. Weather radar. Autopilots-Basic principle, height control, heading control, ILS coupled autopilot control, satellite landing system,

[AERONAUTICAL ENGINEERING MRCET\(UGC-Autonomous\)](#)

speed control and auto throttle. Flight management systems-principles-flight planning-navigation and Guidance, performance prediction and flight path optimization.

OUTCOMES

1. The student would gain understanding of the basic principles of avionics system

TEXT BOOKS

1. Collinson, R.P.G., Introduction to Avionics Systems, second edition, Springer,2003,ISBN 978-81-8489-795-1
2. Moir, I. and Seabridge, A., Civil Avionics Systems, AIAA education Series, AIAA, 2002, ISBN 1-56347589-8

REFERENCE BOOKS

1. Kayton, M., & Fried, W.R, Avionics Navigation Systems, Wiley, 1997, ISBN 0-471-54795-6Z

MALLA REDDY COLLEGE OF ENGINEERING AND TECHNOLOGY

(UGC AUTONOU MOUS – Govt. of INDIA)

IV B.TECH. I SEMESTER – AERONAUTICAL ENGINEERING

AVIONICS (R15)

MODEL PAPER – I

Time: 3 Hours

Max marks: 75

Note: This question paper contains two parts A and B.

Part A is compulsory which carries 25 marks. Answer all questions in Part A. Part B contains of 5 units. Answer any one full question from each unit. Each question carries 10 marks and may have a, b, c as sub questions.

PART –A (25 Marks)

1. (a) Enumerate core avionics systems in modern aircraft. (3)
- (b) List few aircraft state sensors. (2)
- (c) List components of Head-up display (HUD). (3)
- (d) List the limitations of VHF communications against HF Communication system. (2)
- (e) Draw a neat block diagram of a ring laser gyro illustrating various parts. (3)
- (f) List the errors in inertial systems. (2)
- (g) Illustrate the purpose of VHF Omni-range and distance measuring equipment. (3)
- (h) How is the inertial navigation system aligned? (2)
- (i) Explain the principle of autopilot. (3)
- (j) Explain the purpose of flight management system. (2)

PART- B

2. (a) Discuss the importance and role of Avionics in modern aircraft.
- (b) Illustrate the function of ARINC and MIL-STD-1553 B data bus.

OR

3. (a) Explain the method for protecting avionics systems against environmental conditions.
(b) Differentiate between electrical and optical data bus system.
4. (a) Discuss the solid state standby display systems.
(b) Explain Head down displays in military fighter aircraft cockpit.

OR

5. (a) With the help of a neat diagram, explain the principle of radio voice communication.
(b) Explain the principle of satellite communications.
6. (a) Explain the principle of mechanical gyroscopes.
(b) Explain the functioning of differential global positioning system.

OR

7. (a) Explain the functioning of spring restrained pendulous accelerometers.
(b) Explain the requirement and process of integration of GPS and INS.
8. (a) Discuss the principle of strap-down inertial navigation system.
(b) With neat diagram explain the purpose and functioning of attitude and heading reference system.

OR

9. (a) Explain the purpose and functioning of Kalman filters.
(b) Explain the functioning of automatic direction finders in an aircraft.
10. Write short notes on.
(a) Traffic collision and avoidance system (TCAS)
(b) Enhanced ground proximity warning system (EGPWS)

OR

11. Explain the principle of following auto pilot.
(a) Height control (b) Heading control.

MALLA REDDY COLLEGE OF ENGINEERING AND TECHNOLOGY

(UGC AUTONOU MOUS – Govt. of INDIA)

IV B.TECH. I SEMESTER – AERONAUTICAL ENGINEERING

AVIONICS (R15)

MODEL PAPER – II

Time: 3 Hours

Max marks: 75

Note: This question paper contains two parts A and B.

Part A is compulsory which carries 25 marks. Answer all questions in Part A. Part B contains of 5 units. Answer any one full question from each unit. Each question carries 10 marks and may have a, b, c as sub questions.

PART –A

1. (a) Enumerate various outside world sensors. (2)
- (b) List the purpose and method of avionics packaging. (3)
- (c) List the purpose of helmet mounted display. (2)
- (d) List the various head down displays in fighter aircraft. (3)
- (e) Explain the basic principle of accelerometer as sensor. (2)
- (f) Differentiate between strap-up and strap-down inertial navigation system. (3)
- (g) What do you mean by gyro compassing with respect to inertial navigation system? (2)
- (h) Discuss the functioning of localizer with a diagram in landing system. (3)
- (i) Discuss the role of Mode S transponder. (3)
- (j) Explain the purpose of ILS coupled autopilot control. (2)

PART-B

2 Explain the requirement of Avionics equipment and systems with respect to

- (i) Environment
- (ii) Reliability

OR

- 3 (a) Discuss how various avionics systems are interfaced with the pilot.
(b) Discuss the functioning of MIL-STD-1553B data bus.
4. (a) Discuss intelligent display management systems in modern aircraft.
(b) Explain the functioning of data recorder systems in an aircraft.

OR

5. (a) Explain ACARS data communication systems.
(b) Write short notes on
(i) Audio management system
(ii) In-flight entertainment system

- 6 (a) Explain the functioning of micro machined vibrating mass rate gyro.
(b) Discuss the principle and functioning of torque balancer pendulous accelerometer.

OR

7. With the help of neat diagram explain the principle and various segments of a global positioning system.
8. (a) Discuss the principle and components of Radio-navigation system.
(b) How are the angular rate and acceleration corrections provided in inertial navigation system?

OR

- 9(a) Explain the principle of strap-down INS computing.
(b) Explain the functioning of glide-slope and marker systems in ILS.
10. (a) Discuss the principle of weather radar systems.
(b) How is auto-stabilization achieved in an aircraft?

OR

11. (a) Explain the functioning of speed control and auto throttle control systems.
(b) Write short note on flight management system.

MALLA REDDY COLLEGE OF ENGINEERING AND TECHNOLOGY

(UGC AUTONOU MOUS – Govt. of INDIA)

IV B.TECH. I SEMESTER – AERONAUTICAL ENGINEERING

AVIONICS (R15)

MODEL PAPER – III

Time: 3 Hours

Max marks: 75

Note: This question paper contains two parts A and B.

Part A is compulsory which carries 25 marks. Answer all questions in Part A. Part B contains of 5 units. Answer any one full question from each unit. Each question carries 10 marks and may have a, b, c as sub questions.

PART –A (25 Marks)

1. (a) Enumerate core avionics systems. (3)
- (b) What are the reliability requirements of avionics system? (2)
- (c) List the components of head tracking system. (3)
- (d) What is the purpose and meaning of data fusion in displays? (2)
- (e) List the basic principles of gyroscope. (3)
- (f) What is the purpose of integration of INS with GPS? (2)
- (g) How is INS aligned? (3)
- (h) List the categories of Instrument landing systems. (2)
- (i) Enumerate the functioning of air traffic control systems. (3)
- (j) Draw the block diagram of speed control system. (2)

PART-B

2. (a) Explain the purpose and functioning of electrical data bus systems.
- (b) What are the various task automation systems? How do they function?

OR

3. (a) Discuss briefly ARINC specifications.
(b) Write short note on avionics packaging.
4. (a) Explain the display systems in modern military aircraft.
(b) Discuss the functioning of helmet mounted displays.

OR

5. (a) With neat diagram explain the functioning of data communication system.
(b) Discuss the role and functioning of audio management system in a modern civil aircraft.
6. (a) Discuss the principle of ring laser gyro with the help of a diagram.
(b) Discuss the purpose and functioning of differential GPS.

OR

7. (a) Write short note on augmented satellite navigation system.
(b) What are the sources of errors in inertial systems? Explain.
8. (a) Explain the purpose and operation of attitude and heading reference system.
(b) How is angular rate correction done in inertial system?

OR

9. Explain the principle of instrument landing system including localizer, glide slope and marker systems.
10. (a) Explain the operation of airborne weather warning radar system and associated display.
(b) Discuss the purpose and functioning of stability augmentation system.

OR

11. (a) Explain the principle and operation of height hold autopilot with the help of neat diagram.
(b) How is the response of an aircraft determined due to longitudinal control? Briefly explain.

MALLA REDDY COLLEGE OF ENGINEERING AND TECHNOLOGY

(UGC AUTONOU MOUS – Govt. of INDIA)

IV B.TECH. I SEMESTER – AERONAUTICAL ENGINEERING

AVIONICS (R15)

Time: 3 Hours

Max marks: 75

MODEL QUESTION PAPER- IV

Note: This question paper contains two parts A and B.

Part A is compulsory which carries 25 marks. Answer all questions in Part A. Part B contains of 5 units. Answer any one full question from each unit. Each question carries 10 marks and may have a, b, c as sub questions.

PART –A

1. (a) List core avionics systems. (2)
- (b) What are the main types of dead reckoning navigation systems? (3)
- (c) List the main advantages of head-up display in civil aircraft. (3)
- (d) Draw the block diagram of an intelligent display management system. (2)
- (e) Elaborate multi-path error in GPS. (2)
- (f) Discuss the requirement of integration of INS and GPS. (3)
- (g) List various range and bearing radio navigation aids. (3)
- (h) What are the various angular rate correction terms? (2)
- (i) Write the purpose of stability augmentation system. (2)
- (j) List the functions performed by flight management system. (3)

PART-B

2. (a) Discuss various task automation systems in modern aircraft.
- (b) Briefly explain electrical data bus systems.

OR

3. (a) Discuss integrated avionics system architecture in a civil aircraft.
(b) Discuss environment and reliability requirements of avionics equipment.

4. (a) Briefly explain the working of head tracking systems.
(b) Discuss the functions of solid state standby display systems.

OR

5. (a) Discuss the components of voice communication systems in an aircraft.
(b) Explain the functioning and purpose of data recorder systems in an aircraft.
6. (a) Explain the principle of micro electro-mechanical systems (MEMS) technology rate gyros.
(b) Explain the functioning of simple spring restrained pendulous accelerometer.

OR

7. (a) Write short notes on
(i) Differential GPS
(ii) Augmented satellite navigation systems.
(b) Discuss various errors in inertial systems.
8. (a) Discuss the basic principle and attributes of inertial navigation.
(b) Discuss the effect of accelerometer bias and Gyro drift on the errors in inertial navigation system.

OR

9. Explain the functioning of aided INS and Kalman filters.
10. (a) Discuss the purpose and functioning of speed control and auto-throttle systems.
(b) Explain how performance prediction and flight path optimization is achieved.

OR

11. (a) Discuss the purpose and process of flight planning.
(b) Discuss how a coordinated turn is achieved in an aircraft. Derive the necessary relation between bank angle, rate of turn and aircraft velocity.

MALLA REDDY COLLEGE OF ENGINEERING AND TECHNOLOGY

(UGC AUTONOU MOUS – Govt. of INDIA)

IV B.TECH. I SEMESTER – AERONAUTICAL ENGINEERING

AVIONICS (R15)

Time: 3 Hours

Max marks: 75

MODEL QUESTION PAPER- V

Note: This question paper contains two parts A and B.

Part A is compulsory which carries 25 marks. Answer all questions in Part A. Part B contains of 5 units. Answer any one full question from each unit. Each question carries 10 marks and may have a, b, c as sub questions.

PART –A (25 Marks)

1. (a) List various aircraft state sensors. (2)
- (b) List the task performed by flight management system. (3)
- (c) Write the advantages of HF communication systems. (2)
- (d) What are the components of HUD electronics? (3)
- (e) Explain the purpose of gyro and accelerometer in inertial system. (3)
- (f) What is the purpose of INS and GPS integration? (2)
- (g) Explain the purpose of initial alignment in INS. (3)
- (h) Explain the purpose of markers in instrument landing system. (2)
- (i) Write the purpose of mode S transponder. (3)
- (j) Draw the block diagram of a height control autopilot. (2)

PART-B

2. Discuss the requirements of avionics equipment with respect to following:

- (i) Environment (ii) Weight (iii) Reliability.

OR

3. Discuss the purpose and functioning of various data bus systems in civil and military aircraft.

4. Write short notes on

(i) Data fusion in displays.

(ii) Head down displays in military cockpit.

OR

5. Write short notes on

(i) In-flight entertainment system

(ii) ACARS data communication system.

6.(a) Explain the functioning and components of global positioning system.

(b) Explain the functioning of differential GPS.

OR

7. Explain various errors and their compensation methods in inertial navigation systems.

8. Write short notes on

(i) VHF omni-range (ii) Distance measuring equipment (iii) Automatic direction finding.

OR

9. Explain the function of instrument landing system including localizer, glide slope and marker beacons.

10. Write short notes on

(i) TCAS (ii) EGPWS

OR

11. Discuss in detail longitudinal and lateral control and response of aircraft.

UNIT-I

Introduction to Avionics

Index

SI No	Name of the topic	Page no
1	Importance and Role of Avionics	20
2	Core Avionics System	21
3	Aircraft State Sensors	22
4	Outside world Sensors	23
5	Requirement of Avionics Equipment	24
6	Standardization & Specifications	27
7	Electrical & Optical data Bus	30
8	Integrated Modular Avionics architecture	33

UNIT-I Introduction to Avionics.

1.1 Importance and Role of Avionics in Modern Aircraft:

(a) "Avionics" is a word derived from the combination of aviation and electronics. The term 'avionics system' means any system in aircraft which is dependent on electronics for its operation, although the system may contain electro-mechanical elements. The avionics industry is a major **multi-billion dollar** industry world-wide and the avionics equipment of a modern military or civil aircraft can account for around 30% of the total cost of the aircraft. This can go up to 75% of the total cost in the case of an airborne early warning aircraft (AWACS).

(b) Avionics systems are essential to enable the flight crew to carry out the **aircraft mission safely and efficiently**, whether the mission is carrying passengers to their destination in the case of civil airliner, or, in the military case, intercepting a hostile aircraft, attacking a ground target, reconnaissance or maritime patrol.

(c) A major driver in the development and introduction of avionics system has been the need to meet the **mission requirements with minimum flight crew**. This is only made possible by reducing the crew workload by automating the tasks which used to be carried out by the navigator and flight engineer. The reduction in number of aircrew has very considerable economic benefits for the airline in a highly competitive market with consequent saving of crew salaries, expenses and training cost. The reduction in weight is also significant and can be translated into more passengers or longer range on less fuel. In military aircraft, a single seat fighter or strike (attack) aircraft is lighter and costs less than equivalent two seat version. The elimination of second crew member has also **significant economic benefits** in terms of reduction in training costs.

(d) Other very important drivers for avionics system are **increased safety, air traffic control requirements, all weather operation, and reduction in fuel consumption**, improved aircraft performance and control and handling and reduction in maintenance cost.

(e) Military avionics systems are also being driven by continuing increase in the threats posed by the **defensive and offensive capabilities** of potential aggressors.

1.2 Core Avionics Systems and interface with the pilot. Core avionics systems are shown in fig 1.1. It can be seen that the main avionic sub-system has been grouped into five layers according to their role and function. These are briefly summarized below in order to provide an overall picture of the roles and functions of the avionics systems in an aircraft.

1.2.1 Systems Which Interface directly with the pilot (Man-machine interface): These comprise displays, communications, data entry and control and flight control. The Display Systems provide the visual interface between the pilot and the aircraft systems and comprise head up displays (HUDs), helmet mounted displays (HMDs) and head down displays (HDDs). Most combat aircraft are now equipped with a HUD. The HMD is also an essential system in modern combat aircraft and helicopters.

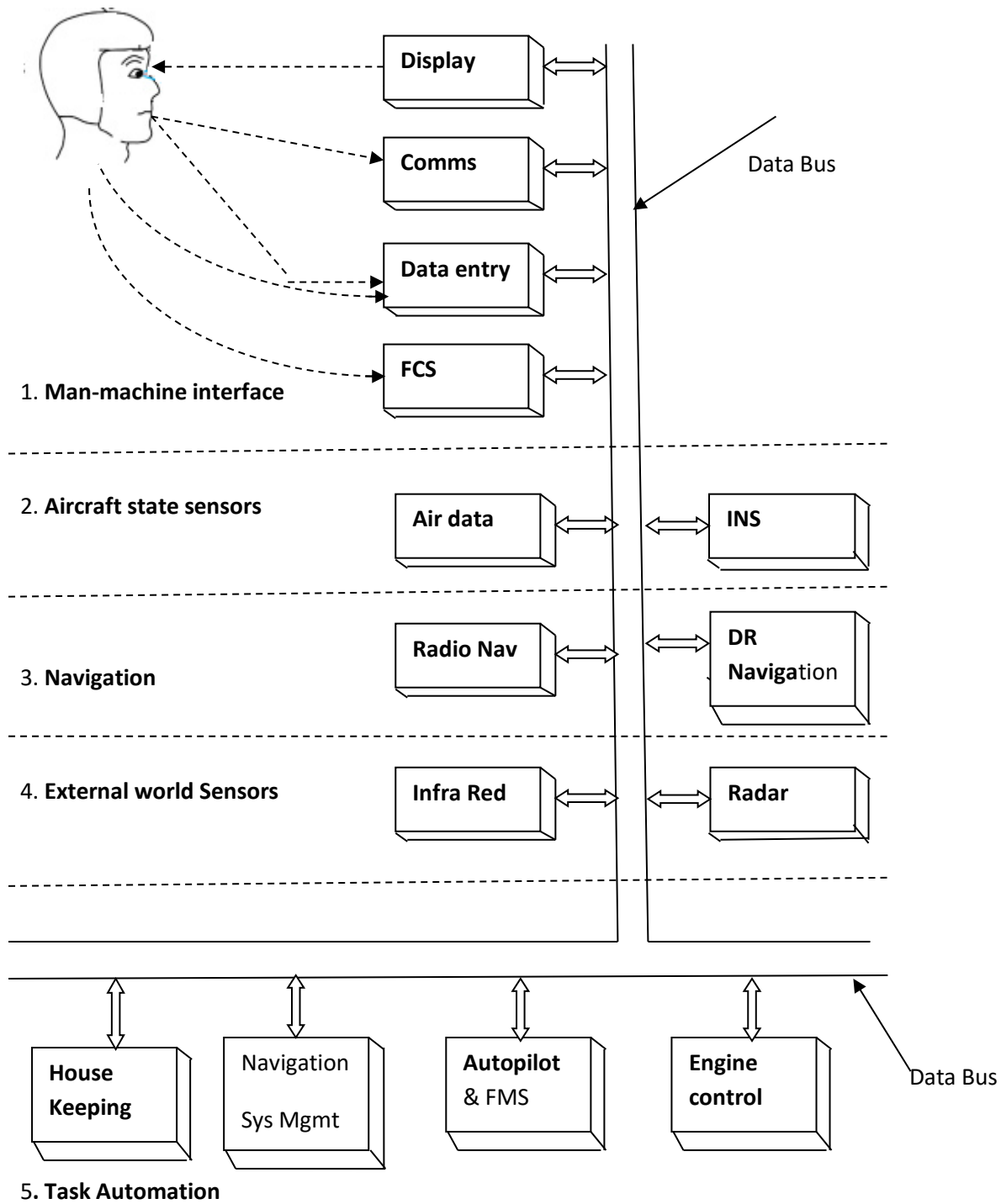


Fig 1.1: Core Avionics System

The prime advantage of the HUD and HMD are that they project the display information into the pilot's field of view so that pilot can be head up and can concentrate on the outside world.

The HUD now provides the primary display for presenting the essential flight information and in military aircraft has transformed weapon aiming accuracy. The HUD can also display a forward looking infrared video picture one to one with outside world from a fixed FLIR imaging sensor installed in the aircraft. The infrared picture merges naturally with the visual scene enabling operations to be carried out at night or in condition of poor visibility due to haze or clouds. The HMD enables the pilot to be presented with information while looking in any direction, as opposed to the limited forward field of view of the HUD. An essential element in the overall HMD system is the Helmet tracker system to derive the direction of the pilot's sight line relative to the aircraft axes. This enables the pilot to designate a target to the aircraft missiles. The HMD can also form part of an indirect viewing system by driving a gimbaled infrared imaging sensor to follow the pilot's line of sight.

The multi-function color displays provide the primary flight displays of height, airspeed, Mach number, vertical speed, artificial horizon, pitch angle, bank angle and heading, and velocity vector. The weather radar display can display also be superimposed on the HIS display.

The Communication Systems play a vital role; the need for reliable two way communication between the ground bases and the aircraft or between aircraft is self evident and is essential for air traffic control. Long range communication is provided by high frequency (HF) radios operating in the band 2-30 MHz. Near to medium range communication is provided in civil aircraft by very high frequency (VHF) radios operating in the band 30-300 MHz, in military aircraft by ultra high frequency (UHF) radio operating in the band 250-400 MHz. (VHF and UHF are line of sight propagation system). Satellite communications (SATCOM) systems are also installed in many modern aircraft and these are able to provide very reliable worldwide communication.

The Data Entry and Control Systems are essential for the crew to interact with the avionics systems. Such systems range from keyboards and touch panels to the use of direct voice input (DVI) control, exploiting speech recognition technology, and voice warning systems exploiting speech synthesizers.

The Flight control Systems exploit electronic system technology for auto-stabilization systems and fly-by-wire (FBW) flight control systems. Most combat aircraft require three axis auto-stabilization systems to achieve acceptable control and handling characteristics across the flight envelope. FBW provides continuous automatic stabilization of the aircraft by computer control of the control surface from appropriate motion sensors.

1.2.2. Aircraft State Sensor Systems: These comprise the air data systems and inertial sensor systems. The Air Data Systems provide accurate information on the air data quantities that is the altitude, calibrated airspeed, vertical speed, true airspeed, Mach number and airstream incidence angle. These are derived from the very accurate sensors which measure the static pressure, total pressure and the outside air temperature. The inertial Sensor Systems provide the information on aircraft attitude and the direction in which it is heading which is essential information for the pilot in executing a maneuver or flying in conditions of poor visibility. The use of very high accuracy gyros and accelerometers to measure the aircraft's motion enables an inertial navigation system (INS) to be mechanized which

provides very accurate attitude and heading information together with the aircraft's velocity and position data (ground speed, track angle and latitude/longitude co-ordinates). The INS is thus a very important aircraft state sensor system- it is also completely self-contained and does not require any access to the outside world.

1.2.3 Navigation System. Accurate navigation information, that is the aircraft's position, ground speed and track angle (direction of motion of the aircraft relative to true North) is clearly essential for the aircraft's mission, whether civil or military. Navigation system is divided into dead reckoning (DR) systems and position fixing systems; both types are required in the aircraft.

The Dead Reckoning Navigation Systems derive the vehicle's present position by estimating the distance travelled from a known position from knowledge of the speed and direction of motion of the vehicle. They have the major advantages of being completely self contained and independent of external systems. The main types of DR navigation systems used in aircraft are:

(a) Inertial Navigation Systems. They are most accurate and widely used systems.

(b) Doppler/heading reference systems. These are widely used in helicopters.

(c) Air data/heading reference systems. These systems are mainly used as a reversionary navigation system being of lower accuracy than (a) and (b).

A characteristic of all DR navigation systems is that the position error builds up with time and it is, therefore, necessary to correct the DR position error and update the system from position fixes derived from a suitable position fixing system.

The Position Fixing Systems used are now mainly radio navigation systems based on satellite or ground based transmitters. A suitable receiver in the aircraft with a supporting computer is then used to derive the aircraft's position from the signals received from the transmitters. The prime position fixing system is without doubt GPS (Global positioning system). This is a satellite navigation system of outstanding accuracy which has provided a revolutionary advance in navigation capability since the system started to come into full operation in 1980.

There are also radio navigation aids such as VOR/DME and TACAN which provide the range and bearing (R/ θ) of the aircraft from ground beacon transmitters located to provide coverage of the main routes. Approach guidance to the airfield/airport in conditions of poor visibility is provided by the ILS (Instrument landing system), or by the later MLS (Microwave landing system). A navigation system on the aircraft is very comprehensive and can include INS, GPS, VOR/DME, ILS, and MLS.

1.2.4 Outside World Sensor System: These systems, which comprise both radar and infrared sensor, systems enable all weather and night time operation and transform the operational capability of the aircraft.

The *Radar Systems* installed in civil airlines and many general aviation aircraft provide weather warning. The radar looks ahead of the aircraft and is optimized to detect water droplets and provide warning of storms, cloud turbulence and severe precipitation so that aircraft can alter course and avoid such conditions, if possible. It should be noted that

in severe turbulence, the violence of the vertical gusts can subject the aircraft structure to very high loads and stresses. These radars can also generally operate in ground mapping and terrain avoidance modes.

Modern fighter aircraft generally have a ground attack role as well as the prime interception role and carry very sophisticated multi-mode radars to enable them to fulfill these dual roles. In the airborne interception (AI) mode, the radar must be able to detect aircraft up to 100 miles away and track while scanning and keeping tabs on several aircraft simultaneously (Typically at least 12 aircraft). The radar must also have a 'look down' capability and be able to track low flying aircraft below it. In the ground attack mode, the radar system is able to generate a map display from the radar returns from the ground, enabling specific terrain features to be identified for target acquisition.

The **Infrared Sensors Systems** have the major advantage of being entirely passive systems. Infrared (IR) sensor systems can be used to provide a video picture of the thermal image scene of the outside world either using a fixed FLIR sensor, or alternately, a gimbaled IR imaging sensor. The thermal image picture at night looks very like the visual picture in daytime, but highlights heat sources, such as vehicle engines, enabling real targets to be discriminated from camouflaged decoys.

1.2.5. Task Automation Systems: these comprise the systems which reduce the crew work load and enable minimum crew operation by automating and managing as many tasks as appropriate so that the crew role is a supervisory management one. The tasks and roles of these are very briefly summarized below.

The **Autopilot and flight management Systems** have been grouped together because of the very close degree of integration between these systems on modern aircraft. The auto pilot relieves the pilot of the need to fly the aircraft continuously with consequent fatigue and so enables the pilot to concentrate on other tasks associated with the mission. Apart from basic modes, such as height hold and heading hold, a suitably designed high integrity autopilot system can also provide a very precise control of the aircraft flight path for such applications as automatic landing in poor or even zero visibility conditions. In military applications, the autopilot system in conjunction with suitable guidance system can provide automatic terrain following, or terrain avoidance. This enables the aircraft to fly automatically at high speed at very low altitudes (100 to 200 ft) so that the aircraft can take advantage of terrain screening and stay below the radar horizon of enemy radars.

The tasks carried out by **flight management systems** (FMS) include:

- flight planning
- Navigation management
- Engine control to maintain the planned speed or Mach number.
- Flight envelop monitoring
- Minimizing fuel consumption.
- Control of the aircraft flight path to follow the optimized planned route.

-Control of the vertical flight profile.

-Ensuring the aircraft is at the planned 3D position at the planned time slot; often referred to as 4D navigation. This is very important for air traffic control.

The engine Control and Management Systems carry out the task of control and the efficient management and monitoring of the engines. Many modern jet engines have a full authority digital engine control system (FADEC). This automatically controls the flow of fuel to the engine combustion chambers by the fuel control unit so as to provide a closed-loop control of the engine thrust in response to the throttle command. The control system ensures the engine limits in terms of temperatures, engine speeds and accelerations are not exceeded and the engine responds in an optimum manner to the throttle command. Other important engine avionics systems include engine health monitoring systems which measure, process and record a very wide range of parameters associated with performance and health of the engines. This gives an early warning of engine performance deterioration, excessive wear, fatigue damage, high vibration levels, excessive temperature levels, etc.

House Keeping Management is the term used to cover the automation of the background tasks which are essential for the aircraft's safe and efficient operation. Such tasks include:

- Fuel management
- Electrical power supply management
- Hydraulic power supply system management
- Cabin/Cockpit pressurization system
- Warning system
- Environmental control systems.
- Maintenance and monitoring systems.

The paragraph 1.1 to 1.5 summarizes the role and importance of the avionics systems shown in fig 1.1.

Many systems on military aircraft have not been mentioned.

1.3. Requirements of Avionics equipment and systems-Environment, weight, reliability.

1.3.1 The Avionics Environment: Avionics systems equipment is very different in many ways from ground-based equipment carrying out similar functions. The reason for these differences is briefly outlined as follows:

(a) The importance of achieving minimum weight.

(b) The adverse operating environment particularly in military aircraft in terms of operating temperature range, acceleration, shock, vibration, humidity range and electro-magnetic interference.

(c) The importance of very high reliability, safety and integrity.

(d) Space constraints particularly in military aircraft requiring an emphasis on miniaturization and high packaging densities.

1.3.2 Environmental Requirements. Compared to civil aircraft environment, avionics equipment has to operate in a very severe and adverse environment in military aircraft. The operating temperature range is usually specified from -40°C to +70°C. Clearly, the pilot will not survive at these extremes but if the aircraft is left out in the Arctic cold or soaking in the Middle-East sun, for example, the equipment may well reach such temperatures.

Vibration is usually quite severe and, in particular, airframe manufacturers tend to locate the gun right under the display. Power spectral energy levels of $0.7g^2$ per Hz at very low frequencies are anticipated.

The equipment must also operate under the **maximum acceleration** or g to which the aircraft is subjected during maneuvers. This can be 9g in a modern fighter aircraft and the specification for the equipment would call up at least 20g.

The electromagnetic compatibility (**EMC**) requirements are also very demanding. The equipment must not exceed the specified emission levels for a very wide range of radio frequencies and must not be susceptible to external source of very high levels of RF energy over a wide frequency band.

The equipment must also be able to withstand **lightning strikes** and the very high electromagnetic pulses (EMP) which can be encountered during such strikes.

1.3.3 Weight. There is gearing effect on unnecessary weight which is of the order of 10:1. For example a weight saving of 10 Kg enables an increase in the payload capability of the order of 100 kg. The process of the effect of additional weight is a vicious circle. An increase in the aircraft weight due to say, an increase in weight of the avionics equipment, requires the aircraft structure to be increased in strength, and therefore made heavier, in order to withstand the increased load during maneuvers. (Assuming the same maximum normal acceleration, or g, and the same safety margins on maximum stress levels are maintained). This increase in aircraft weight means that more lift is required from the wings and the accompanying drag is thus increased. An increase in engine thrust is therefore required to counter the increase in drag and the fuel consumption is thus increased. For the same range it is thus necessary carry more fuel and the payload has to be correspondingly reduced, or, if the payload is kept the same, the range is reduced. For these reductions tremendous efforts are made to reduce the equipment weight to minimum and weight penalties can be imposed if equipment exceeds the specified weight.

1.3.4. Reliability. Reliability is very important consideration in the aircraft. It is clearly not possible to repair equipment in flight so that equipment failure means aborting the mission or significant loss of performance or effectiveness in carrying out the mission. The cost of equipment failures in airline operation can be very high-interrupted schedules, loss of income during 'aircraft on the ground' situations etc. In military operations, aircraft availability is lowered and operational capability lost.

Every possible care is taken in the design of avionics equipment to achieve maximum reliability. The **quality assurance (QA)** aspects are very stringent during the manufacturing process and also very frequently call for what is referred to as '**reliability shake-down testing**', or **RST**, before equipment is accepted for delivery. RST is intended to duplicate the most severe environment conditions to which the equipment could be subjected, in order to try to eliminate the early failure phase of the equipment cycle.

A typical RST cycle requires the equipment to operate satisfactorily through the cycle described below.

- Soaking in an environmental chamber at a temperature of +70°C for a given period.
- Rapidly cooling the equipment to -55°C in 20 minutes and soaking at that temperature for a given period.
- Subjecting the equipment to vibration, for example 0.5g amplitude at 50 Hz, for periods during the hot and cold soaking phase.

A typical specification would call for twenty RST cycles without a failure before acceptance of the equipment. If a failure should occur at the nth cycle, the failure must be rectified and the remaining (20 – n) cycles repeated.

All failures in service (and in testing) are investigated by the QA team and remedial action taken, if necessary.

1.4 Standardization and specifications of avionics equipment and systems-the ARINC and MIL specifications.

1.4.1 Objectives of standardization and specification of avionics equipment and systems.

- (a) To enhance interchangeability, reliability, and maintainability of military/civil aircraft.
- (b) To optimize the variety of items (including subsystems), process, and practices used in acquisition.
- (c) To ensure that products of requisite quality and minimum essential need are specified & obtained.
- (d) Ensure that specifications & standards are written to facilitate tailoring of prescribed requirements to the particular needs.
- (e) Because of interchangeability there is a freedom of choice in the selection of airborne equipment from different sources. 'Box' dimensions, type & pin connection, interfacing, coding etc are covered.

Examples of standards and specifications could be 'environmental testing procedure', 'Technical standard of HF/VHF radio equipment' and 'Open avionics architecture'.

1.4.2 ARINC Specifications. ARINC stands for Aeronautical Radio, INC., a private corporation organized in 1929, & is comprised of airlines, aircraft manufacturers & avionics equipment manufacturers as corporate shareholders. ARINC

was developed to produce specifications and standards for avionics equipment outside the government for domestic & oversees manufacturer.

ARINC copy writes & publishes standards produced by Airlines Electric Engineering Committee (AEEC). The AEEC is an international standard organization made up of major airline operator, avionics equipment manufacturers and ARIC members. The AEEC sets standards for avionics equipment & systems & provides industry defined requirements for standardization of form, fit & function between various manufacturer products.

ARINC Specifications are used to define

-Physical packaging & mounting of avionics equipment.

-Data communication standards.

-High level computer language.

ARINC Standards: These are definitions of the form, fit & function of avionics equipment. These documents are equipment specific & define how a unit will operate.

The **ARINC 500 series** of specifications define older analog avionics equipment whereas the ARINC 700 series are current documents & are typically digital versions of the analog devices.

400 series documents are general design & support documentation for the 500 series avionics equipment characteristic.

600 series documents are general design & support documentation for the 700 series avionics equipment characteristics.

The **800 Series** comprises a set of aviation standards for aircraft, including fiber optics used in high-speed data buses.

ARIN 429 specifications establishes how avionics equipment & systems communicate on commercial aircraft. The specification defines electrical characteristics, word structures and protocol necessary to establish bus communication. ARINC 429 utilizes the simplex, twisted shielded pair data bus system.

1.4.3 MIL specifications: A USA defense standard, often called a military standard, "**MIL-STD**", "**MIL-SPEC**", or (informally) "**Mil Specs**", is used to help achieve standardization objectives by the U.S. Department of defense. Standardization is beneficial in achieving interoperability; ensuring products meet certain requirements, commonality, reliability, total cost of ownership, compatibility with logistics systems, and similar defense-related objectives. Defense standards are also used by other non-defense government organizations, technical organizations, and industry. Although the official definitions differentiate between several types of documents, all of these documents go by the general rubric of "military standard", including defense specifications, handbooks, and standards. Strictly speaking, these documents serve different purposes. Military specifications "describe the physical and/or operational characteristics of a product", while military

standards "detail the processes and materials to be used to make the product." Military handbooks, on the other hand, are primarily sources of compiled information and/or guidance. Standards and specifications are often used interchangeably.

Acronym	Type	Definition
MIL-HDBK	Defense Handbook	Guidance document containing standard procedural, technical, engineering, or design information about the material, processes, practices, and methods covered by the DSP. MIL-STD-967 covers the content and format for defense handbooks.
MIL-SPEC	Defense Specifications	A document that describes the essential technical requirements for purchased material that is military unique or substantially modified commercial items. MIL-STD-961 covers the content and format for defense specifications.
MIL-STD	Defense Standard	A document that establishes uniform engineering and technical requirements for military-unique or substantially modified commercial processes, procedures, practices, and methods. There are five types of defense standards: interface standards, design criteria standards, manufacturing process standards, standard practices, and test method standards. MIL-STD-962 covers the content and format for defense standards.
MIL-PRF	Performance Specification	A performance specification states requirements in terms of the required results with criteria for verifying compliance, but without stating the methods for achieving the required results. A performance specification defines the functional requirements for the item, the environment in which it must operate, and interface and interchangeability characteristics.
MIL-DTL	Detail Specification	A specification that specifies design requirements, such as materials to be used, how a requirement is to be achieved, or how an item is to be fabricated or constructed. A specification that contains both performance and detail requirements is still considered a detail specification.

Some important Mil Specifications/standards are listed below:

-MIL-STD-1553, a digital communications bus.

- MIL-STD-2196, pertains to optical fiber communications.
- MIL-STD-810, test methods for determining the environmental effects on equipment.
- MIL-STD-202, test methods for electronic and electrical parts.

1.5 Electrical and optical data bus systems. Data bus systems are the essential enabling technologies of avionic system integration. They can be broadly divided into electrical data bus system where the data are transmitted as electrical pulses by wires, and optical data bus systems where the data are transmitted as light pulses by optical fibers. Serial digital data buses are used for interconnecting sub-units and sub-systems. Parallel data buses are used within a unit or rack for interconnecting the individual modules.

1.5.1 Electrical Data Bus Systems: There are several electrical serial digital data bus systems in use in avionics systems. These systems can be broadly divided into two categories in terms of their data rate transmission capabilities, namely, data bus systems operating with a maximum throughput of 1 to 2 Mbits/s and high speed data bus systems with a throughput of 50 Mbits/s to 100 Mbits/s. MIL STD 1553 data bus system is very widely used in military aircraft worldwide, although it originated in the US. It has become the established and dominant standard data bus system since its introduction in 1975. It receives and transmits the data at 1 Mbits/s and is a relatively sophisticated data bus system. ARIN 429 is a point to point system of lower capabilities (10 Kbits/s data rate) used in civil avionics systems. The ARINC 629 data bus system has data rate of 2 Mbits/s and is installed in the Boeing 777 airliner which entered service in 1995. There are two standard high speed data buses which have been developed in the US for military applications. These are the 'Linear Token Passing Bus', LTPB, which operates at 50 Mbits/s and the 'High Speed Ring Bus', HSRB, which operates at 100 Mbits/s. For civil airliners Ethernet data bus system is very widely used in commercial computing systems. It has a data transmission rate capability of 100 Mbits/s and is mainly used for data file transfer. The version which has been adapted for airborne application is known as the 'Avionics Full Duplex Switched Ethernet', which has been shortened to 'AFDX Ethernet' network.

1.5.1.1 MIL STD 1553 Bus System: MIL STD 1553B is a US military standard which defines a Time Division Multiplexing (TDM) multiple-source-multiple-sink data bus system which is very widely used in military aircraft in many countries. The basic bus configuration is shown in fig 1.5.1. The system is a command-response system with all data transmissions being carried out under the control of the bus controller. Each sub-system is connected to the bus through a unit called a remote terminal (RT). Data can be transmitted from one RT and received by another RT following a command from the bus controller (BC) to each RT. The protocol exercised by the bus controller hence ensures that there are no data clashes on the bus as only one RT is transmitting at any time. The bus controller thus initiates all data transfers and monitors the status of all transfers. It is generally incorporated in one of the sub-systems-usually the one generating the most traffic. The bus is formed as a single twisted cable pair with one layer of shielding and jacketing and with maximum length of 100 m. Although direct coupling to the bus is allowed, this is generally not used in order to avoid the risk of one terminal shorting out the bus. The bus connection is typically via a transformer coupled stub so that shorting is isolated from the bus. The data transmission rate is 1 Mbits/s. The data word size is 20 bits so that the maximum data transmission rate is 50,000 words per second. A maximum of 31 terminals can be connected to the bus. The bus operation is asynchronous, each terminal having an independent clock source for transmission. The technique adopted for data encoding is known as 'Manchester' bi-phase, encoding where

there must be an active transmission for every bit, i.e. for '0' and '1' signals. This is shown in fig 1.5.2. There are three types of words transferred; command words, status words and data words.

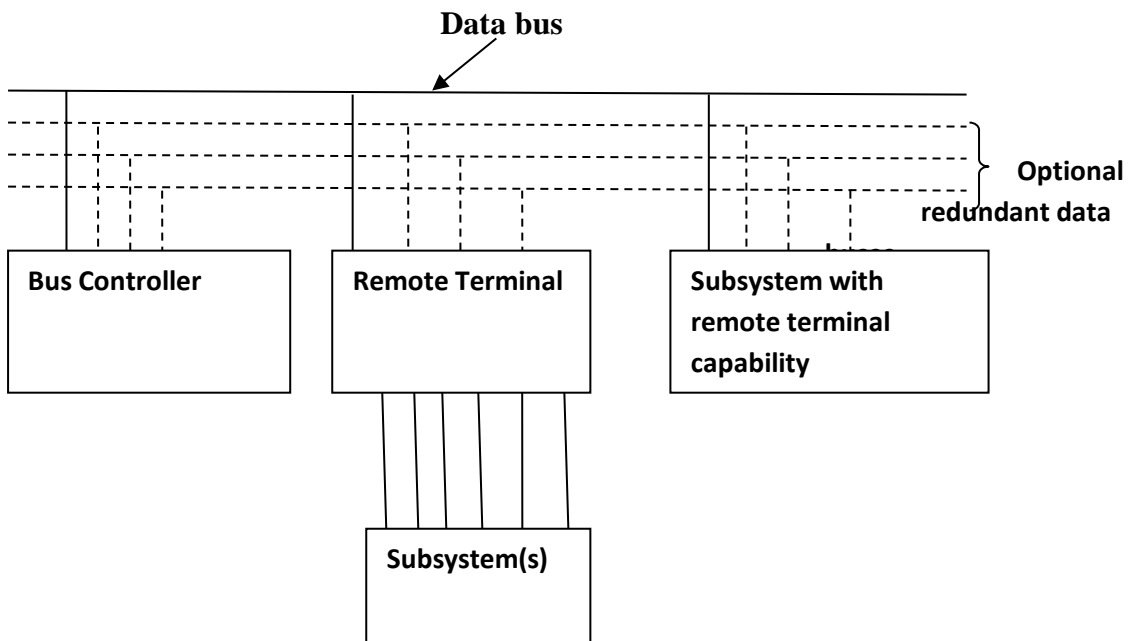


Fig 1.5.1: Typical multiplex data bus system architecture

There are three most commonly used data transfer formats. They are

- BC to RT
- RT to BC

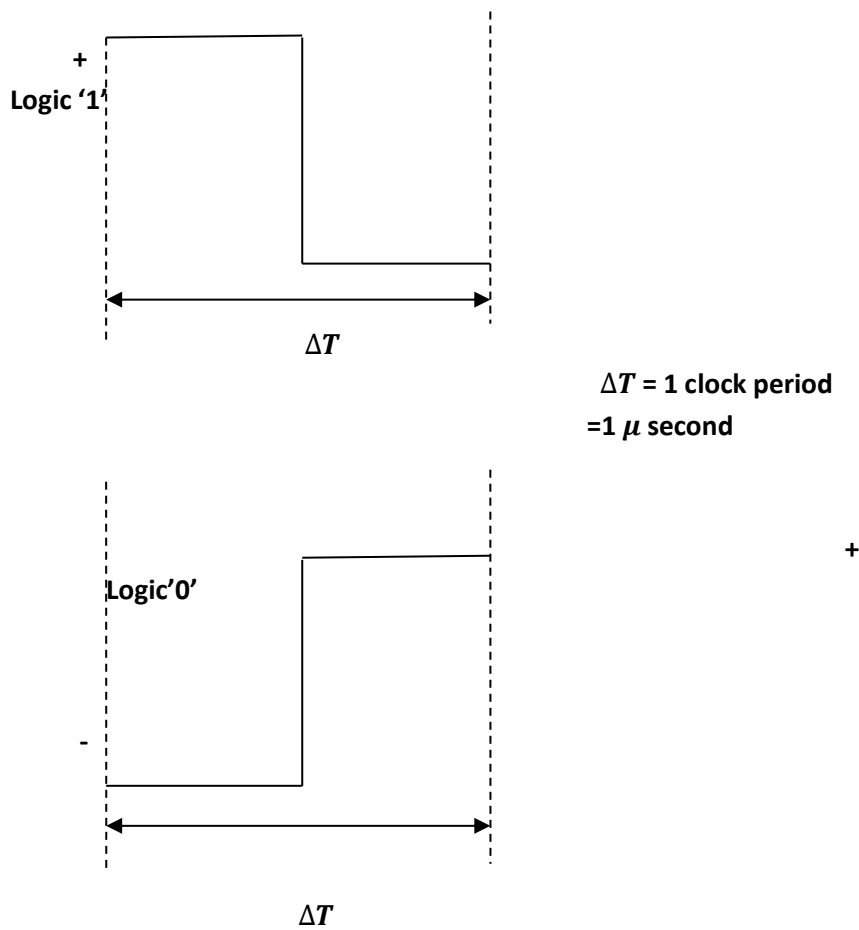


Fig 1.5.2: Logic '1' and logic '0'

1.5.2 Optical Data Bus. Optical fibers data bus offer major advantages over electrically signaled data bus. Some of these are listed below:

- (a) High data rate capability (> 10 Gbits/s using single mode fiber).
- (b) Insensitivity to electro-magnetic interference.
- (c) Electrical isolation.
- (d) No line capacitance or mutual coupling.
- (e) Low-cross talk

(f) Low power dissipation

(g) reduced weight and volume requirements.

An optical fiber basically comprises a central core of a suitable glass material (for example pure silica) with a very low optical transmission loss and with an outer cladding of a material with slightly lower refractive index than the core. In multi-mode fiber optics, the diameter of the core is large compared with the wavelength of the light being transmitted. For example, a typical core diameter is around $100 \mu\text{m}$ and the operating wavelength around $1 \mu\text{m}$. A ray entering the fibre at an incident angle θ to the axis of the fibre less than the critical angle, $\theta_{\text{critical}} = \text{Cos}^{-1} n_2/n_1$, will undergo total reflection at the core/cladding interface. This ray will undergo total internal reflection at the lower interface and will thus be guided through the core by repeated internal reflections.

In **single mode** there is only one value of θ and hence only one ray path for the light to travel along the fibre by multiple reflections so that there is only one velocity of propagation for a light pulse.

Multi-mode optical fiber can be used in avionics system applications because of the relatively short lengths involved and the current data rate requirements of 50 Mbips/s. the reason for its use is primarily due to the need for demountable connectors in avionics equipment for ease of servicing and replacement of a failed unit.

1.6 Integrated Modular Avionics (IMA) Architecture. The avionics currently account for some 30% of the total cost of a new aircraft. Reducing these costs must thus play a major role in containing overall system costs and halting the cost spiral inherent in federated architectures as increasing performance and capability are sought. The IMA architectures provide higher levels of performance and system capability, increased equipment availability and reduced levels of maintenance, so lowering costs right across the system life cycle.

Avionics architecture is the total set of design choices which make up the avionics system and result in it performing as a recognizable whole. In effect, the architecture is the total avionics system design.

The system complexity means that there are very many parts of an avionics architecture and the architecture is best viewed as a hierarchy of levels comprising :

(a) **Function allocation level.** The arrangement of the major system components and the allocation of system functions to those components.

(b) **Communication Levels.** The arrangement of internal and external data pathways and data rates, transmission formats, protocols etc.

(c) **Data processing level.** Central or distributed processing, processor type, software languages, documentation and CASE (Computer aided software engineering) design tools.

(d) **Sensor Level.** Sensor type, location of sensor processing, extent to which combining of sensor outputs is performed.

(e) **Physical level.** Racking, box or module outline dimensions, cooling provisions, power supplies.

The **software concept** is also modular, comprising a number of application programs running under the control of an executive operating system. The basic system requirements are:

- Suitable specifications for interconnection between modules, both hardware and software.
- Hardware that is independent of the application in which it will be used.
- Executive and application software that is independent of the hardware on which it will run.
- Standard interface between the executive and the hardware for input/output. This is often referred to as three levels and is shown in Fig 1.6.

The modular avionics concept relies on the use of a limited range of standard modules which are packaged in a standard modular format and installed in a small number of common racks. Integrated modular avionics approach consists of:

- (a) The use across a range of aircraft platforms of standard 'F³ I' form, that is 'form, fit, function and interface', interchangeable modules procured from an 'avionics supermarket'.
- (b) The integration of data and signal processing across traditionally separate aircraft sub-systems enabling wide scale use of reconfiguration to improve availability.
- (c) The use of sufficient built in test to enable faulty modules to be correctly diagnosed and replaced at first line without additional test equipment.

The use of a small number of standard modules potentially reduces the initial development and procurement cost of equipment through competition and eventually through the economics of scale in the production of the modules. It also reduces the maintenance costs by reducing spare holding.

However, with these advantages there are many implications for the way equipment is currently contracted for and built. The integrated system design increases enormously both system complexity and the potential for interactions between sub-systems. At the same time it blurs the traditional line of responsibility that exists in the industry and it therefore requires a very care ful and systematic design approach if integrated systems are to be put together successfully. To implement such highly integrated systems, very close collaboration between systems engineers from different avionics, airframe and software suppliers is required.

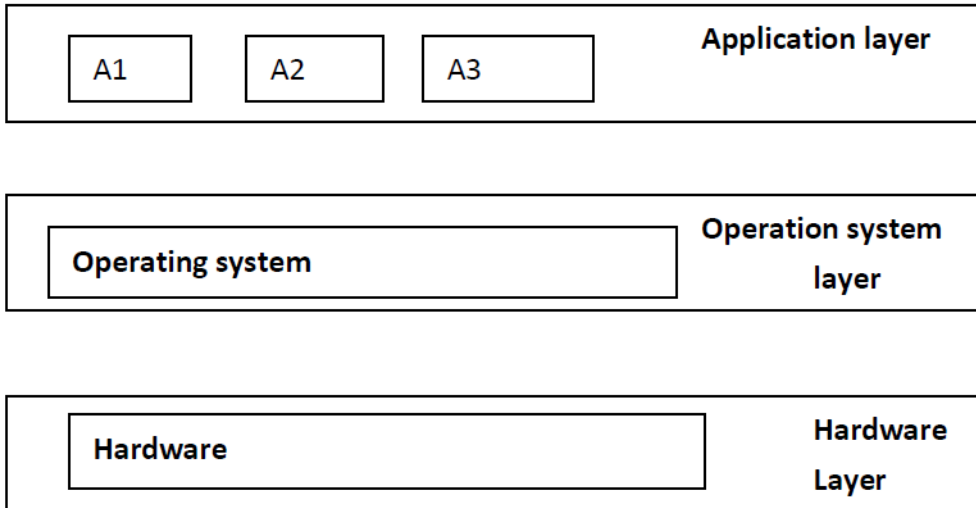


Fig: 1.6: The 'three layers stack' modular software concept.

Line Replaceable Units (LRUs) were developed as a way of removing functional elements from an avionics system with minimum disruption. LRUs have logical functional boundaries associated with the task they perform in the aircraft. LRU formats were standardized to the following standards:

1. Air Transport Radio (ATR). The origins of ATR standardization may be traced back to the 1930s when United Airlines and ARINC established a standard racking system called the air transport radio (ATR) unit case. ARINC 11 identified three sizes defined by box width: $\frac{1}{2}$ ATR, 1 ATR, $1\frac{1}{2}$ ATR, with the same height and length. In a similar time-scale, standard connector and pin sizes were specified for the wiring connections at the rear of the unit. The use of standardized form boxes

led to the use of standard card sizes, connector types, mounting tray assemblies, and internal layout design. The US military and the military authorities in the United Kingdom adopted these standards although to differing degrees, and they are still in use in military parlance today. Over the period of usage, ATR 'short' ~ 12.5" length and ATR 'long' ~ 19.5" length have also been derived. ARINC 404A developed the standard to the point where connector and cooling duct positioning were specified to give true interchangeability between units from different suppliers. The relatively dense packaging of modern electronics means the ATR 'long' boxes are seldom used. The range of module sizes increased to include half-height boxes known as dwarf and elfin.

2. Modular Concept Unit (MCU). The civil airline community took the standardization argument further by developing the MCU. An 8 MCU box is virtually equivalent to 1 ATR width, and boxes are sized in MCU units. A typical small aircraft systems control unit today might be 2 MCU, while a larger avionics unit such as an Air Data and Inertial Reference System (ADIRS), combining the Inertial Reference System (IRS) with the air data computer function, may be 8 or 10 MCU (1 MCU is roughly equivalent to ~ $1\frac{1}{4}$ ", but the true method of sizing an MCU unit is given in Fig. 2.23). An 8 MCU box will therefore be 7.64" high \times 12.76" deep \times 10.37" wide. The adoption of this concept was in conjunction with the most recent ARINC 600 standard, which specifies connectors, cooling air inlets, etc., in the same way as ARINC 404A did earlier.

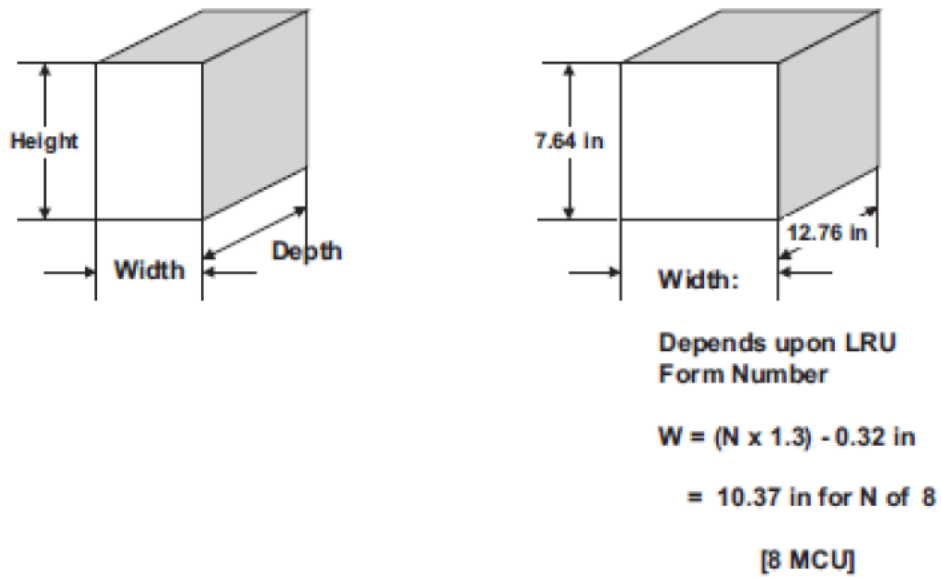


Fig: 2.23: MCU Sizing.

UNIT-II

Display-Man-Machine Interaction and Communication System

Index

SI NO	Topics	Page No
1	Introduction to Aircraft Display	39
2	Head-Up Display	39
3	Helmet Mounted Display	46
4	Head Down Display	51
5	Military Display	56
6	Intelligent Display Management	58
7	Introduction to Data Communication	59
8	HF/VHF Communication	59
9	Satellite Communication System	60
10	Flight Data Recorder	61
11	Flight Entertainment System	63
12	Airborne Communication & Addressing System	64

Unit-II: Displays-Man Machine Interaction and Communication Systems

2.1 Introduction to aircraft displays. The cockpit display systems provide a visual presentation of the information and data from the aircraft sensors and systems to the pilot (and crew) to enable the pilot to fly the aircraft safely and carry out the mission. They are thus vital to the operation of any aircraft as they provide the pilot, whether civil or military, with:

- Primary flight information,
- Navigation information,
- Engine data,
- Airframe data,
- Warning information.

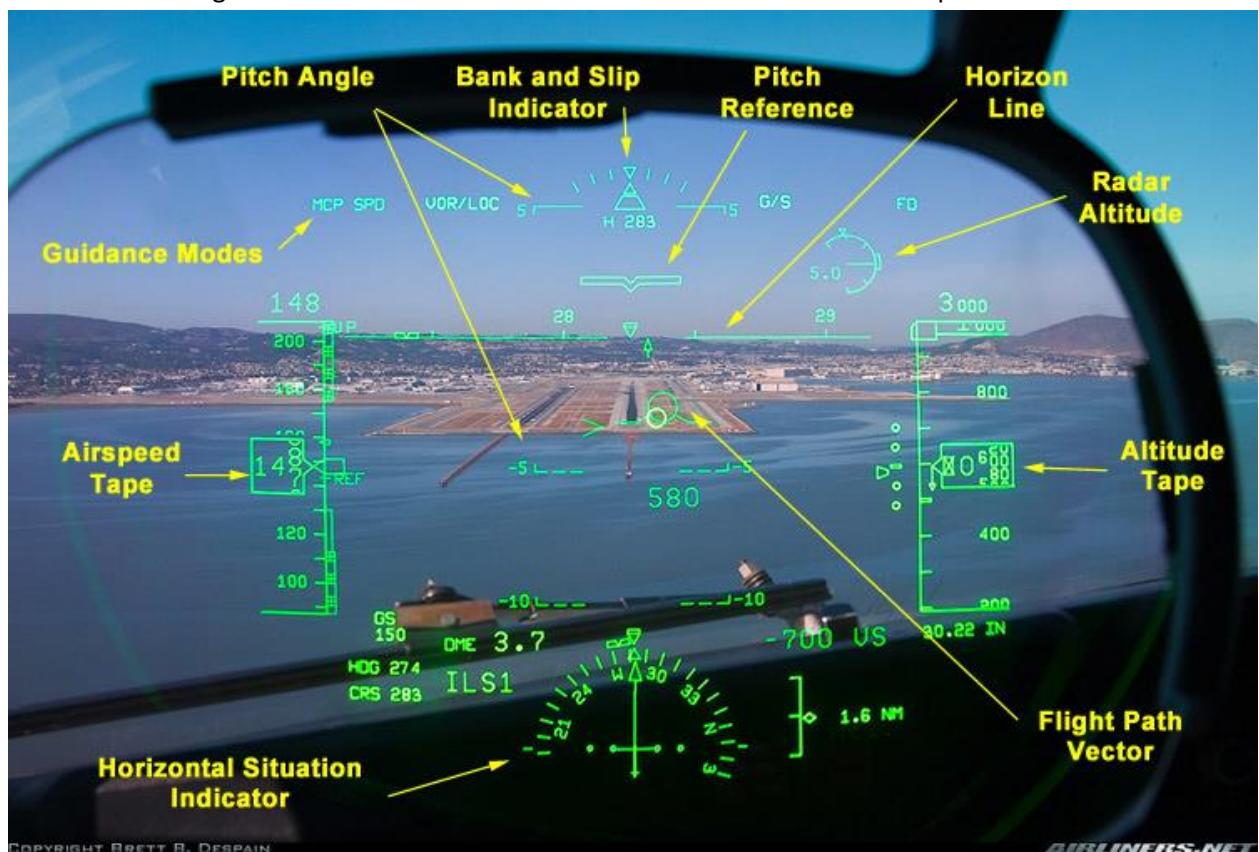
The military pilot has also a wide array of additional information to view, such as:

- Infrared imaging sensors,
- Radar,
- Weapon aiming,
- Threat warnings.

The pilot is able to rapidly absorb and process substantial amounts of visual information but it is clear that the information must be displayed in a way which can be readily assimilated, and unnecessary information must be eliminated to ease the pilot's task in high work load situations. A number of developments have taken place to improve the pilot-display interaction and this is a continuous activity as new technology and components become available. Examples of these developments are:

- Head up display,
- Helmet mounted displays
- Multi-function color displays,
- Digitally generated color moving map displays,
- Synthetic pictorial imagery,
- Display management using intelligent knowledge-based system (IKBS) technology,
- Improved understanding of human factors and involvement of human factors specialized from the initial cockpit design stage.
- Equally important and complementary to the cockpit display systems in 'the man machine interaction' are the means provided for the pilot to control the operation of the avionics systems and enter data. Again, this is the field where continual development is taking place. Multi-function keyboards and multi-function touch panel displays are widely used. Speech recognition technology has now reached sufficient maturity for 'direct voice input' control to be installed in the new generation of military aircraft. Other methods of data entry which are being evaluated include the use of eye trackers.

2.2 Head-up displays (HUD). The HUD has enabled a major improvement in man-machine interaction (MMI) to be achieved as the pilot is able to view and assimilate the essential flight data generated by the sensors and systems in the aircraft whilst head up and maintaining full visual concentration on the outside world scene. A HUD basically projects a collimated display in the pilot's head up forward line of sight so that he can view both the display information and the outside world scene at the same time. Because the display is collimated, that is focused at infinity (or a long distance), the pilot's gaze angle of the display symbology remains conformal or stabilized with the outside world scene. The pilot is thus able to observe both distant outside world objects and display data at the same time without having to change the direction of gaze or refocus the eyes. There are no parallax errors and aiming symbols for either a flight path director, or for weapon aiming in the case of a combat aircraft, remain overlaid on a distant 'target' irrespective of the pilot's head movement. The advantage of head up display presentation of essential flight path data such as artificial horizon, pitch angle, bank angle, flight path vector, height, airspeed and heading can be seen in fig 2.1 which shows a typical head up display as viewed by the pilot during the landing phase. The pilot is thus free to concentrate on the outside world during the maneuvers and does not need to look down at the cockpit instruments or head down



displays.

Fig 2.1: Head up Presentation of primary flight information

It should be noted that there is a transition time of one second or more to re-focus the eyes from viewing a distant object to viewing near objects a meter away or less away, such as the cockpit instruments and displays and adapt to the cockpit environment. In combat situations, it is essential for survival that the pilot is head up and scanning for possible threat from any direction. The very high accuracy which can be achieved by HUD and computerized aiming system together with the ability to remain head up in combat have made the HUD an essential system on all modern combat aircraft.

By using a **Forward Looking Infrared (FLIR)** sensor, an electro-optical image of the scene in front of the aircraft can be overlaid on the real-world scene with a raster mode HUD. The TV picture generated from the FLIR sensor video is projected on to the HUD and scaled one to one with outside world enabling the pilot to fly at low level by night in fair weather. This provides a realistic night attack capability to relatively simple day ground attack fighters. HUDs are now being installed in **civil aircraft** for reasons such as:

- Inherent advantages of head-up presentation of primary flight information including depiction of the aircraft's flight path vector, resulting in improved situational awareness and increased safety in circumstances such as wind shear or terrain/traffic avoidance maneuvers.
- To display automatic landing guidance to enable the pilot to land the aircraft safely in conditions of very low visibility due to fog, as back up and monitor for the automatic landing system. The display of taxi-way guidance is also being considered.
- Enhanced vision using a raster mode HUD to project a FLIR video picture of the outside world from a FLIR sensor installed in the aircraft, or, a synthetic picture of the outside world generated from a forward looking millimetric radar sensor in the aircraft. This enhanced vision systems are being actively developed and will enable the pilot to land the aircraft in conditions of very low or zero visibility at airfields not equipped with adequate all-weather guidance systems such as ILS.

2.2.1 HUD Basic Principles. The basic configuration of a HUD is shown schematically in fig 2.3. The pilot views the outside world through the HUD combiner glass (and wind screen). The combiner glass is effectively a 'see through' mirror with high optical transmission efficiency so that there is little loss of visibility looking through the combiner and wind screen. It is called combiner as it optically combines through collimated display symbology with the outside world screen viewed through it. Referring to fig 2.3, the display symbology generated from the aircraft sensors and systems (such as the INS and air data system) is displayed on the surface of a cathode ray tube (CRT). The display images are then relayed through a relay lens system which magnifies the display and corrects for some optical errors which are otherwise present in the system. The relayed display images are then reflected through an angle of near 90 deg by the fold mirror and thence to collimating lens which collimates the display images which are then reflected from the combiner glass into the pilot's forward field of view. The virtual images of the display symbology appear to the pilot to be at infinity and overlay the distant world scene, as they are collimated. The function of the fold mirror is to enable a compact optical configuration to be achieved so that the HUD occupies the minimum possible space in the cockpit. A collimator is defined as an optical system of finite focal length with an image source at the focal plane.

Rays of light, emanating from a particular point on the focal plane, exit from the collimating system as a parallel bunch of rays, as if they came from a source at infinity. Fig 2.4 (a) and (b) show a simple collimating lens system with the rays traced from a source at the center, o, and point, D, on the focal plane respectively. A ray from a point on the focal plane which goes through the center of the lens is not refracted and is referred to as the 'non-deviated ray'. The other rays emanating from the point are parallel to the non-deviated ray after exiting the collimator. Collimating lens is made of several elements to minimize the unacceptable shortcoming of a single lens. It can be seen from fig 2.4(a) that an observer looking parallel to the optical axis will see point O at eye positions A, B and C, and the angle of gaze to view O is independent of the displacement of the eye from the optical axis. Similarly, it can be seen from fig 2.4(b) that the angle of gaze from the observer to see point D is the same for eye position A, B and C and is independent of translation.

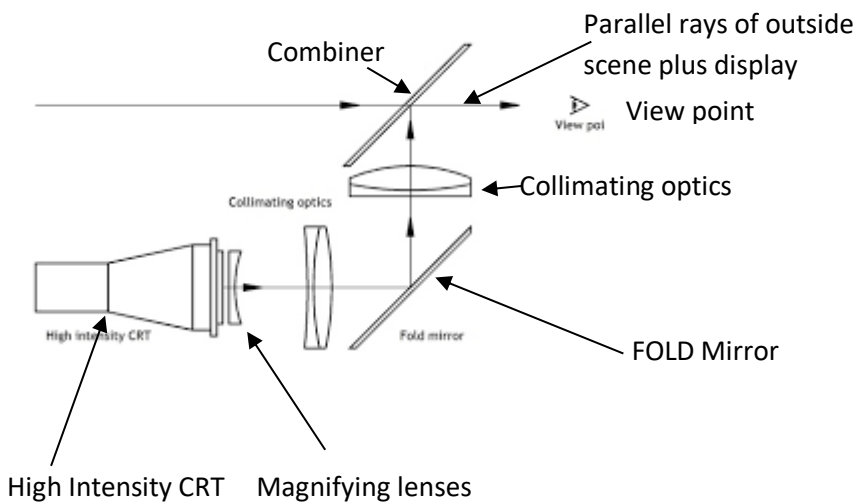


Fig: 2.3 HUD Schematic

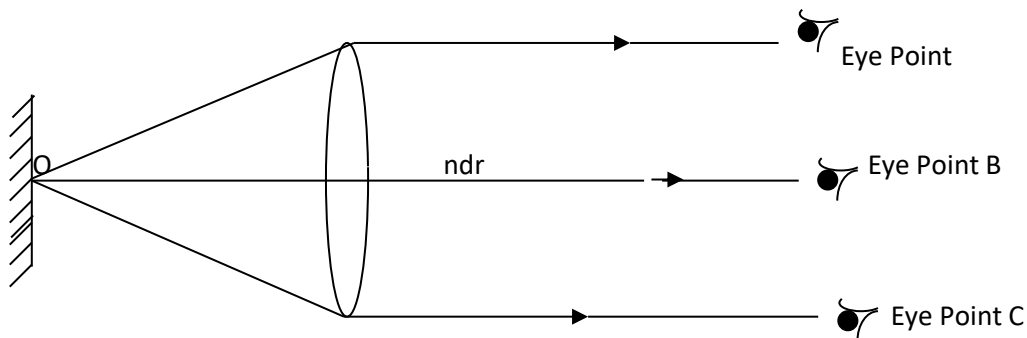


Fig 2.4 (a): simple optical collimator

ndr= non-deviated ray

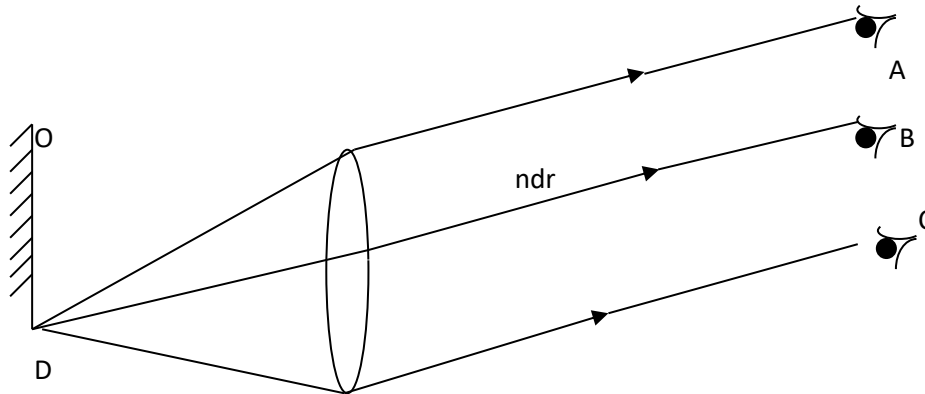


Fig 2.4 (b): Simple optical collimator

It is important to distinguish between the field of view (IFOV), which should be as large as possible within the severe space constraints imposed by the cockpit geometry. A large horizontal field of view is particularly important to enable the pilot 'to look into turns' when the HUD forms part of a night vision system and the only visibility the pilot has of the outside world is the FLIR image displayed on the HUD.

It is important to distinguish between the instantaneous field of view (IFOV) and the total field of view (TFOV) of a HUD as the two are not the same in the case of refractive HUD. The instantaneous field of view is the angular coverage of the imagery which can be seen by the observer at any specific instant and is shown in the simplified diagram in Fig 2.5 (a). It is determined by the diameter of the collimating lens, D , and the distance, L , of the observer's eyes from the collimating lens.

$$\text{IFOV} = 2 \tan^{-1} D/2L$$

The total field of view is the total angular coverage of the CRT imagery which can be seen by moving the observer's eye position around. TFOV is determined by the diameter of the display, A , and effective focal length of the collimating lens, F .

$$\text{TFOV} = 2 \tan^{-1} A/2F$$

Reducing the value of L increases the IFOV as can be seen in Fig 2.5 (b) which shows the observer's normal eye position brought sufficiently close to the collimating lens for the IFOV to equal to the TFOV. However, this is not practical with the conventional type HUD using refractive optics. This is because of the cockpit geometry constraints on the pilot's eye position and the space constraints on the diameter of the collimating lens. The IFOV is generally only about two thirds of the TFOV. It can be seen from Fig 2.5(c) that by moving the head up or down or side to side the observer can see a different part of the TFOV, although the IFOV is unchanged. Typical IFOVs range from about 13° to 18° with corresponding TFOV of about 20° to 25° . A typical HUD installed on an aircraft is shown in fig 2.6.

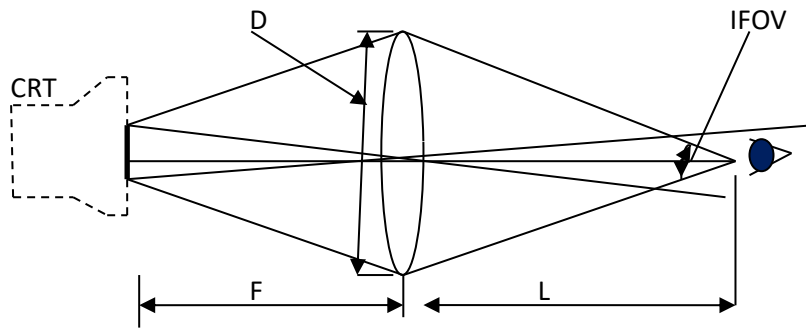


Fig 2.5 (a)

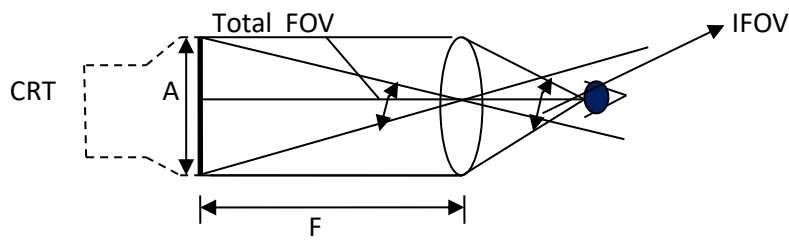


Fig 2.5 (b)

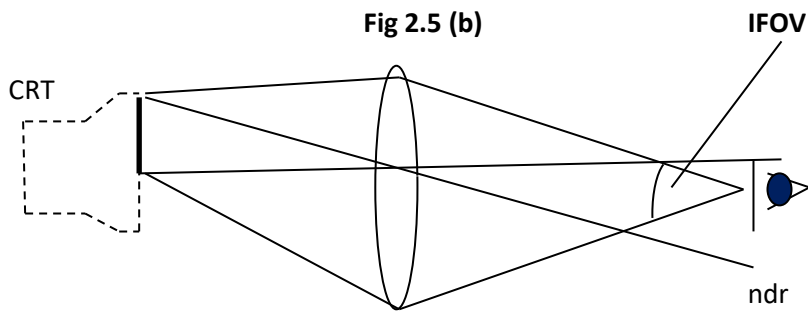


Fig 2.5 (c)

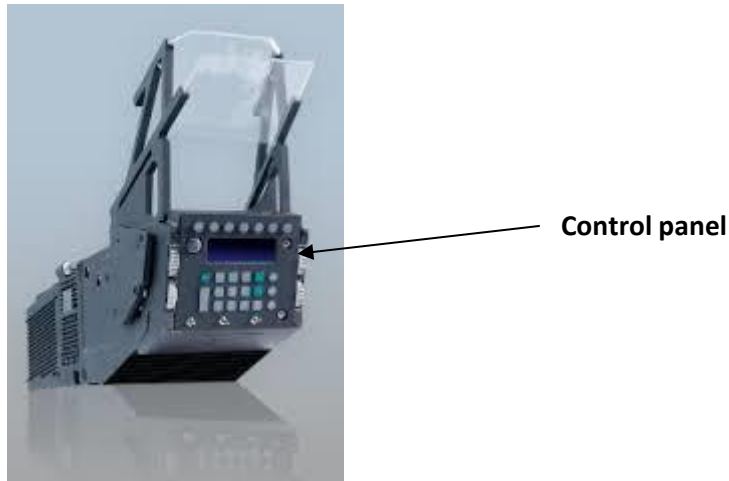


Fig 2.6 HUD

2.2.2 Holographic HUD. The requirement for a large FOV is driven by the use of the HUD to display a collimated TV picture of the FLIR sensor output to enable the pilot to ‘see’ through the HUD FOV in condition of poor visibility, particularly night operation. It should be noted that the FLIR sensor can also penetrate through haze and many cloud conditions and provide ‘enhanced vision’ as the FLIR display is accurately overlaid one to one with the real world. The wider azimuth FOV is essential for the pilot to see into the turn. In a modern wide FOV holographic HUD, the display collimation is carried out by the combiner who is given optical power (curvature) such that it performs the display image collimation. Fig 2.7 shows the basic configuration of a modern single combiner holographic HUD. The CRT display is focused by the relay lens system to form an intermediate image at the focus of the powered combiner. The intermediate image is then reflected from the fold mirror to the combiner. This acts as a collimator as the tuned holographic coating on the spherical surface of the combiner reflects the green light from the CRT display and forms a collimated display image at the pilot’s design eye position.

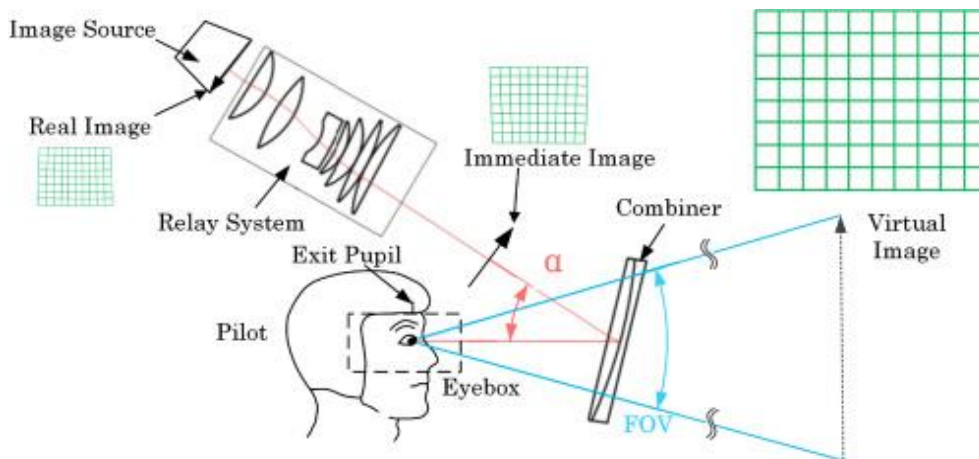


Fig 2.7: Holographic combiner HUD Configuration.

2.2.3 HUD Electronics. The basic elements of HUD electronics systems are shown in Fig 2.8. These function elements may be packaged so that complete system is contained in a single unit as shown in fig 2.6. The data bus interface decodes the serial digital data from the aircraft data bus (MIL STD 1553B data bus) to obtain the appropriate data from the aircraft sub-systems and inputs this data to the display processor. The input data includes height, airspeed, vertical speed, pitch and bank angles, headings, flight path velocity vector. The display processor processes this input data to derive the appropriate display formats, carrying out tasks such as axis conversion, parameter conversion and format management. In addition, the processor also controls the following functions:

- Self test
- Brightness control
- Calibration
- Power supply control

The symbol generator carries out the display waveform generation task (digitally) to enable the appropriate display symbology (e.g. lines, circles, alpha-numeric, etc.) to be stroke written on the HUD CRT. The necessary D to A conversions are carried out in the symbol generator which outputs the appropriate analogue x and y deflection voltage waveforms and 'bright up' wave forms to control the display drive unit of the HUD CRT.

Data Bus

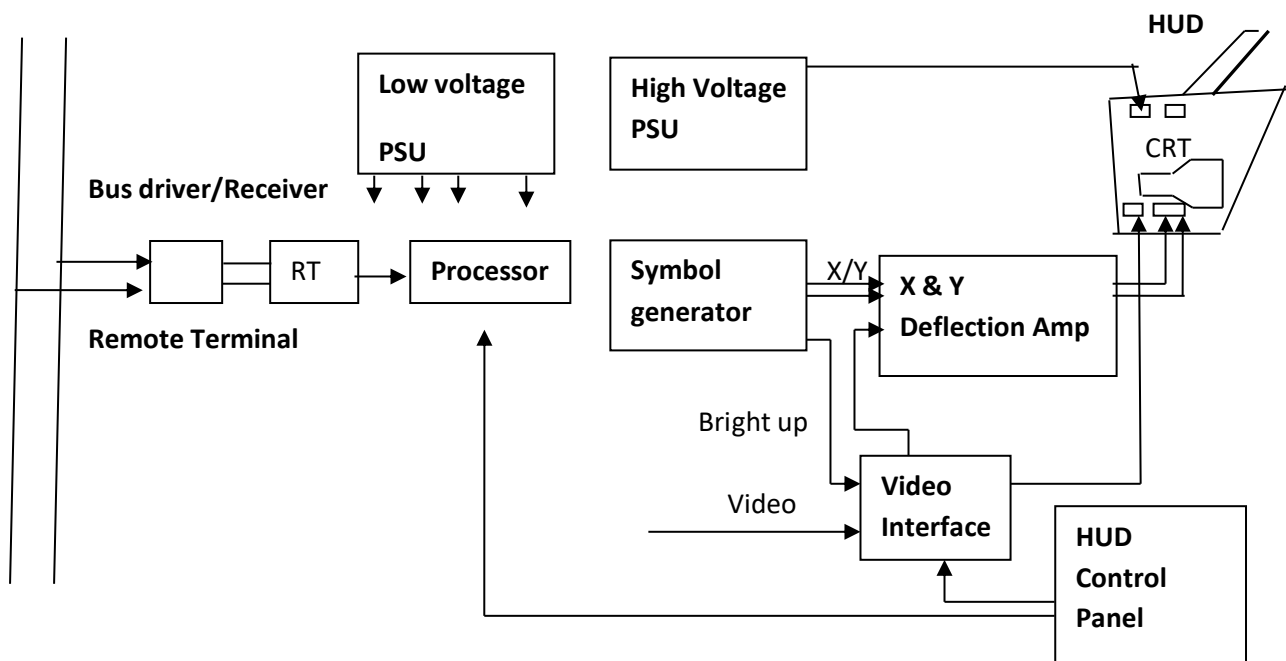


Fig 2.8: HUD Electronics

2.3 Helmet Mounted Displays(HMD).

2.3.1 Introduction. The HUD presents the information in the pilot forward field of view, which even with a wide FOV holographic HUD is limited to about 30° in azimuth and 20° to 25° in elevation. Significant increases in this FOV are not possible because of the cockpit geometry constraints. The pilot requires visual information head up when he is looking in any direction and this requirement can only be met by a helmet mounted display (HMD). Fig 2.9 shows the comparison between HUD and HMD FOV. HMD can provide, in effect, a 'HUD on the helmet'. This can display all the information to the pilot which is normally shown on a HUD but with the pilot able to look in any direction (attitude information is referenced to his line of sight (LOS)). The HMD can also have a wide FOV ranging from 35° to 40° for a fighter aircraft application to over 50° for a helicopter application. It should be appreciated that the FOV moves with the head, unlike the HUD, and a larger FOV reduces scanning head movement in an HMD. It is still very useful, however, to allow peripheral information to enter the eyes, so that the FOV is not just that of optics.

The HMD also enables a very effective night/poor visibility viewing system to be achieved by displaying the TV picture from a gimbaled infrared sensor unit which is slaved to follow the pilot's line of sight. The pilot's LOS with respect to the airframe is measured by a head position sensing system. Such a helmet can also incorporate image intensification devices with a video output to provide a complementary viewing system.

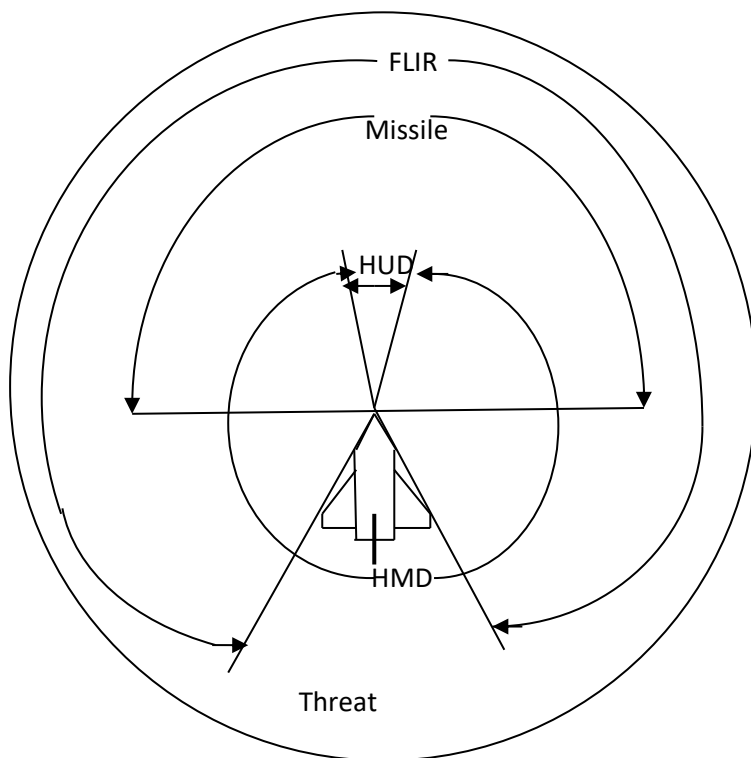


Fig 2.9: Comparison of HUD and HMD Field of View

2.3.2 Helmet Design factors. It is important that the main functions of the conventional aircrew helmet are appreciated as it is essential that the integration of a helmet mounted display system with the helmet does not degrade these functions in any way. The basic functions are:

- To protect the pilot's head and eye from injury when ejecting at high airspeeds. For example, the visor must stay securely locked in the down position when subjected to the blast pressure experienced at indicated airspeed of 650 knots. The helmet must also function as a crash helmet and protect the pilot's head as much as possible in a crash landing.
- To interface with oxygen mask attached to the helmet. Combat aircraft use a special breathing system for high g maneuvering.
- To provide the pilot with an aural and speech interface with the communications radio equipment. The helmet incorporates a pair of headphones which are coupled to the outputs of the appropriate communication channels channel selected by the pilot.
- In addition to the clear protective visor, the helmet must also incorporate a dark visor to attenuate the glare from bright sun light.
- The helmet must also be compatible with NBC (nuclear-biological-chemical) protective clothing and enable an NBC mask to be worn.

The combined mass of the integrated helmet and HMD system must be as low as possible to reduce the strain on the pilot's neck muscles during maneuvers. Modern conventional air crew helmet weigh about 1 kg so that the weight pilot feels on his head during a 9g turn is equal to 9 kg, and this is just acceptable. The typical weight for an integrated helmet incorporating a binocular HMD system is around 1.7 to 2.5 kg. This is limited by current technology and lower weight is sought. The helmet CG should also be in line with the pivoting point of the head on the spine so that there are minimal out of balance moments exerted on the neck's muscles.

2.3.3 Helmet mounted Displays. HMD functions as a 'HUD on the helmet' and provide the display for an integrated night/poor visibility viewing system with the flight and weapon aiming symbology overlaying the projected image from the sensor. Miniature 0.5 inch diameter CRTs are currently used as the display sources. The development of miniature, high resolution liquid crystal display (LCDs), however, has changed this situation. HMDs exploiting these devices are now being produced. A lower weight HMD system can be achieved by the use of a visor projection system in conjunction with a high efficiency optical design. This allows a standard spherically curved air crew visor to be used to carry out the combiner and collimation function by the addition of a neutral density reflection coating. The visor coating provides high display brightness whilst maintaining high real world transmission (> 70% can be achieved) with no coloration.

The combiner and collimation function is thus achieved without adding additional weight to the optical system as the visor is essential anyway. To incorporate the night flying capability in combat aircraft Night Vision Goggles (NVGs) are mounted on a bracket on the front of a standard aircrew helmet. The weight of the NVGs and forward mounting creates an appreciable out of balance moment on the pilot's head and precludes the pilot from undertaking maneuvers involving significant g. The NVGs must also be removed before ejecting because of the g experienced during ejection.

NVGs use image intensifiers tube (IIT) which is a phosphor screen emitting green light in the centre of the visual band where eye is most sensitive. In fighter/strike aircraft use is made of IIT which image on to small CCD cameras. The output of the IIT CCD camera is a video signal which is fed back to the remote display drive electronic where it is electronically combined with the symbology and displayed on the helmet mounted CRTs. Fig 2.10 illustrates the concept of electronic combination of IIT and CRT. Fig 2.11 shows a helmet mounted display in the cockpit.

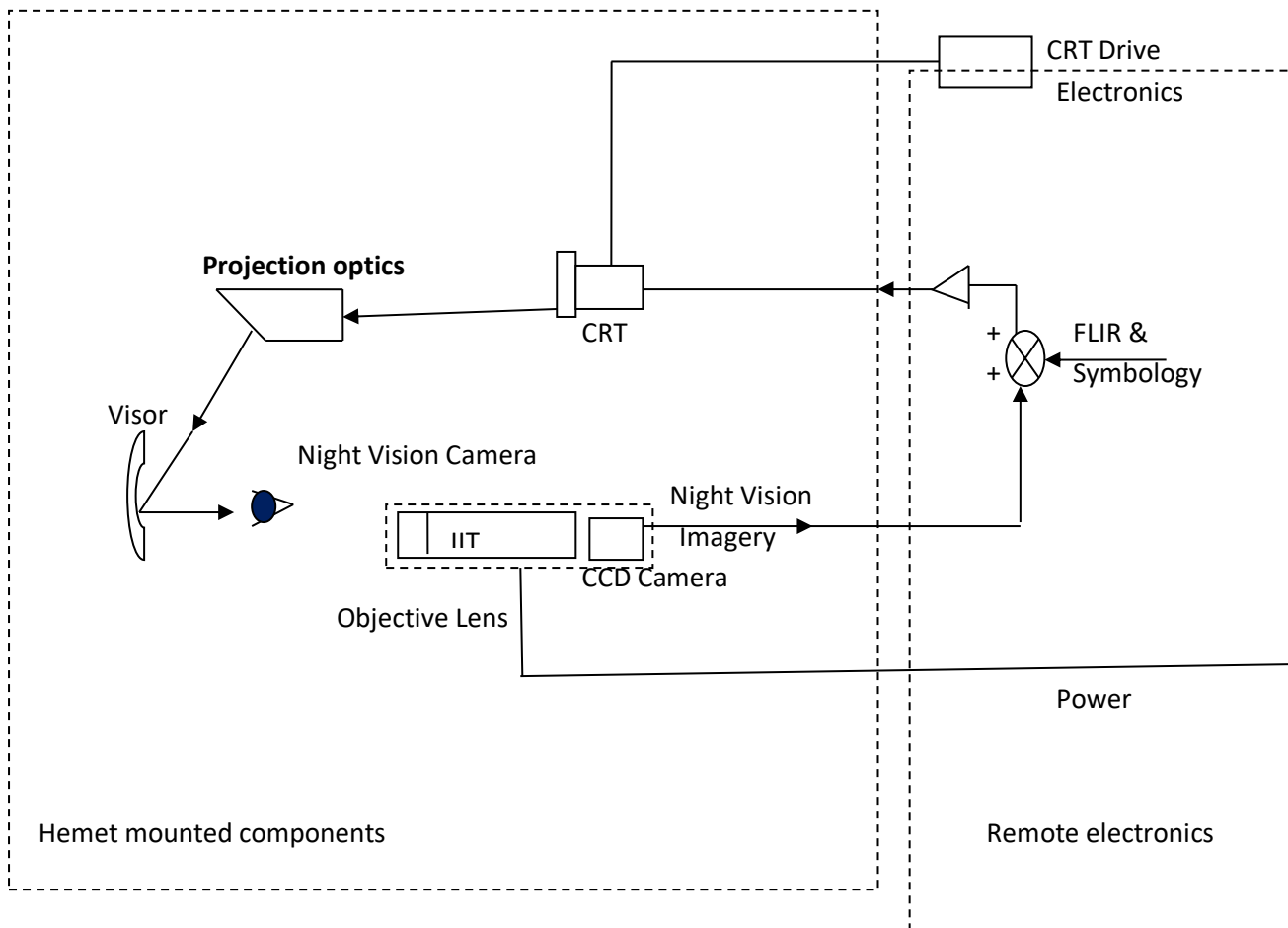


Fig 2.10 Electronics combination of IIT and CRT.



Fig 2.11 Helmet Mounted Display

2.4 Head Tracking Systems. A head tracker system in conjunction with helmet mounted sight (HMS) provides a very effective means for the pilot to designate a target. The pilot moves his head to look and sight on the target using the collimated aiming cross on the helmet sight. The angular co-ordinates of the target sight line relative to the airframe are then inferred from the measurements made by the head tracker system of the attitude of the pilot's head. In air to air combat, the angular co-ordinates of the target line of sight (LOS) can be supplied to the missiles carried by the aircraft. The missile seeker heads can then be slewed to the target LOS to enable the seeker heads to acquire and lock on to the target. (A typical seeker head needs to be pointed to within about 2 deg of the target to achieve automatic lock on.) Missile lock on is displayed to the pilot on the HMS and audio signal is also given. The pilot can then launch the missile. This enables attacks to be carried out at large off-bore sight angles, given agile missiles with high g maneuvering capabilities. The pilot no longer needs to turn the aircraft until the target is within the FOV of the HUD before launching the missile. The maximum off-bore sight angle for missile launch using the HUD is less than 15 deg, compared with about 120 deg with helmet mounted sight (and highly agile missiles). This gives a major increase in air combat effectiveness. Optical head tracking systems work in number of ways, for example,

- (a) Pattern recognition using a CCD camera.
- (b) Detection of LEDs mounted on the helmet.

Magnetic tracking systems measure the field strength at the helmet from a magnetic field radiator located at a suitable position in the cockpit. There are two types of magnetic head tracker system:

- (a) An AC system using an alternating magnetic field with a frequency of around 10 kHz.
- (b) A DC system using a DC magnetic field which is switched at low frequency.

Both systems are sensitive to metal in the vicinity of the helmet sensor. This causes errors in the helmet attitude measurement which are dependent on the cockpit installation. These errors need to be measured and mapped for the particular cockpit and the corrections stored in the tracker computer. The AC system is more sensitive to these errors than DC system which is claimed to be 10 times less sensitive to metal than AC systems. Angular coverage of the magnetic type of head tracker is typically around $\pm 135^\circ$ in azimuth and $\pm 85^\circ$ in elevation. There are other sources of errors in measuring the pilot's direction of gaze apart from the errors present in head tracker system. This is because the pilot's direction of gaze is inferred from the helmet attitude measurement. The pilot can, in fact,

experience great difficulty in keeping the helmet sight on the target when subjected to severe low frequency vibration.. A sinusoidal vibration of 0.5g amplitude at a frequency of 2 Hz corresponds to an up and down motion of ± 31 mm. It has been shown, however, that the pilot's gaze can still be maintained on the target whilst the pilot is experiencing low frequency buffeting type vibration. This is because the control of the eyeball (and hence the direction of gaze) by the eye muscles has a much faster response than the control of the head position by the neck muscles. The 'eyeball servo' has, in fact, a bandwidth of several Hz in control engineering terms. The sight line measurement accuracy can hence be greatly improved by the use of an eye tracker system which measures the direction of gaze of the eye with respect to the helmet. The gaze angle relative to the airframe can then be obtained by combining the eye tracker and tracker outputs.

2.5 Head down Displays.

2.5.1 Introduction. Old aircraft had conventional dial type instruments. With revolution in electronics these displays were replaced by multi-function color CRT display. The only traditional dial instruments which have been retained are the electro mechanical standby instruments such as altimeter, airspeed indicator, artificial horizon and heading indicator. These electro-mechanical standby instruments, however, are now being replaced by all solid state equipment with color LCD display presentation, in the new generation of aircraft entering service, or in avionics upgrade program. The color CRT is still a major display technology in terms of the number of aircraft equipped with color multi-function CRT displays. The situation, however, has changed rapidly over the last decade with the development of high resolution active matrix color liquid displays (AMCD). Flat panel, high resolution, color displays exploiting commercial 'off the shelf' color AMLCDs have displaced color CRT displays in head down display applications in new build civil and military aircraft. It should be noted that the current supremacy of the flat panel AMLCD display may be being challenged in the near future by the organic light emitting diode (OLED) display. OLED displays are emissive display with an inherently wide viewing angle and crisp display characteristics. They have a fast response time of 10 to 20 ns and have wide operating temperature and can have a wide operating temperature range, when properly packaged. They are thin and do not require an illuminating light source like the AMLCD, thus enabling a slim flat panel display to be achieved. HDD displays are driven by a central display processor(s). The size of an HDD is typically defined by an ARINC standard of square format with one inch increments- for example, 5 * 5, 6 * 6 inch, etc.

2.5.2 Civil Cockpit Head Down Displays. A modern civil flight deck is shown in fig 2.10. The displays are duplicated for the captain and Second Pilot and being multi-function, it is possible to reconfigure the display information in the event of the failure of a particular display surface. The electronic Primary Flight Display (PFD) replaces six electro-mechanical instruments i.e. altimeter, vertical speed indicator, artificial horizon/attitude director indicator, heading/compass indicator and Mach meter. A PFD format follows the classic 'T' layout of the conventional primary flight instruments. All the primary flight information is shown on the PFD thereby reducing the pilot scan, the use of color enabling the information to be easily separated and emphasized where appropriate. **Fig 2.11** shows a representative primary flight display. Airspeed is shown on a scale on the left with pressure altitude and vertical speed on the right hand scales. Aircraft heading information is shown on a 'tape' scale type format below the attitude display. The artificial horizon/attitude display has a blue background above the horizon line representing the sky and a brown background below the horizon line representing the ground. This enables 'which way is up' and the aircraft orientation to be rapidly

assimilated by the pilot in recovering from an unusual attitude, for example, as the result of a severe jet upset. Pilot can select various modes of display. A mode shows the aircraft position relative to a specific waypoint. Weather radar displays may be superimposed over the map. Engine/warning and various aircraft systems (For example the fuel system, hydraulic system, and electrical system) can be displayed.



Fig 2.11 Cockpit displays of Airbus 380

2.5.3 Military cockpit head down display. Video head down displays now include FLIR, LLTV and maps. All the HUD functions may be repeated overlaid on the video pictures. Fuel and engine data, navigation waypoints and host of other functions such as hydraulics, pressurization may be displayed. A store management display is also required showing the weapons carried and their status. Typical advanced military cockpits are configured with four head down

displays. There are two large color displays; a Horizontal Situation Display (HSD) providing a 6 * 8 inch map display with symbol overlay of routing and threat data and a Vertical Situation Display (VSD) providing an 8 * 6 inch IR video display showing targeting video at various magnifications. The other two displays are smaller 5 * 5 inch monochrome displays comprising a System Status Display (SSD) displaying system status data and a system control display (SCD) displaying system control data. The advanced cockpits or the new generation of fighter/strike aircraft have just two large color displays as the primary head down displays. Fig 2.12 shows the instrument panel of a strike aircraft. The pilot can divide each screen into several windows enabling a wide variety of information to be displayed at the same time. These flat panel displays are the same type as used in commercial lap-top computer and hardened to withstand the fighter environment by mounting them in rugged bezels.

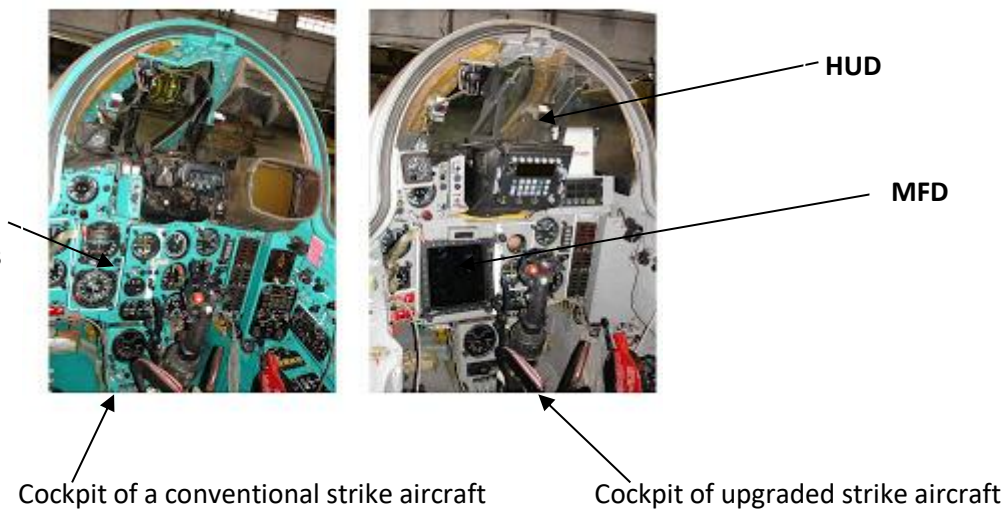


Fig 2.12(a) Cockpit of an old military aircraft & same cockpit after avionics upgrade

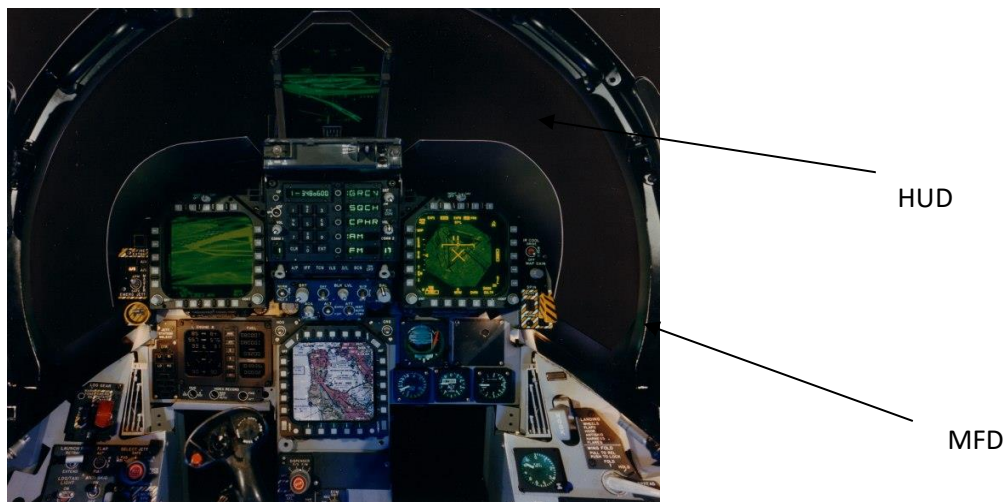


Fig 2.12 (b) Cockpit of a modern fighter aircraft

2.6 Solid State Standby Display Instruments: Till recently, the standby instruments which provide primary flight information to the pilot(s) in the event of loss of the main displays were all electro-mechanical instruments. These were very well proven and reliable instruments having been progressively developed and improved over many years.

The cost of ownership of electro-mechanical instruments, however, is relatively high and is increasing as there is a high skilled labor content in their repair and maintenance, together with the need for high standard clean room facilities. This is because these instruments depend on very low friction precision mechanisms and in the case of gyroscopic instruments there is also inevitable wear and deterioration in the spin axis bearing system. The skilled instrument technicians required to service and repair these instruments are also declining group and are not being replaced by and large as new technology no longer requires their skill. The technology now available has made it possible to produce an all 'solid state' equivalent instrument with a color AMLCD display which is a 'form, fit and function' replacement for the electro-mechanical instrument, or instruments in some cases. The solid state equivalent instrument is packaged in standard instrument case/housing and uses the same electrical connector interfaces. The initial cost of these instruments is competitive with electro-mechanical version, but more importantly they offer a tenfold improvement in reliability and cost of ownership. This is because of the inherent reliability of solid state sensors with no wear or degradation mechanism in their operation. They incorporate very comprehensive built in test and monitoring, and repair is affected by replacing modules and the use of automated testing facilities. Highly skilled instrument technician and clean room facilities are not required. The instruments are also of higher accuracy because of the use of solid state sensors and the ability to apply complex corrections using the embedded micro-processor. Electro-mechanical instruments are limited in the complexity of the corrections which can be made. A recent development is to replace the standby attitude indicator, standby altimeter and standby airspeed indicator with a single solid state integrated standby instrument system. Fig 2.13 illustrates a typical solid state integrated standby instrument system displaying attitude, altitude and airspeed. These integrated standby instrument system comprise of orthogonally mounted solid rate gyros and accelerometers, and color AMLCD display and drive electronics. The microprocessor computes the aircraft attitude from the gyro and accelerometer outputs and altitude and airspeed from the pressure transducer outputs. The system operates from the 28 Volt supply which is supported by the emergency batteries. The integral power conditioning electronics are designed to cope with the variations in battery supply voltage.

2.7 Data Fusion in displays. Data fusion is the name given to the process of combining the data from a number of different sources to provide information which is not present in the individual sources. For example, a synthetic 3D picture can be derived of the terrain in front of the aircraft from an accurate terrain data base and accurate information on the aircraft's position and attitude. The aircraft's position and altitude information are provided by a GPS and an INS. The synthetic picture of the terrain can be overlaid one to one with the outside scene derived from a FLIR sensor and displayed on a HUD or head down display. Ground features which may be hard to detect on the FLIR such as ridge lines can be accentuated together with electricity pylons. This enables the pilot to continue visual flight in conditions of marginal visibility where normally it would be necessary to pull up and fly at a higher altitude. There is research work going on in the development of '3D or 4D' displays or 'path way in the sky'. These displays provide a pictorial presentation of the aircraft's spatial situation and flight path using synthetically generated ground imagery, and exploit data fusion. To generate these pictorial displays is not a problem with the technology now available. There is, however,

a big difference between demonstrating an experimental system and the development of a production system approved by the airworthiness authorities.



Fig 2.13 Solid state integrated standby instruments

The costs involved in achieving certification by the civil airworthiness authorities is a significant sum (as with any airborne system); the software is safety critical and the flight trial to prove the system do not come cheaply.

2.8 Intelligent display Management System. The exploitation of intelligent knowledge based systems (IKBS) technology, frequently referred to as 'expert systems', to assist the pilot in carrying out the mission is the subject of a number of very active research programs, particularly in the United States. The main aim of the program is to reduce the pilot work load in high work load situations in a fighter/strike aircraft. A subset of all the proposed expert systems on an aircraft is an intelligent displays management system to manage the information which is visually presented to the pilot in high work load situations. It is the unexpected or uncontrollable that leads to an excessive work load, examples being:

- Interception by a counter attacking aircraft with very little warning.
- Evasion of ground threat-SAM (surface to air missile).
- Bird strike when flying at low altitude
- Weather aborts or weather diversion emergency.

A block diagram illustrating the concepts of an intelligent displays management system is shown in Figure 2.14. The system comprises an 'aircraft state expert' which deduces 'what is happening' from the aircraft data, pilot input, threat warning systems and the mission plan by the application of an appropriate set of rules. The aircraft state expert

in turn controls the 'display management expert' which determines the information displayed on the various display surfaces e.g. HUD, map, head down displays or HMD according to an appropriate set of goals and priorities.

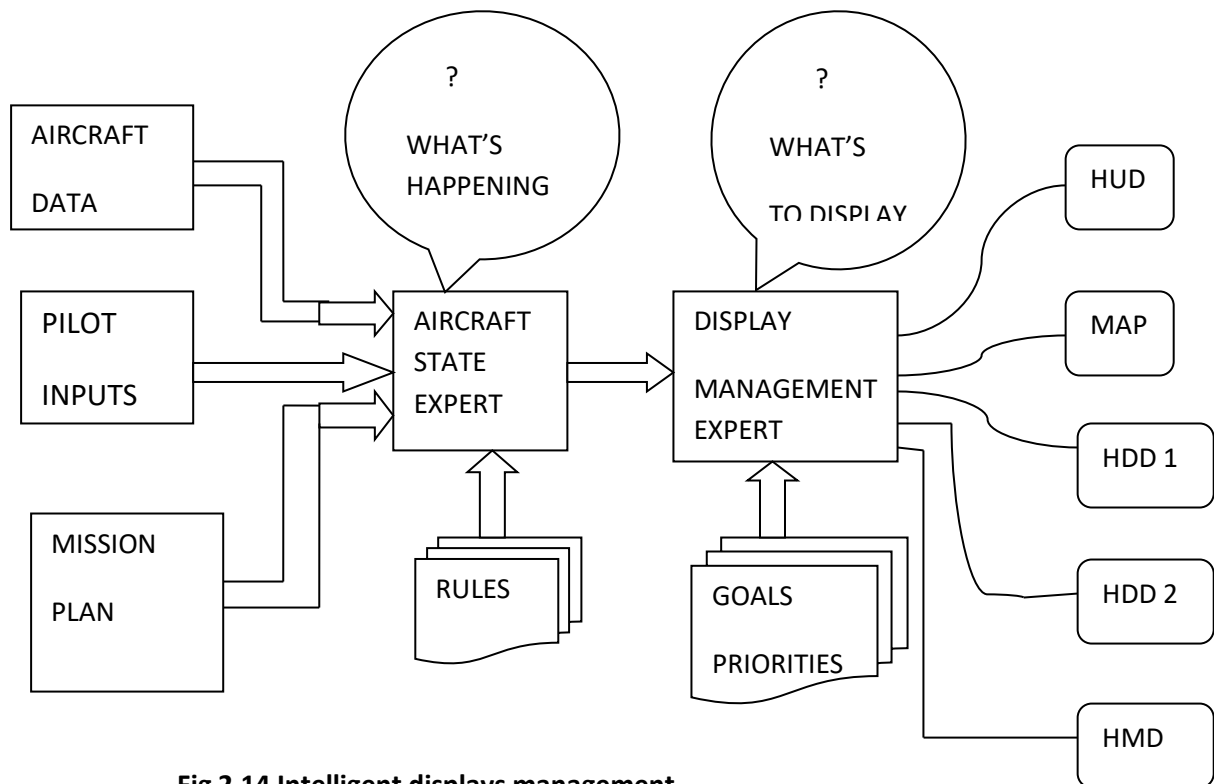


Fig 2.14 Intelligent displays management

2.9 Introduction to Voice and data communication systems.

In aviation, communications between the aircraft and the ground (air traffic/local approach) have historically been by the means of voice communication. More recently, data-link communications have been introduced owing to their higher data rates and in some cases superior operating characteristics. Links are becoming widely used in the HF and VHF bands for basic communications. After selecting the appropriate communications channel selector, the pilot transmits a message by pressing the transmit button which connects the microphone to the appropriate radio. The voice message is used to modulate the carrier frequency, and it is this composite signal that is transmitted. A typical voice signal is shown in Fig 2.15 in the upper part, while the Amplitude Modulated (AM) signal that is transmitted is shown in the lower portion. The receiver demodulates the incoming signal to recover the original voice component. The advantage of this very simple method of transmission is that it is extremely easy to use- all the pilot has to do is speak. A disadvantage of this method is that it occupies a wide bandwidth, typically ≈ 5 kHz, and that speech is not

particularly efficient method of using time and bandwidth compared with data-link applications. The frequency components associated with amplitude modulation are summarized in Fig 2.16. The simple AM case is shown on the left, where it can be seen that the carrier is accompanied by upper and lower sidebands (SBs). The example shows the spectrum that would be produced when a carrier of 2100 kHz (2.1 MHz) is being amplitude modulated by a 1 kHz tone. The three constituent elements are:

- Lower side band (LSB) at (carrier – tone) frequency = $2100 - 1 = 2099$ kHz
- Carrier components at 2100 kHz.
- Upper side band (USB) at (carrier + tone) frequency = $2100 + 1 = 2101$ kHz.

It can be seen that energy is wasted in that power is being transmitted on both side bands and carrier while the effective signal could be decoded from either LSB or USB. Therefore, the technique of Single Side Band (SSB) has been developed which transmits either the upper or lower side band while suppressing the carrier. This SSB operation can yield effectively 8 times more signal power than AM without any power increase at the transmitter. The SSB techniques are used specially in HF communications: the USB is used extensively for aviation, while LSB is used for other services such as amateur radio. The principle of single-sideband LSB and USB operation are shown in the centre and right hand diagrams respectively of Fig 2.16.

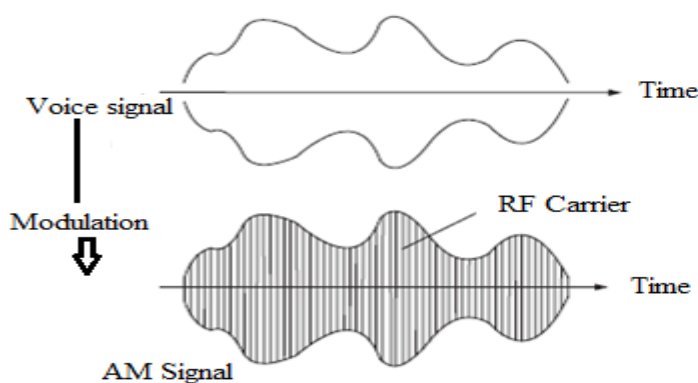


Fig 2.15 Amplitude Modulation

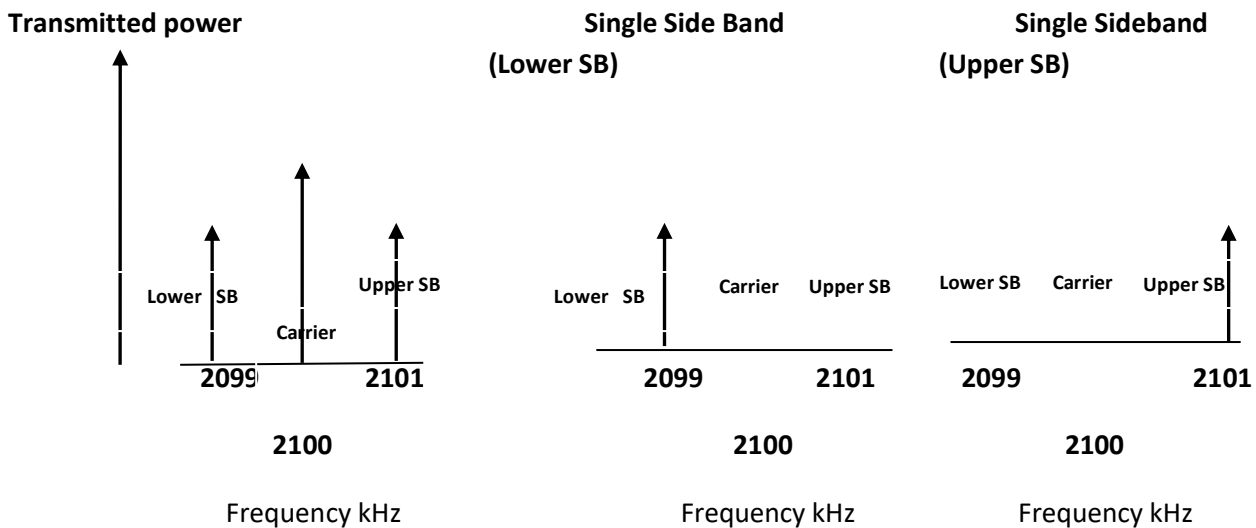


Fig 2.16 Amplitude Modulation and single sideband operation

2.10 HF Communication. High frequency (HF) covers the communication band between 3 and 30 MHz and is very common communication means of land, sea, and air. The utilized band is HF SSB/AM over the frequency range 2.000-29.999 MHz using 1 KHz channel spacing. The primary advantage of HF communication is that this system offers communication beyond the line of sight (LOS). Fig 2.17 shows that there are two main means of propagation, known as sky wave and the ground wave. The sky wave method of propagation relies upon single or multiple-path bounces between the earth and the ionosphere until the signal reaches its intended location. The behavior of the ionosphere is greatly affected by radiation falling on the Earth, notably solar radiation. Times of high sunspot activity are known adversely to affect the ability of the ionosphere as a reflector.

The ground wave method of propagation relies upon the ability of the wave to follow the curvature of the earth until it reaches its intended destination. As for the sky wave, the ground wave may on occasions be adversely affected by atmospheric conditions. Therefore, on occasions HF voice communications may be corrupted and prove unreliable, although HF data links are more resistant to these propagation upsets. HF communications are one of the main methods of communicating over long ranges between air and ground during oceanic and wilderness crossing when there is no line of sight between the aircraft and ground communication stations. For reasons of availability, most long range civil aircraft are equipped with two HF sets, with an increasing tendency also to use HF data link (HF DL) if polar

operations are contemplated. HF Data Link (HFDL) offers an improvement over HF communications owing to the bit encoding inherent in a data link message format which permits the use of error-correcting codes. Furthermore use of more advanced modulation and frequency management techniques allows the data link to perform in propagation conditions where HF voice would be unusable or incomprehensible.

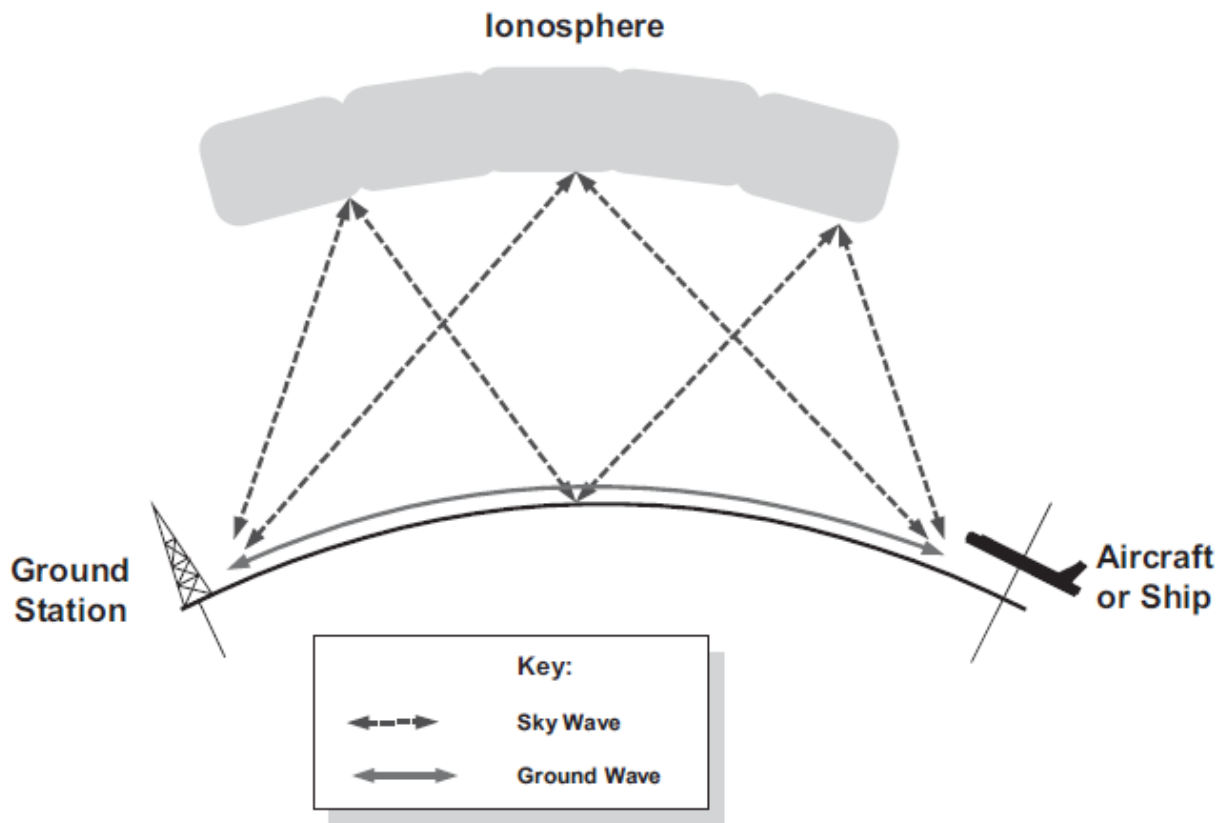


Fig 2.17 HF communication signal propagation

2.11 Very High Frequency (VHF)/Ultra High Frequency (UHF) System. VHF frequency comes under 30-300 MHz and UHF comes under 300 MHz-3000 MHz. VHF voice communication is probably the most heavily used method of communication used by civil aircraft. UHF is mostly used in military aircraft. The VHF band for aeronautical application operates in the frequency range of 118.00-135.975 MHz with channel spacing in recent years of 25 kHz. In recent years, to overcome frequency congestion, and taking advantage of radio technology, channel spacing has been reduced to 8.33 kHz, which permits 3 times more radio channels in the available spectrum. Except in exceptional circumstances VHF/UHF signal will propagate over line of sight. That is, the signal will only be detected by the receiver when it has line of sight or can 'see' the transmitter. VHF/UHF transmissions possess neither of the qualities of HF transmission and accordingly neither sky wave nor ground wave properties apply. This line-of-sight property is affected

by the relative heights of the radio tower and aircraft (see Fig 2.18). The formula that determines the line-of-sight range of VHF/UHF transmission is as follows:

$$R = 1.2 \sqrt{H_t} + 1.2 \sqrt{H_a}$$

Where R is range (nautical miles), H_t is the height of the transmission tower (ft), and H_a is the height of the aircraft (ft). Therefore, for an aircraft flying at 35000 ft, transmission will generally be received by a 100 ft radio tower if the aircraft is within a range of around 235 nautical miles.

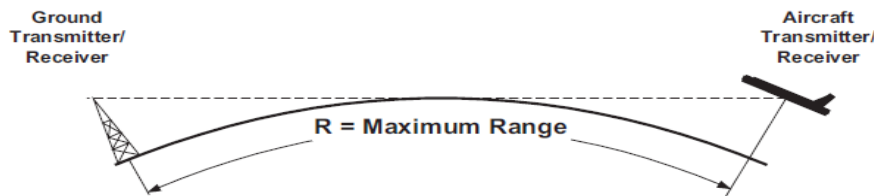


Fig 2.18 VHF/UHF Signal Propagation

2.12 Satellite Communications. System. Satellite communication provides a reliable method of communication using constellation of satellite. Satellite communications, abbreviated to SATCOM, form a useful component of aerospace communications. The principles of operation of STCOM are shown in Fig 2.19. The aircraft communicates via the satellite constellation and remote ground earth station by means of C-band uplinks and downlinks to/from the ground stations and L-band links to/from the aircraft. In this way, communications are routed from the aircraft via the satellite to the ground station and on to the destination. Conversely, communications to the aircraft are routed in the reverse fashion. Therefore, provided the aircraft is within the area of coverage or footprint of a satellite, then communication may be established. The airborne SATCOM terminal transmits on frequencies in the range 1626.5-1660.5 MHz and receives messages on frequencies in the range 1530.0-1559.0 MHz. Upon power-up, the Radio Frequency Unit (RFU) scans a stored set of frequencies and locates the transmission of the appropriate satellite. The aircraft logs onto the ground earth station network so that any ground stations are able to locate the aircraft. Once logged onto the system, communication between the aircraft and any user may begin. The satellite-to-ground C-band uplink/downlink is invisible to the aircraft, as is the remainder of the Earth support network.

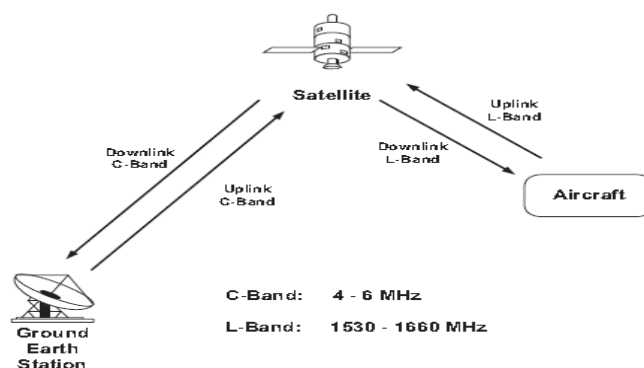


Fig 2.19 Principle of operation of SATCOM

2.13 Flight Data Recorder. All aircraft of a certain size are mandated to carry a flight data recording system, and the requirements for these systems are steadily rigorous. Older Flight Data Recorders (FDRs) recorded various aircraft functions, such as vertical acceleration, heading, airspeed, altitude etc; in analogue form using a stylus and moving oculographic foil medium comprised of steel ally. In modern systems the recording medium is ruggedized to withstand shock, fire, and long-term immersion in seawater using digital solid-state electronic memory. In the US present regulations now dictate that a Digital Flight Data Recorder (DFDR) be used. A Cockpit Voice Recorder (CVR) is used to record crew and ATC conversation using a 'hot mike' located on the flight deck.

The overall system is known as a Digital Flight Data Recording Systems (DFDRS); this comprise the equipment, sensors, wiring, and other installed equipment necessary to perform the function. Where a dedicated sensor has to be installed to provide the DFDR function, then it forms part of DFDRs. Where a sensor is already installed for another purpose, e.g. a lateral accelerometer for automatic flight control, it does not comprise part of the system. The main elements of a DFDRS are:

- DFDR
- Flight Data Acquisition Unit (FDAU). The FDAU has the ability to collect, sample, condition, and digitize analogue signals and provide the data to the DFDR in a digital data stream according to the requirements of ARINC 573. The DFDAU has the ability to receive both analogue parameters and digital data streams and convert them to DFDR digital data format in accordance with ARINC 717.
- Under water Locating Device (ULD) in the form of a sonar locator beacon to aid the location of the unit underwater.

The number of parameters that the DFDRS is required to record has progressively increased in recent years. In essence, all aircraft with provision of carrying ten passengers or more have to a DFDRS fitted.

DFDRs, known colloquially in the media as '**black box recorder**', are actually painted **bright orange** to aid recovery at a crash scene. The reason for increasing the number of recorded parameters was because of the causes of many accidents was not being identified owing to the paucity of data. There is still a problem relating to powering of the DFDRS; when electrical power is lost to part or all of the system, so too are the recorded data, and consideration is being given to alternative electrical power sources to prevent this happening.

2.14 Audio Management System-In-flight Entertainment System.

2.14.1 Audio Management System (AMS). AMS includes those components & subsystems providing air-to-ground, interphone and cabin communications. The system includes the following:

- Audio Integrating System (AIS)
- Communication Radios
- Radio Tuning System

- Cockpit Voice Recorder (CVR)

AIS integrate and manage audio from several audio sources, including crew and service interphone, communication radios & navigation receivers. In addition, the system integrates audio signals, tones & messages from the engine indication & crew alerting system (EICAS) and provides a summation of crew communication to the cockpit voice recorder (CVR). The AIS include the following components

- Audio electronic control unit
- Audio control panel
- Flight compartment speakers
- Microphone & headphones jacks
- Hand held microphones
- Microphone push-to-talk keying switches & External ground interphone jack

Audio electronic control unit is responsible for receiving & processing audio & microphone keying input. The unit integrates with the following

- Ground interphone communications stations
- Communication and navigation aids.
- EICAS & Recording system
- Audio control panel (ACP). ACPs are used to select & control received audio from the communication & navigation systems, as well as to connect audio to the HF/VHF communication radios, and the crew & service interphone. Communication radios include HF and VHF communication trans-receivers. Radio tuning is done primarily using control and display unit (CDU) associated with flight management system (FMS). A block diagram of integrated audio management system in a typical civil aircraft is shown in Fig 2.20.

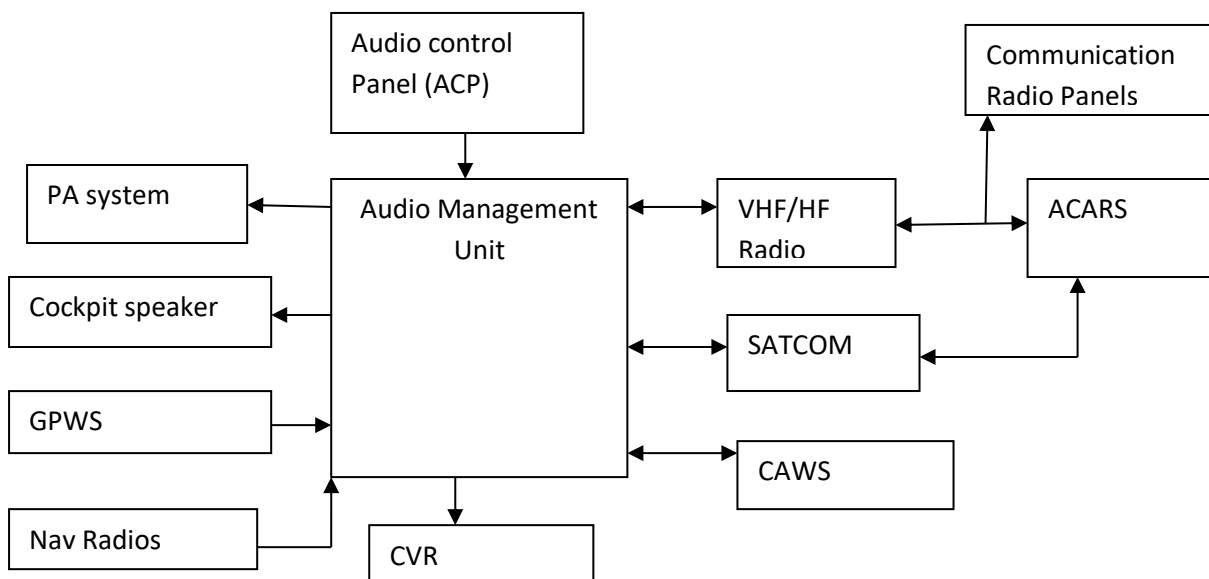


Fig 2.20 Audio Management system

2.14.2 In-flight entertainment (IFE) System. IFE refers to the entertainment available to aircraft passengers during a flight. During the 1990s the demand for better IFE was a major factor in the design of aircraft cabins. Before then, the most a passenger could expect was a movie projected on a screen at the front of a cabin, which could be heard via a headphone socket at his or her seat. Now, in most aircraft, private IFE TV screens are offered on most airlines. Various in-flight entertainment systems are listed below.

(a) Moving-map systems. A moving map system is a real-time flight information video channel broadcast through to cabin project/video screens and personal televisions (PTVs). In addition to displaying a map that illustrates the position and direction of the plane, the system gives the altitude, airspeed, outside air temperature, distance to the destination, distance from the origination point, and local time. The moving-map system information is derived in real time from the aircraft's flight computer systems. This is shown in Fig 2.21.



Fig 2.21 Moving-map System

(b) Audio Entertainment System. Audio entertainment covers music, as well as news, information, and comedy. Most music channels are pre-recorded and feature their own DJs to provide chatter, song introductions, and interviews with artists. In addition, there is sometimes a channel devoted to the plane's radio communications, allowing passengers to listen in on the pilot's in-flight conversations with other planes and ground stations. In audio-video on demand (AVOD) systems, software such as Music-Match is used to select music off the music server. Phillips Music Server is one of the most widely used servers running under Windows Media Center used to control AVOD systems. This form of in-flight entertainment is experienced through headphones that are distributed to the passengers. The headphone plugs are usually only compatible with the audio socket on the passenger's armrest (and vice versa), and some airlines may charge a small fee to obtain a pair. The headphones provided can also be used for the viewing of personal televisions.

(c) Personal Television (PTV). Some airlines have now installed personal televisions (otherwise known as PTVs) for every passenger on most long-haul routes. These televisions are usually located in the seat-backs or tucked away in the armrests for front row seats and first class. Some show direct broadcast satellite television which enables passengers to view live TV broadcasts. Some airlines also offer video games using PTV equipment. Fewer still provide closed captioning for deaf and hard-of-hearing passengers.

(d) In-flight Movies. Personal on-demand videos are stored in an aircraft's main in-flight entertainment system, from whence they can be viewed on demand by a passenger over the aircraft's built-in media server and wireless broadcast system. Along with the on-demand concept comes the ability for the user to pause, rewind, fast forward, or jump to any point in the movie. There are also movies that are shown throughout the aircraft at one time, often on shared overhead screens or a screen in the front of the cabin. More modern aircraft are now allowing Personal Electronic Devices (PED's) to be used to connect to the on-board in-flight entertainment systems.

(e) In-flight games. Video games are another emerging facet of in-flight entertainment. Some game systems are networked to allow interactive playing by multiple passengers. Later generations of IFE games began to shift focus from pure entertainment to learning.

(f) Islamic prayers and directions to Mecca. In several airlines from the Muslim world the AVOD systems provide Qibla directions to allow Muslims to pray toward Mecca. Malaysia Airlines has built-in Qur'an e-books and Garuda Indonesia has a unique Qur'an channel.

(g) Satellite and internal telephony. Some airlines provide satellite telephones integrated into their system. These are either found at strategic locations in the aircraft or integrated into the passenger remote control used for the individual in-flight entertainment. Passengers can use their credit card to make phone calls anywhere on the ground. These systems are usually not capable of receiving incoming calls. There are also some aircraft that allow faxes to be sent and the rate is usually the same as the call rate, but at a per page rate.

(h) Wi-Fi. Several airlines are testing in-cabin wi-fi systems. In-flight internet service is provided either through a satellite network or an air-to-ground network. In the Airbus A380 aircraft, data communication via satellite system allows passengers to connect to live Internet from the individual IFE units or their laptops via the in-flight Wi-Fi access.

2.15 Airborne Communications, Addressing and Reporting System (ACARS).

ACARS is a specific variant of VHF communication operating on 131.5 MHz utilizes a data link rather than the voice transmission. Data link rather than voice transmission is being increasingly used for air-to-ground, and air-to-air communications as higher data rates are being used while at the same time reducing flight crew workload. ACARS is dedicated to down-linking operating data to the airline operational control center. The initial leg is by using VHF communication to an appropriate ground receiver, and thereafter the data may be routed via landlines or microwave links to the airline operations center. At this point it will be allowed access to the internal airline storage and management systems: operational, flight crew, maintenance, etc. Originally, only four basic event parameters were transmitted, OUT-OFF_ON_IN, abbreviated to OOOI:

OUT	Aircraft is clear of the gate and ready to taxi
OFF	Aircraft has lifted off the runway
ON	Aircraft has landed
IN	Aircraft has taxied to the ramp area.

Now, data such as fuel state, aircraft serviceability, arrival and departure time, weather, crew status, and so on are also included in the data message. ACARS was introduced to assist the operational effectiveness of an airline; future data-link application will allow the transfer of more complex data relating to air traffic control routing and flight planning. On-board the aircraft, ACARS introduces a dedicated management unit, control panel, and printer to provide the interface with the flight crew for formatting, dispatching, receiving, and printing messages. This, together with the existing VHF equipment and an interface with the Flight Management System (FMS), forms a typical system as shown in Fig 2.22. All aircraft and air traffic control centers maintain a listening watch on the international distress frequency (121.5 MHz). In addition, military controllers maintain a listening watch on 243.0 MHz on UHF band. These are the international distress frequencies for VHF and UHF band respectively.

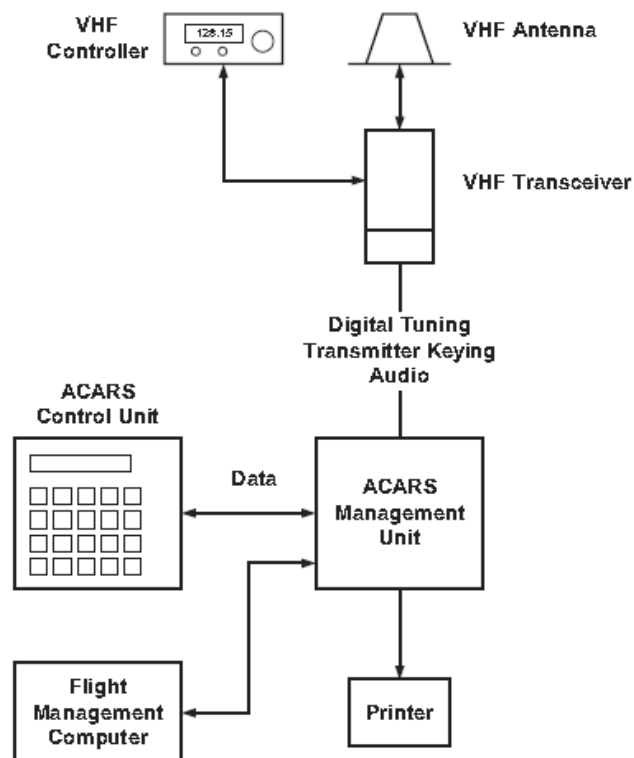


Fig 2.22 Typical ACARS Configuration

UNIT-IV

NAVIGATION, RANGING & LANDING SYSTEMS.

Index

Sl No	Name of the topic	Page no
1	Introduction & Basic Principle of Navigation	65
2	Radio Navigation System	72
3	Inertial Navigation System	74
4	Initial Alignment and Gyro Compassing	87
5	Strap down inertial System	102
6	Attitude Heading Reference	101
7	Instrument Landing Systems	110

Unit-IV Navigation, Ranging and Landing Systems

4.1 Introduction and Basic Principles of navigation.

4.1.1 Introduction. Navigation can be defined as “the act, science or art of directing the movement of a ship or aircraft.”

Navigation thus involves both control of the aircraft’s flight path and guidance for its mission. The measurement of the aircraft’s attitude with respect to the horizontal plane in terms of pitch and bank angles and its heading, that is the direction in which it is pointing in the horizontal plane with respect to North, is essential for both control and guidance. This information is vital for the pilot in order to fly the aircraft safely in all weather conditions, including those when the normal visibility of the horizon and land mark is poor or not available, for example in haze or fog conditions, flying in cloud and night flying. Attitude and heading information is also essential for the key avionics system which enables the crew to carry out the aircraft’s mission. These systems include the autopilot system, navigation system and weapon aiming system. The information is also required for pointing radar beams and infrared sensors.

Accurate knowledge of the aircraft’s position in terms of latitude/longitude co-ordinates, ground speed and track angle, height and vertical speed is also equally essential for the navigation of the aircraft. There is need for accurate and high integrity navigation for civil and military aircraft. For civil aircraft, the density of air traffic on major air routes requires the aircraft in a specified corridor or ‘tube in sky’, these routes being defined by the Air traffic Control authorities. Not only the aircraft follow the defined three-dimensional flight path with high accuracy, but there is also a fourth dimension, namely that of time, as the aircraft’s arrival time must correspond to a specified slot. High accuracy navigation systems are thus essential and form a key part of the flight management system.

For military operations, very accurate navigation systems are essential to enable the aircraft to fly low and take advantage of terrain screening from enemy radar, to avoid known defenses and in particular to enable the target to be acquired in time. The aircraft flies fast and very low so that the pilot cannot see the target until the aircraft is very near to it. There may be then only about six to ten seconds in which to acquire the target, aim and launch the weapon. It is thus necessary to know the aircraft’s position near the target area to within 100 m accuracy. This enables the target sight line to be continuously computed (knowing the target coordinates, including target height, and the aircraft’s height) and a target marker symbol to be displayed on the HUD. This should be near the target and the pilot then slews the marker symbol to exactly overlay the target. This corrects the errors and initializes the weapon aiming process. The use of stand-off weapons which are released several kilometers away from the target also requires an accurate knowledge of the aircraft’s position in order to initiate the mid course inertial guidance system of the missile (the terminal homing phase is achieved with a suitable infrared or microwave radar seeker system. Clearly, the integrity of the navigation system must be very high in both civil and military aircraft as large navigation errors could jeopardize the safety of the aircraft.

4.1.2 Types of Navigation System. There are two basic methods of navigation namely dead reckoning (DR) navigation and position fixing navigation systems. Both systems are used to achieve the necessary integrity.

4.1.2.1 DR Navigation systems: The main types of DR navigation systems are categorized below on the basis of the means used to derive the velocity components of the aircraft. In order of increasing accuracy these are:

(a) Air data-based DR navigation. The basic information used comprises the true air speed TAS(from the air data computer) with wind speed and direction (forecast or estimated) and the aircraft heading from the Attitude Heading Reference System, (AHRS).

(b) Doppler/heading reference systems. These use a Doppler radar velocity sensor system to measure the aircraft's ground speed and drift angle. The aircraft heading is provided by the AHRS.

(c) Inertial Navigation Systems. These derive the aircraft's velocity components by integrating the horizontal components of the aircraft's acceleration with respect to time. These components are computed from the outputs of very high accuracy gyroscopes and accelerometers which measure the aircraft's angular and linear motion.

(d) Doppler inertial navigation systems. These combine the Doppler and INS outputs, generally by means of a Kalman filter, to achieve increased DR navigation accuracy.

The primary DR navigation system which is also the primary source of very accurate attitude and heading information is the Inertial Navigation System (INS). The INS also derive the aircraft's velocity vector in conjunction with the Air Data System which provides barometric height information. This is of great assistance to the pilot when displayed on the HUD. Accurate velocity vector information is also essential for aiming of unguided weapons (guns, bombs and rockets) in military aircraft. The strap-down configuration of the gyros and accelerometers, which is now used in modern systems, enables the INS to provide body angular rates and linear acceleration components for the flight control systems.

A number of manufacturers now provide a combined Air data System and Inertial Reference System as a single unit known as an 'Air Data Inertial Reference System', ADIRS. This has number of advantages such as lower cost, lower weight and occupies less space. Barometric height information is also essential for the vertical inertial channel. Attitude Heading Reference Systems (AHRS) are of lower accuracy than the INS and generally provide a secondary source of attitude and heading information. They use less accurate but lower cost gyros and accelerometers which are insufficiently accurate for Schuler tuning to be effective. A fundamental characteristic of DR navigation systems is that their accuracy is time dependent. For example, a good quality INS has an accuracy of 1 NM/hour so that the aircraft position uncertainty after five hours would be 5 NM.

4.1.2.2 Position fixing system: as mentioned above INS accuracy is time dependent. A position fix system is thus required to constrain the error growth of a DR navigation system and correct the DR position errors. Position fixing navigation systems depend on external references to derive the aircraft's position. For example, radio/radar transmitters on the ground, or in satellites whose orbital positions are precisely known. Unlike DR navigation systems, their errors are not time dependent. The errors are also independent of the aircraft's position in most position fixing systems. The main position fixing systems in current use are briefly summarized below:

(a) Range and Bearing ('R/θ') Radio Navigation Aids. These comprise VOR/DME (VHF Omni Range/Distance Measuring Equipment) and Automatic direction finder (ADF). VOR is an internationally designated short distance radio navigation aid and is an integral part of Air Traffic Control procedures. DME is co-located with VOR and provides the distance from an aircraft to the DME transmitter.

(b) Satellite Navigation System-GPS (Global Position System). GPS is the most important and accurate position fixing system developed to date. It is being used by every type of vehicle-aircraft-ships-land vehicles. Fig 4.1 shows the information flow from the inertial sensor systems, air data system(s) and the position fixing radio navigation systems to the user systems.

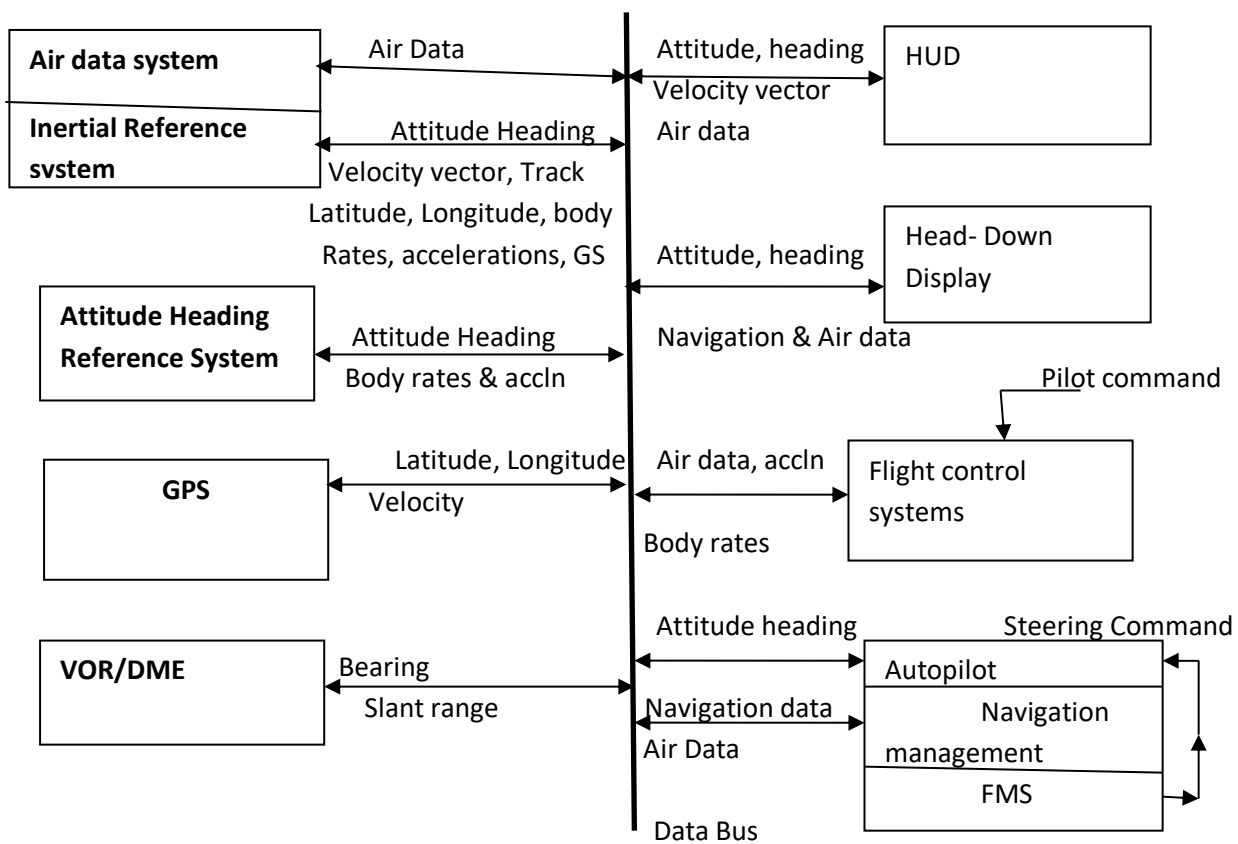


Fig 4.1 Navigation system information flow to user systems

4.1.3 Basic navigation Definitions and principles.

4.1.3.1 Basic Navigation Definitions. Position on the earth's surface is generally specified in terms of latitude and longitude co-ordinates which provide a circular grid over the surface of the Earth.

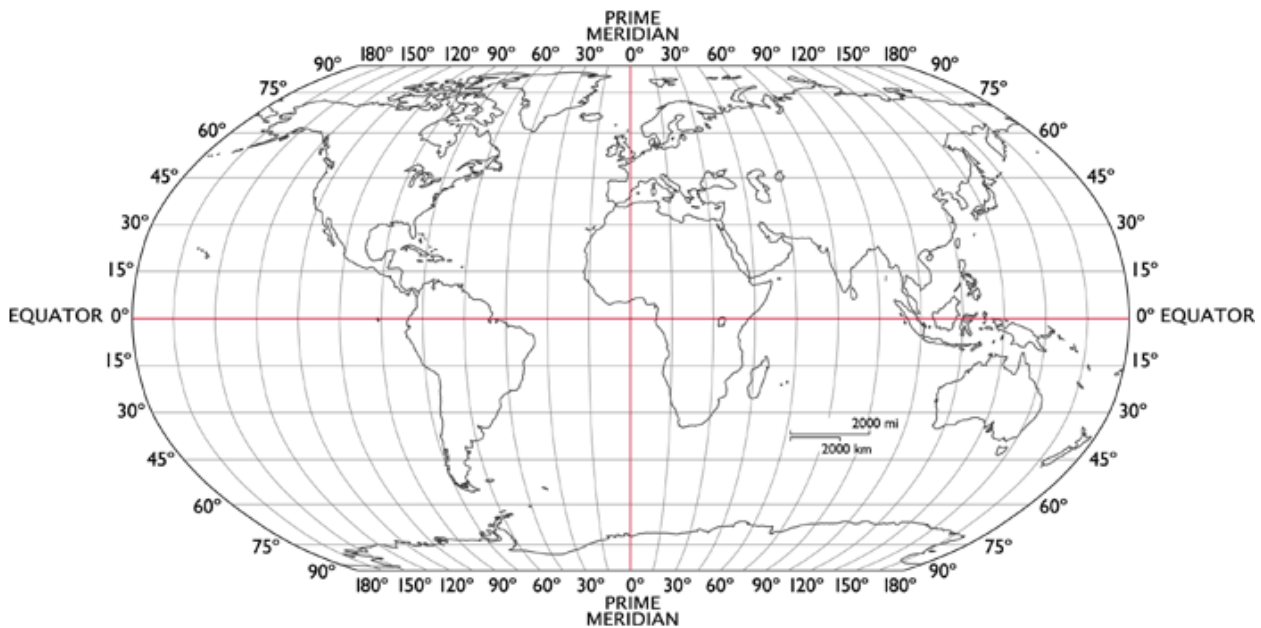


Fig 4.2 Latitude/Longitude co-ordinates

The Earth is basically a sphere-the variation in the radius of the Earth is only about 40 NM in a radius of 3438 NM at the equator, being slightly flattened at the poles. Referring to fig 4.2 and 4.3 latitude and longitude are defined with respect to the polar axis, the equator and the prime meridian. A meridian is a circle round the earth passing through the North and South poles. The prime meridian is the meridian passing through Greenwich which provides the datum for measuring the longitude. The latitude of a point on the earth's surface is the angle subtended at the Earth's centre by the arc along the meridian passing through the point and measured from the equator to the point. The range of latitude angles is from 0° to 90° North and 0° to 90° South. The longitude of a point on the earth's surface is the angle subtended at the earth's centre by the arc along the equator measured East or West of the prime meridian to the meridian passing through the point. The range of longitude angles to cover all points on the Earth's surface is thus 0° to 180° east of the prime meridian and 0° to 180° west of the prime meridian. Latitude and longitude are expressed in degrees, minutes of arc, and seconds of arc. Great circles on the surface of a sphere with centre at the centre of the sphere, that is, the plane of a great circle passes through the Earth's centre. Meridian and the equator are thus great circles. Parallels of latitude which are circles round the Earth parallel to the equator are, however, small circles. The shortest distance between two points on the surface of a sphere is a great circle; hence navigation routes try to follow a great circle path.

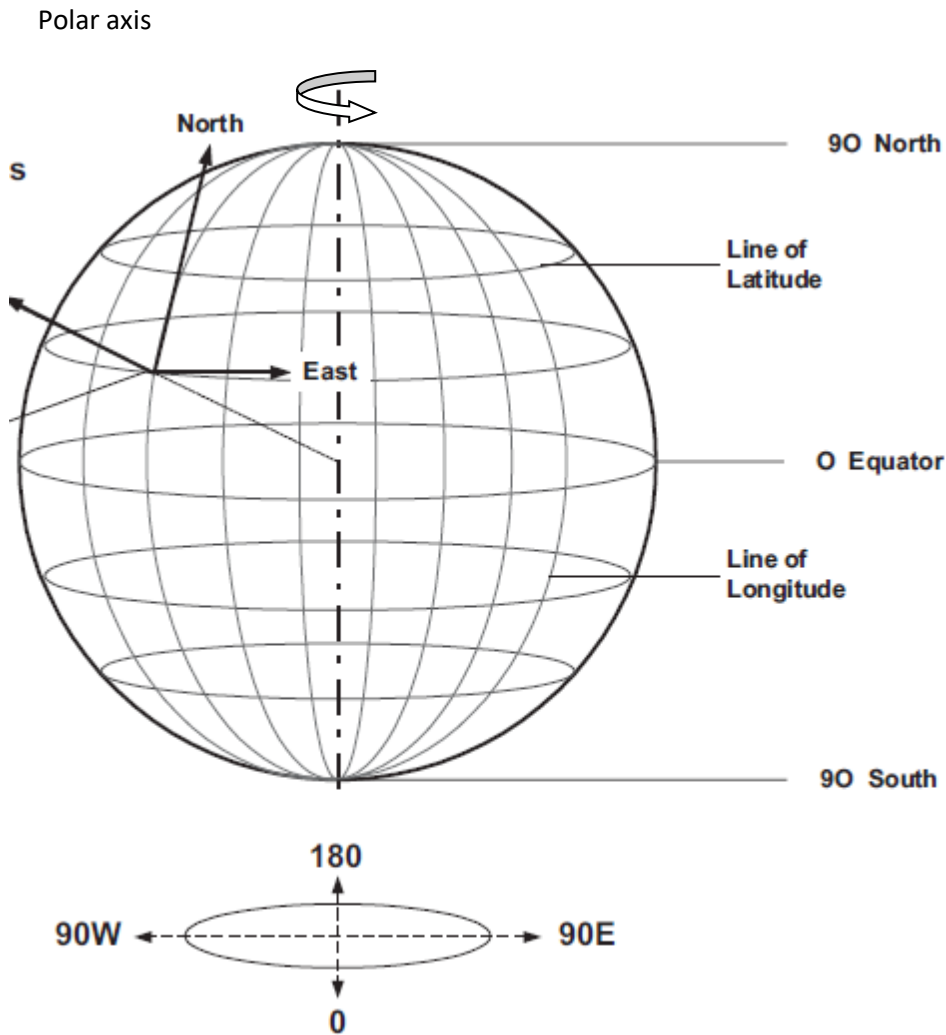


Fig 4.3 Earth referenced co-ordinate system

4.1.3.2 Basic DR Navigation Principles: The basic principles of deriving a DR navigation position estimate are explained below. The following quantities are required:

1. Initial position- latitude/longitude
2. The northerly and easterly velocity components of the aircraft, V_N and V_E .

Referring to fig 4.4 it can be seen that the rate of change of latitude is

$$\dot{\lambda} = \frac{V_N}{R}$$

The rate of change of longitude is

$$\dot{\mu} = \frac{V_E}{R \cos \lambda} \text{ i.e.}$$

$$\dot{\mu} = \frac{V_E}{R} \sec \lambda$$

The change in latitude over time, t , is thus equal to $1/R \int_0^t V_N dt$ and hence the present latitude at time t can be computed given the initial latitude λ_0 . Similarly, the change in longitude is equal to $1/R \int_0^t V_E \sec \lambda dt$ and hence the present longitude can be computed given the initial longitude μ_0 , viz.

$$\lambda = \lambda_0 + \frac{1}{R} \int_0^t V_N dt$$

$$\mu = \mu_0 + \frac{1}{R} \int_0^t V_E \sec \lambda dt$$

It can be seen that a mathematical singularity is approached as λ approaches 90° and $\sec \lambda$ approaches infinity. This method of computing the latitude and longitude of the DR position is hence limited to latitudes below 80° . A different co-ordinate reference frame is used to deal with high latitudes.

The basic computational processes in a DR navigation system using a Doppler/heading reference system are shown in fig 4.5.

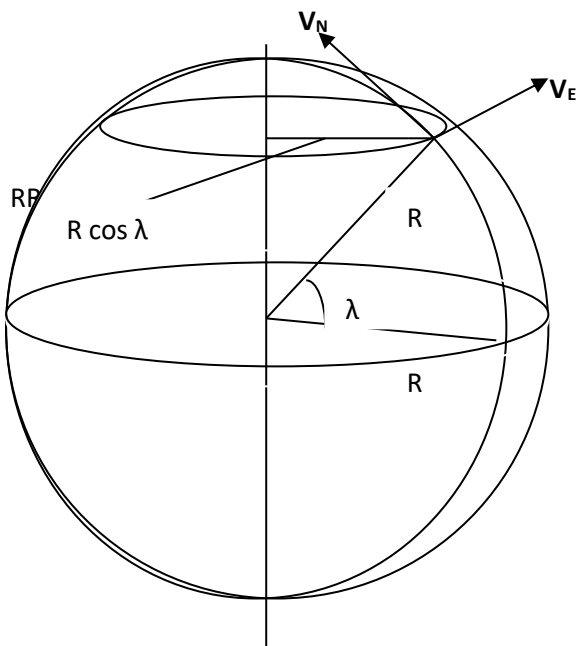


Fig 4.4 Derivation of rates of change of latitude and longitude

In case of a Doppler/heading reference system, the ground speed V_G and drift angle δ are measured directly by the Doppler radar velocity sensor system. The AHRS system provides an accurate measurement of the heading angle, ψ , and hence the track angle, ψ_T can be obtained from

$$\psi_T = \psi + \delta$$

The northerly velocity component of the aircraft, V_N , and the easterly component, V_E , are then derived by resolution of the ground speed vector, V_G .

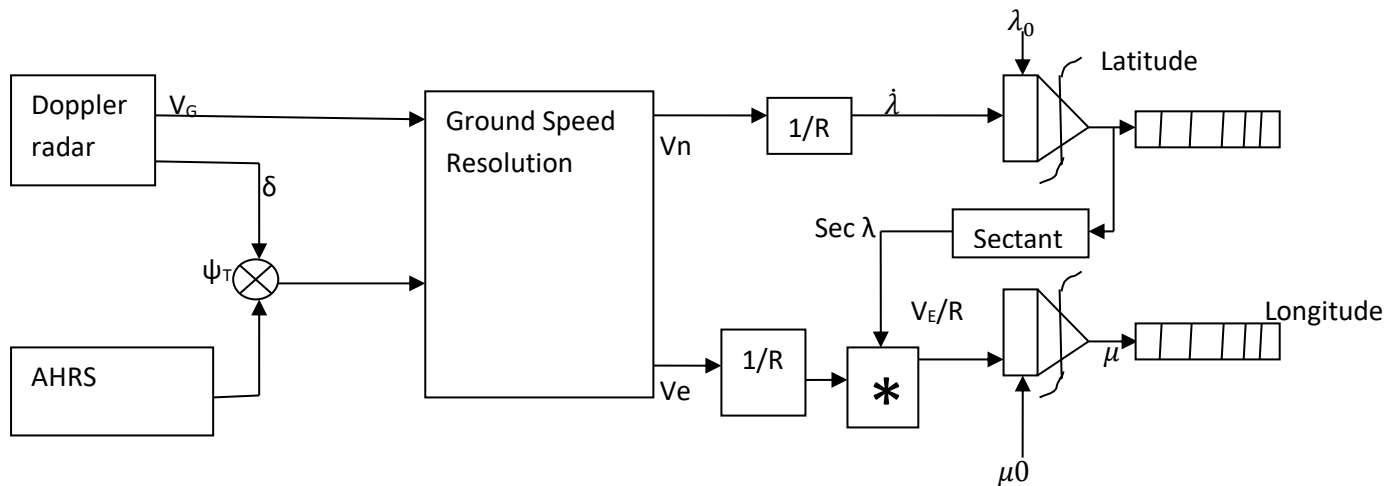


Fig 4.5 Doppler/heading reference DR Navigation system

Hence $V_N = V_G \text{ Cos } \psi_T$

$V_E = V_G \text{ Sin } \psi_T$

In the case of an air data based DR navigation system the northerly and easterly velocity components of the aircraft can be derived as follows:

1. The horizontal velocity component V_H of the true airspeed V_T is obtained by resolving V_T through the aircraft pitch angle θ , viz.

$V_H = V_T \text{ Cos } \theta$

2. The northerly and easterly velocity components of the airspeed are then derived by resolving V_H through the aircraft heading angle ψ , viz.

Northerly airspeed = $V_H \text{ Cos } \psi$

Easterly airspeed = $V_H \text{ Sin } \psi$

3. The forecast (or estimated) wind speed V_w and direction ψ_w is resolved into its northerly and easterly components, viz.

Northerly wind component = $V_w \cos \psi_w$

Easterly wind component = $V_w \sin \psi_w$

4. The northerly and easterly velocity components of the aircraft are then given by:

$$V_N = V_H \cos \psi + V_w \cos \psi_w$$

$$V_E = V_H \sin \psi + V_w \sin \psi_w$$

Such a system provides a reversionary DR navigation system in the absence of Doppler (or an INS) and would generally be used in conjunction with a radio navigation system.

4.2 Radio-navigation Systems. For many years the primary means of navigation over land was by means of radio navigation routes defined by VHF Omni Ranging/Distance measuring Equipment (VOR/DME) beacons as shown in fig 4.5. By arranging the location of these beacons at major navigation or crossing points, and in some cases airfields, it was possible to construct an entire airway network that could be used by the flight crew to define the aircraft flight path from take-off to touch down. Other radio frequency aids include Distance measuring equipment (DME) and Non-Directional Beacons (NDBs).

4.2.1 VHF Omni-range (VOR): The VOR system provides a widely used set of radio beacons operating in the VHF frequency band over the range 108-117.95 MHz with 100 kHz spacing. Each beacon emits a Morse code modulated tone which may be provided to the flight crew for the purpose of beacon identification. The ground station radiates a cardioids pattern that rotates at 30 rev/min, generating a 30 Hz modulation at the aircraft receiver. The ground station also radiates an Omni directional signal which is frequency modulated with a 30 Hz reference tone. The phase difference between the two tones varies directly with the bearing of the aircraft. At the high frequencies at which VHF operates there are no sky wave effects and the system performance is relatively consistent. VOR has the disadvantage that it can be severely disrupted by adverse weather- particularly by electrical storms- and as such it cannot be used as a primary means of navigation for a civil aircraft.

4.2.2 Distance Measuring Equipment. Distance measuring equipment (DME) is a method of pulse ranging used in the 900-1215 MHz band to determine the distance of the aircraft from a designated ground station. The aircraft equipment interrogates a ground based beacon and, upon the receipt of retransmitted pulses (unique to the on-board equipment), is able to determine the range to the DME beacon (see Fig 4.6). DME beacons are able to service requests from a large number of aircraft simultaneously but are generally understood to have capacity to handle about 200 aircraft at once. Specific DME accuracy is 3% or 0.5 nm, whichever is the greater. VOR/DME is organized such that aircraft can navigate the airways by having combination of VOR bearing to and DME distance to run to the next beacon in the airway route structure.

4.2.3 Automatic Direction Finders. Automatic direction Finding (ADF) involves the use of a loop direction finding technique to establish the bearing to a radiating source. This might be to a VHF beacon or a Non-Directional Beacon (NDB) operating in the 200-1600 kHz band. NDBs in particular are the most prolific and widely spread beacons in use today.

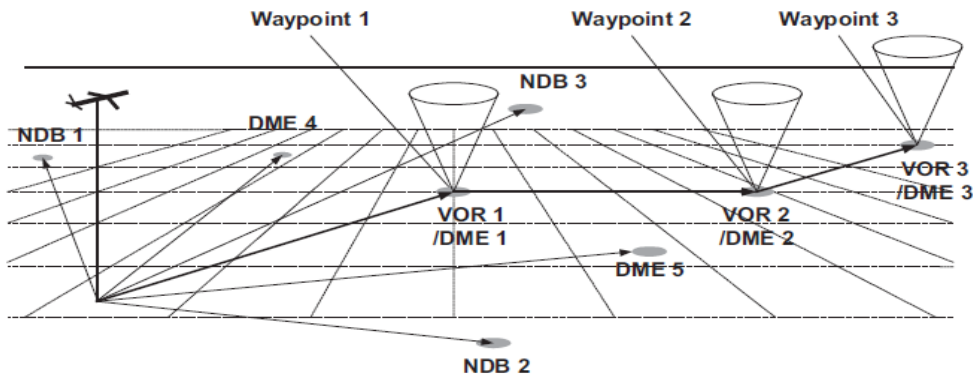


Fig 4.5 Radio Navigation using VOR/DME and ADF

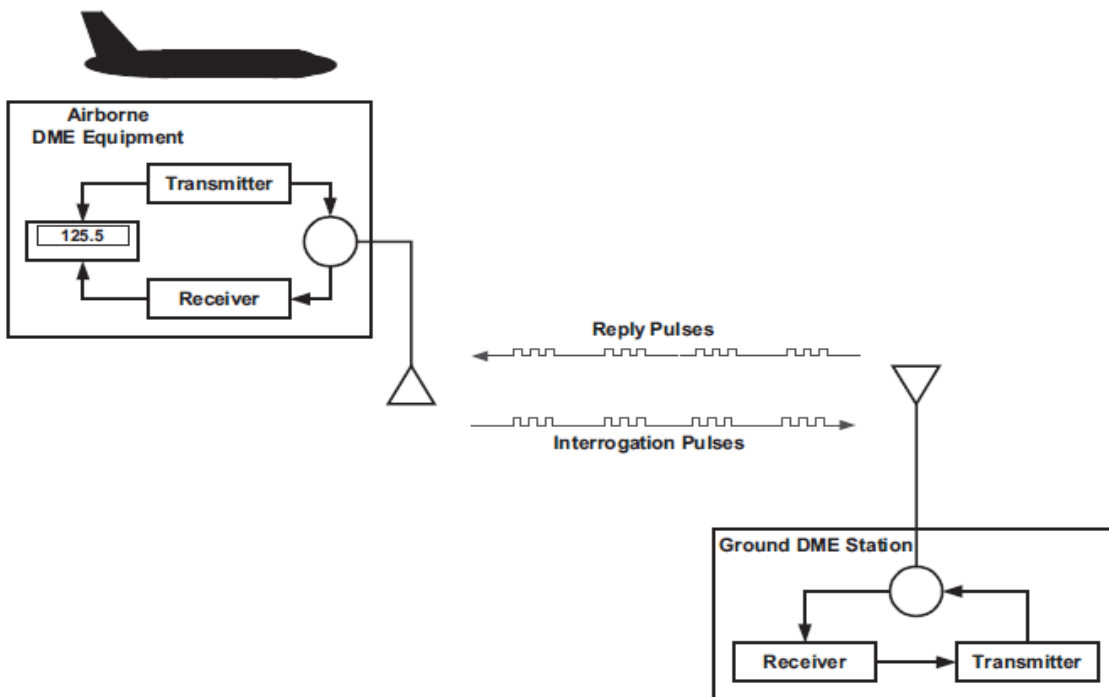


Fig 4.6 DME Principle of operation

The aircraft ADF system comprises integral sense and loop antennae which establish the bearing of the NDB station to which the ADF receiver is tuned. The bearing is shown on the Radio Magnetic Indicator (RMI) or Electronic Flight Instrument System (EFIS) as appropriate. A typical RMI display is shown in fig 4.7.

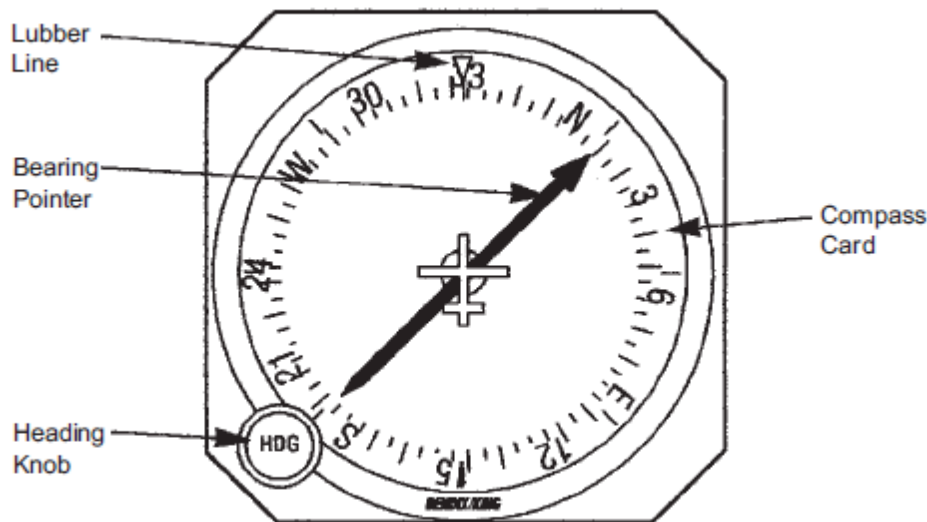


Fig 4.7 Typical Radio Magnetic Indicator

4.3 Inertial Navigation Systems:

4.3.1 Introduction. The attributes of an ideal navigation and guidance system for military applications can be summarized as follows:

- High accuracy
- Self-contained
- Autonomous-does not depend on other system
- Passive-does not radiate
- Un-jammable
- Does not require reference to the ground or outside world.

It was concluded during early 1950s that only system which could meet these requirements was inertial navigation system. INS was developed initially for navigation and guidance of ballistic missiles, strategic bombers, ships and submarines. Huge research and development programs have been carried out worldwide involving many billions of dollars expenditure to achieve viable system. Precession accelerometers had to be developed with bias uncertainties of less than 50 μg . The major task of achieving the required computational accuracies had to be solved and in fact the

first digital computers operating in real time were developed for IN systems. Once these problems had been solved, the INS can provide:

- Accurate position in whatever coordinates are required- e.g. latitude/longitude, etc.
- Ground speed and track angle.
- Euler angles: heading, pitch and roll to very high accuracy.
- Aircraft velocity vector (in conjunction with the air data system).

Accurate velocity vector information together with an accurate vertical reference are essential for accurate weapon aiming and this has led to the INS being installed in military strike aircraft from the early 1960s onwards as a key element of the navigation/weapon aiming system.

The self-contained characteristics of an inertial navigation system plus the ability to provide a very accurate attitude and heading reference led to the installation of IN systems in long range civil transport aircraft from the late 1960s. They are now very widely used in all types of civil aircraft.

4.3.2 Basic Principles and Schuler Tuning of INS. The INS can measure the motion of a vehicle and derive the distance it has travelled without reference to the outside world. It does this by sensing the vehicle's acceleration (and also the gravitational vector) with accelerometers. If the vehicle's acceleration components can then be derived along a precisely known set of axes, successive integration of the acceleration components with respect to time will yield the velocities and distances travelled along the axes. This is true provided the initial conditions are known, that is, the vehicle velocity and position at the start time. Fig 4.8 illustrates the basic concepts of deriving the velocity and distance travelled of the vehicle from its acceleration components.

Put like this it seems very simple. Any errors, however, in deriving the aircraft acceleration components from the accelerometer outputs will be integrated with time, producing velocity errors which in turn are integrated with time generating position errors.

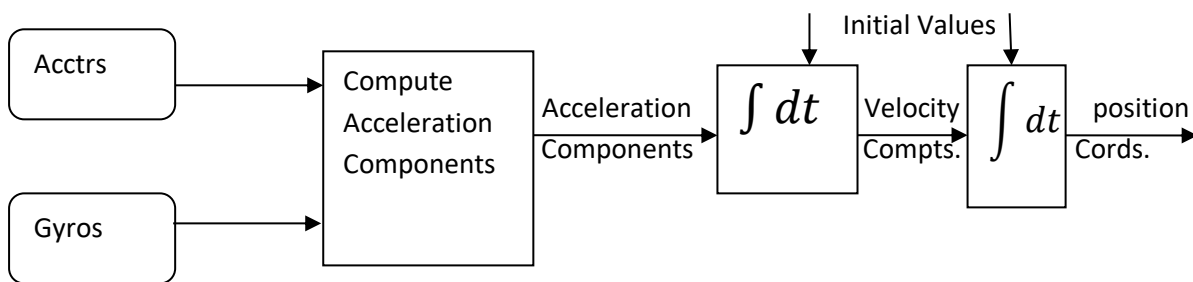


Fig 4.8 Basic principle of inertial navigation

For example, a constant accelerometer bias error, B (which can be equated to an initial tilt error), will result in a distance error which is equal to $\iint B dt dt$, that is $Bt^2/2$. The resulting distance error is thus proportional to the square

of the elapsed time. An accelerometer bias error of $10^{-3}g$ will produce a distance error of 0.45 km after 5 minutes and 1.8 km after 10 minutes, for example.

Errors in deriving the orientation of the accelerometer input axes with respect to the local vertical, that is tilt errors, introduce gravitational acceleration errors in the acceleration measurements. Refer to Fig 4.9. A tilt error, $\Delta\theta$, produces a gravitational error equal to $g \Delta\theta$ ($\Delta\theta$ is small angle). A constant gyro drift rate, W , will cause the tilt error, $\Delta\theta$, to increase linearly with time ($\Delta\theta = W t$) resulting in a gravitational acceleration error $g W t$. This results in a distance error $\iint g W t dt dt$, that is, $g W t^3/6$. The distance error in this case is proportional to the cube of the time. For example, a gyro drift rate of $1^\circ/\text{hour}$ results in a positional error of 0.2 km after 5 minutes and 1.6 km after 1.6 km after 10 minutes. Clearly such types of error propagation are unacceptable except in applications where time of flight is short (e.g., mid- course guidance of short range missiles) or where the system could be frequently corrected by another navigation system. It will be shown that Schuler tuning provides an un-damped closed-loop corrective action to constrain the system tilt errors so that they oscillate about a zero value with an 84.4 minutes period. The 'INS vertical' follows the local vertical irrespective of the vehicle accelerations so that system behaves like a Schuler pendulum. Schuler tuning completely changes the error propagation characteristics from those just described and enables a viable unaided navigation system to be achieved. It is vital and fundamental ingredient of any IN system.

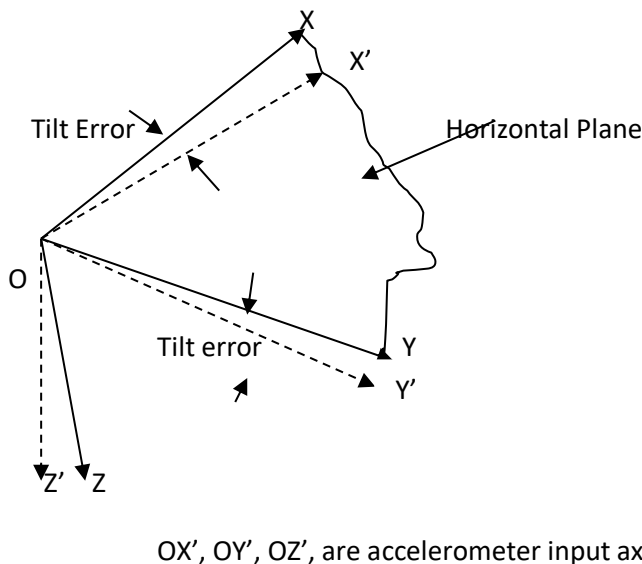


Fig 4.9 Tilt errors

The concept of a pendulum which would be unaffected by accelerations, and would always define the local vertical was originated by the Austrian physicist Max Schuler in 1924. Schuler conceived the idea of a pendulum which would be unaffected by acceleration by considering the behavior of a simple pendulum whose length was equal to the radius of the Earth (see Fig 4.10). The 'plumb bob' of such a pendulum would always be at the Earth's centre and would hence define the local vertical irrespective of the motion, or acceleration, of the point of suspension of the pendulum- any

disturbance to the pendulum bob would cause it to oscillate about the vertical with a period equal to $2\pi\sqrt{\frac{R}{g}}$, where R is the radius of the Earth, g is the gravitational acceleration. Using the accepted values of R and g gives the time period of the Earth radius pendulum (or Schuler pendulum) as 84.4 minutes. A simple pendulum of length equal to the Earth's radius is obviously not feasible. If, however, a pendulous system could be produced with an exact period of 84.4 minutes then it would indicate the local vertical irrespective of the acceleration of the vehicle carrying it. In 1924, the technology was not available to implement a practical system and in fact it was not until the early 1950s that technology became available to implement a practical Schuler tuned IN system. The first successful airborne demonstration of a Schuler tuned navigation system was achieved by Dr. Charles Stark Draper and his team at Massachusetts Institute of Technology (MIT) Boston, USA, around 1952.

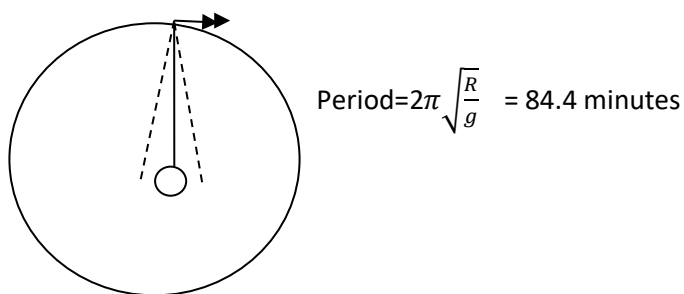


Fig 4.10 Schuler or Earth radius pendulum

The basic principle of any IN system are to derive the components of the aircraft's acceleration along locally level axes, generally the North and east axes, using an orthogonal set of accelerometers and gyros to measure the aircraft's motion. Integration with respect to time of these acceleration components then gives the aircraft's North and East velocity components, knowing the initial conditions. The aircraft's position in terms of its latitude and longitude coordinates can then be determined. It is essential that the system is Schuler tuned to bound the tilt angle errors in deriving the local level plane. The Schuler tuned stable platform was the only viable way of accurately deriving the North and East components of the aircraft's acceleration from the early 1950s to late 1970s. This is because of limitations in angular momentum gyro technology. RLG of inertial accuracy achieved production status in the late 1970s and enabled a strap-down IN system to be implemented. The implementation of a Schuler tuned strap-down INS and a stable platform INS are mathematically identical. The Schuler tuned strap-down INS can thus best be explained and visualized by considering the system to have a mathematical model of a stable platform, that is a virtual stable platform, within the system computer. Fig 4.11 is a block diagram of a Schuler tuned strap-down IN system. The virtual accelerometer outputs are derived from the body mounted accelerometer outputs by the axes transformation processes explained in Unit-III. Their outputs are the same as real accelerometers would have, when mounted on a real stable platform.

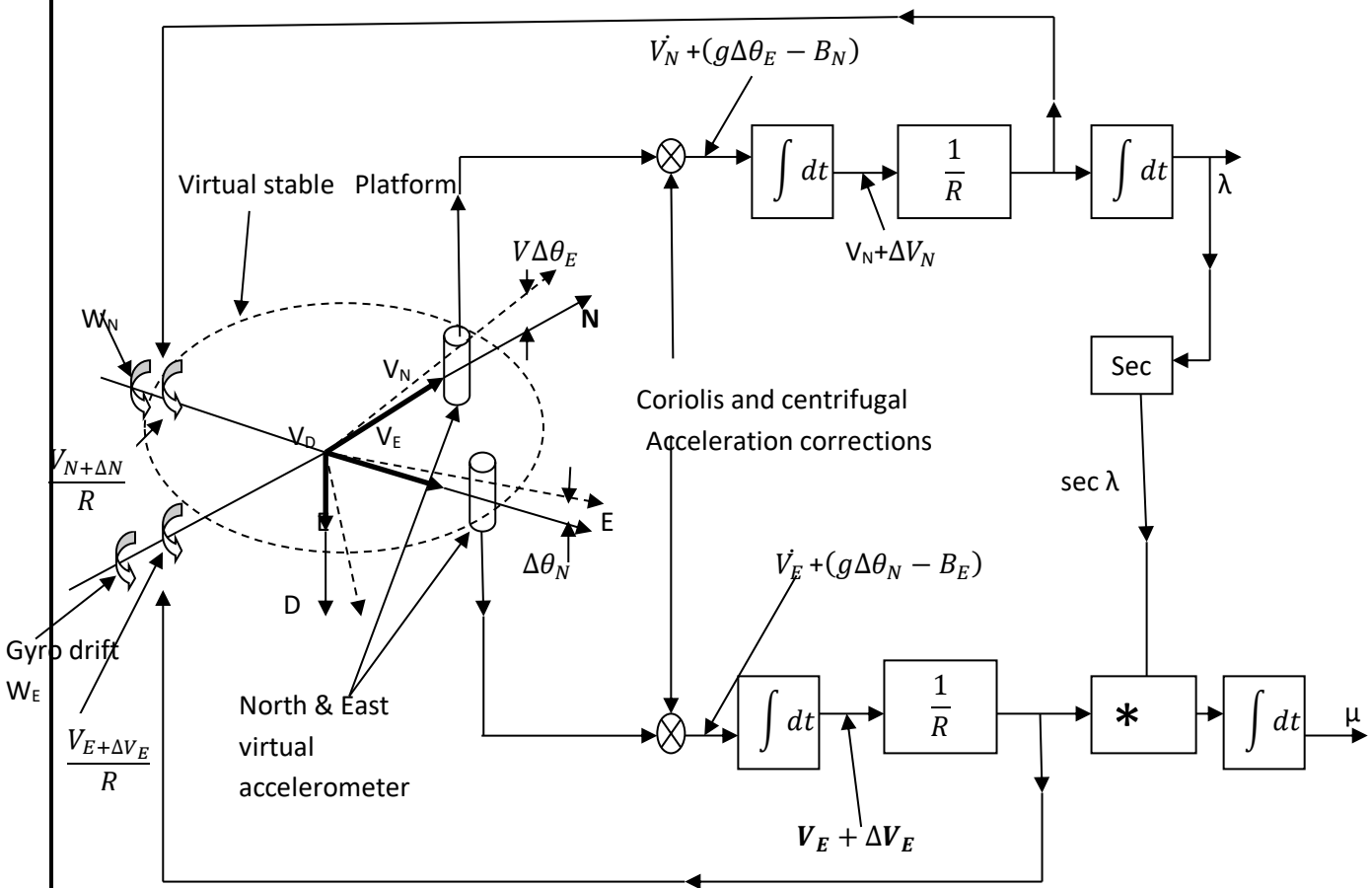


Fig 4.11 Schuler tuned strap-down INS

(Note: The Earth rotation rates about the North and East axes are left out for clarity)

The North and East accelerometers outputs, however, are sensed along North, East, Down (N, E, D), axes which are rotating slowly in space with the Earth's rotation. These axes rotations introduce Coriolis acceleration components. The aircraft also experiences small centrifugal acceleration components as it follows the Earth's curvature. The Coriolis and centrifugal accelerations components are small, $< 0.05 \text{ m/s}^2$, but nevertheless need to be computed, and the real, or virtual, accelerometer outputs corrected before integrating with respect to time to obtain the aircraft's North and East velocity components.

The virtual platform is very accurately aligned with the local NED axes during the initial alignment and gyro compassing phase. Thereafter, it is rotated at the appropriate Earth's rotation rate components and the appropriate vehicle rate components so as to maintain alignment with the local NED axes.

The vehicle rate components are derived by integrating the corrected North and East accelerometer outputs with respect to time, and this inertial derived vehicle rate feedback provides the Schuler pendulum characteristic. The local value of the Earth's radius, R , is used together with the local value of the gravitational constant, g , to achieve accurate Schuler tuning. (The Schuler period is equal to $2\pi\sqrt{\frac{R}{g}}$)

Errors in the derivation of the vehicle rate terms will result in the platform tilting from the horizontal. These errors result from:

1. Accelerometer bias errors which result in bias error, B_N and B_E , in the North and East acceleration component derived from the strap-down accelerometers.
2. Gyro drift rates which introduce a direct error in the applied vehicle rates about the North and East axes of W_N and W_E , and have a major effect on the system accuracy.

These errors in turn produce tilt angle errors, $\Delta\theta_N$ and $\Delta\theta_E$, about the North and East axes. These introduce gravitational acceleration components, $g\Delta\theta_N$ and $g\Delta\theta_E$, into the derived acceleration along the East and North axes.

The resulting velocity errors, ΔV_E and ΔV_N , along the East and North axes are given by

$$\Delta V_E = \int (g\Delta\theta_N - B_E) dt \quad (1)$$

$$\Delta V_N = \int (g\Delta\theta_E - B_N) dt \quad (2)$$

These velocity errors result in vehicle rate errors $\Delta V_E/R$ and $\Delta V_N/R$ about the North and East axes. The sense of the vehicle rate errors in the Schuler loop is such as to slow down or speed up the applied vehicle rate to try to restore $\Delta\theta_N$ and $\Delta\theta_E$ to zero. In fact, due to the two integration taking place in the loop, the system will oscillate about the local vertical, as will be shown mathematically.

The rate of tilt about the North axis is equal to $(\Delta V_E/R + W_N)$. Hence

$$\Delta\dot{\theta}_N = -\frac{1}{R} \int (g\Delta\theta_N - B_E) dt + W_N$$

(The minus sign in the $\Delta V_E/R$ term is because the feedback is negative.) Whence

$$\Delta\theta_N = -\frac{1}{R} \iint (g\Delta\theta_N - B_E) dt dt + \int W_N dt \quad (3)$$

Differentiating twice and re-arranging gives

$$(D^2 + \frac{g}{R}) \Delta\theta_N = \frac{B_E}{R} + DW_N \quad (4)$$

A similar equation for $\Delta\theta_E$ can be obtained with the forcing function being B_N and W_E . It is convenient to drop the suffices N and E in the above equations so that the solution can be applied to either axis.

$$\left(D^2 + \frac{g}{R}\right) \Delta\theta = \frac{B}{R} + DW \quad (5)$$

The local vertical closed-loop tracking system produced by Schuler tuning is shown in the block diagram in Fig 4.12 and provides an error propagation model of an INS.

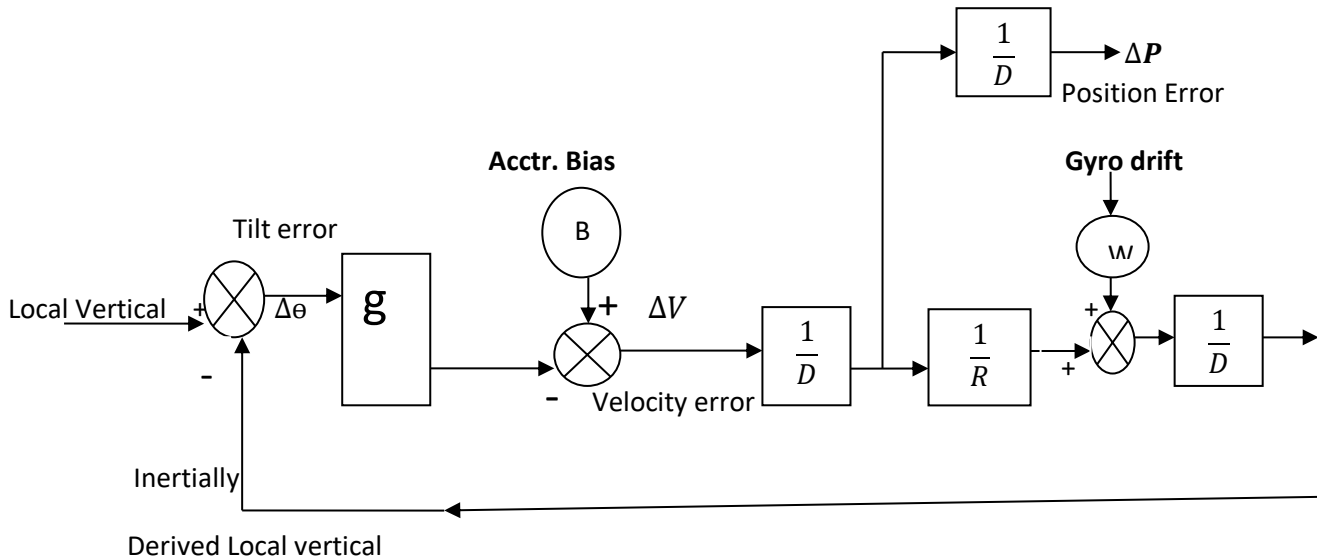


Fig 4.12 Schuler tuned INS error model

The effects of accelerometer bias and gyro drift are considered separately for the sake of simplicity. The effects on the system of a combination of disturbing inputs of accelerometer bias and gyro drift can then be inferred.

(1) Effect of accelerometer Bias.

Assume $W = 0$. The accelerometer bias can be equated to an initial tilt = B/g radians. The solution of equation (5) for initial conditions

$$\Delta\theta(0) = B/g \text{ and } \Delta\dot{\theta}(0) = 0; \text{ hence}$$

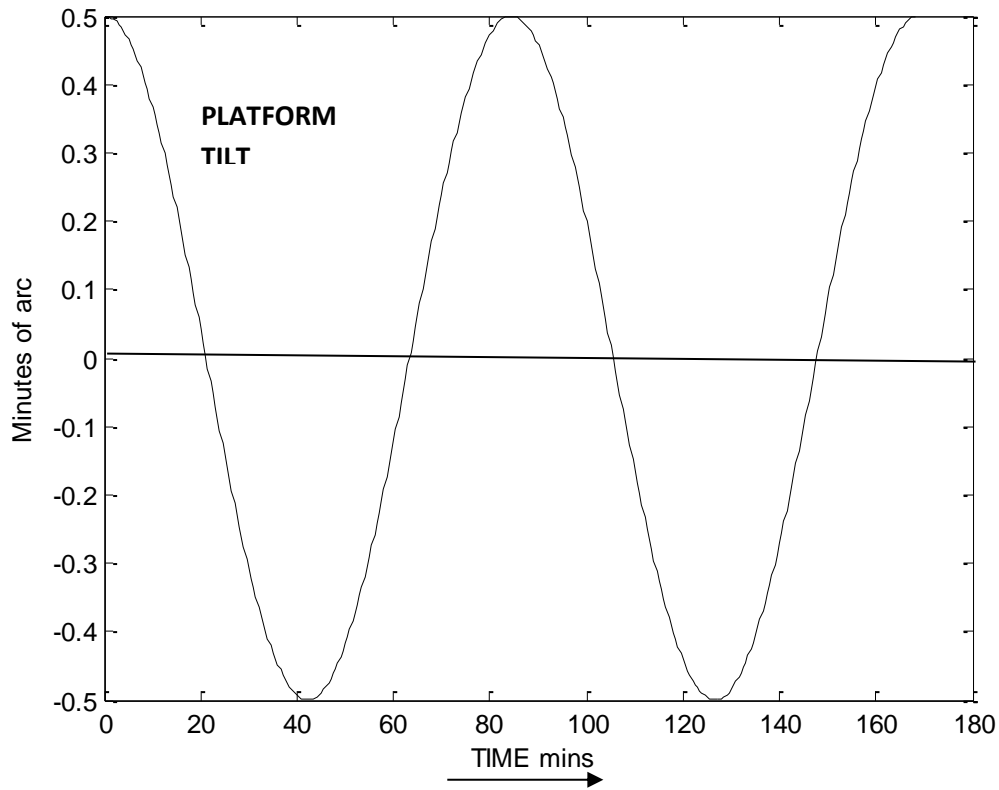
$$\Delta\theta = (B/g) \cos \omega_0 t$$

Where $\omega_0 = \sqrt{g/R}$ is the un-damped natural frequency of Schuler loop. The platform thus oscillates about the local vertical with amplitude B/g and a period is $2\pi\sqrt{R/g} = 84.4$ minutes. The acceleration error is $g\Delta\theta$, the velocity error is $\int B \cos \omega_0 t dt$, and the distance error is $\iint B \cos \omega_0 t dt dt$. Hence

$$\text{Distance error} = \frac{B}{\omega_0^2} (1 - \cos \omega_0 t)$$

Fig 4.13 shows the effect of an accelerometer bias error equivalent to an initial tilt of one half minute of arc ($1.45 \times 10^{-4} g$). This results an oscillatory error between zero and one nautical mile.

(2) Effect of gyro drift: Assume $B=0$ and gyro drift rate, W , is constant. The solution of equation (5) for initial conditions



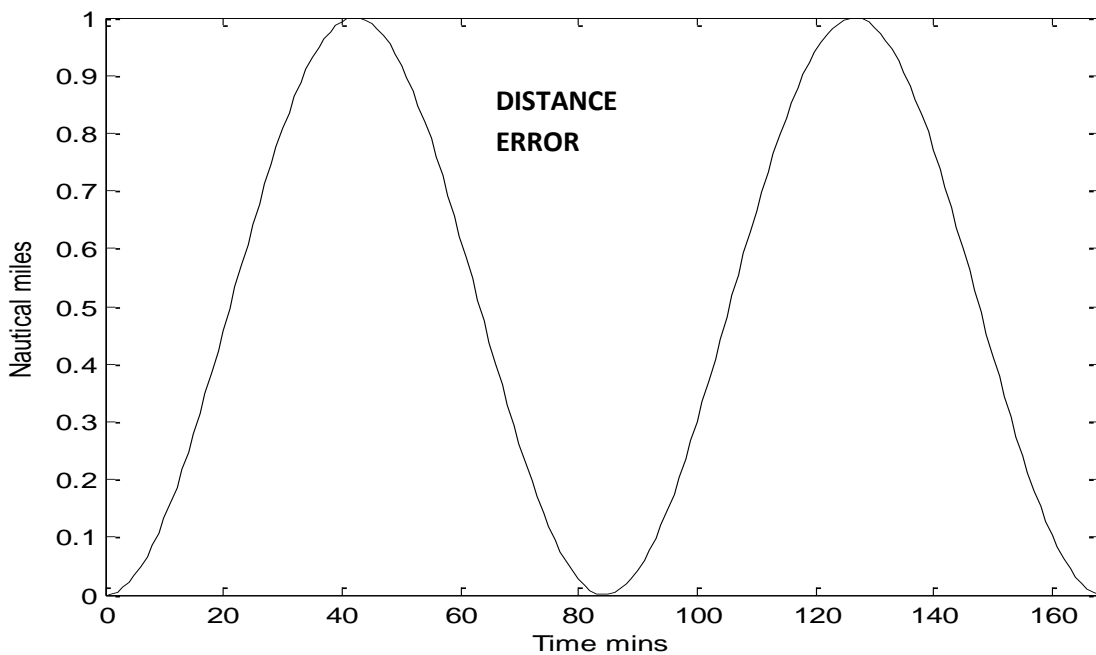


Fig 4.13 Error Propagation due to accelerometer bias of half minute of arc

$\Delta \theta (0) = 0$ and $\Delta \dot{\theta} (0) = W$; Hence

$$\Delta \theta = (W / \omega_0) \sin \omega_0 t$$

The platform thus oscillates about the vertical as before with 84.4 minute period. A gyro drift rate of 0.01 deg/hour results in a very small amplitude oscillation about the local vertical of 0.14 minutes of arc. The velocity error is

$$\int \frac{gW}{\omega_0} \sin \omega_0 t \, dt = WR (1 - \cos \omega_0 t)$$

The velocity error thus oscillates between zero and 2WR.

The distance error is

$$\int WR (1 - \cos \omega_0 t) \, dt = WR (t - \frac{1}{\omega_0} \sin \omega_0 t)$$

The distance error is thus proportional to the time of flight, the small amplitude oscillatory component being swamped after a while.

A constant gyro drift rate of 0.01 Deg/hour (0.6 minutes of arc per hour) will give an average velocity error of 0.6 knot, that is, a distance error which builds up at a rate of 0.6 NM/hour. It should be noted that this represents the error build up along the North and East axes, so that the radial error will be multiplied by $\sqrt{2}$ and hence will be equal to 1

NM/hour. Fig 4.14 illustrates the error growth for a constant gyro of 0.01 Deg/hour. The very accurate vertical reference provided by Schuler tuning can be seen-even a gyro drift as 0.25 deg/hour results in a peak vertical error of only 3.5 minutes of arc.

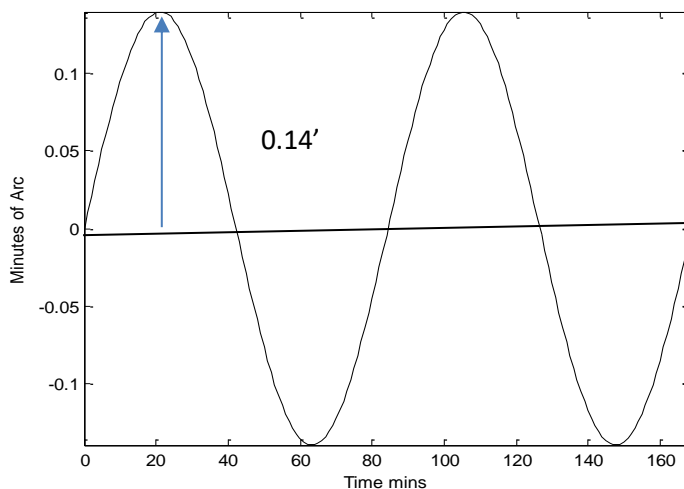
4.3.3 Physical Explanation of Schuler Tuning. A physical explanation of Schuler tuning is explained below, as it is important to have a physical appreciation, as well as a mathematical understanding. Referring to Fig 4.15, suppose that the platform is being rotated at the same rate as the local vertical, but is tilted downwards from the local vertical by small angle, $\Delta \theta$.

At $t = 0$ the platform tilt results in the accelerometer as well as the true acceleration. (Accelerometer input axis tilted downwards results in a negative gravitational acceleration component being measured, as the accelerometer proof mass tends to move in the same direction as when the vehicle is being retarded, i.e., negative acceleration.)

$t = 0$ to 21 minutes. As the aircraft flies over the Earth the negative acceleration error resulting from the platform tilt is integrated with time and causes the computed vehicle rate to become slower than the true vehicle rate. The platform is thus being rotated at a progressively slower rate than the local vertical thereby reducing the tilt error.

At $t = 21$ minutes, the tilt error is zero but the platform is still being rotated at a slower rate than the local vertical so that the platform then starts to tilt the other way (i.e., upwards) after 21 minutes.

$t = 21$ to 42 minutes, the accelerometer error due to platform tilt is now positive so that the platform rate of rotation starts to increase.



PLATFORM TILT

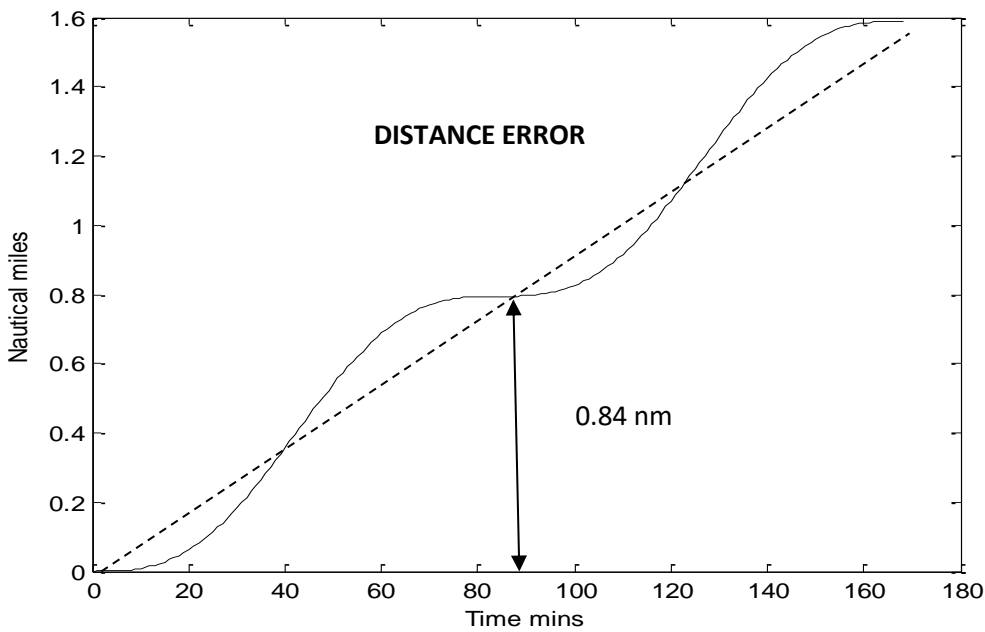


Fig 4.14 Error propagation due to gyro drift of $0.01^\circ/\text{hour}$

At $t = 42$ minutes, the platform is now rotating at the same rate as the local vertical.

$t = 42$ to 63 minutes, after 42 minutes the platform 'vertical' is now starting to rotate at a faster rate than the true vertical and by 63 minutes the platform tilt is zero again. However, the platform is now being rotated at a faster rate than the local vertical. $t = 63$ to 84 minutes, the tilt has changed sign so that the platform rate of rotation now starts to slow down until 84 minutes it is rotating at the same rate as the local vertical. The whole cycle is repeated over the next 84 minutes and so on.

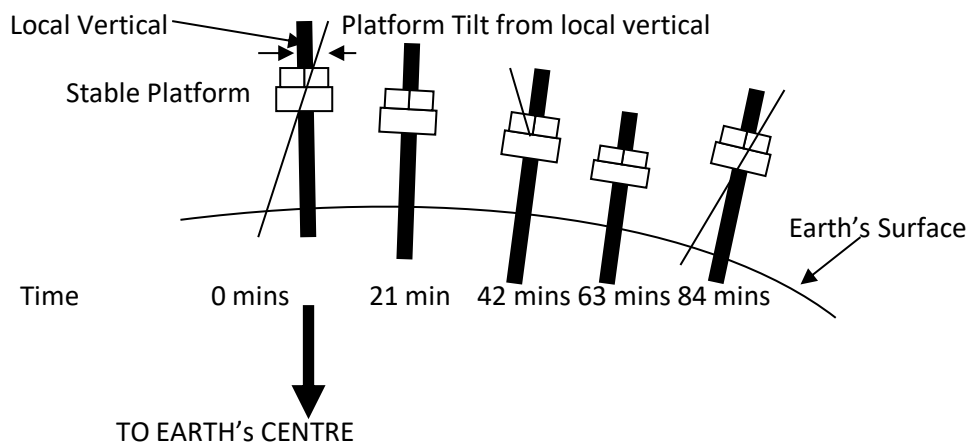


Fig 4.15 Schuler Oscillation

4.4 Platform Axes. The platform or inertial measuring axis frame commonly adopted for latitude below 80 deg is an Earth referenced axis frame known as a 'local level, north slaved axis frame', or local North, East, Down (NED) axes. Alternative coordinate systems are adopted for navigation over Polar Regions. In the case of a stable platform INS mechanism, this enables the gimbal angles to provide a direct read out of the aircraft Euler angles, that is the heading, pitch and bank angles. The term platform is used in general sense and can denote a gimballed stable platform, or, the virtual stable platform maintained in the strap-down INS computer.

4.4.1 Angular Rate Corrections. It is necessary to rotate the gyro derived reference frame at the appropriate rates so that it stays aligned with the local NED axis frame. The Earth's rate and the vehicle rate correction terms are set out in table 4.1, for reference.

Table 4.1 Angular rate correction terms

Rate term	North axis	East axis	Down axis
Earth's rate	$\Omega \cos \lambda$	0	$\Omega \sin \lambda$
Vehicle rate	V_E/R	$-V_N/R$	$-(V_E/R) \tan \lambda$

It should be noted that the quantity, R, in the vehicle rate terms is the distance of the aircraft from the earth's centre and is equal to the Earth's radius, R_0 , plus the aircraft's altitude, H, i.e.

$$R = R_0 + H$$

The value of R_0 is taken as 6,378,137 m. further correction must also be made to allow for the earth being an ellipsoid and not a perfect sphere.

4.4.2 Acceleration correction. The NED axis frame is rotating with respect to an inertial axis frame and this introduces a further complication in deriving the aircraft's rate of change of velocity along the North and East axes. This is because the aircraft's linear motion is defined with respect to these axes which in turn are rotating with the rotation of the Earth. Coriolis accelerations are introduced because of the linear motion with respect to a rotating axis frame, as the path in space is curved one. Coriolis accelerations are named after the French mathematician who formulated the general principles for the study of moving bodies in a rotating frame of reference early in the nineteenth century. Referring to the diagram on fig 4.16, the Coriolis acceleration experienced by a body moving with velocity, V, with respect to an axis frame which is rotating at an angular rate ω rad/s is equal to $2 V\omega$ and is mutually at right angles to the linear velocity and angular velocity vectors. Referring to fig 4.16, the Coriolis acceleration component along the North, East, vertical axes due to the aircraft's linear velocity components V_N, V_E, V_D and the Earth's rotation rate components $\Omega \cos \lambda$ about the North Axis and $\Omega \sin \lambda$ about the vertical axis are:

North axis: $2V_E \Omega \sin \lambda$

East axis: $-2 V_N \Omega \sin \lambda - 2 V_D \Omega \cos \lambda$

Vertical axis: $-2 V_E \Omega \cos \lambda$

The aircraft is also turning in space as it flies over the Earth's surface, as the Earth is spherical, and thus introduces centrifugal acceleration components. The centrifugal (strictly speaking centripetal) acceleration of a body moving with velocity V and turning at a rate ω rad/s is equal to $V\omega$. The centrifugal acceleration component along the North, East and Down axes are set in table 4.2 together with Coriolis acceleration components. The down (or vertical) axis accelerometer measures the gravitational acceleration as well as the vertical acceleration of the aircraft, so that it is necessary to correct the output for the gravitational acceleration g . The gravitational acceleration reduces as the altitude increases and follows as inverse square law. The value of g at an altitude, H , is given by

$g = g_0 (R_0^2) / (R_0 + H)^2$; where g_0 is the value of the gravitational acceleration at the Earth's surface. The local value of the gravitational acceleration, g_0 , varies by a small amount with latitude. This is because of the centrifugal acceleration created by the earth's rate of rotation and the fact that the earth is an oblate spheroid. The relationship is

$g_0 = g_{equ} \{ (1 + k \sin^2 \lambda) / (1 - e^2 \sin^2 \lambda)^{0.5} \}$; Where g_{equ} is equal to $9.780327714 \text{ m/s}^2$, $k = 0.00193185138639$, and $e^2 = 0.00669437999013$

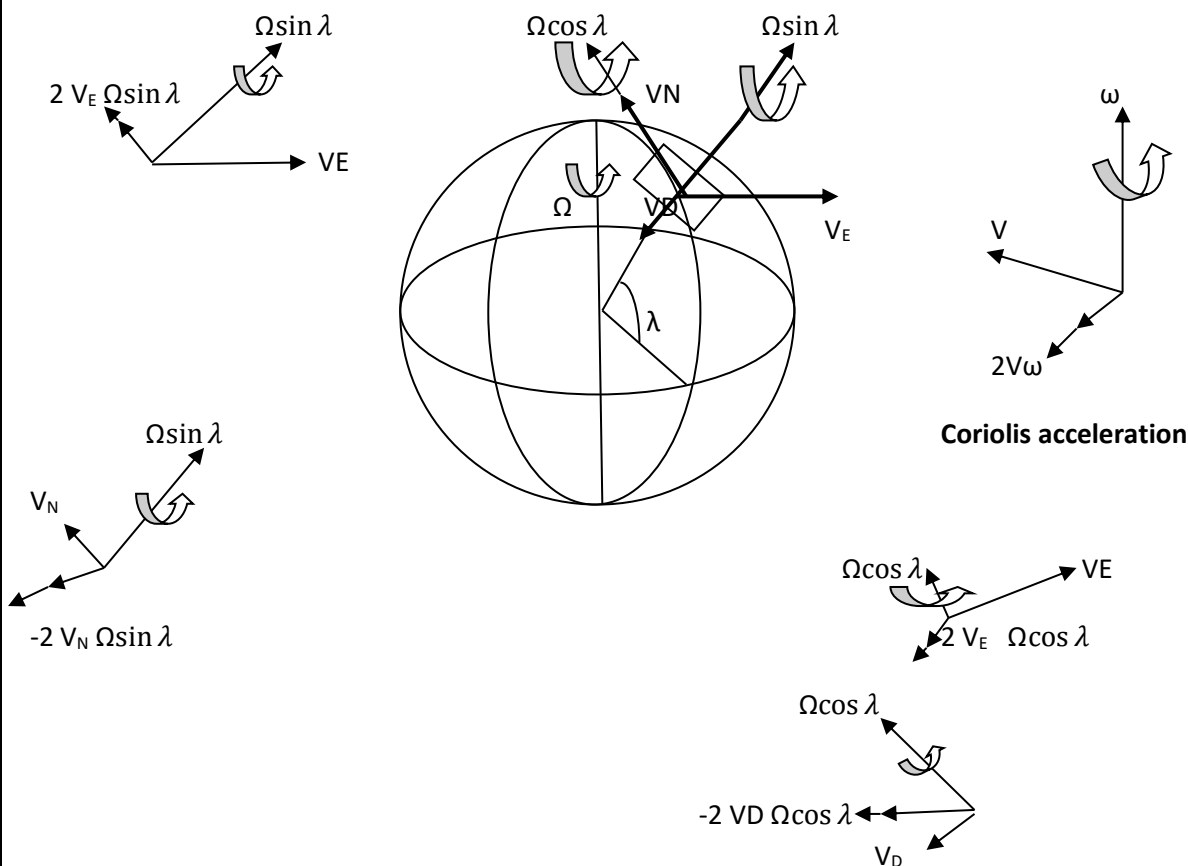


Fig 4.16 Coriolis acceleration due to Earth's rotation

Table 4.2 Acceleration correction terms

Acceleration component	North Axis	East Axis	Down Axis
Coriolis	$2V_E \Omega \sin \lambda$	$-2 V_N \Omega \sin \lambda - 2 V_D \Omega \cos \lambda$	$-2 V_E \Omega \cos \lambda$
Centrifugal	$(V_E^2 \tan \lambda - V_N V_D)/R$	$-(V_E V_N \tan \lambda + V_D V_E)/R$	$(V_N^2 + V_E^2)/R$
Gravitational			$g_0 (R_0^2) / (R_0 + H)^2$

The aircraft rates of change of the aircraft velocity components along NED axes, \dot{V}_N , \dot{V}_E , and \dot{V}_D , are obtained by subtracting the acceleration corrections in table 4.2 from the outputs of the North, East, Down accelerometers, a_N , a_E , a_D . (These are virtual accelerometers in the case of a strap-down INS.) Accurate compensation must be made for the Coriolis and centrifugal acceleration terms.

4.5 Initial alignment and Gyro compassing. Initial navigation can only be accurate as the initial conditions which are set in. It is therefore essential to know the orientation of the accelerometer measuring axes with respect to the gravitational vector, the direction of true North, the initial position and the initial velocity components to very high accuracy. The two basic references used to align an inertial system are the Earth's gravitational vector and Earth's rotation vector.

The initial alignment process is basically the same in a stable platform and strap-down INS. The difference being that in a stable platform INS, the stable platform is physically rotated to bring it into alignment with the local NED axes by applying precession torque to the vertical and azimuth gyros on the platform. It is thus easier to visualize (literally). In case of strap-down system carries out the axis rotation within the system computer to create, in effect, a virtual stable platform. The leveling operation takes place in two stages; a coarse leveling stage followed by a fine leveling stage using the horizontal accelerometer outputs. (In case of strap-down system, these are virtual horizontal accelerometers as the horizontal acceleration components are computed from the body mounted accelerometer outputs using the gyro derived attitude data.) These horizontal accelerometer outputs are directly proportional to the tilt angle from the horizontal of the accelerometer measuring axes when the aircraft is stationary on the ground. They also contain spurious accelerations and the noise due to wind buffet, fueling, crew and passengers moving about the aircraft, etc.

The coarse leveling of a stable platform INS is achieved by feeding the horizontal accelerometer outputs directly into the appropriate torque motors of the vertical gyro(s).

The fine leveling stage, which filters out the noise and spurious accelerations, is achieved by filtering the accelerometer outputs before feeding them into the vertical gyro torque motors. The filtering process is basically the same as in a strap-down INS, which is covered below. It relies on the fact that the integrated horizontal velocity components should be zero as the aircraft is stationary on the ground.

The accelerometer for an aircraft strap-down INS are generally mounted along the aircraft's principal axes so that the 'horizontal' accelerometers mounted along the forward and side-slip axes do not sense a large component of gravity.

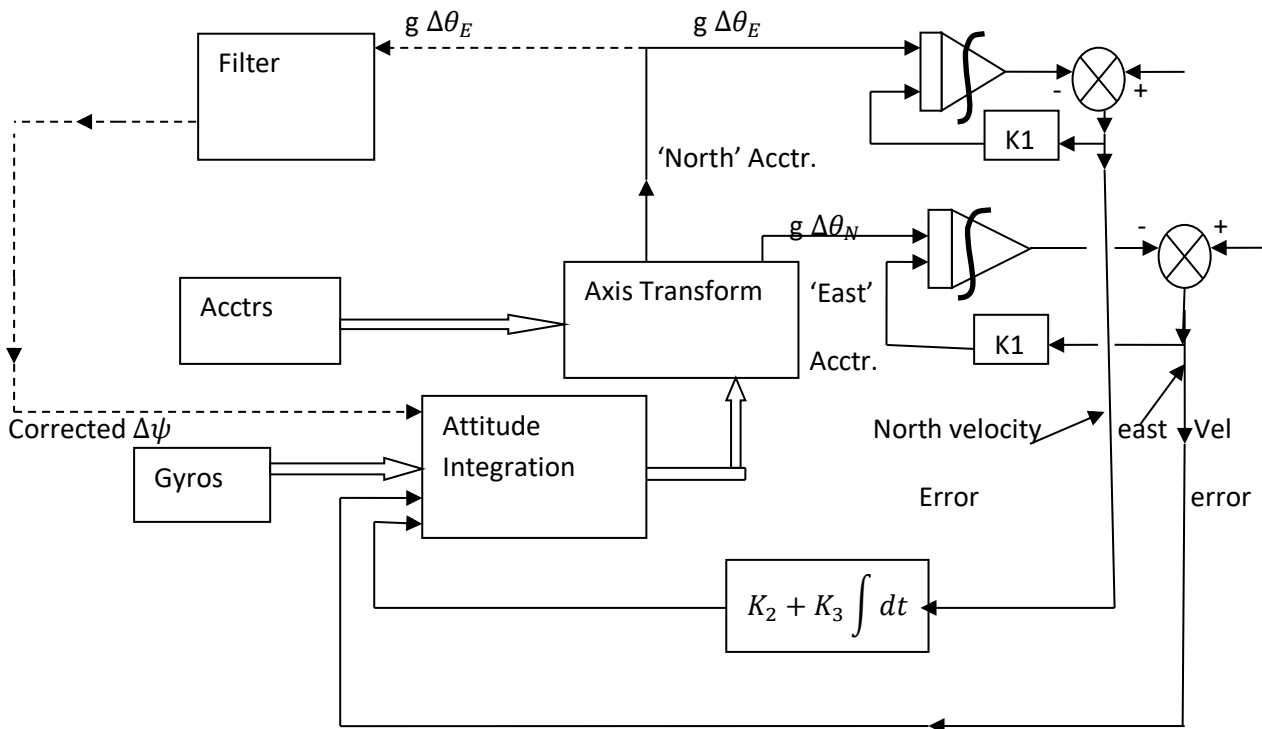
The pitch and bank angles of the aircraft are small as the aircraft is normally fairly level when stationary on the ground. The aircraft attitude integration process, using the incremental body angular rotations measured by the pitch, roll and yaw strap-down gyros, can be initialized by assuming the pitch and bank angles are both zero (if these are not known).

The fine leveling is carried out by using the fact that any tilt errors $\Delta\theta_N$ and $\Delta\theta_E$ about the computed North and East axes will couple gravitational acceleration components $g \Delta\theta_N$ and $g \Delta\theta_E$ into the East and North acceleration components derived from the accelerometers. The horizontal acceleration components are then integrated with respect to time to produce the horizontal velocity components of the aircraft. These horizontal velocity components should be zero as the aircraft is stationary on the ground. Any resulting horizontal velocity components that are measured are therefore fed back appropriately to correct the tilt and level the system. The leveling loops are generally third-order loops using the integral of the velocity errors as well as the velocity errors as control terms. The feedback gains are also varied. Fig 4.17 shows the fine leveling and gyro compassing loops. A coarse azimuth alignment with respect to true North is made to within a degree or so using, say, a magnetic reference. The fine alignment to achieve the required accuracy is accomplished by the process of gyro compassing. During the gyro compassing phase the computed heading is adjusted until the component of the Earth's rotation sensed by the Gyros about the East axis is zero. As shown earlier, the components of the Earth's rate of rotation Ω about the North, East and Down axes at latitude of λ are:

North axis: $\Omega \cos \lambda$

East axis: 0

Vertical axis: $\Omega \sin \lambda$



$\Delta\theta_E$ = tilt angle about east axis

$\Delta\theta_N$ = tilt angle about north axis

$\Delta\psi$ = heading error

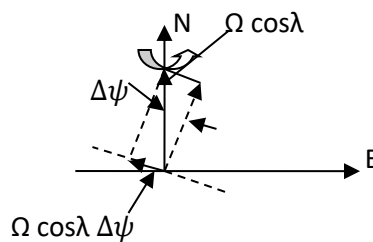


Fig 4.17 Fine leveling and gyro compassing loop

The inset diagram in fig 4.17 shows the components of the Earth's rotation rate which are sensed by the gyros when the derived NED axes are misaligned in the horizontal plane by an amount $\Delta\psi$ from the true North. It can be seen that a rotation rate equal to $\Omega \cos \lambda \cdot \sin \Delta\psi$ is measured about the normal East pointing axis, that is, $\Omega \cos \lambda \cdot \Delta\psi$, if $\Delta\psi$ is small angle.

The north pointing virtual accelerometer will hence be tilting away from the horizontal at a rate $\Omega \cos \lambda \cdot \Delta\psi$ in the absence of any leveling or gyro compassing loops. (This is assuming the appropriate corrections are made to compensate for $\Omega \cos \lambda$ and $\Omega \sin \lambda$ respectively.)

The gyro compassing loop adjusts the computed heading until the east component of the gyro angular rate measurement in the horizontal plane is nulled, the angular rate of rotation about the East axis being estimated from the summed East axis tilt correction

$$\Delta\theta_E = \int (\Omega \cos \lambda \cdot \Delta\psi \, dt)$$

It can be seen that the magnitude of the component of Earth's rate to be sensed decrease with increasing latitude, so that gyro compassing is effectively restricted to latitude below 80 deg.

The major factors which affect alignment accuracy and alignment times are:

- (a) Initial tilt
- (b) Aircraft movements, e.g., effect of wind gusts etc.
- (c) Accelerometer bias errors and gyro drift rates.
- (d) Change of the above quantities (c) with time as the system warms up.
- (e) Accelerometer resolution and gyro threshold.

The loop gains in the leveling and gyro compassing loops are generally controlled by means of a Kalman filter to give an optimal alignment process. Typical alignment times are of the order of seven minutes for full accuracy IN performance.

4.6 Strap-down IN system Computing. The basic computing flow diagram for a strap-down INS is shown in Fig 4.18. A strap-down IN system carries out the same functions as a stable platform type. INS and many elements and functional areas are common to both systems. There are two crucial areas in the strap-down mechanization. These are:

1. Attitude integration whereby the vehicle attitude is derived by an integration process from the body incremental angular rotations measured by the gyros.
2. Accelerometer resolution whereby the corrected outputs of the body mounted accelerometers are suitably resolved to produce the horizontal and vertical acceleration components of the aircraft.

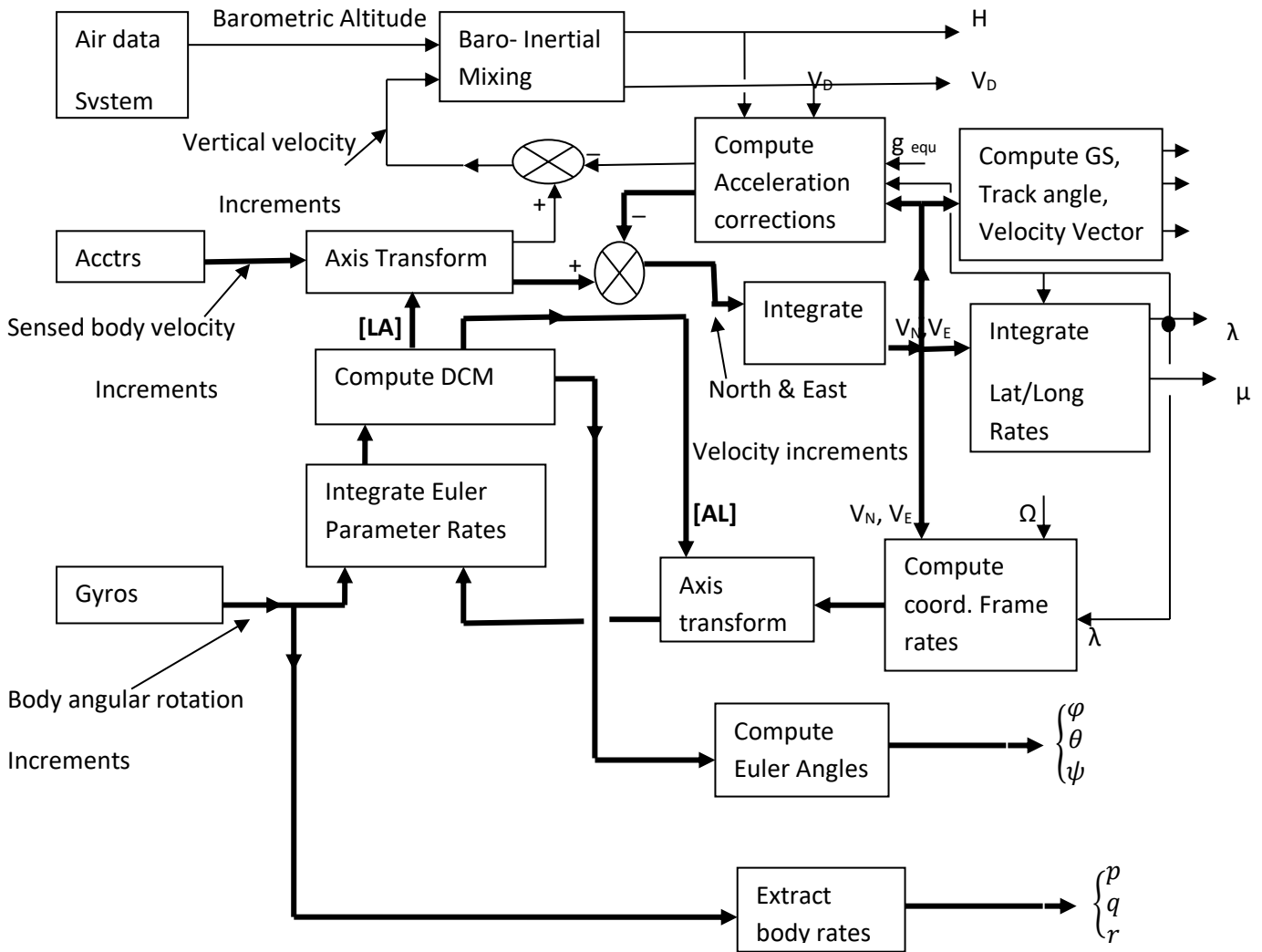


Fig 4.18 Strap-down INS computing flow diagram

The derivation of the aircraft attitude from the strap-down gyro outputs by continuously updating the four Euler symmetrical parameters each iteration period has been explained in Unit-III. Very high accuracy is required in the attitude integration process, the integration period should be as short as possible and accurate integration algorithms must be used (e.g., Runge-Kutta algorithms). The ortho-normalization of the transition matrix is essential using the constraint equation for the Euler parameters, ($e_0^2 + e_1^2 + e_2^2 + e_3^2 = 1$). The derivation of the equivalent (or virtual) horizontal and vertical accelerometer outputs from the body mounted accelerometers is as explained in unit III using the Direction Cosine Matrix derived from the Euler parameters. It should be noted that the velocity increments derived from the pulse rate outputs of the three body mounted accelerometers may need to be corrected to allow for vehicle

rotation during the integration interval when the velocity increments are being accumulated. These error corrections are known as Coriolis body rotation corrections.

The computing system, after deriving the equivalent North, East, Down accelerometer outputs and transforming the co-ordinate frame-rates from local NED axes to aircraft body axes, is then the same as for stable platform mechanization.

The implementation of a strap-down INS is shown in Fig 4.19. The solid state modules comprise:

1. The Inertial Measuring Unit (IMU) comprising three orthogonally mounted laser gyros and three orthogonally mounted accelerometers.
2. The processor Modules carrying out all the processing tasks and also monitoring and self test functions.
3. The Interface Module carrying out all the interfacing tasks.
4. The Power Supply Unit.

The complexity resides in the software and the processor and interface micro-chips.

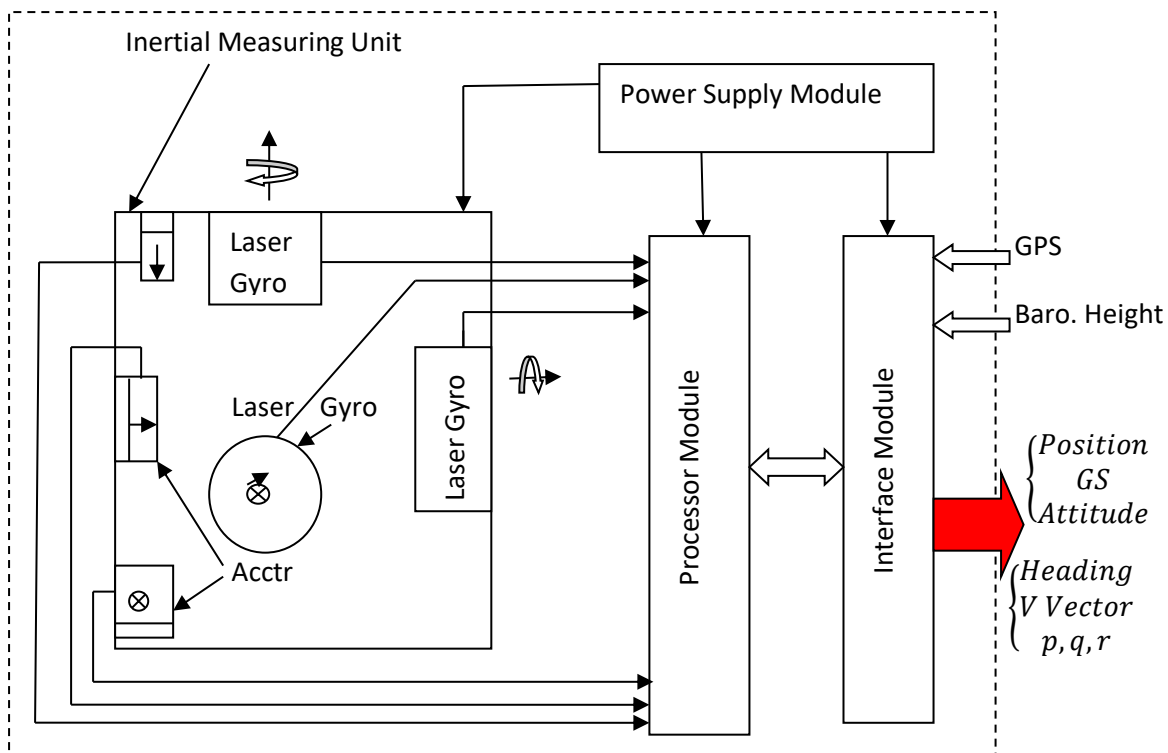


Fig 4.19 Solid state modular implementation of a strap-down INS

The Honeywell laseref VI Micro Inertial Reference System is an example of a current state of the art INS. The inset illustration and data are as shown in Fig 4.20.



Fig 4.20 Honeywell Laseref VI Micro Inertial Reference System

- Overall size: 16.5 cm * 12.3 cm * 12.3 cm)
- Weight: 4.14 kg
- Power consumption: 20 Watts
- Reliability: > 50,000 hours.

Position accuracy (unaided) is 2 NM/hour. Accelerometer is a closed loop, torque balance accelerometer and gyros is laser gyro. The system incorporates GPS integration. Hybrid mode position and velocity accuracy is 12 meters and 0.25 knots (0.13 m/s). GPS integration also enables IRS alignment in motion and even dispatch prior to navigation mode. This feature eliminates while waiting for the IRS to align.

4.7 Aided IN Systems and Kalman Filters. The time dependent error growth of an IN system makes it necessary that some form of aided navigation system using an alternative navigation source is introduced to correct the INS error build up on long distance flight.

A variety of navigation aids can be used for this purpose, for example GPS. Consider, firstly, a simple position reset at each position fix as shown in fig 4.21. The error growth is limited but follows a saw tooth pattern, the amplitude depending on the period between updates and the magnitude of the velocity and tilt errors.

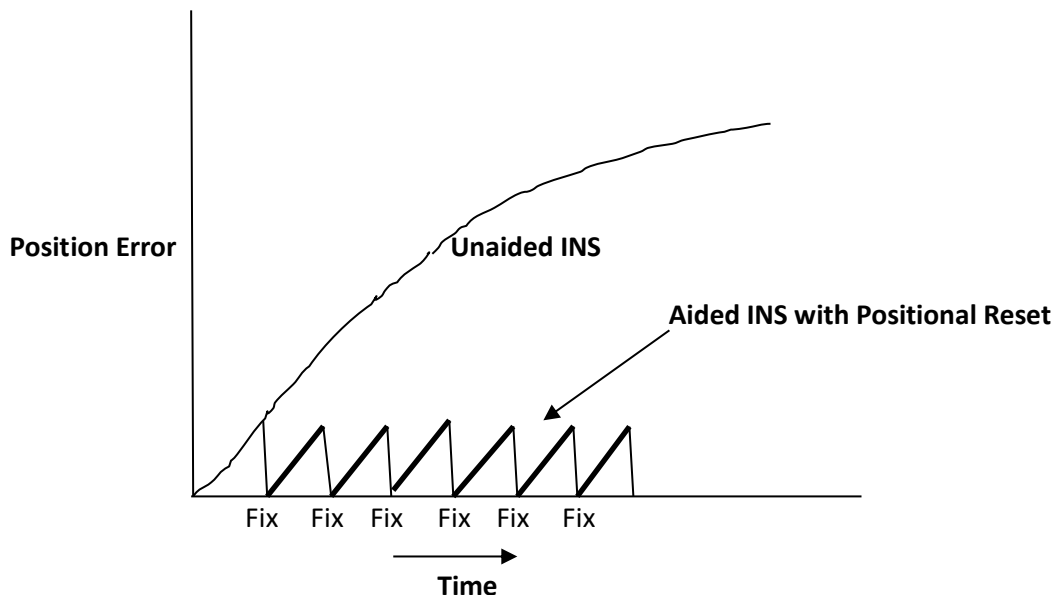


Fig 4.21 Aided INS with simple positional Reset

Now suppose the errors present in the INS, such as attitude errors, velocity errors, gyro drifts, accelerometer errors, etc., could be determined from the position fix information. This is what a Kalman filter does and corrections can then be applied to the INS as shown in the block diagram in Figure 4.22. The Kalman filter provides an optimum estimate of the IN system errors taking into account the errors present in the position fixing system. The resulting error propagation using a Kalman filter to estimate and correct the INS errors follows the pattern shown in fig 4.23- a substantial improvement. An accurate velocity reference system, such as a Doppler radar velocity sensor, can also be used in conjunction with a Kalman filter to estimate and correct the INS errors. In fact, a number of navigational aids can all be combined with an INS in an optimal manner by means of a Kalman filter. The dissimilar nature of the error characteristics of an INS and the various position (and velocity) aids is exploited by the Kalman filter to achieve an overall accuracy and performance which is better than the individual systems. The optimum blending of the individual system characteristics which can be achieved can be seen from the brief summary of the various navigation sources below. Various navigation sources comprise:

1. Position data

- GPS, VOR/DME

- Terrain reference navigation systems
- Radar
- Visual fixes (e.g., use of helmet mounted sight).

2. Velocity data

- Doppler radar
- GPS

3. Altitude data

- Barometric altitude from the air data computer
- Radio altimeter

These sources provide good information on the average at low frequency but are subject to high frequency noise due causes such as instrument noise, atmospheric effects, antenna oscillations, unlevel ground effects, etc. In contrast, IN systems provide good high frequency information content (above the Schuler frequency) despite the vehicle motion. The low frequency information, however, is poor due to inherent long term drift characteristics. The Kalman filter can be used to provide an optimum estimate of the errors in any measuring system and its use is not confined to navigation systems.

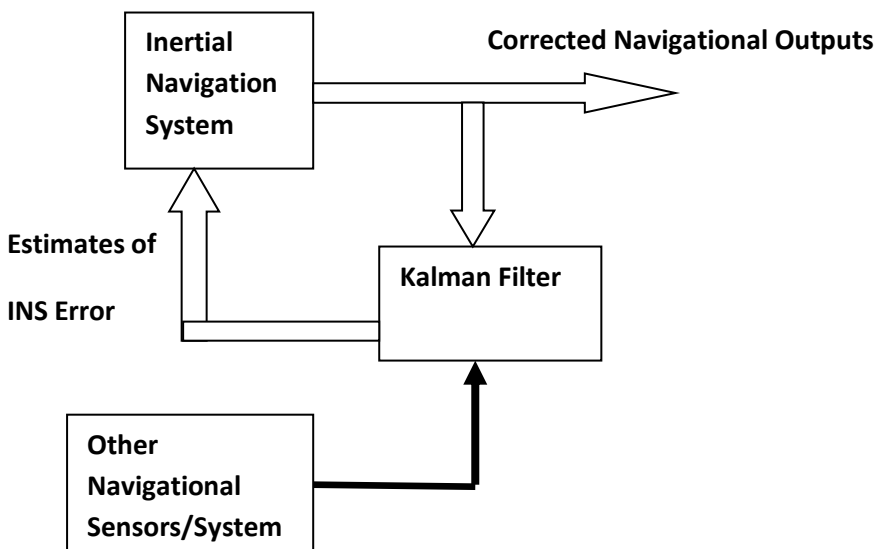


Fig 4.22 Block diagram of aided IN system with Kalman Filter

The Kalman filter was first introduced in 1960 by Dr. Richard Kalman. It is essentially an optimal, recursive data processing algorithm which processes sensor measurements to estimate the quantities of interest (states) of the system using:

1. A knowledge of the system and the measurement device dynamics

2. A statistical model of the system model uncertainties, noises, measurement errors.
3. Initial condition information.

The recursive nature of the filter, that is using the same equations over and over again make it ideally suited to a digital computer. The filter only requires the last value of the state of the system to be stored and does not need the value of the old observations to be retained. This considerably reduces the amount of computer storage required.

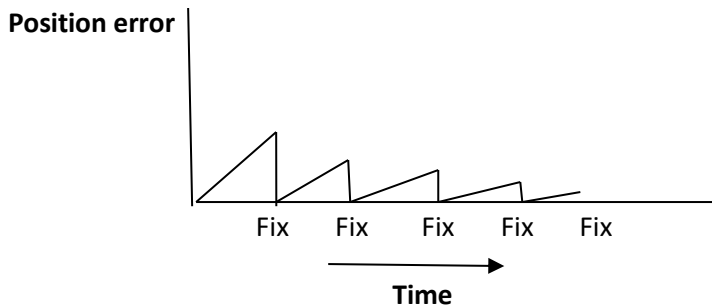


Fig 4.23 Aided INS with Kalman filter

The basic application of a Kalman filter to a mixed navigation system is shown in the flow diagram in Fig 4.24. The filter contains an error model for all the systems involved, enabling the dynamic behavior of the system errors to be modeled. The computer contains a current estimate for each term in the error model and this estimate, which is based on all previous measurements, is periodically updated. At the time of each new measurement, the difference in the outputs of the system is predicted based on the current estimate of the errors in the systems. This difference between the predicted and actual measurements is then used to update each of the estimates of the errors through a set of weighting coefficients- that is the Kalman gains. The weighting coefficients are variables which are computed periodically in the system computer and are based on the assumed statistical error model for the errors. The configuration takes into account the past history of the system including the effects of previously applied information and of vehicle motions which affect the system errors.

A fundamental feature of the Kalman filter is that the error measurements made of one quantity (or set of similar quantities) can be used to improve the estimates of the other error quantities in the system. For example, the Kalman filtering technique generates an improvement in the INS velocity accuracy by virtue of the strong correlation between position error (the measured quantity) and the velocity error.

An essential element in the Kalman filter is the System Error Model which models the dynamic behavior of the system errors. The system dynamic behavior can be represented by n differential equations, where n is the number of state variables in the system. In matrix form this becomes

$$\dot{\mathbf{X}} = \mathbf{AX} + \mathbf{BU}$$

Where \mathbf{X} is the system state vector comprising the state variables, \mathbf{A} is the coefficient or plant matrix, \mathbf{B} is the driving matrix and \mathbf{U} is the input state vector. (Bold letters denote matrices).

In deriving the Kalman filter, \mathbf{U} is assumed to be a vector of unbiased, white, Gaussian noise sequence.

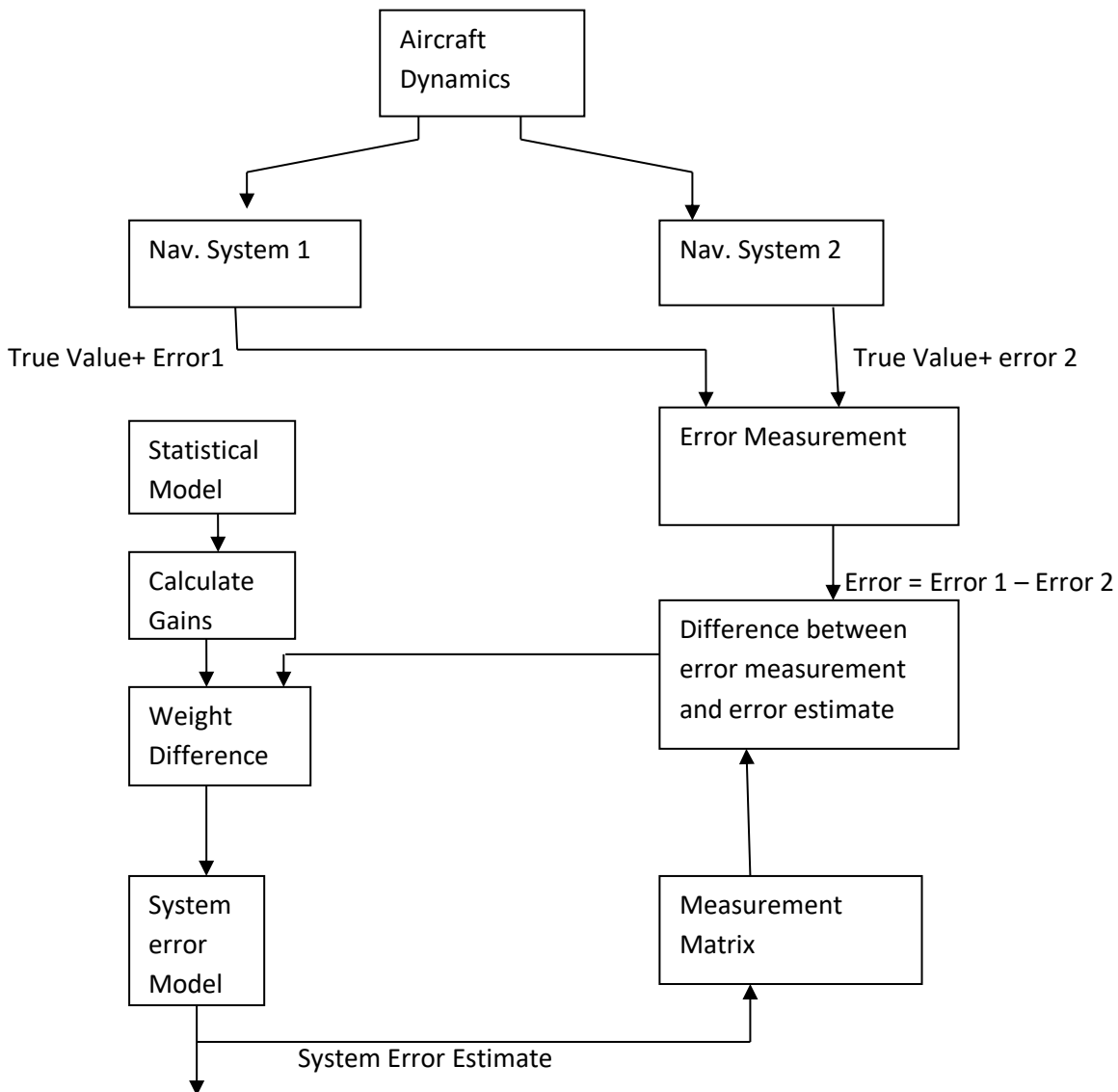


Fig 4.24 Application of Kalman filter to mixed navigation systems

The state equations for the errors in one axis of an IN system are derived below as an example. Referring to the simplified block diagram, Fig 4.12, the position error is ΔP , the velocity error is ΔV , the tilt error is $\Delta \theta$, the gyro drift error is W , and the accelerometer bias error is B .

The relationship between these variables is set out below:

$$\Delta \dot{P} = \Delta V$$

$$\Delta \dot{V} = -g \Delta \theta + B$$

$$\approx \Delta \dot{\theta} = \frac{1}{R} \Delta V + W$$

These equations can be represented more compactly in matrix form as shown below

$$\begin{bmatrix} \Delta \dot{P} \\ \Delta \dot{V} \\ \Delta \dot{\theta} \end{bmatrix} = \begin{bmatrix} 0 & 1 & 0 \\ 0 & 0 & -g \\ 0 & \frac{1}{R} & 0 \end{bmatrix} \begin{bmatrix} \Delta P \\ \Delta V \\ \Delta \theta \end{bmatrix} + \begin{bmatrix} 1 & 0 \\ 0 & 1 \end{bmatrix} \begin{bmatrix} B \\ W \end{bmatrix}$$

i.e.,

$$\dot{X} = AX + BU$$

The state transition matrix Φ_n , relates the system state vector at time nT , that is X_n , to the system state vector at time $(n+1)T$, that is $X_{(n+1)}$ where T is the iteration period. The relationship is shown below:

$$X_{(n+1)} = \Phi_n \cdot X_n$$

Assuming a linear system

$$\Phi_n = e^{At} = I + At + \frac{(At)^2}{2} + \dots$$

If the iteration period T is short

$$\Phi_n \approx I + At + A^2 \frac{T^2}{2}$$

$$\Phi_n = \begin{bmatrix} 1 & 0 & 0 \\ 0 & 1 & 0 \\ 0 & 0 & 1 \end{bmatrix} + \begin{bmatrix} 0 & 1 & 0 \\ 0 & 0 & -g \\ 0 & \frac{1}{R} & 0 \end{bmatrix} T + \begin{bmatrix} 0 & 1 & 0 \\ 0 & 0 & -g \\ 0 & \frac{1}{R} & 0 \end{bmatrix} \begin{bmatrix} 0 & 1 & 0 \\ 0 & 0 & -g \\ 0 & \frac{1}{R} & 0 \end{bmatrix} \frac{T^2}{2}$$

$$\Phi_n = \begin{bmatrix} 1 & T & -gT^2/2 \\ 0 & (1 - gT^2/2R) & -gT \\ 0 & T/R & (1 - gT^2/2R) \end{bmatrix}$$

Hence

$$\Delta P_{(n+1)} = \Delta P_n + T\Delta V_n - g\frac{T^2}{2} \cdot \Delta\theta_n$$

Etc.

From initial estimates of the uncertainties in ΔP , ΔV , $\Delta \theta$ at time, $t = 0$, the values at time $t = (n+1) T$ can thus be derived by a step by step integration process using the transition matrix at each iteration. As stated earlier this is a simplified example to illustrate the process of deriving a dynamic error model. A typical Kalman filter INS error model consists of 17-22 error states. The 19 state model comprises the following error states: two horizontal position errors, two horizontal velocity errors, three attitude errors, three gyro scale factor errors, three accelerometer bias errors, three accelerometer scale factor errors. The vertical channel is not modeled since it is unstable because gravity compensation with altitude which results in the positive feedback of altitude errors. The barometric altitude information from the air data system is combined with INS vertical channel. The GPS received error model typically comprises the 12 states.

The measurement matrix, H , is used to select the part or the component of the state vector X which is being measured. For example, suppose the state vector

$$X = \begin{bmatrix} \Delta P \\ \Delta V \\ \Delta \theta \\ \Delta P_2 \end{bmatrix}$$

Where ΔP , ΔV , $\Delta \theta$ are the inertial system errors and ΔP_2 is the error in the position reference system. To extract $(\Delta P - \Delta P_2)$ the measurement matrix $H = [1 \quad 0 \quad 0 \quad -1]$

$$H \cdot X = [1 \quad 0 \quad 0 \quad -1] \begin{bmatrix} \Delta P \\ \Delta V \\ \Delta \theta \\ \Delta P_2 \end{bmatrix} = \Delta P - \Delta P_2 \quad ;$$

The covariance matrix of the estimation errors is formed by multiplying the error state vector matrix by its transpose- the transpose of a matrix means interchanging the rows and columns of the matrix. The covariance matrix, P , of a state vector X , comprising position, velocity and tilt errors, that is

$$X = \begin{bmatrix} \Delta P \\ \Delta V \\ \Delta \theta \end{bmatrix}$$

is thus

$$P = X X^T;$$

$$\mathbf{P} = \begin{bmatrix} \Delta P \\ \Delta V \\ \Delta \theta \end{bmatrix} \begin{bmatrix} \Delta P & \Delta V & \Delta \theta \end{bmatrix}$$

$$\mathbf{P} = \begin{bmatrix} \Delta P^2 & \Delta P \cdot \Delta V & \Delta P \cdot \Delta \theta \\ \Delta V \cdot \Delta P & \Delta V^2 & \Delta V \cdot \Delta \theta \\ \Delta \theta \cdot \Delta P & \Delta \theta \cdot \Delta V & \Delta \theta^2 \end{bmatrix}$$

It should be noted that the covariance matrix is symmetrical about a diagonal, with the diagonal elements comprising the mean square position, velocity and tilt errors respectively. The off-diagonal terms are cross-correlation between these same three quantities. The covariance matrix changes with time as the initial errors propagate with time. It is modified with time by means of the transition matrix using the following relationship:

$$\mathbf{P}_{(n+1)} = \boldsymbol{\varphi}_n \cdot \mathbf{P}_n \cdot \boldsymbol{\varphi}_n^T$$

($\boldsymbol{\varphi}_n^T$ is the transpose of $\boldsymbol{\varphi}_n$)

The use of the Kalman filter equations is briefly set out below. The purpose of the Kalman filter is to provide an optimum estimate of the system state vector at iteration n. This is denoted by $\widetilde{\mathbf{X}}_n$; the circumflex indicating a best estimate. The filter may be described in two stages. 'Extrapolation' indicates the period during which the filter simulates the action of the system between measurements. 'Update' occurs when a measurement is made on the system and is incorporated into the filter estimate. Quantities after extrapolation, immediately preceding the nth update are shown in the manner $\widetilde{\mathbf{X}}_n(-)$, and those immediately succeeding that update as $\widetilde{\mathbf{X}}_n(+)$. During extrapolation the filter estimate of the system state vector is modified according to the best available knowledge of the system dynamics

$$\widetilde{\mathbf{X}}_n(-) = \boldsymbol{\varphi}_{n-1} \cdot \widetilde{\mathbf{X}}_{n-1}(+).$$

The error covariance matrix is also extrapolated

$$\mathbf{P}_n(-) = \boldsymbol{\varphi}_{n-1} \cdot \mathbf{P}_{n-1}(+) \cdot \boldsymbol{\varphi}_{n-1}^T + \mathbf{Q}$$

where \mathbf{Q} is the covariance matrix of the random system disturbances.

During the filter update procedure, the difference between the actual measurement and a measurement made of the estimated state is weighted and used to modify the estimate state

$$\widetilde{\mathbf{X}}_n(+) = \widetilde{\mathbf{X}}_n(-) + \mathbf{K}_n \cdot [\mathbf{Z}_n - \mathbf{H}\widetilde{\mathbf{X}}_n(-)]$$

\mathbf{Z}_n is the actual measurement made of the state variables and \mathbf{K}_n is the Kalman gain matrix.

The weighting factors, or Kalman gains, are calculated from the current estimate of the error covariance.

$$\mathbf{K}_n = \mathbf{P}_n(-) \cdot \mathbf{H}^T \cdot [\mathbf{H} \cdot \mathbf{P}_n(-) \cdot \mathbf{H}^T + \mathbf{R}]^{-1}$$

where \mathbf{R} is the measurement noise covariance matrix.

The error covariance matrix is then also updated

$$\mathbf{P}_n(+)= [\mathbf{I} - \mathbf{K}_n\mathbf{H}]. \mathbf{P}_n(-)$$

4.7 Attitude Heading Reference System.

4.7.1 Introduction. Modern attitude heading reference Systems are strap-down systems exploiting solid state gyros and accelerometers and are basically similar to modern strap-down IN systems. The major differences are in the accuracy of the inertial sensors and their consequent cost. There is no significant differences in reliability between the two systems as both exploit solid state implementation.

The key feature of Schuler tuning using very high accuracy gyros and accelerometers is very high (and essential) vertical reference accuracy the system provides-around 0.3 minutes of arc for good quality INS. This accuracy is not dependent on the aircraft's acceleration profile; a fundamental characteristic of Schuler tuning. The lower limits in terms of gyro and accelerometer accuracies for Schuler tuning to be effective in providing acceptable vertical reference accuracy in an AHRS system is around 0.3 degree/hour gyro drift rate uncertainty and 500 μg (2 minutes of arc tilt) accelerometer bias uncertainty. It can be seen that such sensor errors would produce vertical errors of 4.2 minutes of arc and 2 minutes of arc respectively and the resulting stand alone vertical accuracy would be around 0.1°.

An alternative method of monitoring the vertical reference which enables lower performance and hence lower cost gyros and accelerometers to be used in an AHRS is based on the use of an independent velocity source. The technique is known as Doppler/Inertial or air data/inertial mixing depending on the source of the aircraft's velocity. The errors in the vertical reference resulting from the effects of accelerations during maneuvers can be kept small with such a monitoring system, given an accurate velocity source. Small transients' errors can be induced in the vertical reference due to changes in gyro drift rates or accelerometer bias errors. The gyros and accelerometers should thus be of reasonable accuracy although they can be up to two orders of magnitude below inertial standards. The method uses the same techniques as used in IN systems to derive the aircraft velocity components from the AHRS accelerometers by integrating the suitably corrected accelerometer outputs with respect time from known initial conditions. The major source of error in the inertially derived velocity components arises from the vertical errors (or tilt errors) in the AHRS producing gravitational acceleration errors which are integrated with time. The inertially derived velocity components are, therefore, compared with velocity components measured by the reference velocity system. The velocity differences are then fed back to correct the vertical errors in the attitude reference and the inertial velocity errors. Fig 4.25 illustrates the basic concepts.

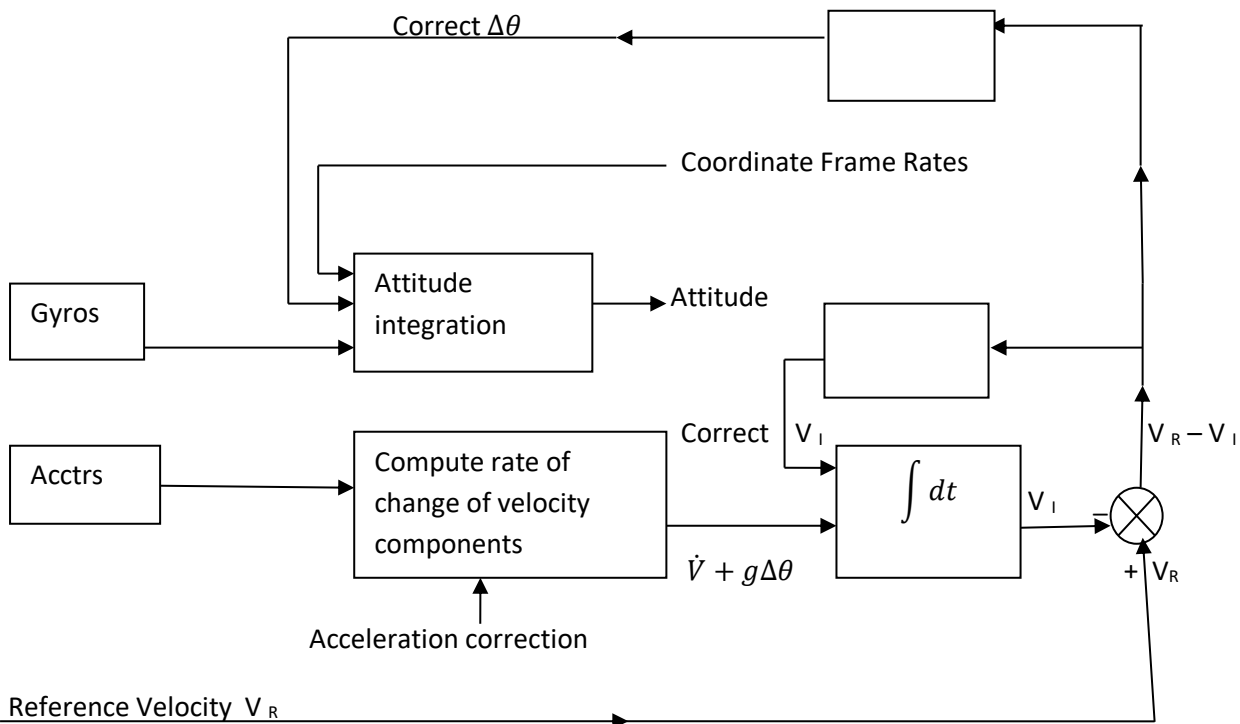


Fig 4.25 Vertical monitoring using Doppler or air data/inertial velocity mixing

In the case of a Doppler velocity sensor, the Doppler and inertially derived velocities are compared along local NED axes, as the Doppler is a key part of the navigation system. In the case of lower accuracy AHRS systems, the comparison of the air data and inertial velocity components is generally made along the aircraft body axes. The mechanization of an air data/inertial velocity mixing system to monitor the vertical reference of a strap-down AHRS is described below to show:

- The use of air data derived velocity as opposed to Doppler
- The use of aircraft body axes as reference frame of axes.
- The application to a lower accuracy AHRS with lower cost gyros in the few degrees/hour bias uncertainty performance bracket.

The basic stages involved in the vertical monitoring system are set out below.

Derivation of velocity components from the air data system: The air data system provides outputs of true air speed, V_T and the angle of attack, α , and the side slip incidence angle, β . The air data derived forward velocity, U_A , side slip velocity V_A , and vertical velocity, W_A , are computed from the air data system outputs V_T , α and β , the suffix A being used henceforth to denote the source of U, V, W (i.e., $U = U_A, V = V_A, W = W_A$).

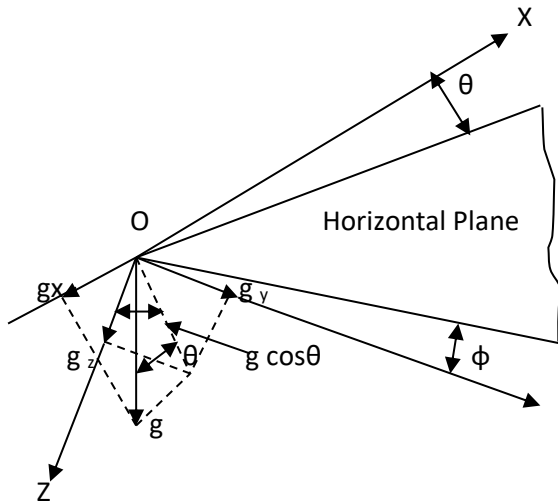


Fig 4.26 resolution of gravity vector

Inertial derivation of forward velocity and side-slip velocity: The aircraft acceleration components along the body axes are derived from the following equations:

- Acceleration along forward axis, $OX = \dot{U} - V r + W q$.
- Acceleration along side-slip axis, $OY = \dot{V} + U r - W p$.
- Acceleration along vertical axis, $OZ = \dot{W} - U q + V p$.

Referring to fig 4.26 it can be seen that the gravitational acceleration components g_x , g_y , g_z along OX , OY , and OZ respectively are

$$g_x = -g \sin \theta \quad (1)$$

$$g_y = g \cos \theta \sin \phi \quad (2)$$

$$g_z = g \cos \theta \cos \phi \quad (3)$$

The outputs of the forward, sideslip and vertical accelerometers are denoted by a_x , a_y , and a_z respectively

$$a_x = \dot{U} - V r + W q + g_x \quad (4)$$

$$a_y = \dot{V} + U r - W p + g_y \quad (5)$$

$$a_z = \dot{W} - U q + V p + g_z \quad (6)$$

The accelerometer bias errors are ignored at this stage for simplicity. From equation (4) and (5) it can be seen \dot{U} and \dot{V} can be obtained by computing the centrifugal acceleration component terms $(-V r + W q)$ and $(U r - W p)$ and the gravitational acceleration component g_x and g_y ; and subtracting these components from the accelerometer

outputs a_x and a_y respectively. The inertially derived velocity components U_i and V_i are then obtained by integrating \dot{U} and \dot{V} with respect to time.

The air data/inertial velocity mixing loops: The overall air data/inertial velocity mixing loops are shown in fig 4.27. The computed centrifugal acceleration component terms $(-V r + W q)$ and $(U r - W p)$ are derived from the air data velocity components U_A, V_A, W_A and so are computed with respect to wind axis. The gravitational acceleration component g_x and g_y are computed from the values of the pitch angle, θ and bank angle ϕ , derived from the attitude computations using the incremental angular data from the strap-down gyros. Integrating \dot{U} and \dot{V} with respect to time yields U_i and V_i and these values are subtracted from the air data derived values of U_A and V_A yield $(U_A - U_i)$ and $(V_A - V_i)$.

The Coriolis acceleration components have been ignored for simplicity. (The air mass, of course, rotates with the Earth.) the major errors in deriving U_i and V_i are due to the tilt errors $\Delta \theta$ and $\Delta \phi$ in deriving the pitch angle, θ , and bank angle ϕ , from the gyro outputs, assuming the errors in the computed centrifugal accelerations are small. The accelerometer bias errors are also assumed to be small.

These tilt errors, $\Delta \theta$ and $\Delta \phi$, result in acceleration errors $g \Delta \theta$ and $g \Delta \phi$ (assuming $\Delta \theta$ and $\Delta \phi$ are small angles) in the computation of g_x and g_y which are integrated with time causing a divergence between U_i and U_A and V_i and V_A unless corrected. The air data/inertial velocity errors $(U_A - U_i)$ and $(V_A - V_i)$ are thus fed back as shown in fig 4.27.

- To the U_i and V_i integrators to slave U_i to U_A and V_i to V_A .
- To the attitude computer to correct the pitch and bank angle tilt errors and reduce these to zero.

Proportional plus integral control, viz.

$$K_2 (\text{Velocity error}) + K_3 \int (\text{velocity error}) dt$$

is used in the feedback to the attitude computer to eliminate steady-state tilt errors due to gyro bias. The values of the feedback gains, K_1, K_2 and K_3 are selected to ensure good damping of the closed loops and good overall accuracy. These loops are also used to align AHRS when the aircraft is stationary on the ground as U_A and V_A are both zero. Any velocity errors result from initial tilt errors and so are fed back to correct the vertical reference. It should be noted that when the aircraft is on the ground so that pitch and bank angles are generally small. The coarse values of pitch and bank angles used to initialize the attitude computation from the gyro incremental outputs can thus be set at zero and subsequently corrected by the alignment process using the accelerometer outputs.

The gyro derived attitude information is coupled in through a high pass filter with pass frequencies of the order of 0.003 Hz, (period of 5.6 minutes approximately), or lower so that the short term measurement of the attitude changes of the aircraft is provided mainly by the gyros. The attitude reference derived from the accelerometers is filtered by a low pass filter which smoothes the noise present and attenuates short period fluctuation but retains the long term accuracy of the gravitational reference.

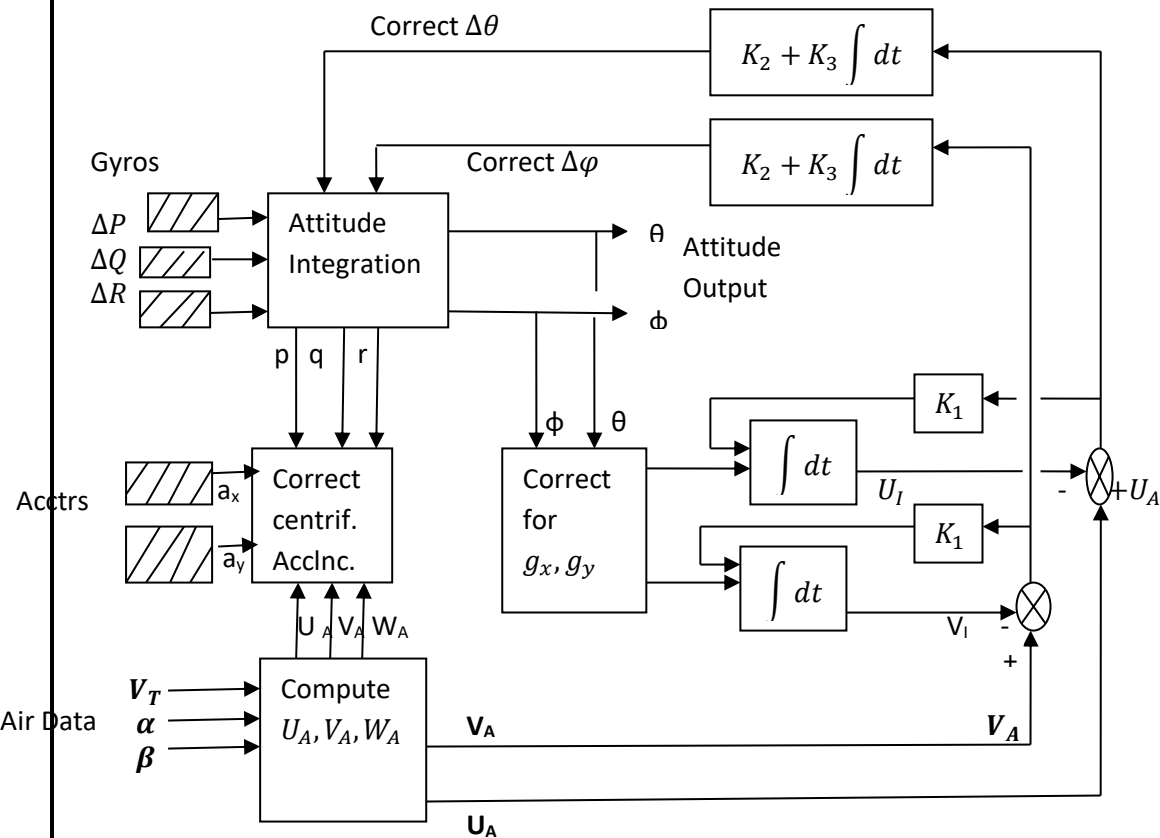


Fig 4.27 Air data vertical monitoring

4.7.2 Azimuth Monitoring Using a Magnetic Heading Reference: Gyro compassing is not suitable for an AHRS with lower accuracy gyros—alignment errors of 1° would result from using gyros with $0.1^\circ/\text{hour}$ bias uncertainty. Typical AHRS gyros are in the $0.3^\circ/\text{hour}$ to $5^\circ/\text{hour}$ bias uncertainty bracket so that it can be seen that other methods must be used for initial alignment and subsequent monitoring of the aircraft heading. (The heading can be unmonitored for several hours if the gyro drift is less than $0.01^\circ/\text{hour}$.) Magnetic monitoring, using the Earth's magnetic field as the directional reference, is generally used for the alignment and monitoring of the heading output of an AHRS using gyros which are not of inertial quality. This is a self-contained and simple system of relatively low cost and high reliability. Using modern magnetic sensors with computer compensation of the sensor errors together with an accurate vertical reference from an AHRS enables the heading errors to be constrained generally to less than 0.7° for latitude up to about 60° . A magnetic heading reference is also used for coarse initial alignment of an INS with the fine alignment carried out by gyro compassing. The magnetic heading is measured by an instrument known as a three axis flux-gate detector in conjunction with an AHRS which provides the vertical reference for the fluxgate detectors. The system comprises three magnetic field sensors, which are mounted orthogonally in a block directly fixed to the airframe with the sensor axes parallel to the principal axes of the aircraft. The components of the Earth's magnetic field with respect to the aircraft's principal axes are denoted by H_x , H_y , and H_z along the forward, sideslip and vertical axes respectively (refer to Figure 4.28). These true components H_x , H_y , H_z of the Earth's magnetic field along each axis

can be expressed in terms of a set of equations which relate the total measurement x_m, y_m, z_m of the three fluxgates. This is to account for axis misalignment and the 'hard iron' and 'soft iron' effects which are characteristic of the fluxgates and their environment in the aircraft.

The set of equations is of the form

$$H_x = a_1 x_m + b_1 y_m + c_1 z_m + d_1 \quad (1)$$

$$H_y = a_2 x_m + b_2 y_m + c_2 z_m + d_2 \quad (2)$$

$$H_z = a_3 x_m + b_3 y_m + c_3 z_m + d_3 \quad (3)$$

The coefficients a_1, a_2, a_3 and b_1, b_2, b_3 and c_1, c_2, c_3 and d_1, d_2, d_3 are measured and stored in the AHRS computer so that the flux gates measurements can be corrected and the true components H_x, H_y and H_z of the Earth's magnetic field determined. Referring to fig 4.28, the resolved components of the earth's magnetic field in the Horizontal plane along the heading axis, H_1 , and at right angles to the heading axis, H_2 , are given by

$$H_1 = H_x \cos \theta + H_y \sin \phi \sin \theta + H_z \cos \phi \sin \theta \quad (4)$$

$$H_2 = H_y \cos \phi - H_z \sin \phi \quad (5)$$

The horizontal component of the Earth's magnetic field, H_H , is therefore equal to

$$H_H = \sqrt{H_1^2 + H_2^2}$$

The aircraft's magnetic heading, ψ_M , is thus given by

$$\psi_M = \cos^{-1} H_1/H_H \text{ or } \sin^{-1} H_2/H_H \quad (6)$$

The computational processes in deriving the magnetic heading, ψ_M , are shown in Fig 4.28 and comprise:

1. computation of the true components H_x, H_y, H_z of the Earth's magnetic field with respect to aircraft axes from the measurement outputs of the three fluxgates x_m, y_m, z_m and the stored coefficients $a_1, a_2, a_3, b_1, b_2, b_3, c_1, c_2, c_3, d_1, d_2, d_3$ using equation (1), (2) and (3).
2. Computation of the horizontal components of the Earth's magnetic field along the heading axis, H_1 , and at right angles to the heading axis, H_2 , using equation (4) and (5).
3. Computation of the magnetic heading angle, ψ_M , from

$$\psi_M = \cos^{-1} H_1/\sqrt{H_1^2 + H_2^2} \text{ or } \sin^{-1} H_2/\sqrt{H_1^2 + H_2^2}$$

The gyro/magnetic heading monitoring system are illustrated in fig 4.29, a basic second order mixing system shown for simplicity. (More complex mixing systems using Kalman filter can be employed.).

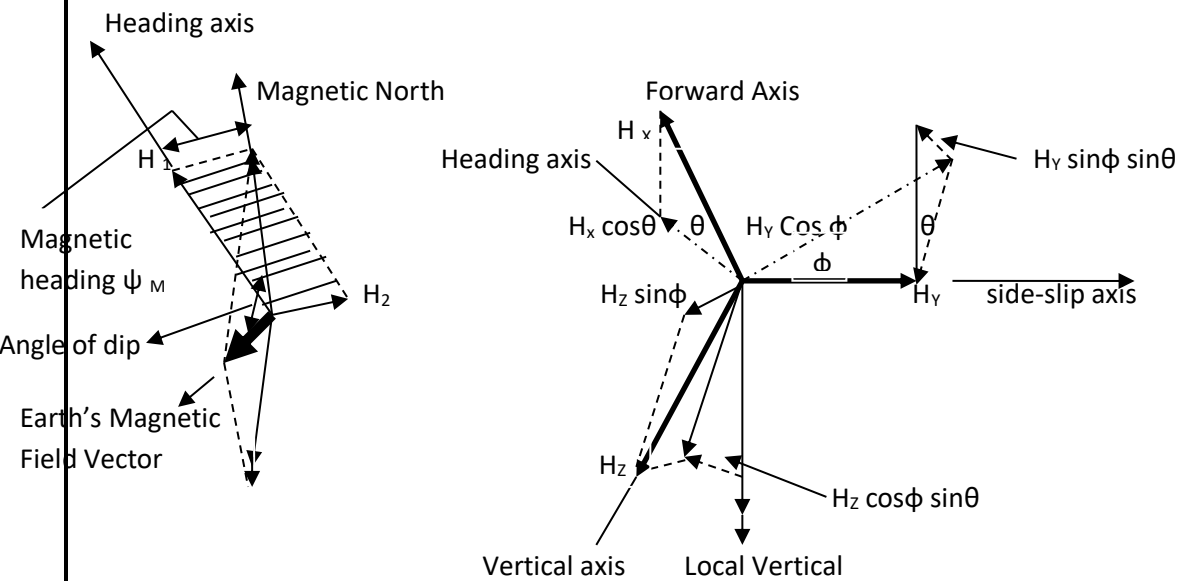


Fig 4.28 Components of the Earth's magnetic field

Referring to fig 4.29:

Ψ_G = Gyro derived heading from the strap-down AHRS

$$\Psi_G = \Psi + \int W dt$$

Where Ψ is the true heading angle and W is gyro drift rate; $\Psi_{G/M}$ is the gyro/magnetic heading; K_1 is the mixing gain for $(\Psi_M - \Psi_{G/M})$ feedback; and K_2 is the mixing gain for $\int (\Psi_M - \Psi_{G/M}) dt$ feedback. From the block diagram it can be seen that

$$\Psi_{G/M} = \Psi_G + K_1 \int (\Psi_M - \Psi_{G/M}) dt + K_2 \int \int (\Psi_M - \Psi_{G/M}) dt dt \quad (7)$$

Differentiating equation (7) twice and substituting $\dot{\Psi} + W$ for $\dot{\Psi}_G$ gives

$$(D^2 + K_1 D + K_2) \Psi_{G/M} = (K_2 + K_1 D) + D^2 \Psi + D W \quad (8)$$

The dynamic response of the system is that of a simple second-order system with undamped natural frequency, $\omega_0 = \sqrt{K_2}$ and damping ratio, $\xi = K_1 / 2 \sqrt{K_2}$. The integral feedback gain K_2 , determines the undamped natural frequency and the proportional feedback gain, K_1 determines the damping. K_1 and K_2 are determined by the value of the gyro bias uncertainty, W , and the need to have a well damped closed-loop response with ξ equal to or near to 1. From equation (8):

$$\frac{\omega_0^2 \left(1 + \frac{2\xi D}{\omega_0}\right)}{(D^2 + 2\xi\omega_0 D + \omega_0^2)} \cdot \psi_M + \frac{D^2}{(D^2 + 2\xi\omega_0 D + \omega_0^2)} \cdot \psi + \frac{D}{(D^2 + 2\xi\omega_0 D + \omega_0^2)} \cdot W$$

Ignoring the gyro bias uncertainty term W , as it has zero contribution to $\Psi_{G/M}$ if W is constant.

$$\Psi_{G/M} = F_1(D) \Psi_M + F_2(D) \Psi$$

$$F_1(D) = \frac{\omega_0^2 \left(1 + \frac{2\xi D}{\omega_0}\right)}{(D^2 + 2\xi\omega_0 D + \omega_0^2)} \quad \text{and} \quad F_2(D) = \frac{D^2}{(D^2 + 2\xi\omega_0 D + \omega_0^2)}$$

The magnetic heading, Ψ_M , component of $\Psi_{G/M}$ is coupled through a low pass filter of transfer function $F_1(D)$. This greatly attenuates the magnetic noise content of the Ψ_M output and short term transients' error such as would be caused by flexure of the structure at the fluxgate sensor location under maneuver loads. The gyro measured component of $\Psi_{G/M}$ is coupled through a high pass, or, 'wash-out' filter of transfer function $F_2(D)$. This enables the changes in heading to be measured without lag but ensures that the steady gyro bias, W , is 'DC blocked' (or 'washed-out'). The complementary filtering thus enables the 'the best of both worlds' to be achieved. The basic accuracy and repeatability of the magnetic heading sensor is retained but any noise and transients' errors during maneuvers are heavily smoothed and filtered. The excellent dynamic response of the gyro system is retained and the gyro bias is DC blocked. There are also no steady-state magnetic heading errors due to gyro bias.

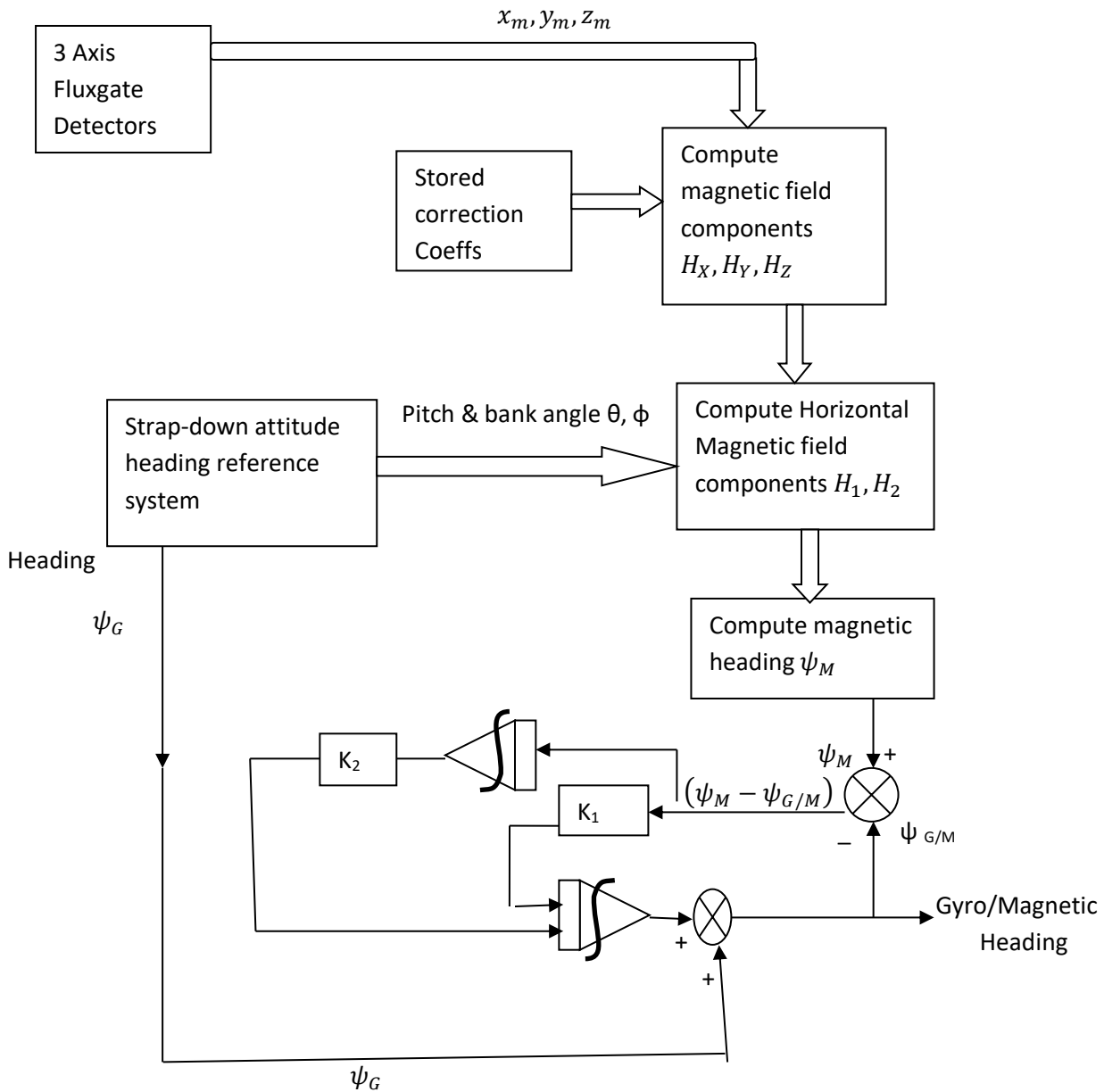


Fig 4.29 Magnetic monitoring of gyro heading

4.8 Instrument Landing System

4.8.1 Principle of operation. *Instrument landing system* operates as a ground-based instrument approach system that provides precision lateral and vertical guidance to an aircraft approaching and landing on a runway, using a combination of radio signals to enable a safe landing during instrument meteorological conditions (IMC) such as low ceilings or reduced visibility due to fog, rain, or blowing snow.

Radio-navigation aids must provide a certain accuracy (set by international standards of ICAO); to ensure this is the case, flight inspection organizations periodically check critical parameters with properly equipped aircraft to calibrate and certify ILS precision.



Fig 4.30 Details of five antennas of the ILS at Pisa Airport, Italy



Fig 4.31: The pilot has to correct to the left and a little upwards.

An aircraft approaching a runway is guided by the ILS receivers in the aircraft by performing modulation depth comparisons. Many aircraft can route signals into the autopilot to fly the approach automatically. An ILS consists of two independent sub-systems. The localizer provides lateral guidance; the glide slope provides vertical guidance. An ILS consists of two independent sub-systems. The localizer provides lateral guidance; the glide slope provides vertical guidance.

4.8.2 Localizer. A localizer antenna is centered on the runway to provide lateral (left-right) guidance (Refer fig 4.30). A total of 40 operating channels are available within the band 108-112 MHz. The localizer provides left and right lobe signals that are modulated by different frequencies (90 and 150 Hz) so that one signal or other will dominate when the aircraft is off the runway center-line. The beams are arranged such that the 90 Hz modulated signal will predominate when the aircraft is to the left, while the 150 Hz signal will be strongest to the right. The difference in signal is used to drive a cross-pointer deviation needle so that the pilot is instructed 'fly right' when the 90 Hz signal is strongest, and 'fly left' when the 150 Hz signal dominates. When the aircraft is on the center – line, the cross-pointer deviation needle is positioned in the central position. This deviation signal is proportional to azimuth out to $\pm 5^\circ$ of the center line (refer fig 4.31).

4.8.3 Glide slope. A glide slope antenna is located beside the runway threshold to provide vertical guidance (up-down). Forty operating channels are available within the frequency band 329-335 MHz. As for the localizer, two beams are located such that the null position is aligned with the desired glide slope, usually set at a nominal 3° . In the case of glide slope, the 150 Hz modulated signal predominates below the glide slope and the 90 Hz signal is stronger above. When the signals are balanced, the aircraft is correctly positioned on the glide slope and the glide slope deviation needle is positioned in a central position. As for the localizer needle, the pilot is provided with 'fly up' or 'fly down' guidance to help him or her acquire and maintain the glide slope. Fig 4.32 shows the general arrangement of ILS. Fig 4.33 illustrates how guidance information is portrayed for the pilot according to the aircraft position relative to the desired approach path. In a modern aircraft this information is displayed on the Primary Flight Display. The ILS localizer, glide slope, and DME channels are so paired such that only the localizer channel needs to be tuned for all three channels to be correctly tuned.

4.8.3 Marker Beacon systems. Marker beacons are located at various points down the approach path to give pilot information as to what stage on the approach has been reached. These are the outer, middle, and inner markers. Location of the marker beacons are:

- Outer marker approximately 4-7 nm from the runway threshold,
- Middle marker ~3000 ft from touchdown
- Inner marker ~ 1000 ft from touchdown.

The high speed of most modern aircraft renders the inner marker almost superfluous and it is seldom used.

The marker beacons are all fan beams radiating on 75 MHz and provide different Morse code modulation tones that can be heard through the pilot's headset. The layout of the marker beacons with respect to the runway is shown in Fig 4.34. The beam pattern is $\pm 40^\circ$ along track and $\pm 85^\circ$ across track. The overall audio effect of the marker beacon is to convey an increasing sense of urgency to the pilot as the aircraft nears the runway threshold.

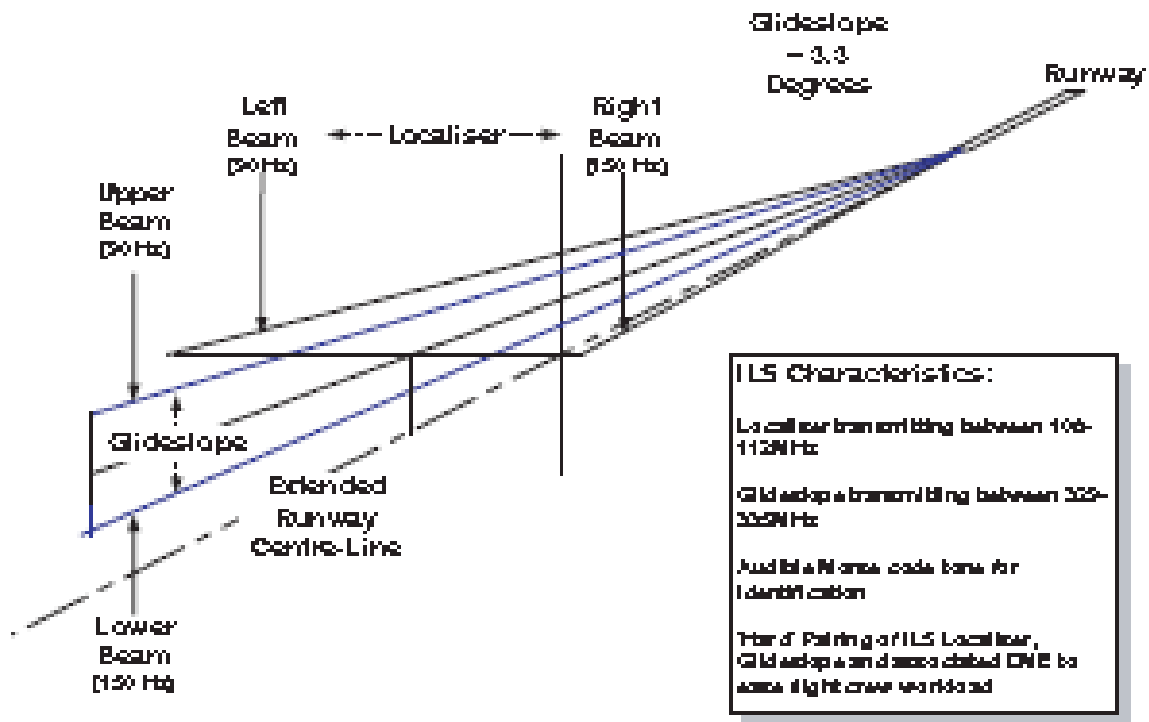


Fig 4.32 ILS glide slope and localizer

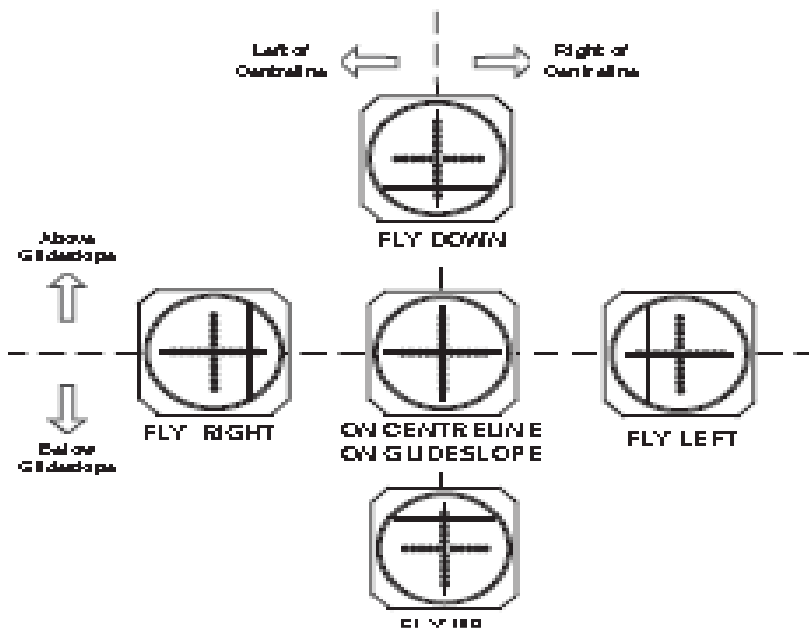


Fig 4.33 ILS guidance display

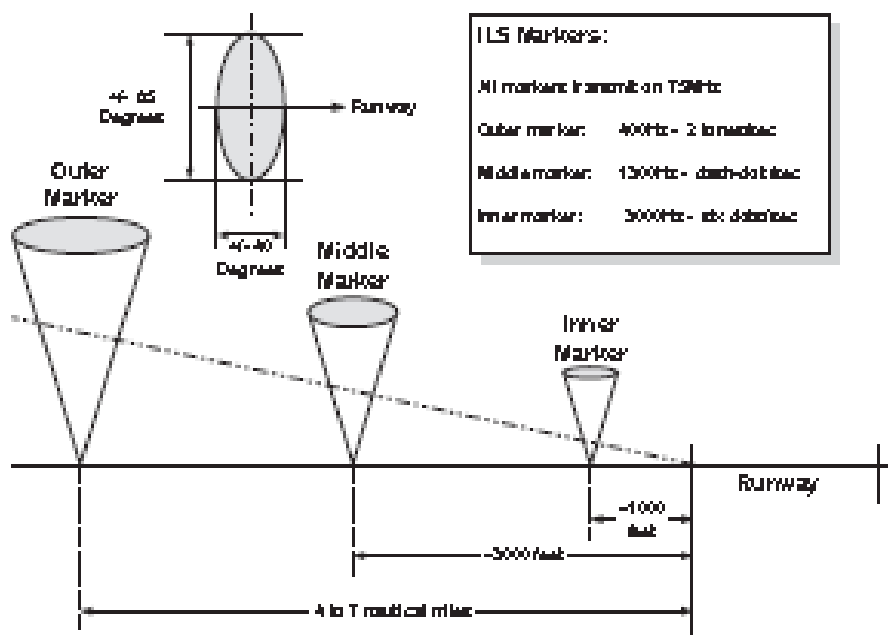


Fig. mark

Fig 4.34 ILS Approach markers

4.8.4 Decision Altitude/Height. Once established on an approach, the pilot follows the ILS approach path indicated by the localizer and descend along the glide path to the decision height. This is the height at which the pilot must have adequate visual reference to the landing environment (i.e. approach or runway lighting) to decide whether to continue the descent to a landing; otherwise, the pilot must execute a missed approach procedure, then try the same approach again, try a different approach, or divert to another airport.

4.8.5 Categories of Instrument Landing systems. There are three categories of ILS equipment which support similarly named categories of approach/landing operation. Information below is based on ICAO, and FAA.

ICAO classifies ILS approaches as being in one of the following categories:

ILS categories for precision instrument approach and landing

Approach category	<u>Decision height</u>	<u>Runway visual range (RVR)</u>	Visibility minimum	Notes
I	200 ft (61 m) or more	1,800 ft (550 m); at some airports, 1,210 ft (370 m) is approved. ¹ For single crew operations, increased to 2,600 ft (790 m).	800 m (2,600 ft).	Either visibility not less than 800 m (2,600 ft) or a runway visual range (RVR) not less than 550 meters (1,800 ft) on runway with touchdown zone and centerline lighting. FAA Order 8400.13D allows for special authorization of CAT I ILS approaches to a decision height of 150 feet (46 m) with RVR ≥ 1,400 feet (430 m). ^[10] The aircraft and crew must be approved for CAT II operations and a heads-up display in CAT II or III mode must be used to the decision height. CAT II/III missed approach criteria apply.
II	less than 200 ft and	1,000 feet (300 m)	N/A	ICAO and FAA: 350 meters (1,150 ft)

AERONAUTICAL ENGINEERING MRCET(UGC-Autonomous)

	more than 100 ft (30 m)			
IIIa	less than 100 ft and more than 50 ft (15 m)	600 feet (180 m)	N/A	
IIIb	less than 50 ft (15 m) or none	150 feet (46 m)	N/A	
IIIc	No limitations	None ¹	N/A	As of 2012, this category is not yet in operation anywhere in the world, as it requires guidance to taxi in zero visibility as well. Category IIIc is not mentioned in EU-OPS.

Smaller aircraft generally are equipped to fly only a CAT I ILS. On larger aircraft, these approaches typically are controlled by the flight control system with the flight crew providing supervision. CAT I relies only on altimeter indications for decision height, whereas CAT II and CAT III approaches use radio altimeter (RA) to determine decision height.

An ILS must shut down upon internal detection of a fault condition. Higher categories require shorter response times; therefore, ILS equipment is required to shut down faster. For example, a CAT I localizer must shut down within 10 seconds of detecting a fault, but a CAT III localizer must shut down in less than 2 seconds.

Unit-III: Inertial Sensors and Global Positioning Systems.

3.1 Basic principles of gyroscopes and accelerometers. Gyroscopes (abbreviated as gyros) and accelerometers are known as inertial sensors. This is because they exploit the property of inertia, namely the resistance to a change in momentum, to sense angular motion in the case of the gyro and changes in linear motion in the case of the accelerometer. They are fundamental to the control and guidance of an aircraft. For example, in a FBW aircraft the rate gyros and accelerometers provide the aircraft motion feedback which enables a maneuver command control to be achieved and aerodynamically unstable aircraft to be stabilized by the flight control system. Gyros and accelerometers are also the essential elements of the spatial reference system or attitude/heading reference system (AHRS) and the inertial navigation system (INS). Gyroscopes based on other operating principles also exist, such as the electronic, microchip-packaged MEMS gyroscopes found in consumer electronics devices, solid-state ring lasers, fibre optic gyroscopes, and the extremely sensitive quantum gyroscope

3.1.1 Principle of momentum gyro.

(a) Attitude Measurement: A mechanical or angular momentum gyro is a spinning wheel or disc in which the axis of rotation is free to assume any orientation by itself (see Fig 3.1). When rotating, the orientation of this axis is unaffected by tilting or rotation of the mounting, according to the conservation of angular momentum. Because of this, gyroscopes are useful for measuring or maintaining orientation.

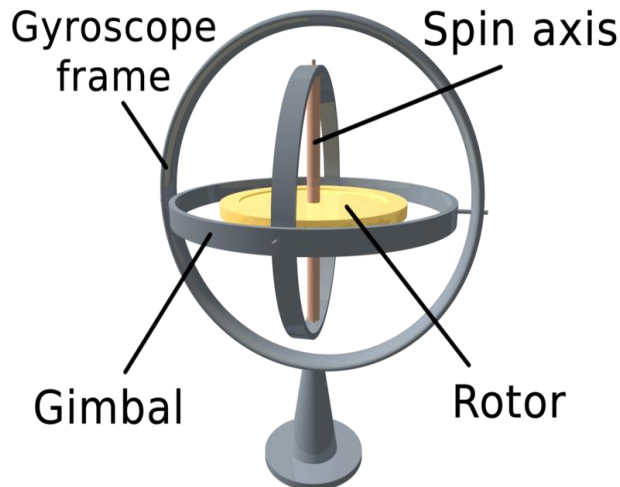


Fig 3.1 Mechanical Gyro

Within mechanical systems or devices, a conventional *gyroscope* is a mechanism comprising a rotor free to spin about one axis, the rotor being mounted in an inner gimbal or ring; the inner gimbal is free for oscillation in an outer gimbal. The **outer gimbal** or ring, which is the gyroscope frame, is mounted so as to pivot about an axis in its own plane determined by the support. This outer gimbal possesses one degree of rotational freedom and its axis possesses none. The next **inner gimbal** is mounted in the gyroscope frame (outer gimbal) so as to pivot about an axis in its own plane that is always perpendicular to the pivotal axis of the gyroscope frame (outer gimbal). This inner gimbal has two degrees of rotational freedom. The axle of the

spinning wheel defines the spin axis. The rotor is mounted to spin about an axis, which is always perpendicular to the axis of the inner gimbal. So the rotor possesses three degrees of rotational freedom and its axis possesses two. The wheel responds to a force applied about the input axis by a reaction force about the output axis (See Fig 3.2). The Gyros are based on the principle of rigidity and precession. Rigidity is the ability of a freely rotating mass to maintain its plane of spin when any external force is applied to it. If a rotating wheel is so maintained as to be free to move about any axis passing through its centre of mass, its spin axis will remain fixed in space. This principle is used in attitude measuring system as shown in Fig 3.1. The principle of precession states that when a torque acts on a spinning mass with an axis perpendicular to that of spin, then the latter will precess about an axis perpendicular to both aforementioned axes, at an angular velocity, $\Omega = T/I \omega$. Where T is the applied torque, 'I' is the moment of inertia and ω is the angular speed of rotation of the spinning mass.

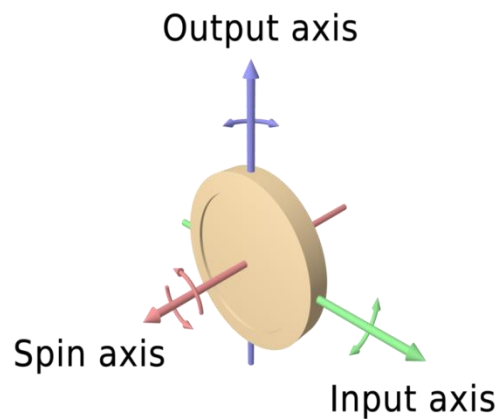


Fig 3.2: Three axis of the gyro

(b) **Rate Gyros.** This is used to measure the angular rate of the body. This has only two planes of freedom. Springs limit the amount of precession. Fig 3.3 shows turn rate gyro on the left and roll rate gyro on the right.

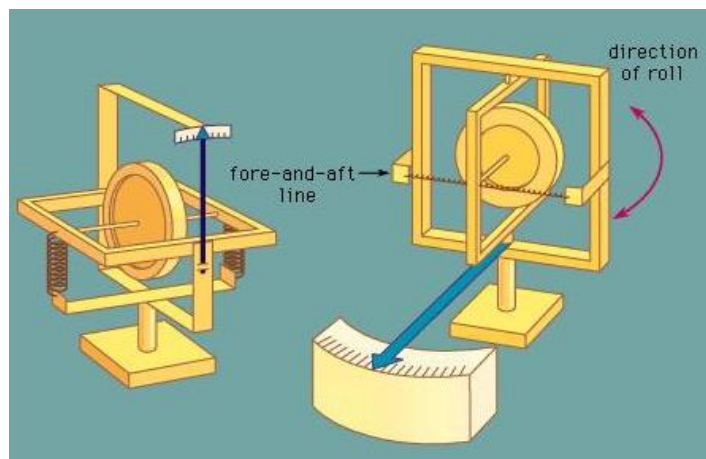


Fig 3.3 Turn Rate and Roll Rate Gyroscope.

$$\text{Rate of displacement of gyro} = \text{spring torque/angular momentum} = \frac{k\lambda}{I\omega}$$

Where

k= spring constant

λ = spring deflection

I = Moment of inertia

ω = angular velocity

Hence $\dot{\theta} \propto \lambda$

3.1.2 Principle of Accelerometer. The measurement of acceleration always relies on classical Newton's mechanics. Normally the acceleration to which a body is subjected is of interest; the accelerometer being rigidly attached to that body. The transducers make use of a sensing element consisting of a proof mass which is suspended by a spring; acceleration causes a force to act on the mass which is consequently deflected by a distance 'x' as shown in fig. 3.1.2. Some form of damping is required; otherwise the system would oscillate at its natural frequency 'Tn' for any input signal. To derive the motion equation of the system, D'Alembert's principle is applied, where all real forces acting on the proof mass are equal to the inertia force on the proof mass. We can write the equation of motion as:

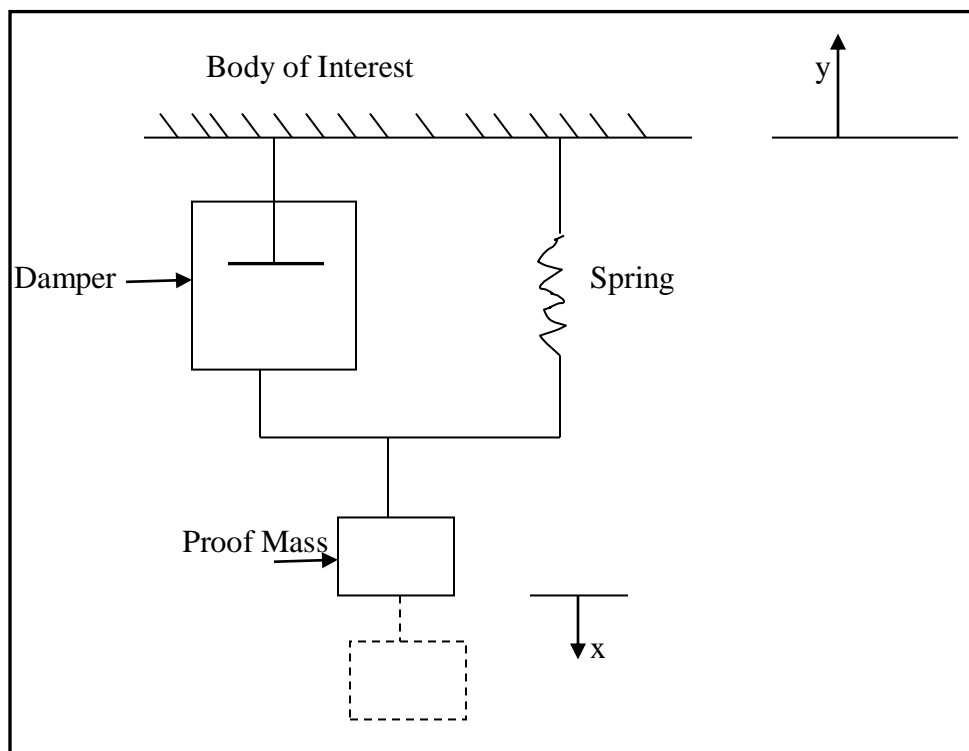


Fig 3.1.2 Principle of operation of a sensing element of an accelerometer

$$m \frac{d^2y}{dt^2} = m \frac{d^2x}{dt^2} + b \frac{dx}{dt} + kx \quad (1)$$

Where: m: mass of the proof mass,

y: movement of the body of interest,

x: movement of the proof mass,

b: damping factor (assumed to be constant, for this consideration),

k: spring constant.

The second derivative of ‘y’ with respect to time is the acceleration ‘a’ of the body of interest.

In the steady state condition, that is with constant acceleration ‘a’ and constant deflection ‘x’,

$$m a = k x$$

$$\text{Or } a = k x / m$$

Sensitivity of the accelerometer is

$$S = a/x = k/m$$

Dynamic performance is derived by taking the Laplace transform of equation (1)

$$\frac{x(s)}{a(s)} = \frac{m}{ms^2 + bs + k} = \frac{1}{s^2 + \frac{bs}{m} + \frac{k}{m}}$$

From this equation natural frequency Tn is given by

$$T_n = \sqrt{\frac{k}{m}}$$

An upper boundary of the bandwidth of an open loop accelerometer is its natural frequency. It can be seen that the bandwidth of an accelerometer sensing element has to be traded off with its sensitivity since $S = 1/T_n^2$ (This trade-off can be partly overcome by applying feedback) Furthermore the bandwidth of the accelerometer can be increased past the natural frequency of the sensing . For the dynamic performance of an accelerometer the damping factor ‘b’ is crucial. For maximum bandwidth the proof mass should be critically damped; it can be shown that for $b = 2mT_n$ this is the case. It should be noted here that in micro machined accelerometers the damping originates from the movement of the proof mass in a viscous medium.

Closed Loop Accelerometer: The accelerometer discussed above, in which the deflection of the proof mass provides a measure for the acceleration, is commonly referred to as an open loop accelerometer. High performance transducers have traditionally made use of some form of feedback where an external force is used to compensate the inertia force on the proof mass due to the acceleration, thus keeping the proof mass at zero deflection ($x = 0$). This can be approximately achieved by a closed loop structure depicted in **fig. 3.1.3**. The external force has

to be derived by a residual deflection of the proof mass. The position of the proof mass is sensed and converted into a voltage, providing the output signal. The same voltage is used to generate a feedback force on the proof mass opposing the accelerating input force. Consequently, the proof mass is only being deflected by the difference between these two forces which can be considered as the error signal. Some sort of compensation may be required to ensure the stability of the loop. In a closed loop accelerometer the sensitivity 'S' is not inversely proportional to the square of the natural frequency 'Tn' of the sensing element but depends on the loop gain and the form of compensation. Another advantage is that possible nonlinearities of spring and the damping are reduced considerably if the proof mass stays at or close to its rest position.

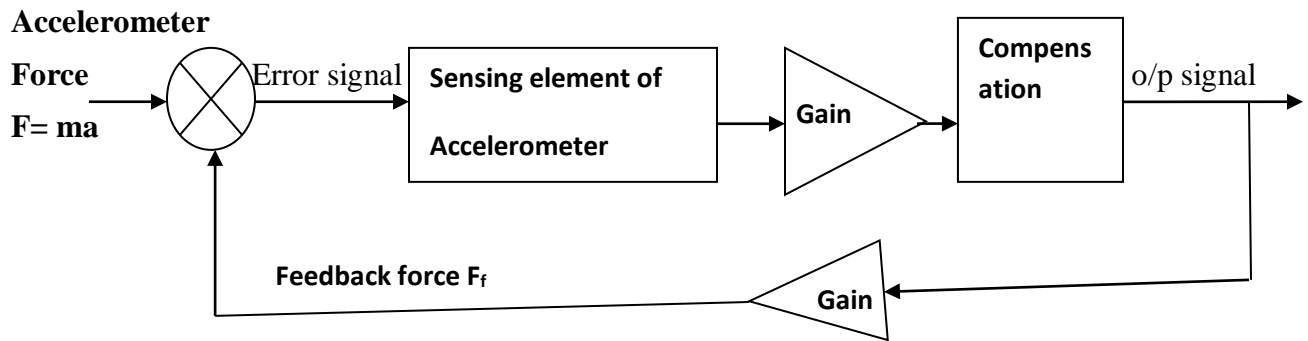


Fig 3.1.3 Closed Loop Accelerometer

3.2 Dynamically Tuned Gyro. Inertial sensors (gyroscopes and accelerometers) are important component for a number of civil and military applications. They are used for the stabilization of weapons and radars, missiles in military applications. The gyroscopes usually involve high cost manufacturing process, sophisticated technology and expertise, so that necessary performance on vehicle navigation or device positioning can be achieved. A dynamic tuned gyroscope, the so called DTG, is one of the options nowadays that can provide the required performance for many applications at a reasonable price. They demand considerable less investment in materials, machinery, processes and man power when compared to other usual sensors such as the ring-laser gyro. **DTG is a two degree-of-freedom sensor that measures the angular rates** and can achieve precision better than $0.01^\circ/h$, in full-scale range of $200^\circ/s$. The DTG operation principle is based on an inertia rotor suspended by a universal joint with flexure (**Fig 3.4**). The flexure spring stiffness is independent of spin rate. However, the dynamic inertia (from the gyroscopic reaction effect) from the gimbal provides negative spring stiffness proportional to square of the spin speed. Therefore, at a particular angular speed, called the tuning speed, the two moments cancel each other, freeing the rotor from torque, a necessary condition for an ideal gyroscope (**figure 3.5**).

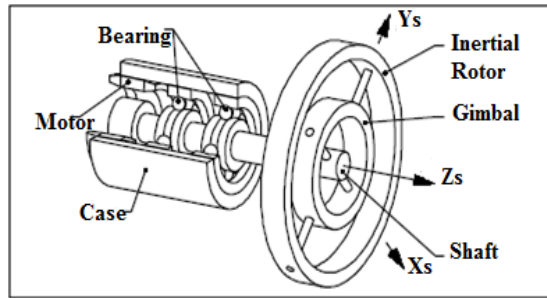


Fig 3.4 Dynamically Tuned Gyro

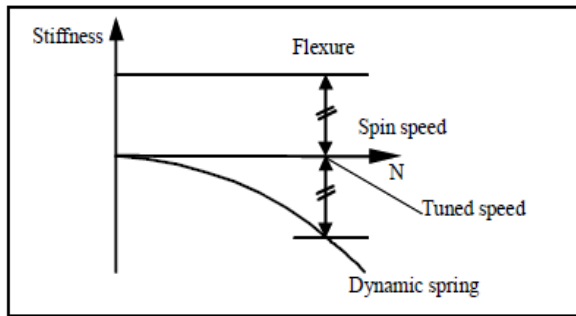


Fig 3.5: The Tuning speed

3.3 Micro machined vibrating mass rate gyroscope:

3.3.1 Basic Principle. Micro machined gyroscopes are actually based on Coriolis Effect gyroscope. Coriolis Effect is shown in fig 3.5 and 3.6. Coriolis acceleration arises in a rotating reference plane & is proportional to the rate of rotation.

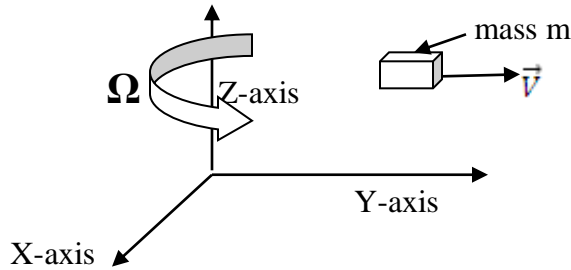


Fig 3.5: Coriolis Acceleration

Coriolis acceleration is given by the equation:

$$\vec{a}_{cor} = 2 \vec{V}_{pm} \times \vec{\Omega}$$

Where; \vec{a}_{cor} = Coriolis acceleration; \vec{V}_{pm} = Velocity of the proof mass; $\vec{\Omega}$ = Rate of rotation

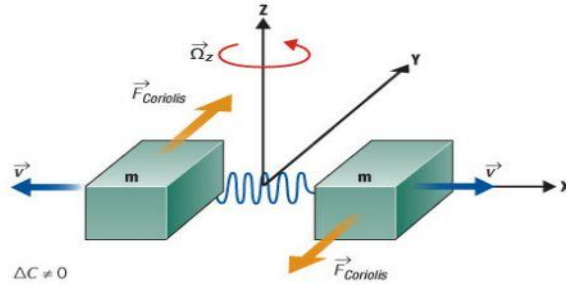


Fig 3.6 Coriolis force on two bodies connected by a spring & forced to vibrate along x-axis.

In **fig 3.7** the proof mass m is supported by two springs and two dampers, equivalently. Assume that x -axis is the driving direction, y -axis is the sensing direction. When the proof mass works under simple harmonic vibration by applying an electrostatic, piezo electric, electromagnetic force, and the displacement along x -axis is

$$x(t) = A_x \text{Cos} (\omega_x t)$$

Where A_x is the amplitude, ω_x is the driving angular frequency. When there is an angular rate Ω_z input rotation about z -axis, this will cause Coriolis acceleration about y -axis:

$$a_y = 2\Omega_z \times \frac{dx}{dt} = -2\Omega_z A_x \omega_x \text{Sin} (\omega_x t)$$

The proof mass will vibrate along the y -axis because of the Coriolis force. The input angular rate Ω_z can be calculated by detecting the y -axis displacement. When drive and sense modes are fully matched i.e. $\omega_x = \omega_y$, the responsive amplitude along y -axis achieves the maximum, while the band width achieves the minimum one. In general sense mode and drive mode should be matched for optimized sensitivity and bandwidth. Kindly refer Fig 3.7 (a) & (b)

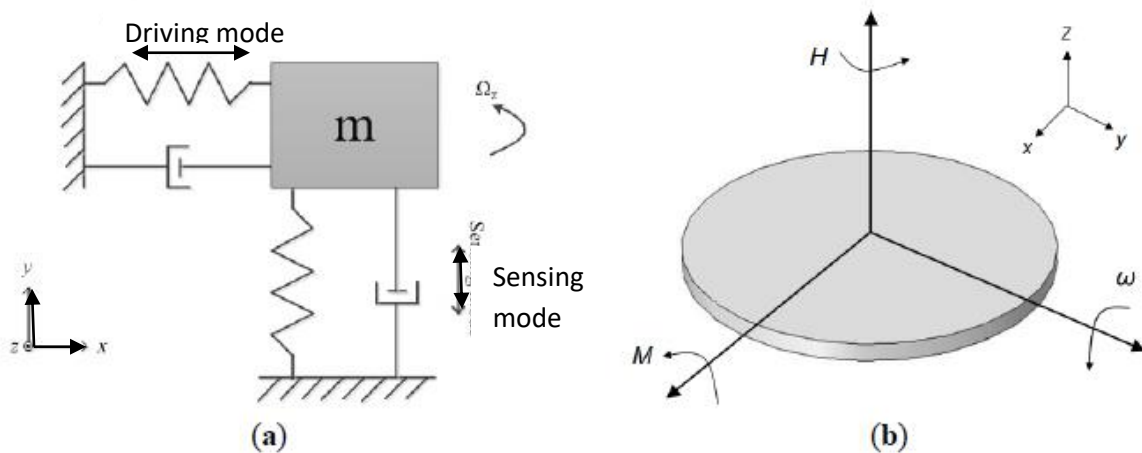


Fig 3.7 Principle of Micro machined gyroscope (a) Coriolis Effect (b) Precession principle

The conservation of angular momentum is shown in fig 3.6 (b). The Micro machined gyroscope based on precession principle usually has a rotor which is rotating around the spin axis (z-axis) at a constant speed to maintain an angular momentum H . when an angular momentum rate orthogonal to the spin axis is applied, such as around y-axis, a precession moment M of the rotor is generated around x-axis by the equation:

$$\mathbf{M} = \boldsymbol{\omega} \times \mathbf{H}$$

This moment M causes the spin axis of the rotor to make a precession around the x-axis.

3.3.2 Vibrating quartz tuning Fork rate gyro. The basic configuration of a vibrating quartz tuning fork rate gyro is shown in **fig 3.8**. The system comprises of a vibrating quartz tuning fork to sense angular rate which is coupled to a similar fork as a pick-up to produce the rate output signal. The piezo-electric drive tines are driven by an oscillator to vibrate at precise amplitude. An applied rotation rate about an axis parallel to the vibrating tines causes a sine wave of torque to be produced resulting from the Coriolis acceleration as explained earlier. This oscillatory torque in turn causes the tines of the pick-up fork to move up and down in and out of the plane of the fork assembly. This causes an electrical output signal to be produced by the Pick-up Amplifier which is amplified and phase sensitive rectified to provide a DC signal which is directly proportional to the input rate.

The pair of tuning forks and their support flexures and frames is batch fabricated from thin wafers of single crystal piezo-electric quartz and is micro-machined using photo-lithographic processes similar to those used to produce millions of digital quartz wristwatches each year. Standard rate ranges are from $50^\circ /s$ up to $1000^\circ /s$. The threshold resolution is $\leq 0.004^\circ /s$ and the BW is greater than 60 Hz. Start-up time is less than 1 second and power consumption is less than 0.7 Watt. Mean time between failures (MTBF) is over 100,000 hours

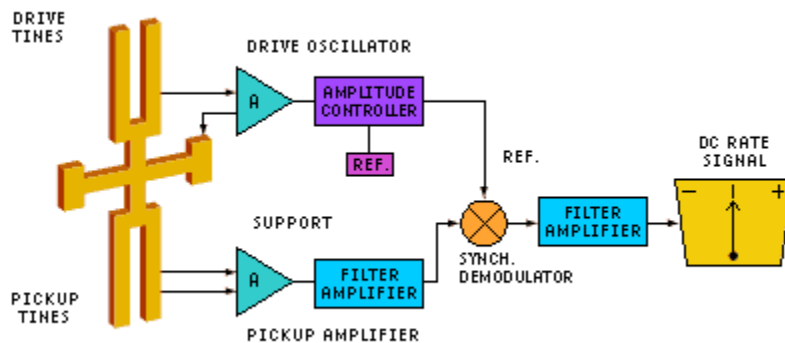


Fig 3.8 Vibrating Quartz rate Sensor

3.4 Introduction to optical gyroscope. Optical gyroscopes such as the ring laser gyro and the fibre optic gyro measure angular rate of rotation by sensing the resulting difference in the transit times for laser light waves travelling around a closed path in opposite direction. The time difference is proportional to the input rotation rate and the effect is known as the ‘Sagnac effect’ after the French physicist G. Sagnac who, in fact, demonstrated that rotation rate could be sensed

optically with the Sagnac interferometer as long ago as 1913. Sagnac provided the first demonstration of the feasibility of an optical experiment capable of indicating the state of rotation of a frame of reference, by making measurements within that frame. A schematic diagram of his interferometer is shown in Fig. 3.9(a). Light from the light source is split into two beams by the beam splitter. Two counter-propagating beams then circulate in the interferometer. The beams interfere on the beam splitter. There are two output ports of the interferometer, one back towards light source; the other towards the detector. The Fig 3.9 (b) shows a circular Sagnac interferometer of radius, r , rotating at an angular speed, Ω_{rot} . The shift in path lengths of two counter rotating beams, t_+v and t_-v , is shown. The fringe pattern recorded at the output of this interferometer is sensitive to any phase difference between the two counter-propagating beams. One beam is rotating clock wise (cw) and another anti clock wise (acw) direction. In the case that the whole interferometer is rotating in its plane, at an angular frequency, Ω_{rot} , it is possible to follow a simple derivation to obtain the value of the phase shift, $\Delta\phi$. Consider a circular interferometer of radius, r , as shown in Fig. 3.9(b).

The time taken for the two beams to complete one circuit of the interferometer, t_+ and t_- is given by,

$$t_+ = (2\pi r + r \Omega_{rot} t_+) / v; \quad (1)$$

$$t_- = (2\pi r - r \Omega_{rot} t_-) / v; \quad (2)$$

v is the speed of propagation of light around the Sagnac loop.

Hence from equation (1) & 2 we get

$$t_+ = \frac{2\pi r}{v - r\Omega_{rot}}$$

$$t_- = \frac{2\pi r}{v + r\Omega_{rot}}$$

Therefore difference in propagation time between two counter propagating beams, δt , is given by

$$\delta t = t_+ - t_- = \frac{2\pi r}{v - r\Omega_{rot}} - \frac{2\pi r}{v + r\Omega_{rot}}$$

$\therefore \delta t = \frac{4\pi r^2 \Omega_{rot}}{v^2 - (r\Omega_{rot})^2}$ Area of the interferometer, A , is equal to πr^2 . In vast majority of the cases

$$v^2 \gg (r\Omega_{rot})^2$$

It follows that,

$$\delta t = \frac{4A\Omega_{rot}}{v^2} \quad (4)$$

The phase difference between two propagating beams is given by $\left(\frac{v\delta t}{\lambda}\right)$;

$$\Delta\phi = \frac{4\vec{A} \cdot \vec{\Omega}_{rot}}{\lambda v} \quad (5)$$

Here \vec{A}/A is the unit area perpendicular to the surface of interferometer. In the case of light $v = c$. The sensitivity of this interferometer depends only on the wavelength and the projection of the

rotation onto the area enclosed in the interferometer. The center of rotation and shape of the loop have no bearings on the sensitivity. The sensitivity however, depends upon the angle between plane of rotation and the plane of interferometer.

The difference in optical path length ΔL is given by, $\delta t * v$

$$\text{Hence } \Delta L = \frac{4A\Omega_{rot}}{c} \quad (6)$$

The frequency difference, Δf , resulting from a difference in optical path length, ΔL , is given by

$$\frac{\Delta L}{L} = \frac{\Delta f}{f} \text{ substituting the value } \Delta L \text{ from equation (6) we get}$$

$$\Delta f = \frac{4A\Omega_{rot}}{cL} \text{ where } c = v$$

The wavelength of the laser transition $\lambda = c/f$, hence

$$\Delta f = \frac{4A}{\lambda L} \dot{\theta} \quad ; \text{ where } \dot{\theta} = \Omega_{rot}$$

$$\therefore \Delta f = K_0 \dot{\theta} \quad ; \text{ where } K_0 \text{ is the } \mathbf{gyro \ scale \ factor} = \frac{4A}{\lambda L}$$

This is shown in Fig 3.10.

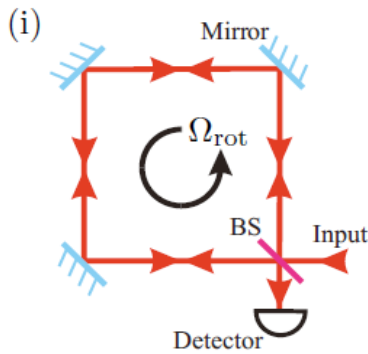


Fig 3.9 (a)

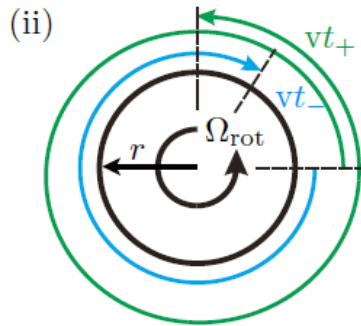


Fig 3.9 (b)

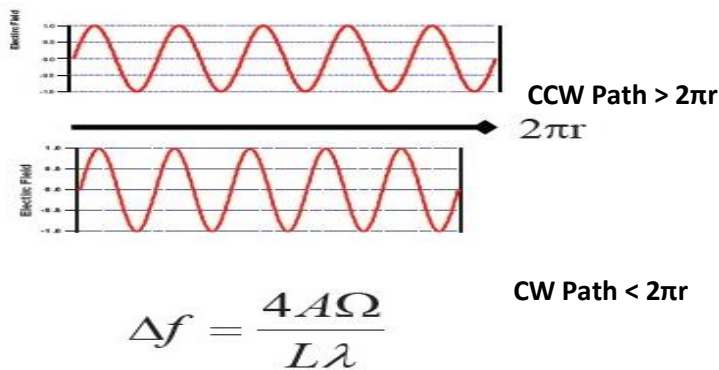


Fig 3.10: Change in frequency

3.5 The Ring Laser Gyros-principles. The basic elements of the RLG are shown schematically in Fig 3.11. The two counter rotating laser beams are generated from the lasing action of a helium-neon gas discharge within the optical cavity, the triangular closed path being formed by reflecting mirrors at each corner of the triangle. This closed path forms the resonant cavity and the longitudinal mode frequency, f , is determined by the cavity optical path length, L , being given by $f = nc/L$ where n is an integer and c is the velocity of light. At zero rotation rate, the cw and acw path lengths are equal and there is zero difference between the frequencies of the cw and acw waves. When the RLG is rotated about an axis normal to the plane of the closed path there is a difference in the path length of the cw and acw travelling waves, as shown earlier, which causes a frequency difference between the two waves. This frequency difference is measured by allowing a small percentage of the two laser beams to be transmitted through one of the mirrors. A corner prism is generally used to reflect one of the beams so that it can be combined with the other to generate a fringe pattern at the read out detector photo-diodes. An input rotation rate causes the fringe pattern to move relative to the read out photo-diode at a rate and in direction proportional to the frequency difference (positive or negative). A sinusoidal output signal is generated by each fringe as it passes by the photo-diodes these are spaced so that there is a 90 deg phase difference between their outputs so that direction of rotation can be determined from which photo-diode output is leading. The photo-diode outputs are then converted into positive (or negative) pulses by suitable pulse triggering and direction logic.

As discussed earlier $\Delta f = K_0 \dot{\theta}$; the gyro thus behaves as an integrating rate gyro

$$\int_0^T \Delta f dt = K_0 \int_0^{\theta} d\theta$$

The angle turned through about the gyro input axis in the time period, T , is equal to the net number of positive (or negative) pulses counted in that period. The RLG thus provides a direct digital output of the input angular rotation with a process of inherent integration carried out in the optical domain.

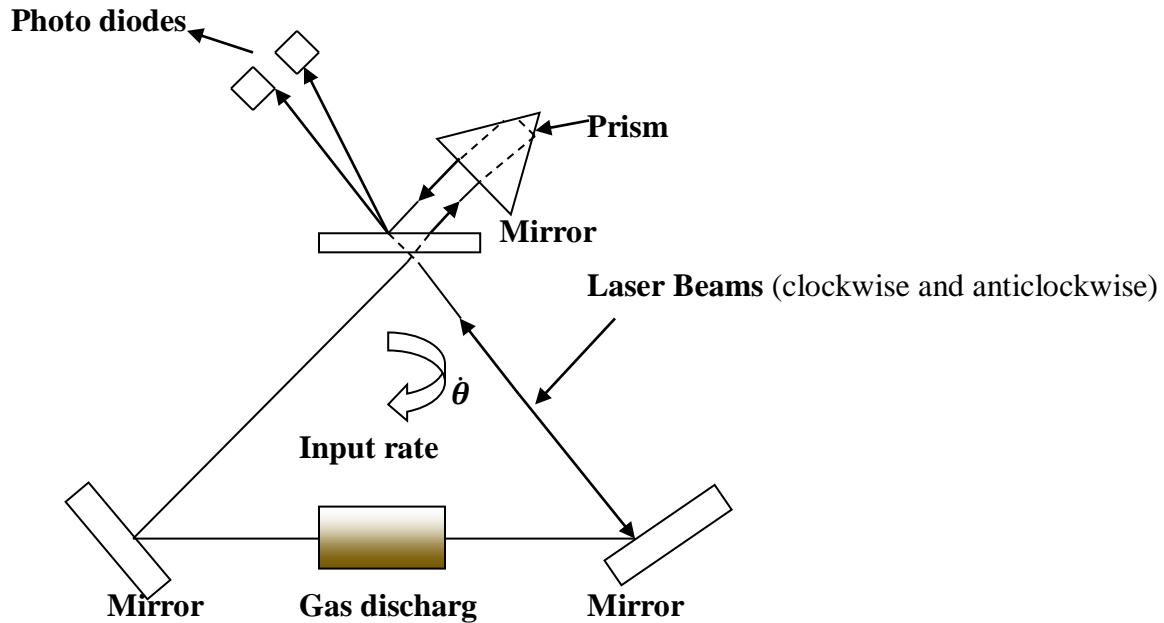


Fig 3.11 Laser gyro schematic

Another explanation of the RLG is as follows. The counter propagating waves set up by the lasing action will beat together and set up a standing wave pattern in the cavity. This standing wave pattern remains fixed in space irrespective of the angular rotation of cavity. The standing wave pattern remains fixed in space irrespective of the angular rotation of the cavity. An observer rotating with the cavity, in this case the read out photo-diodes, will thus see a succession of light and dark fringes as the read-out moves past the spatially fixed standing wave. Figure 3.12 illustrates the principle. The fact that the standing wave pattern remains fixed in the space as the cavity rotates can be interpreted as a manifestation of the inertia which electro-magnetic

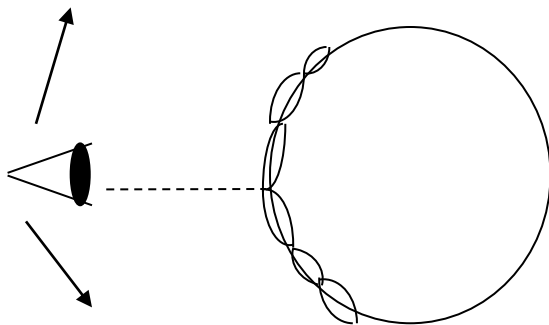


Fig 3.12 Laser Gyroscope Principle

energy possesses in view of its mass equivalence. Fig 3.13 illustrates the construction of a typical RLG. The equivalent triangular cavity is machined from a solid block of a vitreous-ceramic material known as 'CERVIT' which has a very low coefficient of thermal expansion. The three mirrors are mounted on the block by optical contact for stability and ruggedness. The mirrors have multi-dielectric coatings and have a reflectivity of more than 99.9%. The optical path length of the cavity is adjusted by means of a piezo-electric transducer attached to one of the cavity mirrors. The position of the mirror being controlled by a servo loop so that laser oscillates at its peak average power. High voltages of the order of 2,000 volts dc are applied between the two separate anodes and the common cathode to ionise the He-Ne gas mixture and provide the required lasing action. A major problem which has had to be overcome with the RLG is the phenomenon known as 'lock-in'. This arises because of imperfection in the lasing cavity, mainly in the mirrors. For low rotation rates below a threshold known as the 'lock-in rate', the two beams lock together at the same frequency so that there is zero output and a dead zone results. The fig 3.14 (a) illustrates the effect of lock-in under steady input rate conditions. This lock-in zone is of the order of 0.01 to 0.1°/s compared with 0.01°/hour accuracy required for an INS. A very effective method of overcoming this problem is to mechanically dither the laser block about the input axis at a typical frequency of about 100 Hz with the peak velocity of about 100°/s. The amplitude of the dither rate and acceleration are so chosen so that the dwell time in the lock-in zone is so short that lock-in can not occur. The fig 3.14 (b) illustrates the effect of dither on removing the dead zone. The dither signal can be removed from the output by mounting the read-out reflector prism on the gyro case and read-out photo-diodes on the block so as to produce an optical cancellation of the dither signal. Alternatively the read-out prism and read-out photo-diode can both be mounted on the block and the unwanted dither signal can be removed by a digital filter.

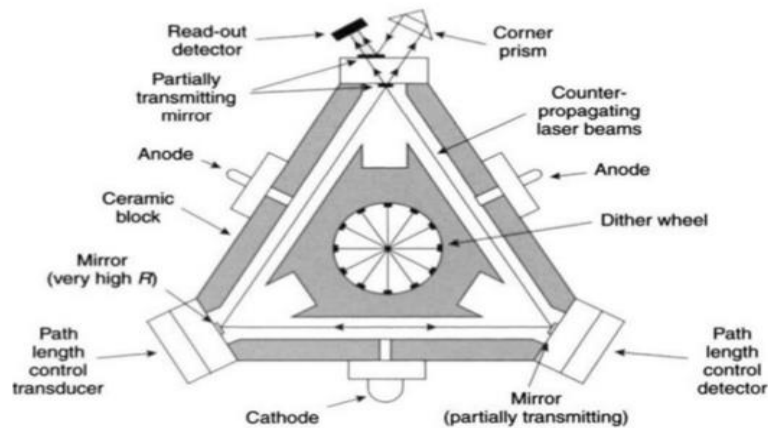


Fig 3.13 Ring Laser gyro

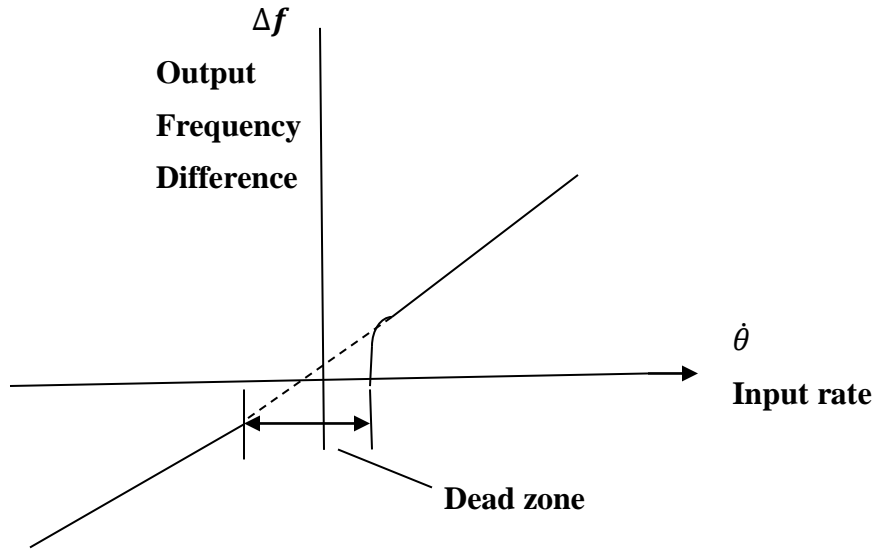


Fig 3.14 (a) Lock-in effect of mechanical dither

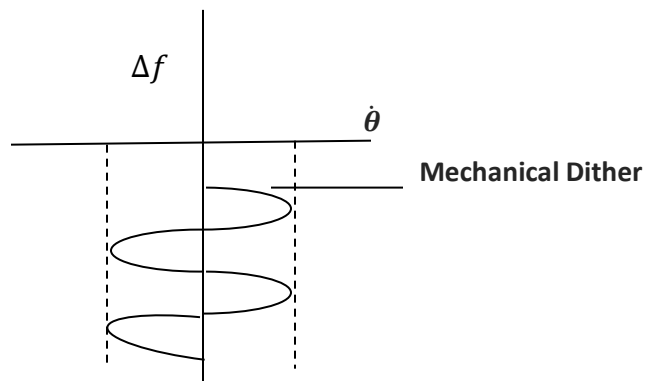


Fig 3.14 (b)

3.6 Specific force measurements with accelerometers. The acceleration of a vehicle can be determined by measuring the force required to constrain a suspended mass so that it has the same acceleration as the vehicle on which it is suspended, using Newton's second law: Force = mass \times acceleration.

The measurement is complicated by the fundamental fact that it is impossible to distinguish between the force acting on a suspended mass due to the Earth's gravitational attraction and the force required to overcome the inertia and accelerate the mass so that it has the same acceleration as the vehicle. The vehicle acceleration, \mathbf{a} , being produced by a vector sum of the external forces acting on the vehicle, namely, the propulsive thrust, \mathbf{T} , Lift, \mathbf{L} , drag, \mathbf{D} , and the gravitational force, $m\mathbf{g}$, acting on the aircraft mass, m . (The bold print denotes the quantities are vector quantities).

$$\vec{T} + \vec{L} + \vec{D} + \vec{mg} = \vec{ma}$$

$$\vec{a} = (\vec{T} + \vec{L} + \vec{D})/m + \vec{g}$$

The vector sum of the external forces excluding the gravitational force divided by the aircraft mass, that is $(\vec{T} + \vec{L} + \vec{D})/m$, is known as the 'specific force'. The force, F_a , required to constrain the suspended mass, m_a , is thus given by

$$\vec{F}_a + \vec{m}_a\vec{g} = \vec{m}_a\vec{a}$$

$$\frac{\vec{F}_a}{m_a} + \vec{g} = \vec{a} = (\vec{T} + \vec{L} + \vec{D})/m + \vec{g}$$

Hence

$$\vec{F}_a = m_a = (\vec{T} + \vec{L} + \vec{D})/m$$

i.e. the accelerometer will thus measure the specific force component along its input axis and not the vehicle acceleration components. It is thus essential to know the magnitude and orientation of the gravitational vector with respect to the accelerometer input axis in order to compute the vehicle acceleration component from the accelerometer outputs. Only if the accelerometer axis is exactly orthogonal to the gravity vector (i.e. horizontal) so that there is zero gravitational component will the accelerometer measure the vehicle acceleration component along its input axis. An accelerometer is a primary sensor responsible for measuring inertial acceleration, also known as specific force, acting on its input axis. There are several types of accelerometers, the mechanical accelerometer is here given as a model example. From physics we know that velocity is the change in position over time.

$$\bar{v} = \frac{\Delta x}{\Delta t}$$

Acceleration is the change in velocity over time. Based upon classical mechanics we know that the acceleration a body is subjected to is proportional to the force acting upon it. This is also known as Newton's second law.

$$\mathbf{F} = m\mathbf{a} \quad \rightarrow \quad \mathbf{a} = \mathbf{F}/m$$

An accelerometer can be thought of as a weight suspended on two sides with springs. The weight is known as the "proof mass" and the direction that the mass is allowed to move is known as the sensitivity axis. This is shown in fig 3.15.

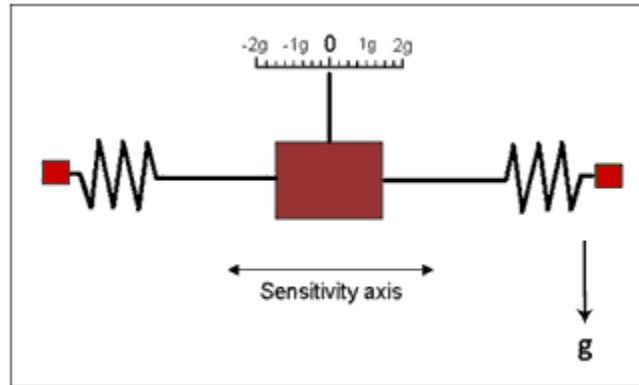


Fig 3.15 Principle of Accelerometer (input axis orthogonal to gravity vector)

If the accelerometer was subjected to a linear acceleration, the proof mass would attempt to remain at rest, in accordance with Newton's first law, which states that an object at rest tends to remain at rest. As we can imagine acceleration would cause the proof mass to shift to one side compressing one of the springs. The amount of deflection in this spring is proportional to the net acceleration. Now consider rotating the above accelerometer so that the sensitivity axis is aligned with gravity as shown in Fig 3.16.

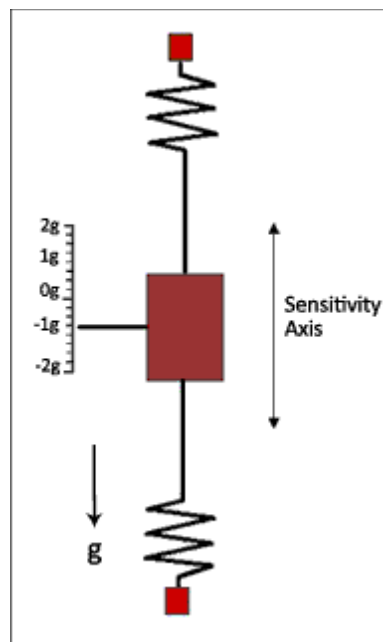


Fig 3.16 Input axis parallel to gravity vector

In this case gravity would act on the proof mass causing the bottom spring to compress. As such an accelerometer measures both the linear acceleration due to motion and the pseudo-acceleration caused by gravity. It is called pseudo-acceleration since this acceleration due to gravity doesn't necessarily result in a change in velocity or position. Because of this it isn't completely accurate to even call it acceleration, and this is why many refer to this more accurately as a specific force. The deflection of the springs is proportional to the force acting on the proof mass, which is equivalent to the linear acceleration of the accelerometer package plus the gravitational acceleration due to gravity. Simply put just remember that the output of an accelerometer is affected by both linear acceleration and gravity. Note that the accelerometer is only capable to react to specific forces and unable to measure directly field forces (the gravitational component). The gravitational component is only detectable when there is a reaction specific force to it (the Normal for example). The sensor output is a displacement related to the input and not properly an inertial acceleration.

3.7 Spring restrained pendulous accelerometers. A simple spring restrained pendulous

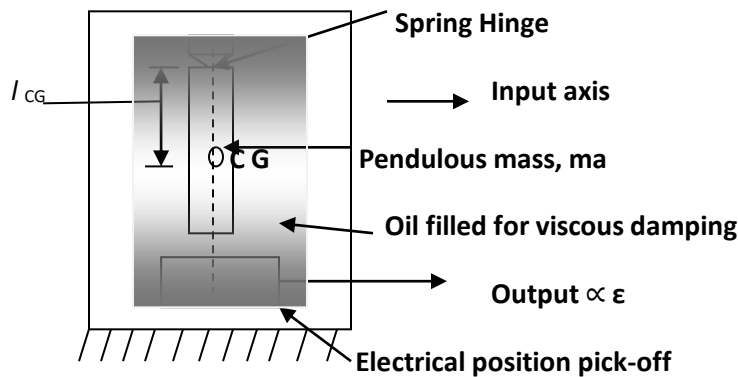


Fig 3.17 Simple spring restraint pendulous accelerometer

accelerometer is shown in Fig 3.17. This comprises an unbalanced pendulous mass which is restrained by the spring hinge so that it can move only in one direction that is along the input axis. The spring hinge exerts a restoring torque which is proportional to the angular deflection from the null position. When the case is accelerated the pendulum defects from the null position until the spring torque is equal to the moment required to accelerate the centre of mass of the pendulum at the same acceleration as the vehicle. This simple type of accelerometer is typically oil filled to provide viscous damping so that transient response is adequately damped. An electrical position pick-off measures the deflection of the pendulum from the null position and provides the output signal.

The transfer function of the simple accelerometer described above is a simple quadratic lag filter of the type

$$\frac{\text{Output}}{\text{Input acc'n}} = \frac{K_0}{s^2 + 2\xi\omega_0 s + \omega_0^2}$$

K_0 is the accelerometer scale factor, and the un-damped natural frequency $\omega_0 = \sqrt{\frac{K}{I}}$, where K is torsional spring stiffness of hinge and I is the moment of inertia of the pendulum about hinge axis. The simple spring restrained accelerometer is used in applications where the accuracy requirements are not demanding, e.g. 1 to 2 % bracket.

The maximum angular deflection of the pendulum from the null position is limited to about $\pm 2^\circ$ to minimize cross-coupling error. This results in maximum cross-axis coupling error of $\sin 2^\circ$ that is approximately 3.3% of any acceleration acting along an axis normal to the input axis. The acceleration input range thus determines the spring stiffness, or rate, and hence the bandwidth of the sensor. For example, consider an accelerometer with maximum input range of say $\pm 10g$ and an un damped natural frequency of 25 Hz. The same basic accelerometer designed for an input range of $\pm 3g$ would have a bandwidth of only 14 Hz approximately, being reduced by a factor $\sqrt{\frac{3}{10}}$.

3.8 Torque balance pendulous accelerometers. Accelerometers are devices that measure acceleration along a particular axis. The measurement of acceleration can be integrated using computers used to derive aircraft velocity and position. All accelerometers use the principle of sensing the force on a loosely suspended mass, from which the acceleration may be calculated. A common accelerometer used today is the pendulous torque balance accelerometer shown in Fig 3.18. The device is fixed to the body structure whose acceleration is to be taken (shown as the structure at the right). As the structure and the pendulous arm move, the pick-off at the end of the pendulous arm moves with respect to two excitation coils. By sensing this movement, a corrective current is applied to the restoring coil that balances the pick-off to the null position. As the restoring coil is balanced between two permanent magnets above and below, the resulting current in the restoring coil is μ proportional to the applied acceleration- in this example in the vertical direction. Typical accelerometer accuracies may vary from 50 mg ($50 \times 10^{-3}g$) down to a few μg ($1 \mu g = 1 \times 10^{-6}g$)

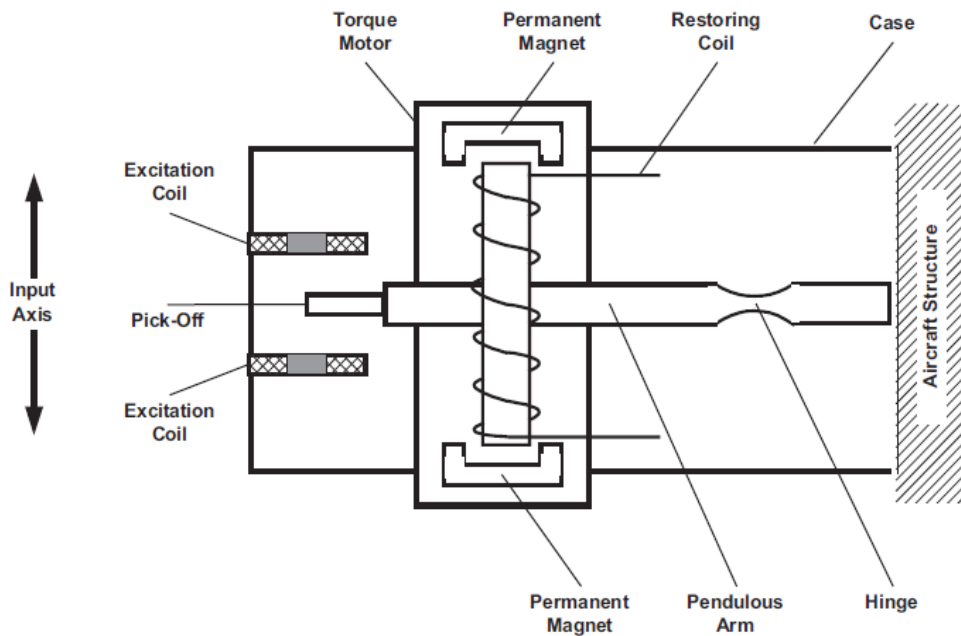


Fig 3.18 Pendulous torque balance accelerometer

A generic closed loop pendulous accelerometer might be constructed as shown in Fig 3.19. This accelerometer consists of a proof mass, a hinge, some damping, a pick-off, a Forcer, and a servo loop. The three principal accelerometer axes-the input, output (hinge), and pendulous axes (IA, OA, and PA)- are also defined in the figure. The pendulosity (the product of proof mass and the pendulous length) acts as the scaling parameter between acceleration and torque. Under acceleration along the IA, the OA torque is

$$T = F \times k = m \times a \times k = a \times p$$

Where

F = inertia force

K= length from hinge to proof mass CG

M = proof mass

a= acceleration

p = pendulosity = m × k

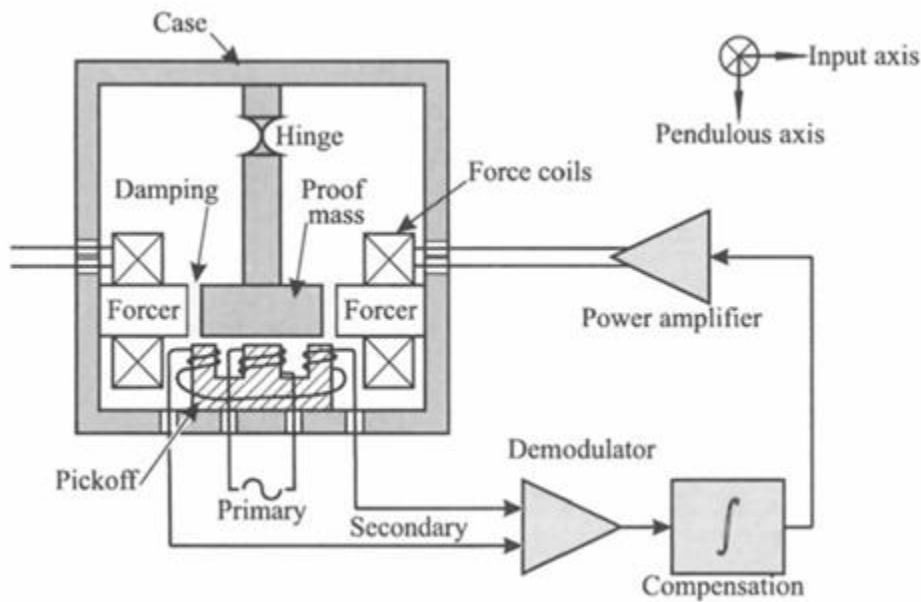


Fig 3.19 Pendulous torque balance accelerometer

Therefore

$$a = T/p$$

In analog instruments torque is proportional to the feedback current, i

$$T = k_F \times i$$

Where, k_F is forcer scale factor. Then $a = k_F \times i/p$

The instrument scale factor is

$$K = \text{output/Input}$$

$$K = i/a = p/ k_F$$

For high scale factor and sensitivity, we require high pendulosity, that is, large mass m and k . But mass should not be so large that under shock loads it creates stress levels that damage the hinge. Mission dynamics affect the choice of pendulum length. In strap-down systems, k should be small to minimize angular acceleration error.

Another torque balance accelerometer is shown in fig 3.20. The pendulous mass 'A' develops a torque proportional to the product of its mass unbalance and the applied acceleration. The movement of mass 'A' is detected by the position sensor 'B' whose output signal is connected to an amplifier. The resulting current is fed into the torque motor 'C' which then develops a torque exactly equal to, but directly opposed to the initial torque from the pendulous mass 'A'. Mass

'A' stops moving assuming a position minutely differing from its zero 'g' position. Simultaneously, the current to the torque motor is fed through a stable resistor to provide an output voltage proportional to the applied acceleration. The system is damped by means of a phase advancing network within the installation by applying an independent current input to the torque motor.

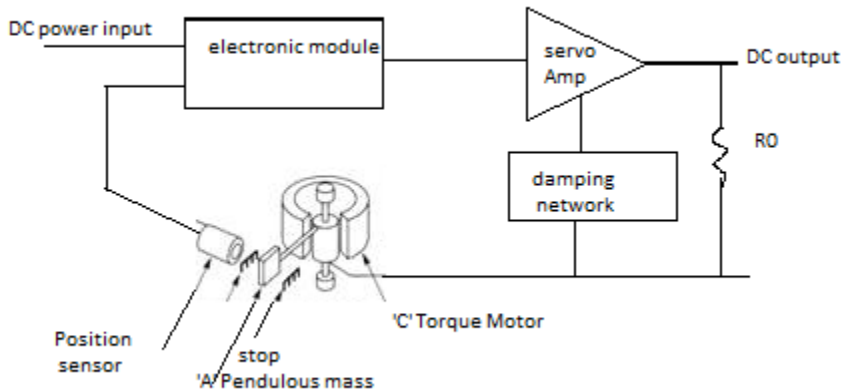


Fig 3.20 Torque balance accelerometer

3.9 Stable Platform System. In stable platform the inertial sensors are mounted on a platform which is isolated from any external rotation motion. In other words the platform is held in alignment with the global frame. This is achieved by mounting the platform using gimbals (frames) which allows the platform freedom in all three axes as shown in **Fig 3.21**. The platform mounted gyroscope detects any platform rotations. These signals are feedback to torque motors which rotate the gimbals in order to cancel out such rotations, hence keeping the platform aligned with the global axis. Resolvers provide angular information about the aircraft in relation to the platform, and hence aircraft attitude (Euler Angles) can be determined.

Gimbal Angular Pick-off signals \longrightarrow Euler angles

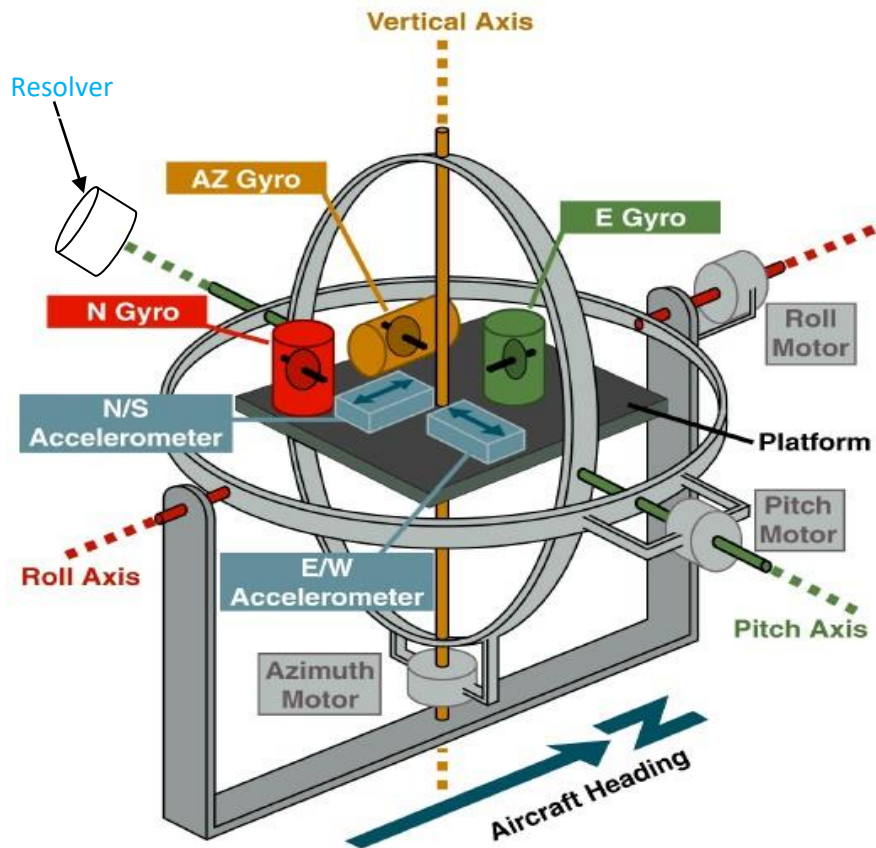


Fig 3.21 Stable Platform system

Equation that governs the rotating body

$$\vec{T} = \vec{\Omega} \times \vec{L}$$

\vec{L} is the angular momentum whose magnitude is $I \times \omega$

$\vec{\Omega}$ is the angular precession velocity of this momentum vector

\vec{T} is the torque vector.

Torque T is sensed at the gyro bearing point. Through feedback control, the gimbal motors react to negate this torque thus maintaining stable platform. Three orthogonal gyros are mounted on the stable platform. The gyros on the platform in conjunction with gimbal motors maintain the platform at a fixed attitude in an inertial frame, while the mounting frame may rotate. Thus the platform is called the stable platform.

3.10 Strap down systems. Fig 3.22 illustrates the strap down concept. The system has three gyros (for measuring roll rate (p), pitch rate (q) and yaw rate(r), three accelerometers (a_x , a_y , a_z) mounted on the rigid frame or block which is directly fixed, that is ‘strapped-down’, to the airframe. The input axes to these accelerometers are aligned along with the aircraft body axis X, (a_x), Y, (a_y) and Z (a_z). The gyros and accelerometers thus measure the angular and linear motion of the aircraft with respect to the aircraft’s body axes. The Euler angles are then computed from the body rate information by the system computer. It should be noted that a stable platform system and a strap-down system are mathematically equivalent systems. The function of the mechanical gimbals is carried out by the strap-down system computer which in effect contains a mathematical model of the gimbals.

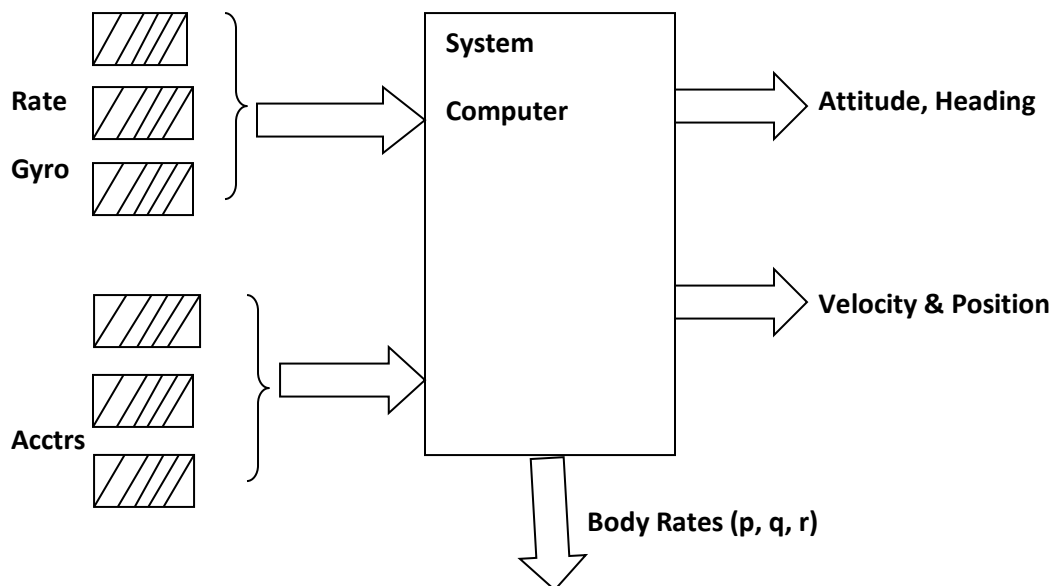
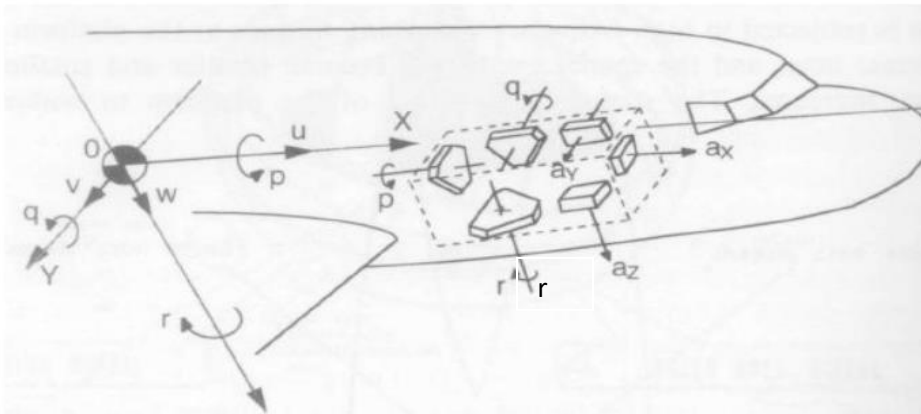


Fig 3.22 Strap-down system schematic

3.10.1 Attitude Algorithms: The Euler angles, ϕ , θ , ψ and the equations relating to body rate p , q and r are related to Euler angular rates $\dot{\phi}$, $\dot{\theta}$, $\dot{\psi}$ by the following three equations

$$\dot{\phi} = p + q \sin \phi \tan \theta + r \cos \phi \tan \theta$$

$$\dot{\theta} = q \cos \phi - r \sin \phi$$

$$\dot{\psi} = q \sin \phi \sec \theta + r \cos \phi \sec \theta$$

These equations can be expressed more compactly in matrix form

$$\begin{bmatrix} \dot{\phi} \\ \dot{\theta} \\ \dot{\psi} \end{bmatrix} = \begin{bmatrix} 1 & \sin \phi \tan \theta & \cos \phi \tan \theta \\ 0 & \cos \phi & -\sin \phi \\ 0 & \sin \phi \sec \theta & \cos \phi \sec \theta \end{bmatrix} \begin{bmatrix} p \\ q \\ r \end{bmatrix}$$

The Euler angles can then be derived from the Euler angle rates by a process of integration using an initial conditions a known attitude at a given point in time. This process becomes meaningless, however, at $\theta = 90^\circ$ when $\tan \theta$ and $\sec \theta$ become infinite. (This is mathematical equivalent of ‘gimbal lock’.) The use of three-parameter Euler algorithm is therefore generally limited to pitch angles between $\pm 30^\circ$ as the error equations are unbounded, and to avoid mathematical singularities. A fully maneuverable system is therefore required where there are no restrictions on the pitch angles. The limitations of the three-parameter Euler systems are overcome by the use of what is known as the *Euler four symmetrical parameters* to define the vehicle attitude.

It can be shown that an axis set may be moved to any required orientation by a single rotation about a suitably positioned axis. Let this axis make angles $\cos^{-1} \alpha$, $\cos^{-1} \beta$, $\cos^{-1} \gamma$ with the inertial axes OX_0 , OY_0 and OZ_0 respectively. Let a single rotation, μ , about this axis bring a moving axis set from OX_0 , OY_0 , OZ_0 into coincidence with OX , OY , OZ , the set whose orientation it is desired to specify.

The Euler four symmetrical parameters are given by

$$\left. \begin{aligned} e_0 &= \cos \mu/2 \\ e_1 &= \alpha \sin \mu/2 \\ e_2 &= \beta \sin \mu/2 \\ e_3 &= \gamma \sin \mu/2 \end{aligned} \right\} \quad (1)$$

Then e_0, e_1, e_2, e_3 can be used to specify the attitude of the vehicle with respect to OX_0, OY_0, OZ_0 .

The following relationship with Euler angles can be derived:

$$\sin \theta = 2(e_0e_2 - e_3e_1) \quad (2)$$

$$\tan \psi = \frac{2(e_0e_3 + e_1e_2)}{e_0^2 + e_1^2 - e_2^2 - e_3^2} \quad (3)$$

$$\tan \varphi = \frac{2(e_0e_1 + e_1e_3)}{e_0^2 - e_1^2 - e_2^2 + e_3^2} \quad (4)$$

It can be shown that

$$\begin{bmatrix} \dot{e}_0 \\ \dot{e}_1 \\ \dot{e}_2 \\ \dot{e}_3 \end{bmatrix} = \frac{1}{2} \begin{bmatrix} -e_1 & -e_2 & -e_3 \\ e_0 & -e_3 & e_2 \\ e_3 & e_0 & -e_1 \\ -e_2 & e_1 & e_0 \end{bmatrix} \begin{bmatrix} p \\ q \\ r \end{bmatrix} \quad (5)$$

Because four parameters are being used to describe the orientation when only three are necessary, a constraint equation exists of the form

$$e_0^2 + e_1^2 + e_2^2 + e_3^2 = 1 \quad (6)$$

These two equations have great advantages over the equivalent Euler angle equations:

- They apply to all attitudes
- The error equations are bounded by the constraint equation.
- The numerical value of each parameter always lies in the range -1 to +1, so easing the scaling problems in the computing mechanism.

Equation (5) can be re-arranged into the form

$$\begin{bmatrix} \dot{e}_0 \\ \dot{e}_1 \\ \dot{e}_2 \\ \dot{e}_3 \end{bmatrix} = \frac{1}{2} \begin{bmatrix} 0 & -p & -q & -r \\ p & 0 & r & -q \\ q & -r & 0 & p \\ r & q & -p & 0 \end{bmatrix} \begin{bmatrix} e_0 \\ e_1 \\ e_2 \\ e_3 \end{bmatrix}$$

This can be written more compactly as

$$\dot{\mathbf{X}} = \mathbf{A}\mathbf{X}$$

$$\text{Where } \mathbf{X} = \begin{bmatrix} e_0 \\ e_1 \\ e_2 \\ e_3 \end{bmatrix} \text{ and } \mathbf{A} = \frac{1}{2} \begin{bmatrix} 0 & -p & -q & -r \\ p & 0 & r & -q \\ q & -r & 0 & p \\ r & q & -p & 0 \end{bmatrix}$$

This equation can be solved by approximation integration technique by assuming p, q, r are constant over a short period of time Δt from time t_n to time t_{n+1} .

The predicted value of \mathbf{X} at time t_{n+1} , \mathbf{X}_{n+1} is given by

$$\mathbf{X}_{n+1} = \mathbf{X}_n + \dot{\mathbf{X}}_n \Delta t = \mathbf{X}_n + \mathbf{A}\mathbf{X}_n \Delta t$$

i.e. $\mathbf{X}_{n+1} = (\mathbf{I} + \mathbf{A}\Delta t)\mathbf{X}_n$; 'I' is the unity matrix.

$(\mathbf{I} + \mathbf{A}\Delta t)$ is in fact an approximation to the transition matrix which relates the value of the state vector at time t_{n+1} to the value at time t_n .

The incremental angular rotations measured about the roll, pitch and yaw axes are denoted by $\Delta P, \Delta Q, \Delta R$ respectively.

$$\Delta P = \int_{t_n}^{t_{n+1}} p dt = p \Delta t$$

$$\Delta Q = \int_{t_n}^{t_{n+1}} q dt = q \Delta t$$

$$\Delta R = \int_{t_n}^{t_{n+1}} r dt = r \Delta t$$

Hence the approximation transition matrix is

$$\begin{bmatrix} 1 & 0 & 0 & 0 \\ 0 & 1 & 0 & 0 \\ 0 & 0 & 1 & 0 \\ 0 & 0 & 0 & 1 \end{bmatrix} + \frac{1}{2} \begin{bmatrix} 0 & -\Delta P & -\Delta Q & -\Delta R \\ \Delta P & 0 & \Delta R & -\Delta Q \\ \Delta Q & -\Delta R & 0 & \Delta P \\ \Delta R & \Delta Q & -\Delta P & 0 \end{bmatrix}$$

Hence

$$\begin{bmatrix} e_0 \\ e_1 \\ e_2 \\ e_3 \end{bmatrix}_{t_{n+1}} = \begin{bmatrix} 0 & -\Delta P/2 & -\Delta Q/2 & -\Delta R/2 \\ \Delta P/2 & 0 & \Delta R/2 & -\Delta Q/2 \\ \Delta Q/2 & -\Delta R/2 & 0 & \Delta P/2 \\ \Delta R/2 & \Delta Q/2 & -\Delta P/2 & 0 \end{bmatrix} \begin{bmatrix} e_0 \\ e_1 \\ e_2 \\ e_3 \end{bmatrix}_{t_n}$$

The performance of the numerical integration algorithm can be further improved by using second-order Runge-Kutta algorithm or fourth-order Runge-Kutta algorithms where very high accuracy is required, and by decreasing the integration time constant, Δt with a more powerful computer. The constraint equation $e_0^2 + e_1^2 + e_2^2 + e_3^2 = 1$ is used to correct the transition matrix for the accumulated computational errors in the integration process to maintain orthogonality of the computed axes. The four symmetrical Euler parameters are also mathematical quaternion as it can be shown that they are made up of the sum of a scalar quantity and a vector with orthogonal components. The values of the Euler angles θ, ψ, ϕ are then calculated from equations (2), (3) and (4).

The corresponding initial values of the Euler parameters when the initial values of the Euler angles are θ, ψ, ϕ , are given by

$$\left. \begin{aligned} e_0 &= \cos \psi/2 \cos \theta/2 \cos \phi/2 + \sin \psi/2 \sin \theta/2 \sin \phi/2 \\ e_1 &= \cos \phi/2 \cos \theta/2 \sin \psi/2 - \sin \phi/2 \sin \theta/2 \cos \psi/2 \\ e_2 &= \cos \psi/2 \sin \theta/2 \cos \phi/2 + \sin \psi/2 \cos \theta/2 \sin \phi/2 \\ e_3 &= \sin \psi/2 \cos \theta/2 \cos \phi/2 - \cos \psi/2 \sin \theta/2 \sin \phi/2 \end{aligned} \right\}$$

3.10.1 Generation of Strap-down ‘Equivalent Stable Platform’. Fig 3.23 illustrates the computational process involved in generating an ‘equivalent stable platform’ within the strap-down system computer. The integration of the Euler parameter rates to yield the Euler parameters, enables the Direction Cosine Matrix (DCM) to be computed for the aircraft axes to local North, East, Down (NED) axes conversion, and vice versa. This enables the strap-down accelerometer measurements, a_x, a_y, a_z , of the aircraft acceleration components along the aircraft body axes to be converted into the aircraft acceleration components along the local NED axes, a_N, a_E, a_D . The computing system thus provides the equivalent of accelerometers mounted on a stable platform with their input axes aligned with local NED axes.

The Direction Cosine Matrix for converting to local NED axes from arbitrary body axes is

$$[DCM]_{la} = \begin{bmatrix} e_0^2 + e_1^2 - e_2^2 - e_3^2 & 2(e_1e_2 - e_0e_3) & 2(e_0e_2 + e_1e_3) \\ 2(e_0e_3 + e_1e_2) & e_0^2 - e_1^2 + e_2^2 - e_3^2 & 2(e_2e_3 - e_0e_1) \\ 2(e_1e_3 - e_0e_2) & 2(e_0e_1 + e_2e_3) & e_0^2 - e_1^2 - e_2^2 + e_3^2 \end{bmatrix}$$

Thus the aircraft acceleration components with respect to local NED axes are given by

$$\begin{bmatrix} a_N \\ a_E \\ a_D \end{bmatrix} = [DCM]_{la} \begin{bmatrix} a_x \\ a_y \\ a_z \end{bmatrix}$$

Gyros measure angular motion with respect to an inertial axis frame that is an axis frame which is fixed in space. It is therefore necessary to rotate the gyro-derived reference frame at the appropriate rates so that it stays aligned with the local NED axes because of the earth’s rotation and the vehicle’s motion over the spherical surface of the earth. The latter corrections are known as the vehicle rate corrections. In the case of stable platform, these corrections are made by précisising the vertical and azimuth gyros at the appropriate rates. In the case of strap-down system, the Earth’s rate and vehicle rate corrections are converted by the appropriate DCM to the coordinate frame rates with respect to aircraft axes. These coordinate frame rates are then

summed with the aircraft body rates, p, q, r , so that the subsequent integration will yield the aircraft attitude with respect to local NED axes (Knowing the initial conditions). The DCM for converting the co-ordinate frame rates for the earth's rate and vehicle rate from local NED axes to aircraft body axes is given by

$$[DCM]_{al} = \begin{bmatrix} e_0^2 + e_1^2 - e_2^2 - e_3^2 & 2(e_0e_3 + e_1e_2) & 2(e_1e_3 - e_0e_2) \\ 2(e_1e_2 - e_0e_3) & e_0^2 - e_1^2 + e_2^2 - e_3^2 & 2(e_0e_1 + e_2e_3) \\ 2(e_0e_2 + e_1e_3) & 2(e_2e_3 - e_0e_1) & e_0^2 - e_1^2 - e_2^2 + e_3^2 \end{bmatrix}$$

Earth's rate correction about the North, East, Down axes are $\Omega \cos \lambda, 0, \Omega \sin \lambda$ respectively where Ω is the earth's rate of rotation and λ is the latitude.

The vehicle rate corrections are $V_E/R, -V_N/R, -V_E/R \tan \lambda$ about the North, East, Down axes where V_N and V_E are the components of the aircraft's velocity along the North and East axes and R is the radius of the Earth.

Hence, the vehicle rate and Earth's rate corrections about the aircraft X, Y, Z axes are given by

$$[DCM]_{al} = \begin{bmatrix} \left(\frac{V_E}{R} + \Omega \cos \lambda \right) \\ \frac{-V_N}{R} \\ \left(-\frac{V_E}{R} \tan \lambda + \Omega \sin \lambda \right) \end{bmatrix}$$

The initial value of the direction cosine matrix between the aircraft and the local NED axes is given by

$$[DCM]_{la} = \begin{bmatrix} c\theta c\psi & s\phi s\theta c\psi - c\phi s\psi & c\phi s\theta c\psi + s\phi s\psi \\ c\theta s\psi & s\phi s\theta s\psi + c\phi c\psi & c\phi s\theta s\psi - s\phi c\psi \\ -s\theta & s\phi c\theta & c\phi c\theta \end{bmatrix}$$

Where s is sine and c is cosine.

The initial value of the direction cosine matrix between the local NED axes and the aircraft axes is given by

$$[DCM]_{la} = \begin{bmatrix} c\theta c\psi & c\theta s\psi & -s\theta \\ s\phi s\theta c\psi - c\phi s\psi & s\phi s\theta s\psi + c\phi c\psi & s\phi c\theta \\ c\phi s\theta c\psi + s\phi s\psi & c\phi s\theta s\psi - s\phi c\psi & c\phi c\theta \end{bmatrix}$$

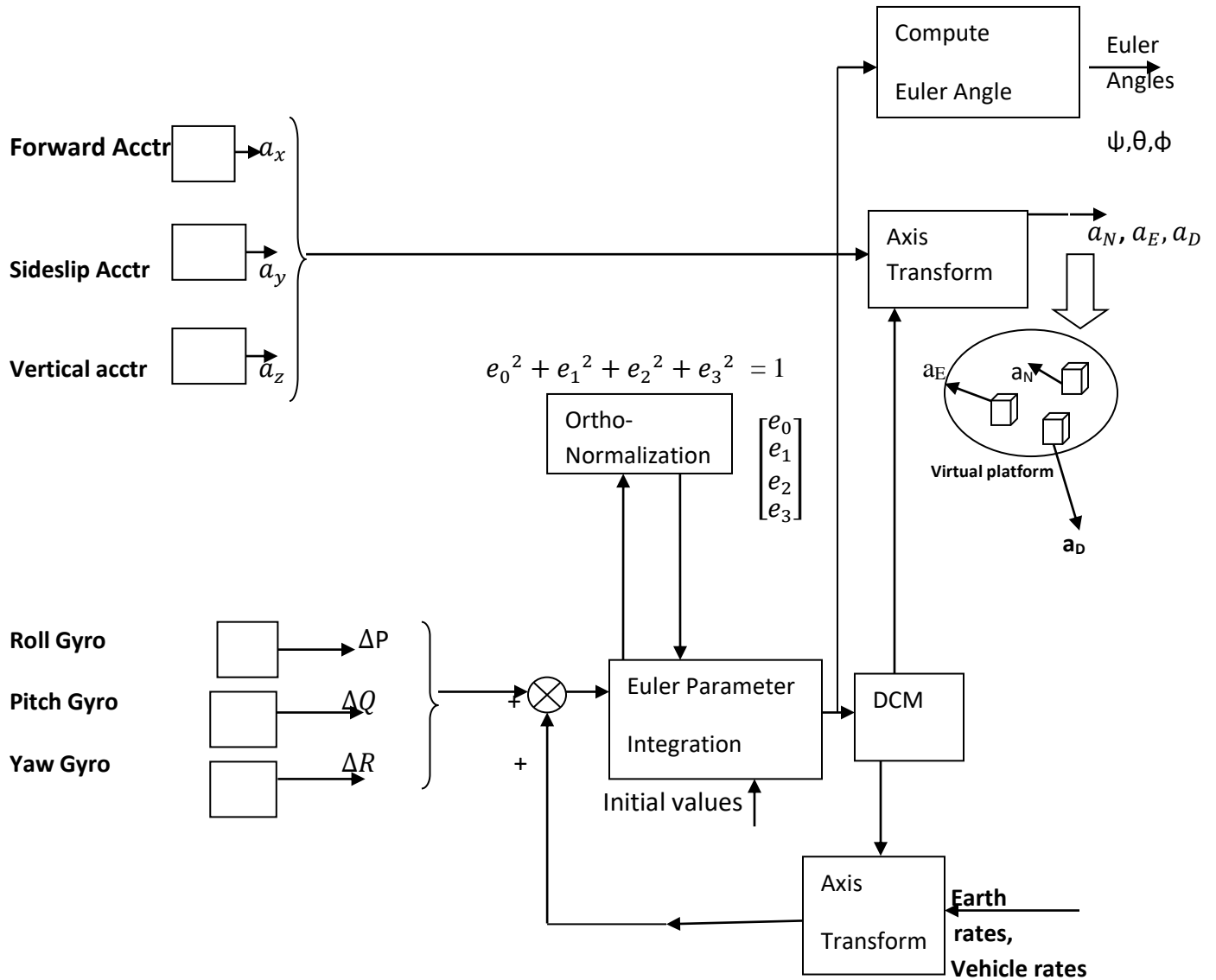


Fig 3.23: Strap-down 'Equivalent Stable Platform'

3.11 Errors in inertial systems and compensations. An inertial measuring unit consists of

- Three accelerometers
- Three gyroscopes
- Digital signal processing software/hardware

Three accelerometers are mounted at right angles to each other, so that accelerations can be measured independently in three axes: X, Y and Z. Three gyroscopes are also at right angles to each other, so that

angular rates can be measured around each of the acceleration axes. Signals from accelerometers and gyroscopes are processed through signal processing at a very high rate. The measurements are then summed, giving a total acceleration and rotation for the IMU sample period. For example, in a 200 Hz IMU, the sample period represents the total motion of the IMU over 5 milliseconds. The information about the motion of the IMU is transmitted to the INS. These measurements are used as input into the INS filter. The end result of combining the IMU information with GPS information is position, velocity and attitude. IMU measurements are integrated with respect to time, as part of the INS filter, so any errors in the measurements grow with time. To reduce the effect of measurement errors, they must be understood, estimated and then corrected. A bias error, if not removed from the measurement, is integrated twice as part of the mechanisation process. In this case, a constant bias (error) in acceleration becomes a linear error in velocity and a cubic error in position. A converged and well designed INS filter, estimates and removes errors from the IMU measurements, leading to higher attitude and longer solution stability during periods of poor GPS coverage.

3.11.1 General Error Terms due to Sensors (Accelerometer and Gyros).

- **Repeatability.** The ability of the sensor to deliver the same output for the same repeated input, assuming all other conditions are the same
- **Stability.** The ability of the sensor to deliver the same output, over time, for the same constant input.
- **Drift.** The change of the output over time (zero drift is the change over time with no input).

Not all of these errors are relevant for all IMU. The various errors are explained in the following paragraphs and shown in Fig 3.24.

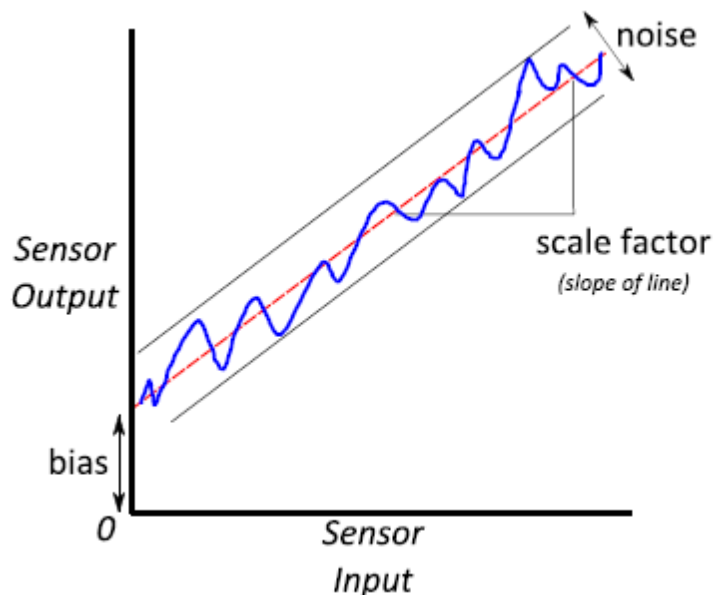


Fig 3.24 Inertial System Errors

(a) Input Range. The input range is the maximum angular rate or acceleration the IMU can meaningfully measure. Acceleration or rotation outside this range results in bad measurements or no measurements. The input range can also be described in terms of shock (linear acceleration with respect to time). Importantly, strong vibrations can lead to a poor solution, as the sensors are already saturated with signal. The actual signal of the vehicle motion (or the body that is the object of the measurement) is more difficult to separate from the noise caused by the vibration. The bandwidth of the sensor plays an important part in the ability of the sensors to measure actual motion. A low bandwidth means high frequency vibration is not properly measured, so the resulting measurement suffers from aliasing. For this reason, vibration isolation is recommended in situations where significant vibration is present or with low bandwidth sensors.

(b) Bias. For a given physical input, the sensor outputs a measurement, offset by the bias. For example, if the IMU is stationary and level, the vertical axis measures the acceleration due to gravity. Gravity has a normal acceleration of 9.81 m/s^2 . But if the measurement is biased, it may measure acceleration of 9.75 m/s^2 . The difference between the measured and real value is the bias. While the IMU is powered on, the initial bias changes over time. This change in bias is often related to temperature, time and/or mechanical stress on the system. In the case of light based gyroscopes (Fibre Optic Gyro (FOG)/Ring laser gyro (RLG)), the optical length increases or decreases with the change in the physical properties of the IMU. Often, IMUs are manufactured with temperature compensation, increasing the stability of the measurements. An INS filter constantly estimates the bias by making use of external source of information (GPS, Barometer). The estimated bias value is removed from the IMU measurements before using them in the mechanization. The process of bias estimating is more effective when stable.

(c) Scale factor. Scale factor is the relation between input and output. If the input is 100%, the expected output is 100%. The actual output is the result of a linear effect, where the output is proportional to the input but scaled. For example, if the input is 10 m/s^2 , but there is a 2% scale factor, the output measurement is 10.2 m/s^2 . This can also be described as a 20000 ppm error. Another method of describing scale factor is the slope of the sensor signal.

(d) Sensor Noise. If a sensor measures a constant signal, random noise is always present. This is described as a stochastic process and is minimised using statistical techniques.

(e) Sensor Non-orthogonality (Misalignment). The three gyroscopes and three accelerometers are mounted orthogonal to each other. The mountings, however, have errors and so are not perfectly 90 degrees. This leads to a correlation between sensors. For example, assume one axis is pointed perfectly up and the IMU is level. The accelerometer on this axis is measuring acceleration due to gravity. If the other two axes were perfectly orthogonal, they would not be measuring any of the gravity effect. If there is misalignment, they would also measure gravity,

leading to a correlation in the measurement. Careful manufacturing, as well as factory calibration, can help minimize this error source. Continuous estimation and correction during system operation is also an approach used to minimise this effect.

(f) G dependency (Acceleration Effect). Some gyroscopes and accelerometers are subject to a change in the bias depending on how the sensor experiences acceleration. This is most common in Micro Mechanical System (MEMS) gyroscopes, when the mass undergoes acceleration along the sensing axis. This effect can be modeled and removed from the measurements and is often included in the IMU signal condition stage before output of the measurements.

(g) Timing Error (Latency). The difference between the time IMU measures motion and the time that external sources like GPS measure the same motion, is very important factor in the quality of the resulting, combined solution. When the INS+GPS timing disagree, by large enough factors, errors become apparent, especially in dynamic situations. Integrated INS equipment corrects for this error in measurement time automatically and removes this error from the output measurements and final navigation solution.

(h) Compensating INS Errors Using INS Filter. As explained, errors in INS increases with time because on integration effect. These errors are removed by combining the INS data with other sensor. One of the most common alternative sensors is a satellite navigation radio, such as GPS. Sensor fusion refers to processes in which signals from two or more types of sensor are used to update or maintain the state of a system. In the case of inertial navigation systems the state generally consists of the orientation, velocity and displacement of the device measured in a global frame of reference. A sensor fusion algorithm maintains this state using IMU accelerometer and gyroscope signals together with signals from additional sensors or sensor systems. There are many techniques for performing sensor fusion, the most popular of which are Kalman filter.

3.11.2 Errors due to digital processing of Attitude information. The strap-down system accuracy is critically dependent on the accuracy of digital signal processing involved in the numerical solution of the attitude algorithm. The major error sources in digital processing are briefly discussed below, together with methods used to minimize these errors.

(a) Commutation. Errors arise in digital processing because of the non-commutativity of angular motion. A different attitude is attained if a series of rotation about the body axes are made in different order. Commutation errors are introduced in the numerical processing because for each solution update of the transformation matrix, the processor operates sequentially on the input angular increments in a fixed order. This may not correspond to the actual time ordered sequence in which the angles were accumulated in the vehicle. Commutation errors can thus arise in deriving the vehicle attitude particularly when subjected to cyclical or repetitive inputs such as conical motion, which can result in a rectification drift of the transformation matrix.

These commutation errors can be minimised by decreasing the angle increment size involved in each computation.

(b) Integration. Errors arise in the integration because of using discrete approximate solutions of a continuous process and equations which have no analytic solution. These errors are minimised by using sophisticated integration algorithms (e.g. Runge-Kutta fourth order) and by increasing the update rate.

(c) Round off. These errors are due to the finite resolution of data and rounding off the computations to the value of the least significant bit. Double precision working (32 bit) for critical operations is used to minimise these errors.

(d) Quantization. These errors result from the process of converting the analog output of the sensors into discrete increments which can be input as a series of pulses into the digital computer. This quantization process causes the input to the computer to always lag the outputs of the sensors. The average value of this quantization(or sensor storage error) is one half of the quantization angle. This information is not lost but received in the next update cycle and results in a quantization noise in the output that needs to be modelled for the best performance. These errors are minimized by decreasing the quantization angle and mathematical modelling.

3.12 Attitude with Respect to Local North, East, Down Axes.

3.12.1 Introduction. The aircraft Pitch and Bank angles are required with respect to the local level plane, that is a plane which is normal to the local vertical, defined as a line through the aircraft to the Earth's centre. The aircraft heading angle is generally required with respect to true North, that is the direction of the local meridian pointing towards the North pole.(The local meridian being a circle round the Earth which passes through the North and South Poles and the aircraft's present position). It is therefore necessary to convert the gyro derived data, which is with respect to inertial axes, to an Earth referenced axis frame.

There are three basic directional references which are used to align an Attitude and Heading Reference System (AHRS) or INS. These comprise:

- Earth's gravitational acceleration vector- This is sensed by the accelerometers and enables the local vertical to be determined.
- Earth's angular Velocity Vector. This can be measured by the gyros, provided they are of sufficient accuracy, and enables the aircraft heading to be determined by a process known as 'Gyro compassing' . It can be shown that a heading accuracy of 0.1 deg, however, requires the gyro bias uncertainty to be less than 0.01 deg/hour. The technique is therefore not suitable for AHRS using lower accuracy gyros.
- Earth's magnetic field. This enables a heading reference to generally within 0.7 deg accuracy to be established at latitude below 60 deg North or South of the equator.

Fig 3.25 illustrates the basic Earth reference axis frame, generally referred to as a 'local level, North slaved axis frame' or 'North, East, Down axes-NED'.

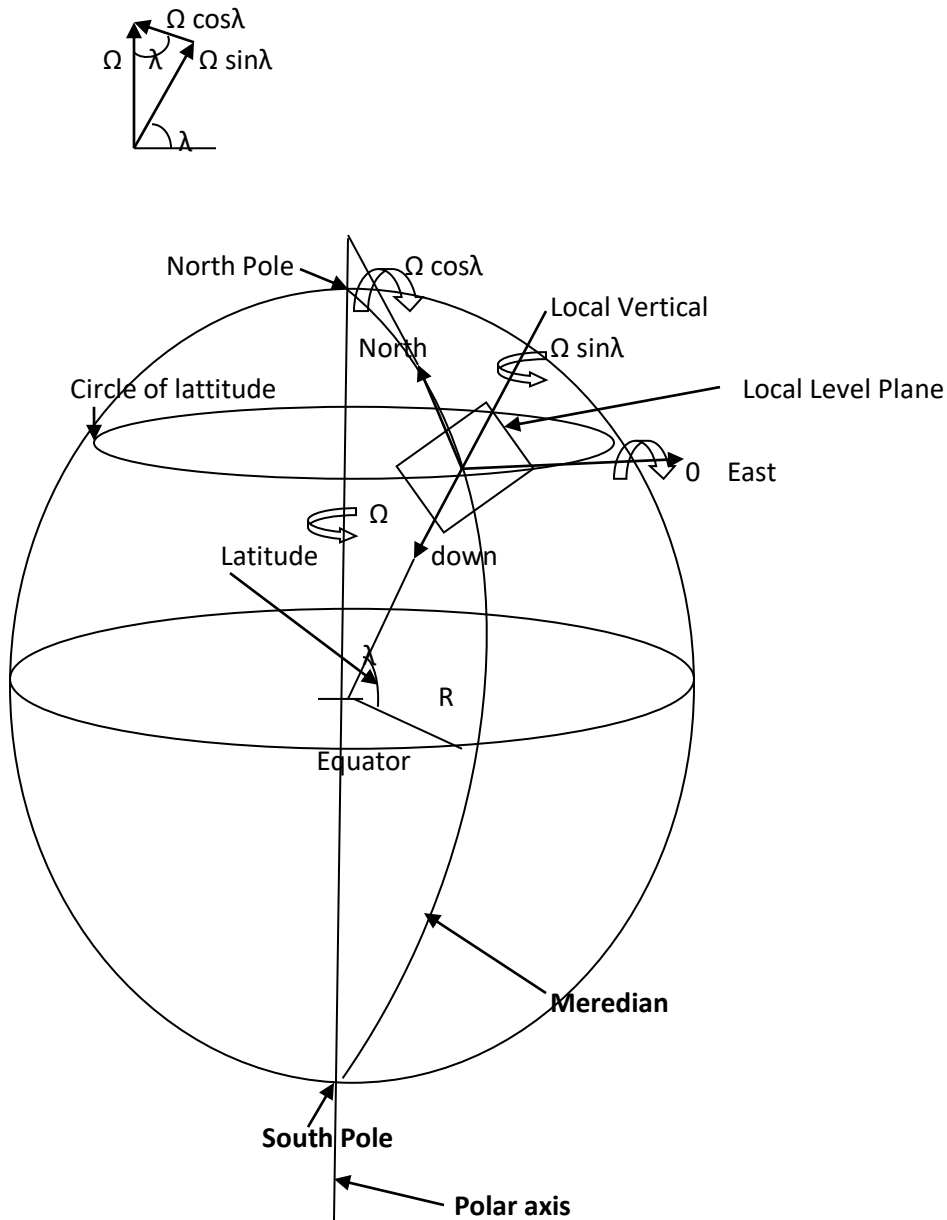


Fig 3.25 Earth's Rotation Rate Components

3.12.2 Angular rate correction for the Earth's Rotation. Fig 3.25 and accompanying vector diagram show the Earth's angular velocity vector, Ω , can be resolved into two components.

(a) Component about the North pointing axis is $\Omega \cos \lambda$, where λ is the latitude angle at the aircraft's position. This correction must be applied to the computer derived axes of the virtual stable platform to maintain a level state. As an example, at a latitude of $51^\circ 30'N$ (London Area), the Earth's rate component about the North axis is $15 \cos 51^\circ 30'$ degrees per hour = $9.3377^\circ/\text{hour}$ ($\Omega = 15^\circ/\text{hour}$).

(b) Component about the local vertical axis is $\Omega \sin \lambda$.

This correction must be applied to the virtual stable platform, if it is desired to maintain it pointing North. It should be noted that there is zero component of the Earth's angular velocity about the East pointing axis and this forms the basis of the gyro compassing alignment technique.

3.12.3 Vehicle rate correction. Fig 3.26 illustrates how local vertical rotates in space as the aircraft flies over the surface of the earth because the Earth is spherical. The angular rates are equal to:

- V_N/R about the East pointing axis, where V_N is the northely component of the aircraft's velocity and R is the radius of the Earth.
- V_E/R about the North pointing axis, where V_E is the Easterly component of the aircraft's velocity.

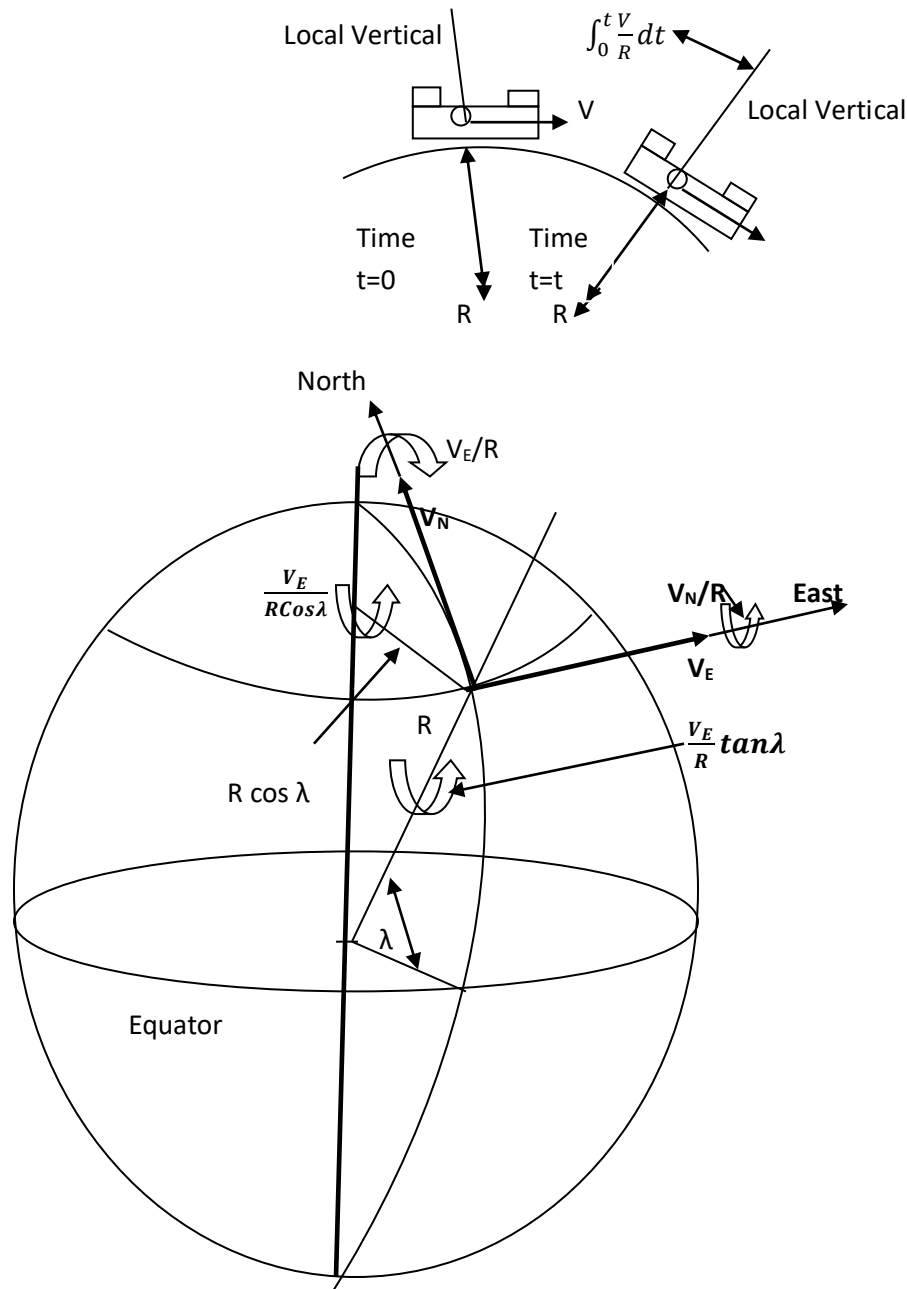


Fig 3.26 Vehicle Rates

These angular rates are referred to as the vehicle rates. It is therefore necessary to rotate the virtual platform about the East pointing and the North pointing axes at angular rates of V_N/R and V_E/R respectively in order to maintain the virtual platform locally level as the aircraft moves over the spherical surface of the Earth. The magnitude of these vehicle rate correction terms is more easily appreciated by expressing the aircraft's velocity in knots (nautical miles/hour) bearing in mind 1 nautical mile is equal to 1 minute of arc at the Earth's surface. For example, an aircraft with a ground speed of 600 knots and track a track angle of 030° has a northely velocity compone $V_N = 600 \cos 30^\circ$, that is 519.615 knots and an easterly velocity component $V_E = 600 \sin 30^\circ$, that is 300 knots. A correction rate equal to $519.6/60$, that is $8.66^\circ/\text{hour}$, about the East axis and $300/60$, that is $5^\circ/\text{hour}$, about the North axis, is required in order to maintain the platform (real, or virtual in the case of a strap-down system) locally level.

An external source of velocity such as a Doppler radar, or less accurately air data, can be used to derive the northing and easting velocity components for the vehicle rate correction terms. The Doppler or air data derived velocity components would generally be combined with the inertially derived velocity componets from the accelerometers. The use of very high accuracy gyros and accelerometers enables the velocity components to be derived directly from the accelrometers and fed back to correct the vertical reference so as to form a Schuler tuned system.

There is also a vehicle rate correction, $(V_E/R) \tan \lambda$, about the local vertical down (axis) which must be applied to the virtual platform in order to maintain the north reference. The fig 3.26 shows the three vehicle rate correction terms V_N/R , V_E/R , $(V_E/R) \tan \lambda$. The $(V_E/R) \tan \lambda$ term is derived by resolving the vehicle rate component about the Earth's polar axis $V_E/(R \cos \lambda)$, through the latitude angle, viz.

$$\frac{V_E}{R \cos \lambda} \sin \lambda = \frac{V_E}{R} \tan \lambda$$

It can be seen that the $(\frac{V_E}{R} \tan \lambda)$ term increases rapidly at high latitudes and becomes infinite at the poles when $\lambda = 90^\circ$. Alternative co-ordinate systems are used to overcome this limitation at high latitudes ($> 75^\circ$).

3.13 Global Navigational Satellite Systems-the Global Positioning System (GPS). GPS is basically a radio navigation system which derives the user's position from the radio signals transmitted from a number of orbiting satellites. GPS provides a superior navigation capability to all previous radio navigation systems. Civilians use of GPS is now wide spread, for example, GPS receivers are fitted in many cars, vans and lorries . Equipment required by the GPS user is entirely passive and requires a GPS receiver only. Electronic miniaturisation has enabled very compact and light weight GPS receivers to be produced. The full positional accuracy of 16m (3D) and velocity accuracy of 0.1 m/s is now available to civil users (previously, only military users were able to achieve this accuracy). Precise time to within a few billionths of a secon is also available. The use of GPS in conjunction with ground station system which transmits corrections to the user system, known as Differential GPS, has enabled a positional accuracy of 1 m to be achieved.

3.13.1 GPS System Description. The overall GPS system comprises three segments, namely the space segment, the control segment and the user segment and is shown in fig 3.27. The three segments are briefly summarised below.

(a) Space segment. This comprises 24 GPS satellites placed in six orbital planes at 55° to the equator in geo-synchronous orbits at 20,000 km above the Earth. The orbit tracks over the Earth, forming an 'egg beater' type pattern. 21 satellites are required for full worldwide coverage and three satellites act as orbiting spares.

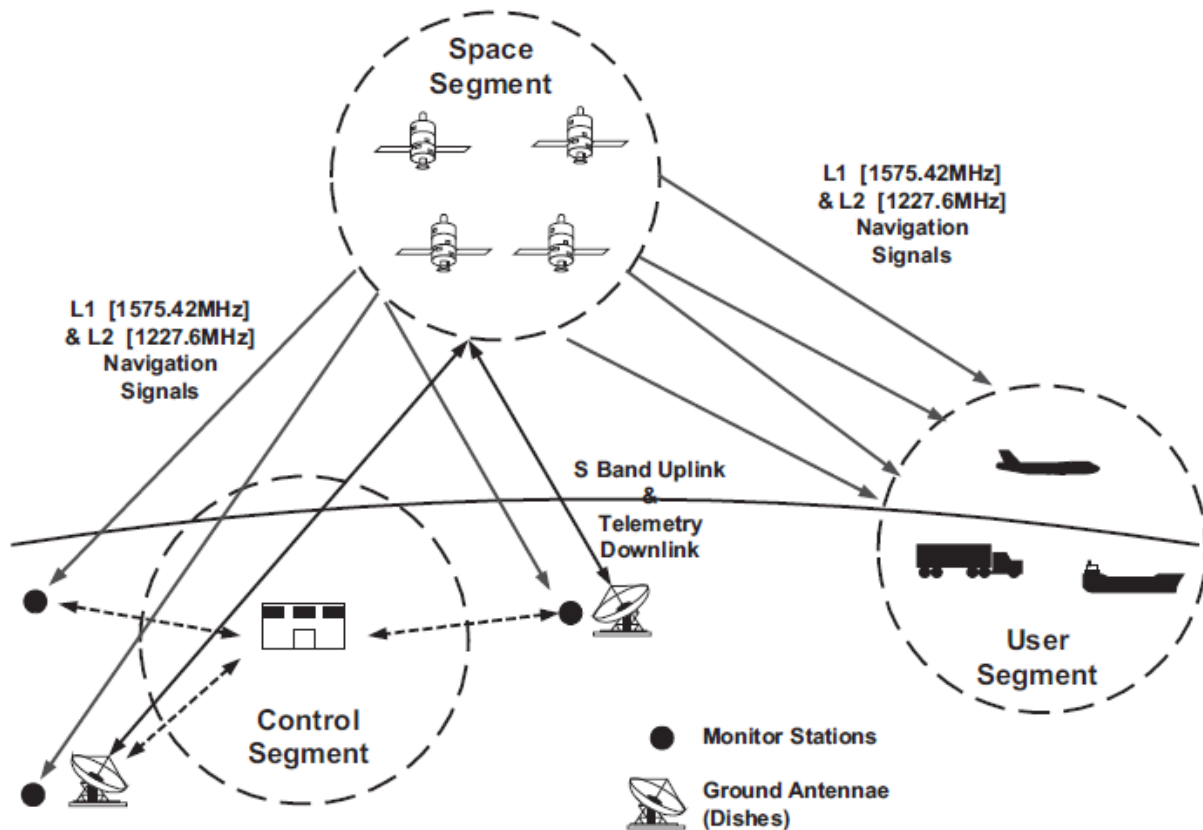


Fig 3.27: The GPS System

The GPS satellites use two frequency transmission, L1 at 1575.42 MHz and L2, at 1227.6 MHz for transmitting the digitally encoded navigation messages data at 50 Hz modulation on both L1 and L2 channels. The navigation message data will comprise the satellite orbital position parameters, clock correction parameters and health information for itself and the other satellites, and almanac data for all the satellites. Spread spectrum techniques are used on both the L1 and L2 frequency channels. The L1 carrier is modulated by a 1.023 MHz clock rate pseudo-random code known as the Coarse/Acquisition (C/A) code; a different C/A code is assigned to each satellite. A quadrature carrier component of the L1 signal is modulated by the Precise (P) code which uses ten times the clock rate of the C/A code.

The L2 transmission is modulated by the P code only and enables corrections to be made for ionospheric delay uncertainties, the dual frequency transmission enabling these corrections to be derived. It should be noted that, until fairly recently, the GPS accuracy available to civil users was deliberately degraded to 100m. The full accuracy of 16 m could only be obtained by military users with access to the P code on the L2 transmission, which was encrypted. The restriction was removed in 2000.

(b) Control Segment. This comprises a Master Control Station at Colorado Springs in the USA and five monitor stations located worldwide. The control segment is operated by the United States Department of Defense (DoD). The control segment tracks the satellites and predicts their future orbital position data and the required satellite clock correction parameters, and the updates each satellite on the uplink as it goes overhead. The GPS full system accuracy is only available when the operational control segment is functioning properly and navigation messages are uploaded on a daily basis. The GPS satellites are, however, designed to function with the control system inoperable for a period of 180 days with gradually degraded accuracy. This gives the GPS system a high degree of robustness.

(c) User Segment. The user segment equipment is entirely passive and comprises a GPS receiver. A very wide variety of compact, light weight and inexpensive GPS receivers are now available, all using the same basic concepts.

The user system operation is very briefly as follows. The operator first enters the estimated present position and the time. The GPS receiver then starts to search for and track satellites. The data coming in identifies the satellite number, locates the satellite in space and establishes the system time. The GPS receiver needs to track the signals from at least four satellites to determine the user's position. The user's 3 D position is determined to an accuracy of 16 m RMS, 3D velocity to 0.1 m/s RMS by measuring the Doppler shifts, and time to within 100 ns (1 sigma).

3.13.2 Basic Principles of GPS. The basic principle of position determining using the GPS system is to measure the spherical ranges of the user from a minimum of four GPS satellites. The orbital positions of these satellites relative to the Earth's surface are known to extremely high accuracy and each satellite transmits its orbital position data. Each satellite transmits a signal which is modulated with the C/A pseudo-random code in a manner which allows the time of transmission to be recovered.

The spherical range of the user from the individual transmitting satellite can be determined by measuring the time delay for the satellite transmission to reach the user. Multiplying the time delay by the velocity of light then gives the spherical range, R , of the user from the transmitting satellite. The user's position lies on the surface of a sphere of radius, R , as shown in Fig 3.28.

The system depends on precise time measurements and requires atomic clock reference standards. The need for extremely high accuracy in the time measurement can be seen from the fact that a 10^{-8} seconds) time error results in a distance error of 3 meters, as the velocity of light is 3×10^{-8} m/s.

Each GPS satellite carries an atomic clock which provides the time reference for the satellite data transmission. Assume that the time is perfect, given a perfect time reference in the user equipment, measurement of the spherical ranges of the three satellites would be sufficient to determine the user's

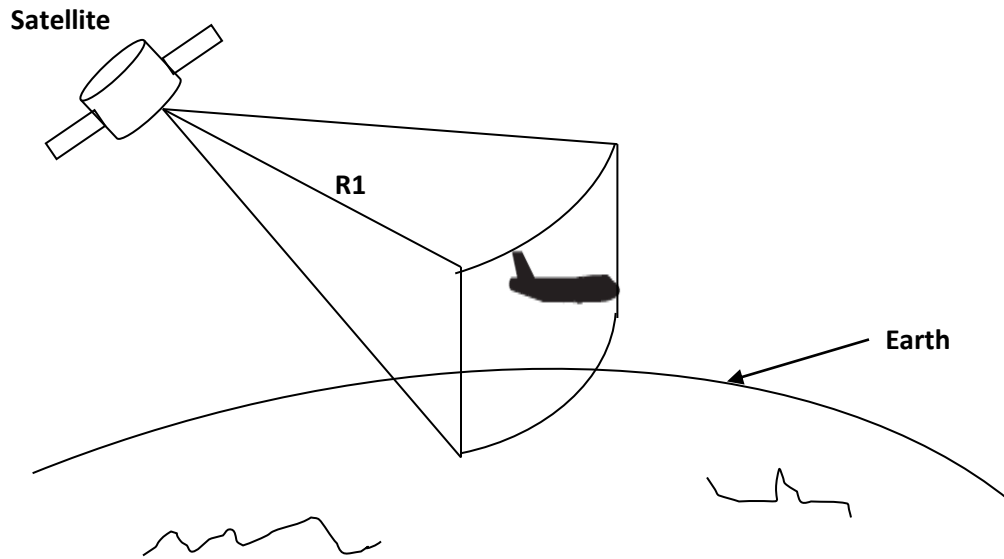


Fig 3.28 GPS spherical ranging

position. The user's equipment, however, has a crystal clock time reference which introduces a time bias in the measurement of the transit times of the satellite transmissions. The measurement of the time delay is thus made of two components. The first component is the transit time of the ranging signal and the second component is the time offset between the transmitter clock and the receiver clock due to non-synchronisation of the clocks.

Measuring the spherical ranges from four satellites as shown in Fig 3.29 enables the user's position to be determined and yields four equations containing four unknowns, viz the three position co-ordinates of the user and the time bias in the user's clock. The position co-ordinates of the user can thus be determined together with very accurate time information. Fig 3.30 shows the data transmission wave forms and illustrates the user time time bias ΔT , and the time delays Δt_1 , Δt_2 , Δt_3 , and Δt_4 for the signals transmitted from the satellites to reach the user.

Four pseudo ranges R_{1p} , R_{2p} , R_{3p} , R_{4p} to the four satellites S1, S2, S3, S4 can be determined, viz.

$$R_{1p} = c\Delta t_1$$

$$R_{2p} = c \Delta t_2$$

$$R_{3p} = c \Delta t_3$$

$$R_{4p} = c \Delta t_4$$

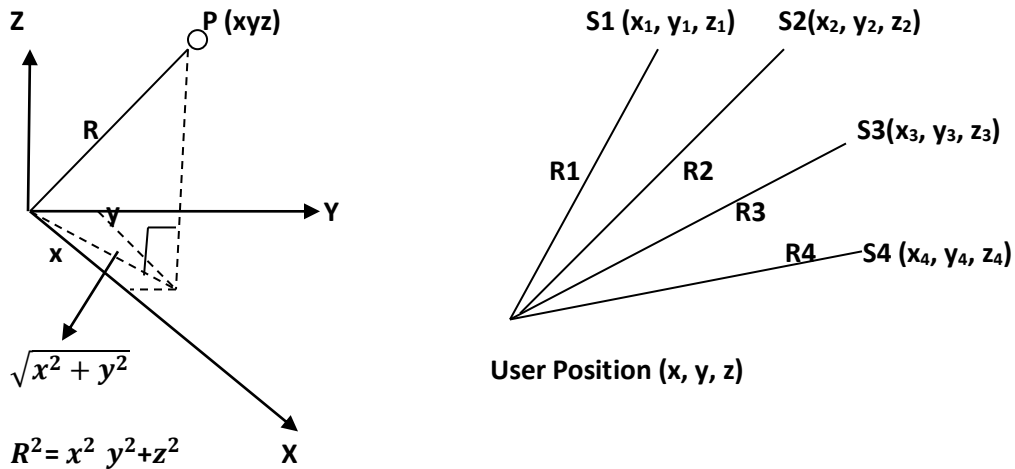


Fig 3.29 User-satellite Geometry

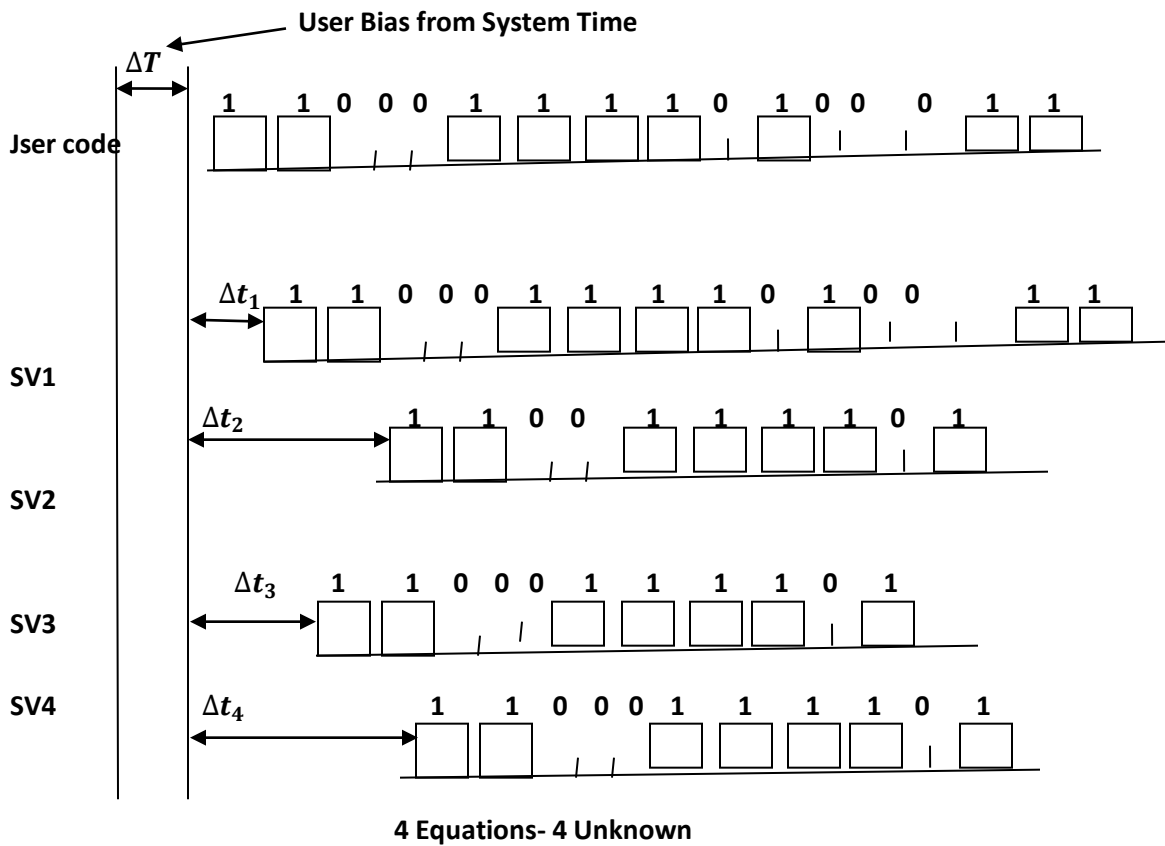


Fig 3.30 GPS Satellite waveforms with perfect satellite clocks

Let the range equivalent of the user's clock offset be T, i.e.

$$T = c \Delta T$$

Hence, from basic 3D co-ordinate geometry (refer Fig 3.28)

$$R_1 = [(X - X_1)^2 + (Y - Y_1)^2 + (Z - Z_1)^2]^{1/2} = R_{1p} - T$$

$$R_2 = [(X - X_2)^2 + (Y - Y_2)^2 + (Z - Z_2)^2]^{1/2} = R_{2p} - T$$

$$R_3 = [(X - X_3)^2 + (Y - Y_3)^2 + (Z - Z_3)^2]^{1/2} = R_{3p} - T$$

$$R_4 = [(X - X_4)^2 + (Y - Y_4)^2 + (Z - Z_4)^2]^{1/2} = R_{4p} - T$$

When R_1, R_2, R_3, R_4 are the actual ranges from the user's position to the four satellites S1, S2, S3, S4 and the coordinates of these satellites are $(X_1 Y_1 Z_1), (X_2 Y_2 Z_2), (X_3 Y_3 Z_3), (X_4 Y_4 Z_4)$ respectively.

These four equations with four unknowns can thus be solved and yield the user's position coordinate (X Y Z) and the user's time offset, ΔT .

The assumption of perfect satellite clock made initially is not valid one and in fact the clocks are slowly but steadily drifting away from each other. The satellite clocks are therefore, mathematically synchronized to a defined GPS Master time which is maintained at the Master Control station. This GPS time is continuously monitored and related to the Universal Time Co-ordinate (UTC) maintained by the United States Naval Observatory. The navigation user requires the Ephemeris parameters, that is the instantaneous position data of the GPS satellites which are used for range measurement, as well as the clock parameters in order to compute the users position. Clock and Ephemeris parameters are down linked to the user at 50 bits per second data rate modulated in both C/A and P code navigation signals. The navigation message uses a basic format consisting of a 1500 bit long frame made up of five sub-frames, each sub-frame being 300 bits long. Each satellite also transmits almanac data of all satellites to the user. This is primarily to facilitate satellite acquisition and to compute what is known as the **geometric dilution of precision** (GDOP) values to assist the selection of satellites to achieve better accuracy. The optimum geometry occurs when one satellite is at the user's zenith (directly over-head) and at least three other satellites are evenly spaced around the user's horizon. Conversely, a large error would occur if the satellites are clustered together, so that their lines of sight tended towards being parallel. Health data of all satellites is also transmitted.

3.14 Integration of GPS and INS. GPS and INS are wholly complementary and their information can be combined to the mutual benefit of both systems. For example:

- Calibration and correction of INS errors- the GPS enables very accurate calibration and correction of the INS errors in flight by means of Kalman filter.
- The INS can smooth out the step change in the GPS position output which can occur when switching to another satellite because of the change in inherent errors.
- Jamming resistance- like any other radio system, GPS can be jammed, albeit over a local area, although it can be given a high degree of resistance to jamming. The INS, having had its errors

previously corrected by the Kalman filter, is able to provide accurate navigation information when the aircraft is flying over areas subjected to severe jamming.

- Antenna obscuration- GPS is a line of sight system and it is possible for the GPS antenna to be obstructed by the terrain or aircraft structure during manoeuvres.
- Antenna location correction-the GPS derived position is valid at the antenna and needs to be corrected for reference to the INS location. The INS provides attitude information which together with the lever arm constants enables this correction to be made.

3.15 Differential GPS(DGPS).

3.5.1 Introduction to DGPS. The horizontal position accuracy available to all GPS users (civil and military) is now 16 m. this was not the case, however, until 2000 when the restriction of 'Selective Availability' was removed. Concerns about potential enemies using GPS to deliver missiles and other weapons against the US had led to a policy of accuracy denial, generally known as selective Availability. The GPS ground stations deliberately introduced satellite timing errors to reduce the positioning accuracy available to civil users to a horizontal positioning accuracy of 100 m to a 95% probability level. This was deemed adequate for general civil navigation use, but in practice it did not satisfy the accuracy or integrity requirements for land or hydrographic surveying, coastal navigation or airborne navigation. It should be borne that even 16 m accuracy, now available, is insufficiently accurate for many applications. For example automatic landing in case of airborne applications.

A supplementary navigation method known as Differential GPS(DGPS) has therefore been developed to improve the positioning accuracy for the growing number of civil applications. DGPS can be defined as:

Positioning of a mobile station in real-time by corrected (and possibly Doppler or phase smoothed) GPS pseudo range. The corrections are determined at a static 'reference station' and transmitted to the mobile station. A monitor station may be part of the system, as a quality check on the reference station transmissions.

3.5.2 Basic principles of DGPS. The basic principle underlying DGPS is the fact that errors experienced by two receivers simultaneously tracking a satellite at two stations fairly close to each other will largely be common to both receivers. The basic differential GPS concept is illustrated in Fig 3.31. The position of the stationary GPS receiver station is known to very high accuracy so that the satellite ranges can be accurately determined, knowing the satellite ephemeris data. The errors in the pseudo-range measurements can then be derived and the required corrections computed and transmitted to the user's receiver over a radio link. The errors present in a GPS system are illustrated in Fig 3.32 and are briefly discussed below:

(a) GPS Satellite clock. GPS satellites are equipped with very accurate atomic clocks and corrections are made via the Ground Stations. Even so, very small timing errors are present and so contribute to the overall position uncertainty. Selective availability deliberately introduced noise equivalent to around 30 m in the individual satellite clock signals.

(b) Satellite ephemeris errors. The satellite position is the starting point for all the positioning computations, so that errors in the Ephemeris data directly affect the system accuracy. GPS satellites are injected into very high orbits and so are relatively free from the perturbing effects of the Earth's upper atmosphere. Even so, they still drift slightly from the predicted orbits and so contribute to the system error.

(c) Atmospheric errors. Radio waves slow down slightly from the speed of light in vacuum as they travel through the ionosphere and the Earth's atmosphere. This is due respectively to the charged particles in the ionosphere and the water vapor and neutral gases present in the troposphere. These delays translate directly into a position error. The use of different frequencies in the L1 and L2 transmission enables a significant correction to be made for ionosphere delays. (It should be appreciated that this facility was not available to civil users prior to 2000.)

(d) Multi-path errors. The GPS satellite signal is received by the direct line of sight (LOS) path, but the signal may also be received as the result of reflections off local obstructions. The reflected signals arrive slightly delayed from the direct LOS signal and are termed multi-path signals. The resulting noise is called multi-path error.

(e) Receiver clock. Internal noise in the GPS receiver clock introduces a small error.

DGPS enables most of the above errors to be counteracted, as they are common to both the Reference station receiver and the user receiver. The exceptions are the multi-path and receiver errors as these are strictly local phenomenon.

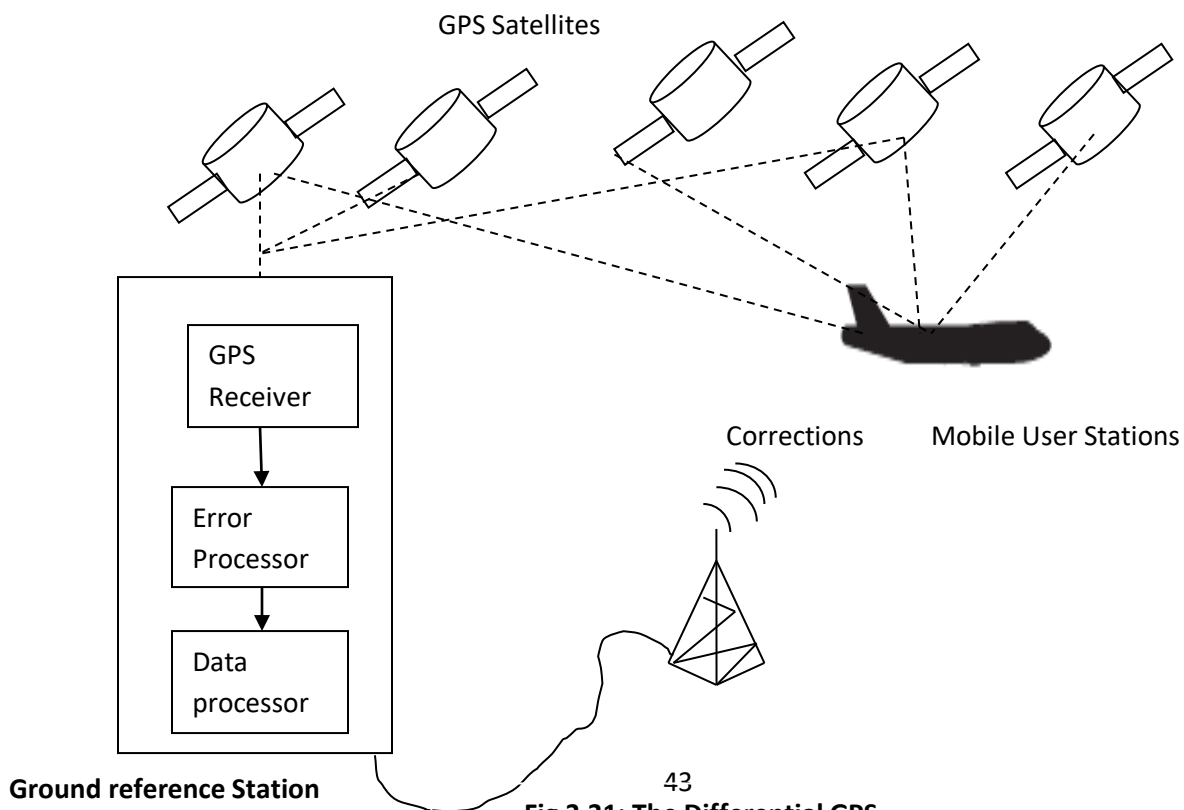


Fig 3.31: The Differential GPS

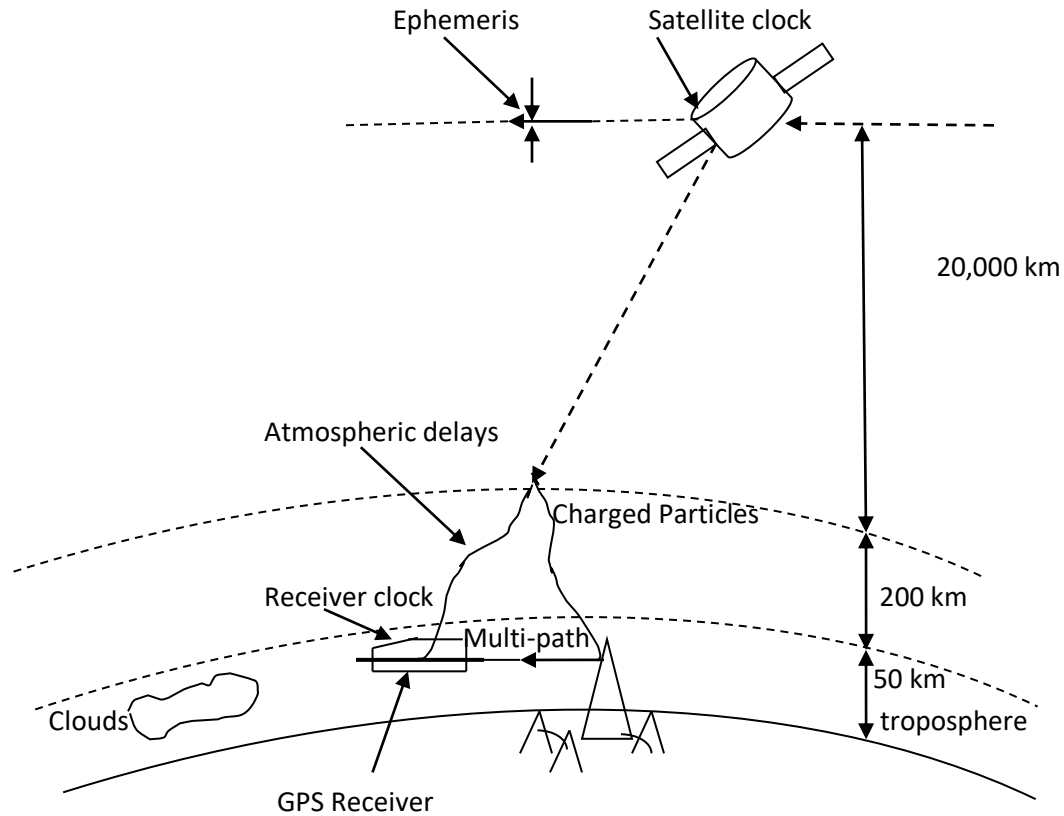


Fig 3.32: GPS error sources

3.6 Augmented satellite navigation systems. The advent of satellite navigation systems and satellite communication links has provided new capabilities for aircraft precision navigation, particularly in civil operations. Integrity and accuracy requirements can only be met, provided navigation systems are able to support all phases of flight including all-weather precision approaches to airports not equipped with ILS (or MLS) installations. In conjunction with satellite communication links, they can also provide the capability for remote air traffic control as shown in Fig 3.33. Successful concept proving trials have been conducted using on-board GPS receivers and SAT COM radios to monitor the aircraft flight path on normal commercial flights from UK to West Indies.

Some reservations exist to whether the integrity of the present GPS systems is sufficiently high to meet the navigation integrity requirements in safety critical phases of the flight and adverse weather conditions. Although the probability of GPS receivers producing erroneous position data is very low, there have been recorded instances of erroneous GPS position data in flight.

There have also been reservations about total reliance on GPS, as it is a military system which is completely under the control of the US military command, although it is freely available to any user. The accuracy available to civil users during the 1990s was limited to 100m by the policy of Selective Availability.

An augmented satellite navigation system provided by additional satellite under international civil control was therefore proposed and studied in detail by the European civil authorities from the late 1990s. The additional ranging signals and monitoring will enable the integrity requirements to be met and will also provide increased accuracy. European Union is developing Galileo system with 40 orbiting satellites. The system will provide a positional accuracy of the order of 1 meter worldwide when it comes to operation. ISRO also is launching satellite for the navigation purpose.

The development of differential GPS has enabled Ground Reference Stations to monitor the quality of the satellite transmissions. They provide an additional check on the GPS system integrity for users within a 500 to 1000 mile radius of these stations and enable differential corrections to be transmitted to these users. Increased accuracy is obtained with errors in the few meter brackets, depending on the range from the Ground Station.

A GPS satellite augmentation system is being developed in the USA under the auspices of the FAA called the Wide Area Augmentation System, WASS. The WASS system is shown in Fig 3.34. This will provide increased integrity by monitoring the GPS satellite transmission from a network of monitor ground stations in the US and increase the system accuracy by transmitting the differential corrections over communication satellite radio links. User position accuracy should be within 3 meters enabling precision approaches to be accomplished in Cat 2 visibility conditions. Extensive trials have been conducted towards the evaluation of WASS by FAA with very promising results.

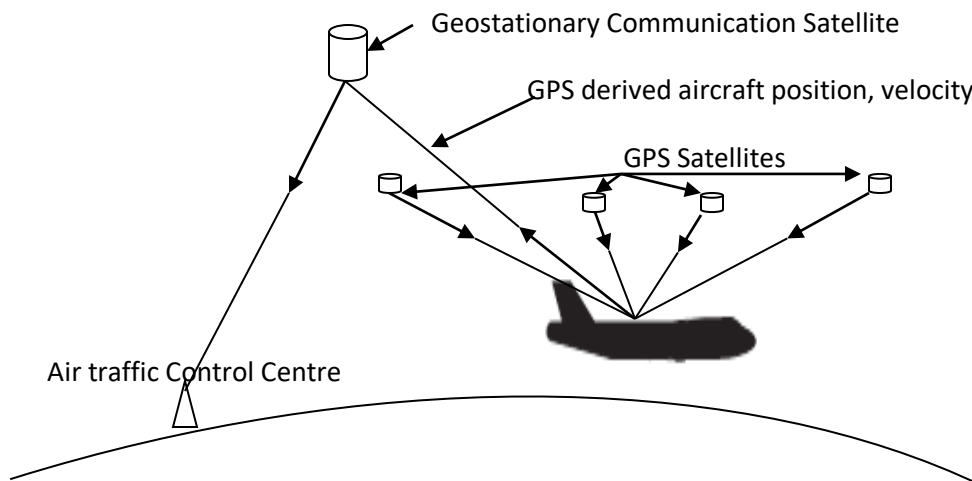


Fig 3.33 Remote air traffic control

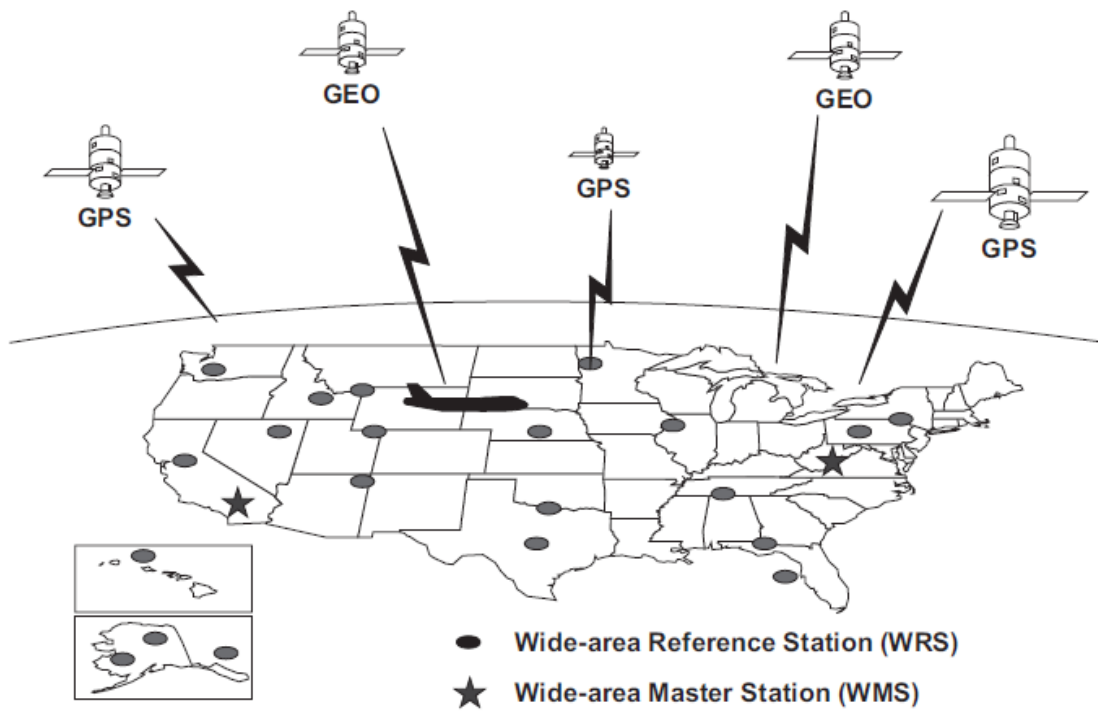


Fig 3.34 Wide Area Augmentation System, WASS, Concept

UNIT-V Surveillance Systems and Auto flight Systems:

5.1 Air traffic control systems (Mode S transponder): as a means to aid the identification of individual aircraft and to facilitate the safe passage of aircraft through controlled airspace, the ATC transponder allows ground surveillance radar to interrogate aircraft and decode data, which enables correlation of a radar track with a specific aircraft. The principle of transponder operation is shown in Fig 5.1. A ground based primary surveillance radar (PSR) will transmit radar energy and will be able to detect an aircraft by means of the reflected energy-termed the aircraft return. This will enable the aircraft return to be displayed on an ATC console at a range and bearing commensurate with the aircraft position. Coincident with the primary radar operation, Secondary Surveillance radar (SSR) will transmit a series of interrogation pulses that are received by the on-board aircraft transponder. The transponder aircraft replies with a different series of pulses that gives information relating to the aircraft, normally aircraft identifier and altitude. If the PSR and SSR are synchronized, usually by being co-bore sighted, then both the presented radar returns and the aircraft transponder information may be presented together on the ATC console. Therefore, the controller will have aircraft identification (e.g. BA 125) and altitude presented alongside the aircraft return, thereby greatly improving the controller's situational awareness.

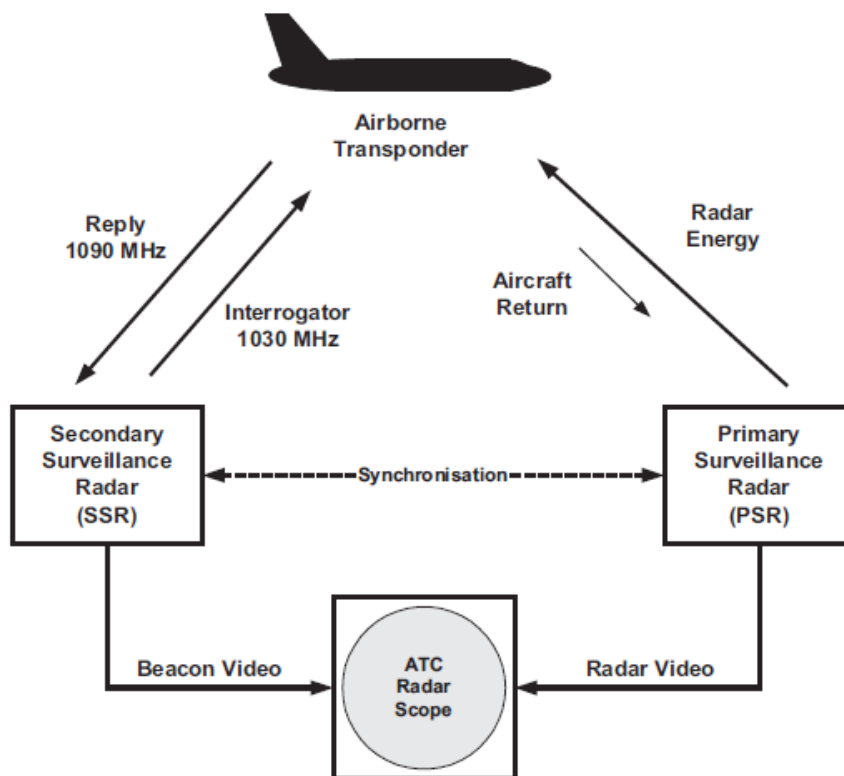


Fig 5.1 principle of transponder operation

The system is also known as Identification Friend or Foe (IFF) secondary Surveillance Radar (SSR), and this nomenclature is common use in the military field. On-board the aircraft, the equipment fit is shown in Fig 5.2. The main elements are:

- ATC transponder controller unit for setting modes and response codes.
- Dedicated ATC transponder unit.
- An ATC antenna unit with an optional second antenna. It is usual to utilize both upper and lower mounted antenna to prevent blanking effects as the aircraft maneuvers.

The SSR interrogates the aircraft by means of a transmission on the dedicated frequency of 1030 MHz which contains the interrogation pulse sequence. The aircraft transponder replies on the dedicated frequency of 1090 MHz with a response that contains the reply pulse sequence with additional information suitably encoded in the pulse stream.

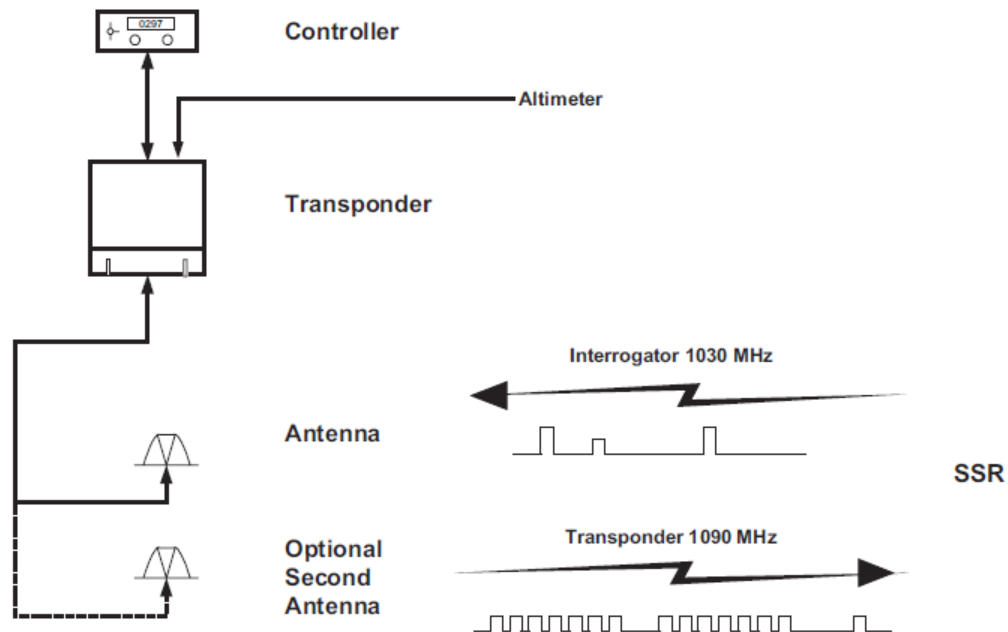


Fig 5.2 Airborne transponder equipment

In its present form, the ATC transponder allows aircraft identification-usually the airline call-sign-to be transmitted when using mode A. When mode C is selected, the aircraft will respond with its identifier, together with altitude information.

More recently, an additional mode- mode S or mode Select-has been introduced with intention of expanding this capability. In ATC mode S, the SSR uses more sophisticated mono-pulse techniques that enable the aircraft azimuth bearing to be determined more quickly. Upon determining the address and location of the aircraft, it is entered into a roll call file. This together with details of all the aircraft detected within the interrogator's sphere of operation forms a complete tally of all the aircraft in the vicinity. Each mode S reply contains a discrete 24 bit address identifier. This unique address, together with the fact that the interrogator knows where to expect

the aircraft from its roll call file, enables a large number of aircraft to in a busy air traffic control environment. ATC mode S has other features that enable it to provide the following:

- Air-to-air as well as air-to-ground communication.
- The ability of aircraft autonomously to determine the precise whereabouts of other aircraft in their vicinity.

Mode S uses an unambiguous identification of each aircraft by its unique 24 bit address. Mode S also protects the data it transmits owing to the inclusion of several parity bits that means that up to 12 erroneous bits may be tolerated by the application of error detection and correction algorithms.

5.2 Traffic alert and collision avoidance systems (TCAS): The TCAS was developed in prototype form during the 1960s and 1970s to provide a surveillance and collision avoidance system to help aircraft avoid collision. It was certified by the FAA in the 1980s and has been widespread use in the USA in its initial form. TCAS is based on the beacon interrogator and operate in similar fashion to the ground-based SSR already described in above. The system comprises two elements: a surveillance system and a collision avoidance system. TCAS detects the range and bearing and altitude of aircraft in the proximity for display to the pilots.

TCAS transmits a mode C interrogation search pattern for mode A and C transponder equipped aircraft and receives replies from all such equipped aircraft. In addition, TCAS transmits one mode S interrogation for each mode S transponder equipped aircraft, receiving individual responses from each one. It will be recalled that mode A relates to range and bearing, while mode C relates to range, bearing and altitude and mode S relates to range, bearing, and altitude with a unique mode S reply. The aircraft TCAS equipment comprises a radio transmitter and receiver, directional antennae, a computer, and flight deck display. Whenever another aircraft receives an interrogation, it transmits a reply and the TCAS computer is able to determine the range from the time taken to receive the reply. The directional antennae enable the bearing of the responding aircraft to be measured. TCAS can track up to 30 aircraft but only display 25, the highest-priority targets being the ones that are displayed. TCAS is unable to detect aircraft that are not carrying an appropriate operating transponder or that have unserviceable equipment. A transponder is mandated if an aircraft flies above 10,000 f or within 30 miles of major airports. TCAS exists in two forms: TCAS I and TCAS II, TCAS I indicates the range and bearing of aircraft within a selected range, usually 15-40 nautical miles forward, 515 nautical miles aft, and 10-20 nautical miles on each side. The system also warns of aircraft within ± 8700 ft of the aircraft's own altitude. The collision avoidance system element predicts the time to, and separation at, the intruder's closest point of approach. These calculations are undertaken using range, closure rate, altitude, and vertical speed. Should the TCAS ascertain that certain safety boundaries will be violated, it will issue traffic advisory (TA) to alert the crew that closing traffic is in the vicinity via the display of certain colored symbol. Upon receiving a TA, the flight crew must visually identify the intruding aircraft and may alter their altitude by up to 300 ft. A TA will normally be advised between 20 and 40 seconds before the point of closest approach with a simple audio warning in the flight crew's headsets. 'TRAFFIC, TRAFFIC'. TCAS I do not offer any deconfliction solution but does provide the

crew with vital data in order that they may determine the best course of action. TCAS II offers a more comprehensive capability, with the provision of Resolution Advisory (RAs). TCAS II determines the relative motion of the two aircraft and determines an appropriate course of action. The system issues an RA via mode S, advising the pilots to execute the necessary maneuver to avoid the other aircraft. An RA will usually be issued when the point of closest approach is within 15 and 35 seconds and the deconfliction symbology is displayed coincident with the appropriate warning. A total of ten audio warnings may be issued. Examples are:

- 'CLIMB, CLIMB, CLIMB'.
- 'DESCEND, DESCEND, DESCEND'.
- 'REDUCE CLIMB, REDUCE CLIMB'.
- Finally, when the situation is resolved, 'CLEAR OF CONFLICT'.

TCAS II clearly requires a high level of integration between the active equipment. Fig 5.3 shows the interrelationship between:

- TCAS transmitter/receiver
- ATC mode S transponder
- VSI display showing vertical guidance for TAs and RAs.
- Optional horizontal situation indicator for RAs that could be the navigation display.
- Audio system and annunciators.
- Antennae for ATC mode S and TCAS.

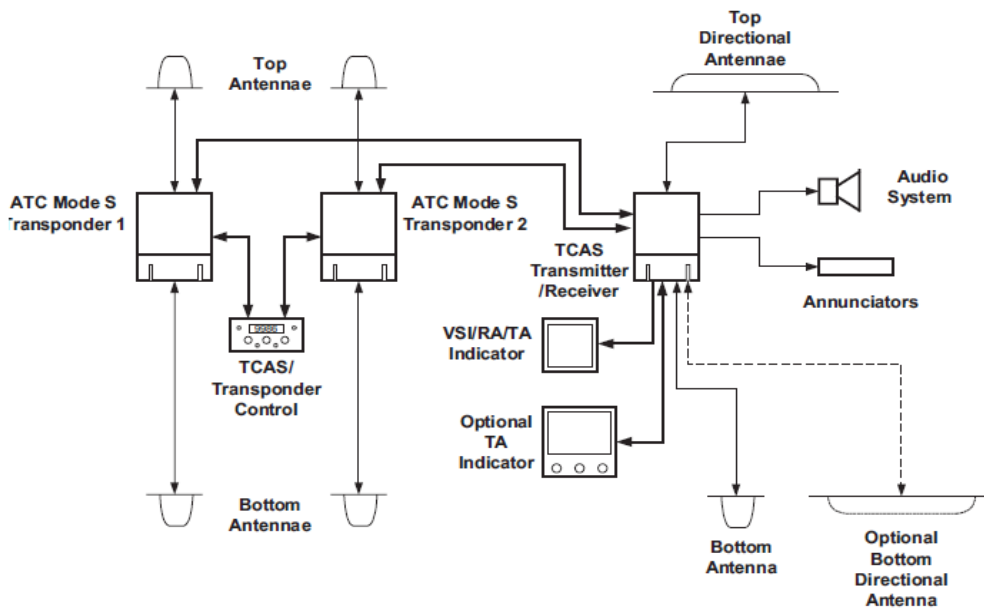


Fig 5.3 TCAS Architecture showing related equipment and displays

5.3 Ground proximity warning system (GPWS) and Enhanced ground proximity warning system (EGPWS): While TCAS is designed to prevent air-to-air collision; the GPWS is intended to prevent unintentional flight into the ground. Controlled Flight into Terrain (CFIT) is the cause of many

accidents. The term describes conditions where the crews are in control of the aircraft, but owing to misplaced sense of situational awareness, they are unaware that they are about to crash into the terrain. GPWS takes data from various sources and generates a series of audio warnings when a hazardous situation is developing.

GPWS uses radar altimeter information together with other information relating to the aircraft flight path. Warnings are generated when the following scenarios are unfolding:

- Flight below the specified descent angle during an instrument approach.
- Excessive bank angle at low altitude.
- Excessive descent rate.
- Insufficient terrain clearance.
- Inadvertent descent after take-off.
- Excessive closure rate to terrain.
- The aircraft is descending too quickly or approaching higher terrain.

Inputs are taken from a variety of aircraft sensors and compared with a number of algorithms that defines the safe envelope within which the aircraft is flying. When key aircraft dynamic parameters deviate from the values defined by the appropriate guidance algorithms, then appropriate warnings are generated.

The installation of GPWS equipment for all airlines flying in US airspace was mandated by the FAA in 1974, since then the number of CFIT accidents has dramatically decreased.

More recently enhanced versions have become available. EGPWS offers a much greater situational awareness to the flight crew as more quantitative information is provided, together with earlier warning of the situation arising. It uses a worldwide terrain database which is compared with the aircraft's present position and altitude. Within the terrain database the Earth's surface is divided into a grid matrix with a specific altitude assigned to each square within the grid, representing the terrain at that point.

The aircraft intended flight path and maneuver envelope for the prevailing flight conditions are compared with the terrain matrix and the result is graded according to the proximity of the terrain as shown in Fig 5.5. Terrain responses are graded as follows:

- No display for terrain more than 2000 ft below the aircraft.
- Light-green dot pattern for terrain between 1000 and 2000 ft below the aircraft
- Medium green dot pattern for terrain between 500 and 1000 ft below the aircraft.
- Heavy-yellow display for terrain between 1000 and 2000 ft above the aircraft.
- Heavy-red display for terrain more than 2000 ft above the aircraft.

The type of portrayal using colored imagery is very similar to that of the weather radar and is usually shown in the navigation display. It is far more informative than the audio warnings given by earlier version of GPWS. The EGPWS also gives audio warnings, but much earlier than those given by the GPWS. The earlier warnings, together with the quantitative color display, give the flight crew a much better overall situational awareness in respect of terrain and more time to react positively to their predicament than did previous systems.

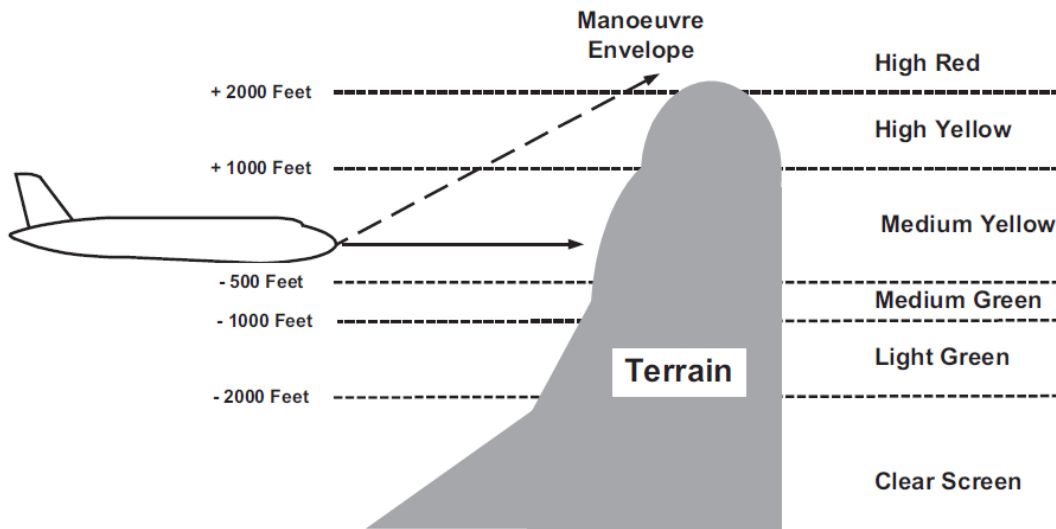


Fig 5.5 Principle of operation of EGPWS

5.4 Weather Radar: Purpose of the weather radar is to alert the flight crew to the presence of adverse weather or terrain in the aircraft's flight path. The weather radar radiates energy in a narrow beam with bandwidth of $\sim 3^\circ$ which may be reflected from clouds or terrain ahead of the aircraft. The radar beam is scanned either side of the aircraft centre-line to give a radar picture of objects ahead of the aircraft. The antenna may also be tilted in elevation by around $\pm 15^\circ$ from the horizontal to scan areas above and below the aircraft. The principle of operation of weather radar is shown in fig 5.6. This shows a storm cloud directly ahead of the aircraft, with some precipitation below, and also steadily rising terrain. Precipitation can be indicative of severe vertical wind shear which can cause a hazard to the aircraft. The radar beam is pointing horizontally ahead of the aircraft with the antenna in its mid-or datum position and will detect the storm cloud through which the aircraft is about to fly. By referring to the weather radar display, the pilot will be able to see if the storm cells can be avoided by altering course left or right. The use of the antenna tilt function is crucial. In the example given, if the antenna is fully raised, the crew will not gain any information relating to storm cloud, precipitation, or rising terrain. If the antenna is fully depressed, the radar will detect the rising terrain, but not the storm cloud or precipitation ahead. For this reason, any weather radars incorporate an automatic tilt feature so that radar returns are optimized for the flight crew in terms of the returns that are received.

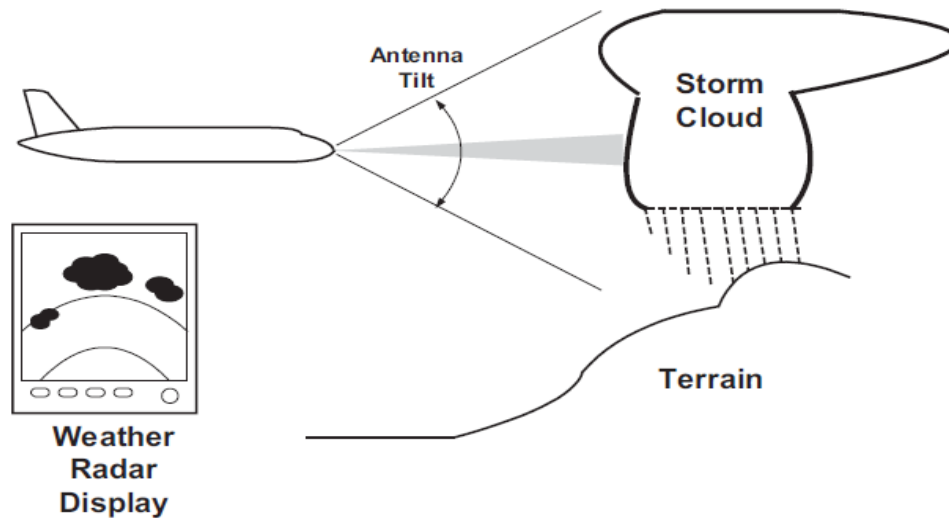


Fig 5.6 Operation of weather radar

Most modern weather radars can use Doppler processing to detect turbulence ahead of the aircraft. This is very useful feature as maximum wind shear does not necessarily occur coincidentally with the heaviest precipitation. In fact, some of the most dangerous wind shear can occur in clear air with the aircraft flying nowhere near any cloud or precipitation.

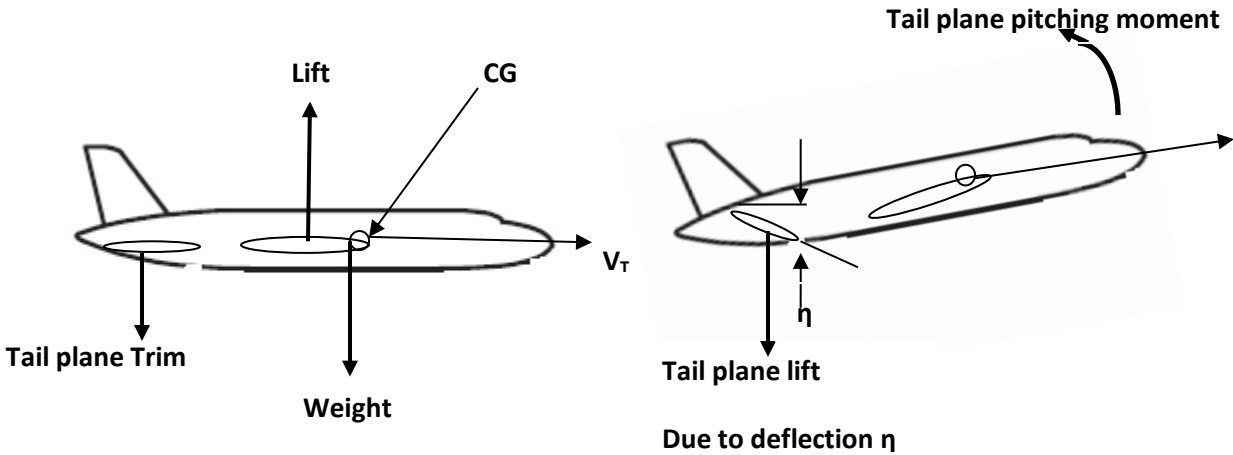
The radar picture may be displayed on a dedicated radar display or overlaid on the pilot or first officer's navigation display. Displays are typically in color, which helps the flight crew to interpret the radar data. Displays have various selectable range markers and are usually referenced to the aircraft heading. Separate display may be provided for weather or turbulence modes. A block diagram of typical weather radar is shown in Fig 5.6. In a weather radar (RDR-4B) of M/s Honeywell, the transmitter operates at 9.345 GHz and the system has three basic modes of operation:

- Weather and map with a maximum range of 320 nm.
- Turbulence (TURB) mode of 40 nm.
- Wind shear detection out to 5 nm.

The radar antenna is stabilized in pitch and roll using aircraft attitude data from an Attitude and Heading Reference System (AHRS) or inertial reference system. The pulse width and pulse frequency depend upon mode of operation.

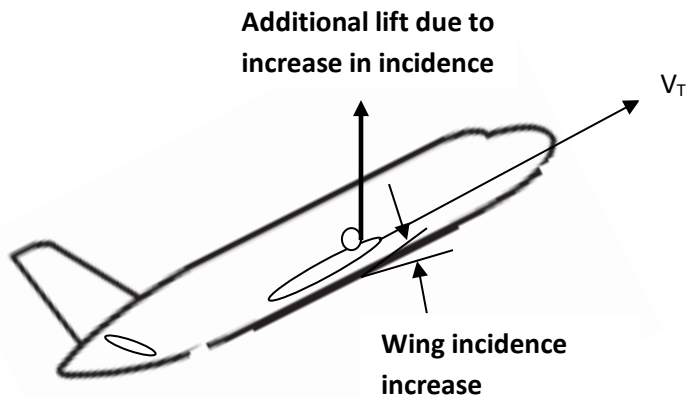
5.5 Longitudinal and lateral control and response of aircraft.

5.5.1 Longitudinal control and response: In conventional (i.e. non-Fly-by-wire) aircraft, the pilot controls the angular movement of the tail plane/elevators directly from the control column, or 'stick', which is mechanically coupled by rods and linkages to the tail plane /elevator servo actuator. (Fully powered controls are assumed.) To maneuver in the longitudinal (or pitch) plane, the pilot controls the tail plane/elevator angle and hence the pitching moment exerted about the CG by the tail plane tilt. This enables the pilot to rotate the aircraft about the its CG to change the wing incidence angle and hence control the wing lift to provide the necessary



(a) Straight & level trimmed flight

(b) Tailplane moved through angle η and pitch maneuvering initiative



(c) Wing incidence increased. Additional lift provided centripetal force to turn in the pitch plane

Fig 5.7 Maneuvering in the pitch plane

normal, or centripetal, force to change the direction of the aircraft's flight path(See Fig 5.7).

The initial response of the aircraft on application of a steady tailplane/elevator angular movement from the trim position as follows.

The resulting pitching moment accelerates the aircraft's inertia about the pitch axis causing the aircraft to rotate about its CG so that the wing incidence angle increases. The wing lift increases accordingly and causes the aircraft to turn in the pitch plane and the rate of pitch to build up. This rotation about the CG is opposed by the pitching moment due to incidence which increases as the incidence increases and by the pitch rate damping moment exerted by the tailplane. A steady condition is reached and the aircraft settles down to a new steady wing incidence angle and a steady pitch rate which is proportional to the tailplane/elevator angular movement from the trim position.

The aircraft's inertia about the pitch axis generally results in some transient overshoot before a steady wing incidence is achieved, the amount of overshoot being mainly dependent on the pitch rate damping generated by the tailplane.

The normal acceleration is equal to the product of the forward speed and the rate of pitch and is directly proportional to the increase in wing lift resulting from the increase in wing incidence angle. For a given constant forward speed, the rate of pitch is thus proportional to the tailplane/elevator angular movement from the trim position which in turn is proportional to the stick deflection. The rate of pitch is reduced to zero by returning, that is 'centralizing', the stick to its trimmed position.

5.5.2 Pitch Rate Response to Tailplane/Elevator Angle. The key to analyzing the response of the aircraft and the modifying control required from the automatic flight control system is to determine the aircraft's basic control transfer function. This relates the aircraft's pitch rate, q , to the tailplane/elevator angular movement, η , from the trimmed position.

This can be derived from the aircraft's equation of longitudinal motion. For small angular movement $q = d\theta/dt$. Transfer function can be written as:

$$\frac{q}{\eta} = \frac{K(D^3 + b_2D^2 + b_1D + b_0)}{(D^4 + a_3D^3 + a_2D^2 + a_1D + a_0)} ; \text{ where } D = d/dt$$

$K, b_2, b_1, b_0, a_3, a_2, a_1, a_0$ are constant coefficients comprising the various derivatives. The transient response (and hence the stability) is determined by the solution of the differential equation $(D^4 + a_3D^3 + a_2D^2 + a_1D + a_0)q = 0$.

$q = Ce^{\lambda t}$, where C and λ are constant, is solution of this type of linear differential equation with constant coefficients. Substituting $Ce^{\lambda t}$ for q yields

$$(\lambda^4 + a_3\lambda^3 + a_2\lambda^2 + a_1\lambda + a_0)Ce^{\lambda t} = 0 ; \text{ i.e.}$$

$$(\lambda^4 + a_3\lambda^3 + a_2\lambda^2 + a_1\lambda + a_0) = 0$$

This equation is referred to as the characteristic equation. This quadratic equation can be split into two quadratic factors which can be further factorized into pairs of conjugate complex factors as shown below:

$$(\lambda + \alpha_1 + j\omega_1)(\lambda + \alpha_1 - j\omega_1)(\lambda + \alpha_2 + j\omega_2)(\lambda + \alpha_2 - j\omega_2) = 0$$

The solution is

$$q = \underbrace{A_1 e^{-\alpha_1 t} \sin(\omega_1 t + \phi_1)}_{\text{Short period motion}} + \underbrace{A_2 e^{-\alpha_2 t} \sin(\omega_2 t + \phi_2)}_{\text{Long period motion}}$$

A_1, ϕ_1, A_2, ϕ_2 are constants determined by the initial conditions, i.e. value of \ddot{q}, \dot{q}, q at time $t = 0$.

For the system to be stable, the exponents must be negative so that the exponential terms decay to zero with time. (Positive exponents result in terms which diverge exponentially with time, i.e. an unstable response.)

The solution thus comprises the sum of two exponentially damped sinusoid corresponding to the short period and long period responses respectively.

The initial basic response of the aircraft is thus a damped oscillatory response known as the short period response. The period of this motion is in the region of 1 to 10 seconds, depending on the type of aircraft and its forward speed, being inversely proportional to the forward speed, e.g. typical fighter aircraft would be about 1 second period whereas a large transport aircraft would be about 5 to 10 seconds period. This short period response is generally fairly well damped for a well behaved (stable) aircraft but may need augmentation with an auto-stabilization system over parts of the flight envelope of height and speed combination.

The second stage comprises a slow lightly damped oscillation with a period ranging from 40 seconds to minutes and is known as the long period/motion. It is basically similar to the phugoid motion and is again inversely proportional to forward speed. The phugoid motion consists of a lightly damped oscillation in height and airspeed whilst the angle of attack remains virtually unchanged and is due to the interchange of potential and kinetic energy as the aircraft's height and speed change. The damping of the phugoid motion is basically a task for the autopilot, the long period making it very difficult for the pilot to control.

Fig 5.8 illustrates the two types of motion in the response. A simpler method of obtaining a good approximation to the q/η transfer function which accurately represents the aircraft's short period response can be obtained by assuming the forward speed remains constant. This is a reasonable assumption as the change in forward speed is slow compared with other variables.

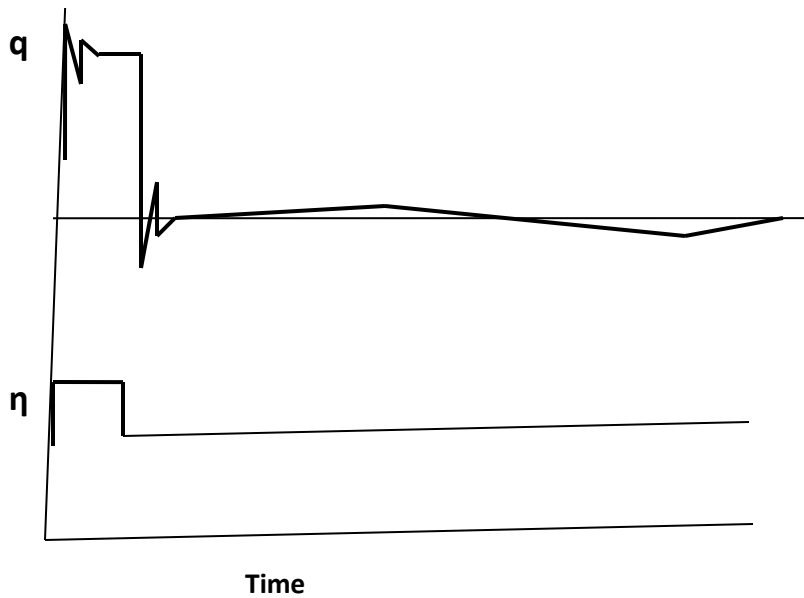


Fig 5.8 Pitch response

5.5.3 Pitch Response Assuming Constant Forward Speed: The transfer function relating to pitch rate and wing incidence to tailplane (or elevator) angle, that is q/η , are derived below from first principles making the assumption of constant forward speed and small perturbations from steady straight and level, trimmed flight.

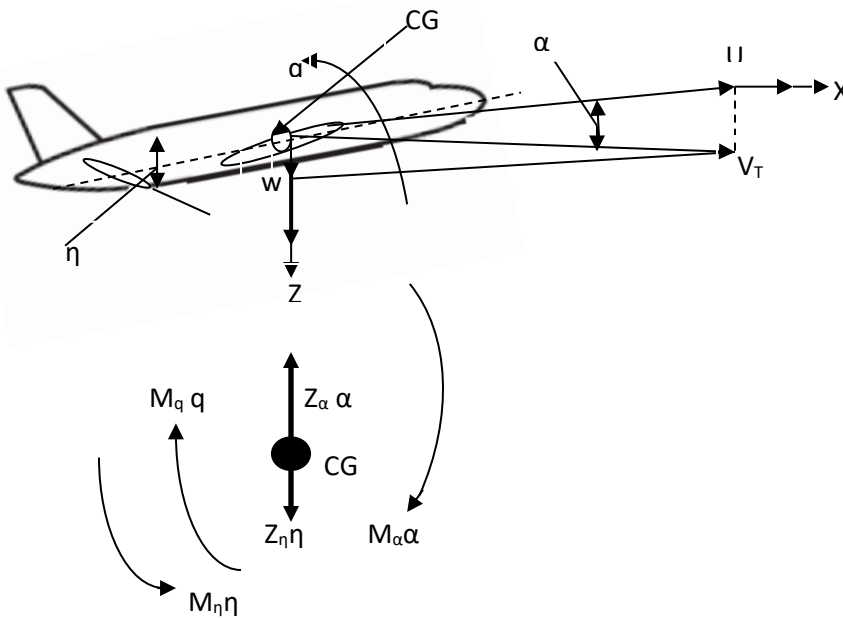


Fig 5.9 Forces & moments-longitudinal plane (stability axes)

Referring to fig 5.9, an orthogonal set of axes OX, OY, OZ moving with the aircraft with the centre o at the aircraft's center of gravity is used to define the aircraft motion. OX is aligned with the flight path vector, OY with the aircraft's pitch axis and OZ normal to the aircraft's flight path vector (positive direction downwards). These axes are often referred to as 'stability axes' and enable some simplification to be achieved in the equations of motion. Velocity along OX axis is U (constant); velocity increment along OZ axis is w; velocity along OY axis is 0; rate of rotation about pitch axis, OY, is q; change in angle of incidence from the trim value is α ; aircraft mass is m; aircraft moment of inertia about pitch axis, OY, is I_y .

Considering forces acting along in OZ direction

1. Change in lift force acting on wing due to change in angle of incidence, α from trim value is $Z_\alpha \alpha$.
2. Change in lift force acting on tailplane due to change in tailplane angle, η , from trim value is $Z_\eta \eta$.

Normal acceleration along OZ axis is $\dot{w} - Uq$, where $\dot{w} = \frac{dw}{dt}$

Equation of motion along OZ axis

$$Z_\alpha \alpha + Z_\eta \eta = m(\dot{w} - Uq) \quad (1)$$

Considering moments acting about CG

1. Pitching moment due to change in tailplane angle, η , from trim value is $M_\eta \eta$.
2. Pitching moment due to change in angle of incidence, α , from trim value is $M_\alpha \alpha$.
3. Pitching moment due to angular rate of rotation, q, about the pitch axis is $M_q q$.

Equation of angular motion about pitch axis, OY

$$M_\eta \eta + M_\alpha \alpha + M_q q = I_y \dot{q} \quad (2)$$

where $\dot{q} = \frac{dq}{dt}$ is angular acceleration and change in angle of incidence is

$$\alpha = \frac{w}{U} \quad (3)$$

These simultaneous differential equations can be combined to give equation in terms of q and η only by eliminating w, or, α and η only by eliminating q. However, it is considered more instructive to carry out this process using block diagram algebra as this gives a better physical picture of the aircraft's dynamic behavior and the inherent feedback mechanism relating q and α . Equation (2) can be written as

$$q = \frac{1}{I_y} \int (M_\alpha \alpha + M_q q + M_\eta \eta) dt \quad (4)$$

Substituting $U\dot{\alpha}$ for \dot{w} in equation (1) and re-arranging yields

$$\alpha = \int \left(q + \frac{Z_\alpha}{mU} \alpha + \frac{Z_\eta}{mU} \eta \right) dt \tag{5}$$

Fig 5.10 represents equation (4) in block diagram form. It should be noted that the sign of the derivatives have been indicated at the summation points in the block diagram. M_q is negative and aerodynamically stable aircraft is assumed that M_α is also negative. The $M_q q$ and $M_\alpha \alpha$ terms are thus negative feedback terms. Fig 5.11 is block diagram representation of equation (5).

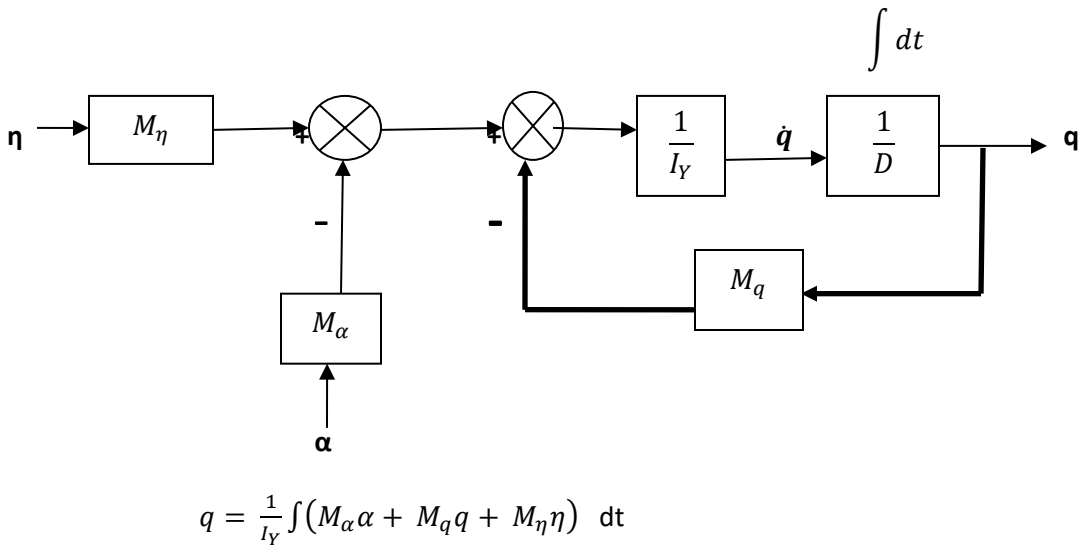


Fig 5.10 Block diagram representation of equation (4)

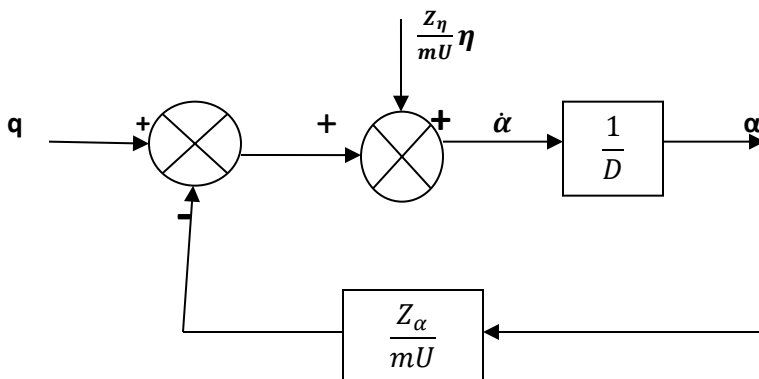


Fig 5.11 Block diagram representation of equation (5)

Considering inner feedback loop $M_q q$ in fig 5.10, we get

$$\frac{q}{(M_\eta \eta - M_\alpha \alpha)} = \frac{\frac{1}{I_y D}}{1 + \frac{1}{I_y D} M_q}$$

$$\frac{q}{(M_\eta \eta - M_\alpha \alpha)} = \frac{1}{M_q} \cdot \frac{1}{(1 + T_1 D)}$$

Where $T_1 = \frac{I_y}{M_q}$

This represents a simple first-order lag transfer function. Referring to fig 5.11, the α/q inner loop can be similarly simplified to

$$\frac{\alpha}{q} = T_2 \cdot \frac{1}{(1 + T_2 D)}$$

Where $T_2 = \frac{mU}{Z_\alpha}$

This represents another first-order lag transfer function. The overall block diagram thus simplifies to fig 5.12. It should be noted that the $\frac{Z_\eta}{mU}$ input term has been omitted for simplicity as it is small in comparison with other terms.

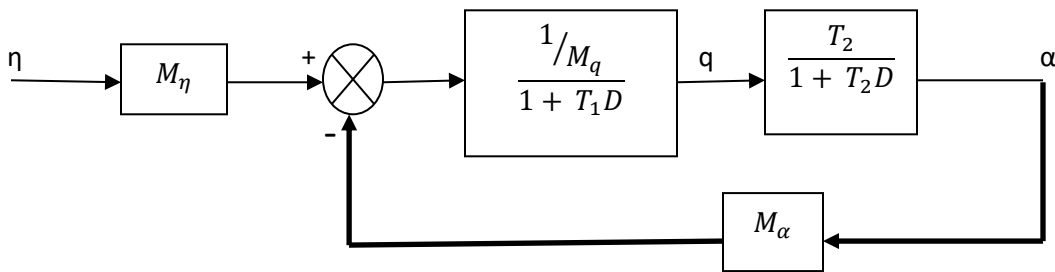


Fig 5.12 Simplified overall block diagram

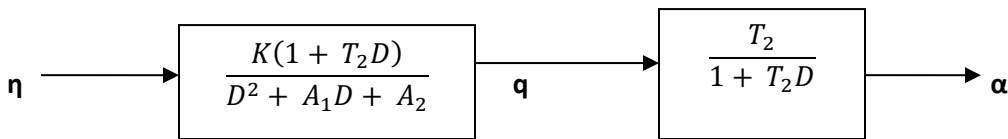


Fig 5.13: Further simplified overall block diagram.

Also, because it is an external input to the loop, it does not affect the feedback loop stability and transient response to a disturbance. Referring to fig 5.12 and applying the block diagram reduction technique yields

$$\frac{q}{\eta} = M_\eta \cdot \frac{\frac{1}{M_q}}{1 + \frac{1}{M_q} \cdot \frac{T_2}{(1 + T_2 D)} M_\alpha}$$

This simplifies to

$$\frac{q}{\eta} = \frac{M_{\eta}}{I_y T_2} \cdot \frac{(1 + T_2 D)}{D^2 + \left(\frac{1}{T_1} + \frac{1}{T_2}\right) D + \frac{M_{\alpha}}{I_y} + \frac{1}{T_1 T_2}}$$

$$\frac{q}{\eta} = \frac{K(1 + T_2 D)}{(D^2 + A_1 D + A_2)} \quad (6)$$

Where

$$K = \frac{M_{\eta}}{I_y T_2} = \frac{M_{\eta} Z_{\alpha}}{I_y m U} \quad ; \quad A_1 = \frac{1}{T_1} + \frac{1}{T_2} = \frac{M_q}{I_y} + \frac{Z_{\alpha}}{m U} \quad ; \quad A_2 = \frac{M_{\alpha}}{I_y} + \frac{1}{T_1 T_2} = \frac{M_{\alpha}}{I_y} + \frac{M_q Z_{\alpha}}{I_y m U}$$

Substituting

$$\alpha = \frac{T_2}{1 + T_2 D} \cdot q \text{ in equation (6) yields}$$

$$\frac{\alpha}{\eta} = \frac{K T_2}{(D^2 + A_1 D + A_2)}$$

The resulting overall block diagram is shown in fig 5.13. From equation (6)

$$(D^2 + A_1 D + A_2) q = K K(1 + T_2 D) \eta$$

The transient response is given by the solution of the differential equation

$$(D^2 + A_1 D + A_2) q = 0$$

The solution is determined by the roots of the characteristic equation

$$(\lambda^2 + A_1 \lambda + A_2) = 0$$

$$\text{Which are } \lambda = -\frac{1}{2} A_1 \pm \frac{\sqrt{A_1^2 - 4A_2}}{2}$$

The solution in this case is an exponential damped sinusoid

$$q = A e^{-\alpha_1 t} \sin(\omega t + \phi)$$

When A & ϕ are constant determined from the initial conditions (value of \dot{q} and q at time t = 0). The coefficient A₁ determines the value of α_1 ($= A_1/2$) and this determines the degree of damping and overshoot in the transient response to a disturbance. The coefficient A₂ largely determines

the frequency, ω , of the damped oscillation $\omega = \frac{\sqrt{4A_2 - A_1^2}}{2}$ and hence the speed of response.

In order for the system to be stable the roots of the characteristic equation must be negative or have negative real part, so that the exponents are negative and exponential terms decay to zero with time. This condition is met provided A₁ and A₂ are both positive. Conversely, an aerodynamically unstable aircraft with positive M_α would in A₂ being negative thereby giving a

positive exponent and a solution which diverges exponentially with time. It is useful to express the quadratic factor ($D^2 + A_1D + A_2$) in terms of two generalized parameters ω_0 and ζ , thus ($D^2 + 2\zeta\omega_0D + \omega_0^2$) where ω_0 is the undamped natural frequency $=\sqrt{A_2}$.

$$\zeta = \text{damping ratio} = \frac{\text{coefficient of } D}{\text{Coefficient of } D \text{ for critical damping}}$$

$$\text{i.e. } \zeta = \frac{A_1}{2\sqrt{A_2}}$$

(Critical damping results in a non-oscillatory response and is the condition for equal roots when $A_1^2 = 4A_2$.)

The transient response to an initial disturbance to a second-order system of the type ($D^2 + 2\zeta\omega_0D + \omega_0^2$) $x = 0$ when x is any variable is plotted in fig 5.14 for a range of values of damping ratio, ζ , and non-dimensional time $T = \omega_0 t$. These graphs can be used for any second order system.

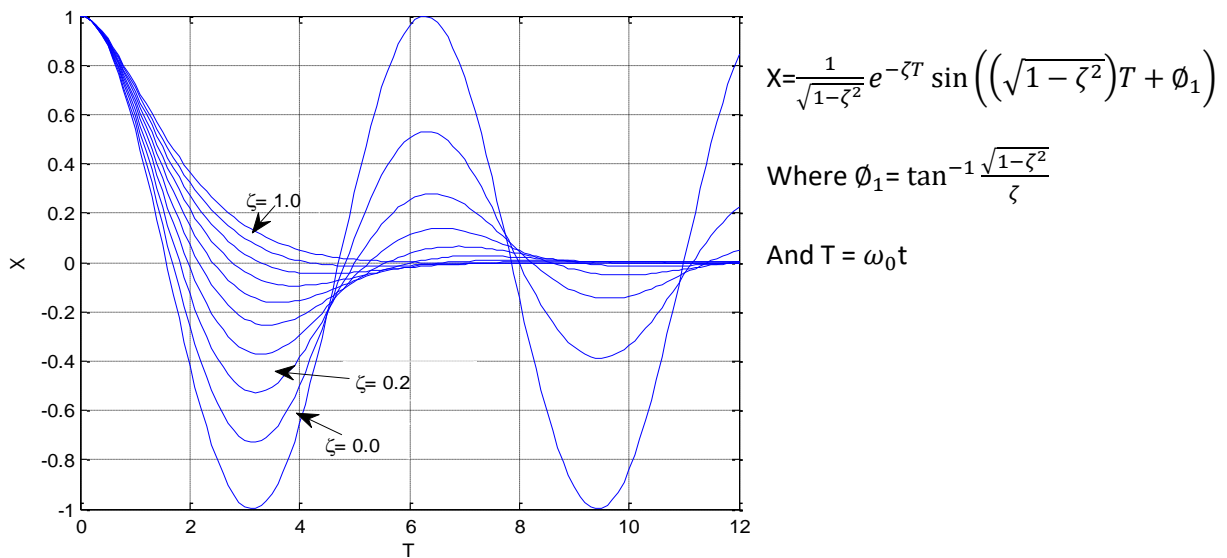


Fig 5.14 Generalized second-order system transient response

5.6 Lateral control.

5.6.1 Aileron Control and Bank to Turn: The primary means of control of the aircraft in the lateral plane are the aileron. These are moved differentially to increase the lift on one wing and reduce it on the other thereby creating a rolling moment so that the aircraft can be banked to turn.

Aircraft bank to turn so that a component of the wing lift can provide the essential centripetal force towards the center of the turn in order to change the aircraft's flight path (See Fig 5.15). The

resulting centripetal acceleration is equal to (aircraft velocity) \times (rate of turn) i.e. $V_T \dot{\psi}$. This centripetal acceleration causes an inertia force to be experienced in the reverse direction, i.e. a centrifugal force. In a steady banked turn with no side slip the resultant force the pilot experiences is the vector sum of the gravitational force and the centrifugal force and is in the direction normal to the wings. The pilot thus experiences no lateral force. Banking to turn is thus fundamental to effective control and maneuvering in the lateral plane because of the large lift forces that can be generated by the wings. The lift force can be up to nine times the aircraft weight in the case of a modern fighter aircraft. The resulting large centripetal component thus enables small radius, high g turns to be executed. Referring to fig 5.15; Horizontal component of the Lift force is $Z \sin \phi$. Equating this to the centrifugal acceleration gives

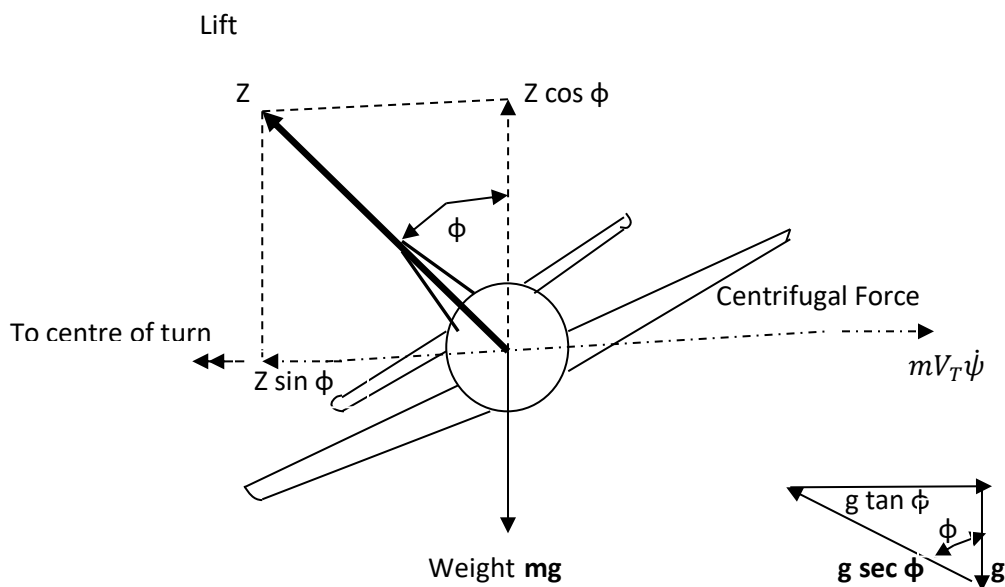


Fig 5.15 Forces acting in a turn

$$Z \sin \phi = m V_T \dot{\psi}$$

Vertical component of the lift force is $Z \cos \phi$. Equating this to the aircraft weight gives

$$Z \cos \phi = mg$$

From which

$$\tan \phi = V_T \dot{\psi} / g$$

Thus the acceleration towards the centre of the turn is $g \tan \phi$.

Referring to the inset vector diagram in fig 5.15, the normal acceleration component is thus equal to $g \sec \phi$. Thus a 60° banked turn produces a centripetal acceleration of 1.73 g and normal

acceleration of 2g. At a forward speed of 100 m/s (200 knots approx.) the corresponding rate of turn would be 10.4 °/s.

The lift required from the wings increases with the normal acceleration and the accompanying increase in drag requires additional engine thrust if the forward speed is to be maintained in the turn. The ability to execute a high g turn thus requires a high engine thrust/aircraft weight ratio. To execute a coordinated turn with no side slip requires the operation of all three sets of control surfaces, that is the aileron and the tailplane (or elevator) and to a lesser extent the rudder. It is also necessary to operate the engine throttles to control the engine thrust. The pilot first pushes the stick sideways to move the ailerons so that the aircraft rolls, the rate of roll being dependent on the stick movement. The rate of roll is arrested by centralizing the stick when the desired bank angle for the rate of turn has been achieved. The pilot also pulls back gently on the stick to pitch the aircraft up to increase the wing incidence and hence the wing lift to stop loss of height and provide the necessary centripetal force to turn the aircraft. A gentle pressure is also applied to the rudder pedals as needed to counteract the yawing moment created by the differential drag of the ailerons. The throttle are also moved as necessary to increase the engine thrust to counteract the increase in drag resulting from the increase in lift and hence maintain speed.

The response of the aircraft from aileron can be derived from following simplified assumption:

Angular movement of the ailerons from the trim position, ξ , produces a rolling moment equal to $L_\xi \xi$ where L_ξ is the rolling moment derivative due to aileron angle moment. This is opposed by a rolling moment due to the rate of roll which is equal to $L_p p$.

The equation of motion is thus

$$L_\xi \xi + L_p p = I_x \dot{p}$$

where I_x is moment of inertia of the aircraft about the roll axis.

This can be expressed in the form

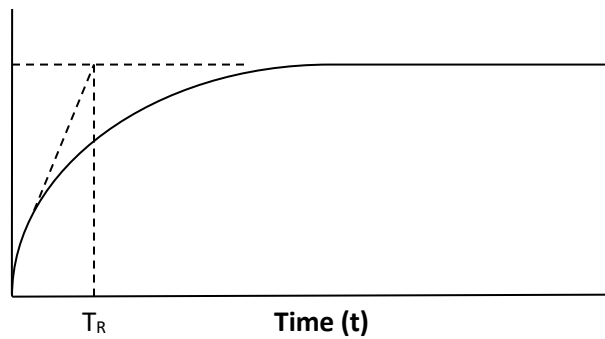
$$(1 + T_R D)p = L_\xi \xi / L_p .$$

Where T_R is the roll response time constant = $I_x / -L_p$ (note L_p is negative).

This is a classic first-order system, the transient solution being $p = A e^{-t/T_R}$, where A is a constant determined by the initial conditions. For a step input of aileron angle, ξ_i the response is given by

$$p = \frac{L_\xi}{L_p} (1 - e^{-t/T_R}) \xi$$

This is illustrated in Fig 5.16.

Roll Rate (p)**Fig 5.16 Roll rate response**

It can be seen that variation in the derivative L_p and L_ξ over the flight envelope will affect both the speed of response and the steady-state rate of roll for a given aileron movement. It should be noted that aerodynamics also refers to the roll response as a subsidence as this describes the exponential decay following a roll rate disturbance.

5.6.2 Rudder control: Movement of the rudder creates both a lateral force and a yawing moment. The control action exerted by the rudder is thus used to:

- Counteract the yawing moment due to movement of the ailerons to bank the aircraft to turn as already explained in Para 5.6.1 above.
- Counteract side slipping motion.
- Counteract asymmetrical yawing moments resulting, say, from loss of engine power in the case of multi-engine aircraft or carrying asymmetrical stores/weapons in the case of a combat aircraft (or both).
- Deliberate execution of a side slipping maneuver. The yawing moment created by the rudder movement will produce a sideslip incidence angle, β , and this will result in a side force from the fuselage and fin. This side force enables a flat side slipping turn to be made. However, the sideways accelerations experienced in flat turns are not comfortable for the pilot (or crew and passengers for that matter). In any case the amount of sideways lift that can be generated by the fin and the fuselage body will only enable very wide flat turns to be made in general.
- To 'kick-off' the drift angle just prior to touch down when carrying out a cross-wind landing. This is to arrest any sideways motion relative to the runway and to avoid side forces acting on the undercarriage at touchdown.

Directional stability in the lateral plane is provided by the fin and rudder. A side-slip velocity, v , with the aircraft's fore and aft axis at an incidence angle, β , to the aircraft velocity vector V_T , (or relative wind) results in the fin developing a side force. This side force tends to align the aircraft with relative wind in a similar manner to a weather cock.

5.6.3 Short Period Yawing Motion: The weather cock action can result in a lightly damped oscillatory motion under certain flight conditions because of the aircraft's inertia, if the yaw rate damping moment is small. The analysis of this motion can be simplified by assuming pure yawing

motion and neglecting the cross- coupling of yawing motion with rolling motion (and vice versa). The direction of the aircraft's velocity vector is also assumed to be changed. It can be shown that:

$$\text{Side slip velocity, } v = V_T \sin \beta = V_T \beta \text{ (as } \beta \text{ is a small angle)} = V_T \psi$$

As $\beta = \psi$, the incremental change in heading (or yaw) angle.

$$\text{Thus yawing moment due to side slip is } N_v V_T \psi.$$

It should be noted that side slip angle (β) and yawing angle (ψ) are not same except when the direction of the aircraft's velocity vector is unchanged.

The moments acting about the CG are:

1. Yawing moment due to side slip is $N_v V_T \psi$.
2. Yawing moment due to yaw rate is $N_r r = N_r \dot{\psi}$

The equation of motion is:

$$N_v V_T \psi + N_r \dot{\psi} = I_z \ddot{\psi}$$

where I_z is moment of inertia about yaw axis.

That is,

$$\left(D^2 + \frac{-N_r}{I_z} D + \frac{-N_v V_T}{I_z} \right) \psi = 0$$

Note that derivative N_r and N_v are both negative.

This is a second order system with an un-damped natural frequency

$$\omega_0 = \sqrt{\frac{N_v V_T}{I_z}}$$

and damping ratio

$$\zeta = \frac{1}{2} \frac{N_r}{\sqrt{N_v V_T I_z}}$$

The period of oscillation ($\frac{2\pi}{\omega_0}$) and the damping ratio are both inversely proportional to the square root of the forward speed, i.e. $\sqrt{V_T}$. Thus increasing the speed shortens the period but also reduces the damping. The period of the oscillation is of the order of 3 to 10 seconds. The short period yawing motion can be effectively damped out automatically by a yaw axis stability augmentation system (or yaw damper).

In practice there can be significant cross-coupling between yawing and rolling motion and the yawing oscillator motion can induce a corresponding oscillatory motion about the roll axis 90° out of phase known as 'Dutch Roll'. (Reputedly after the rolling-yawing gait of a drunken Dutchman.) The ratio of the amplitude of the rolling motion to that of yawing motion is known as

the 'Dutch roll ratio' and can exceed unity, particularly with aircraft with large wing sweepback angles.

5.6.4 Combined Roll-Yaw-Sideslip Motion: The cross coupling and interaction between rolling, yawing and sideslip motion and the resulting moments and forces equation can be solved to find transient response to a disturbance in the lateral plane. The resulting equation is a fifth order differential equation, which can be factorized into two complex roots and three real roots as shown below:

$$(D^2 + 2\xi\omega_0 D + \omega_0^2) \left(D + \frac{1}{T_R}\right) \left(D + \frac{1}{T_Y}\right) \left(D + \frac{1}{T_{SP}}\right) x = 0$$

where x denotes any of the variables v, p, r.

The transient solution is of the form

$$x = A_1 e^{-\zeta\omega_0 t} \sin\left(\sqrt{1 - \zeta^2} \omega_0 t + \phi\right) + A_2 e^{-t/T_R} + A_3 e^{-t/T_Y} + A_4 e^{-t/T_{SP}}$$

where A_1 , ϕ , A_2 , A_3 and A_4 are constants determined by the initial conditions.

The quadratic term describes the Dutch roll motion with un-damped natural frequency ω_0 and damping ratio ζ . T_R describes the roll motion subsidence and T_Y the yaw motion subsidence. T_{SP} is usually negative and is time constant of a slow spiral divergence. It is a measure of the speed with which the aircraft, if perturbed, would roll and yaw into a spiral dive because of the rolling moment created by the yaw rate. The time constant of this spiral divergence is of the order of 0.5 to 1 minute and is easily corrected by the pilot (or auto pilot).

5.7 Powered Flying Controls (PCU): Hydraulic power control units (typically referred to as PCUs) are used to position primary (or secondary) flight control surfaces. PCUs are a single assembly that combines individual hydraulic components into an assembly. PCUs perform two critical functions: (1) they position the flight control surface in response to mechanical or electrical commands, and (2) they represent a principle structural element capable of withstanding flight loads and providing protection against flutter (unsteady, aerodynamic loads). The requirements of these two functions make PCU design a challenging task.

At the heart of PCU are a servo valve and an actuator (servo actuator). The servo valve can be controlled by a flapper nozzle, jet pipe, solenoid, torque motor or mechanical linkage. Some PCUs contain only a servo actuator. However, PCUs often contain other components to meet performance and failure mode performance criteria. Other components typically found in PCUs are shutoff valves, pressure relief valves, input filter, check valves, and compensator. Another component that is often part of a PCU is one or more servos whose control is based on some performance criteria. These servos can be positioned electronically or by hydraulic pressure (where loss of hydraulic pressure allows a spring to position the servo). A simple PCU is shown in Figure 5.17.

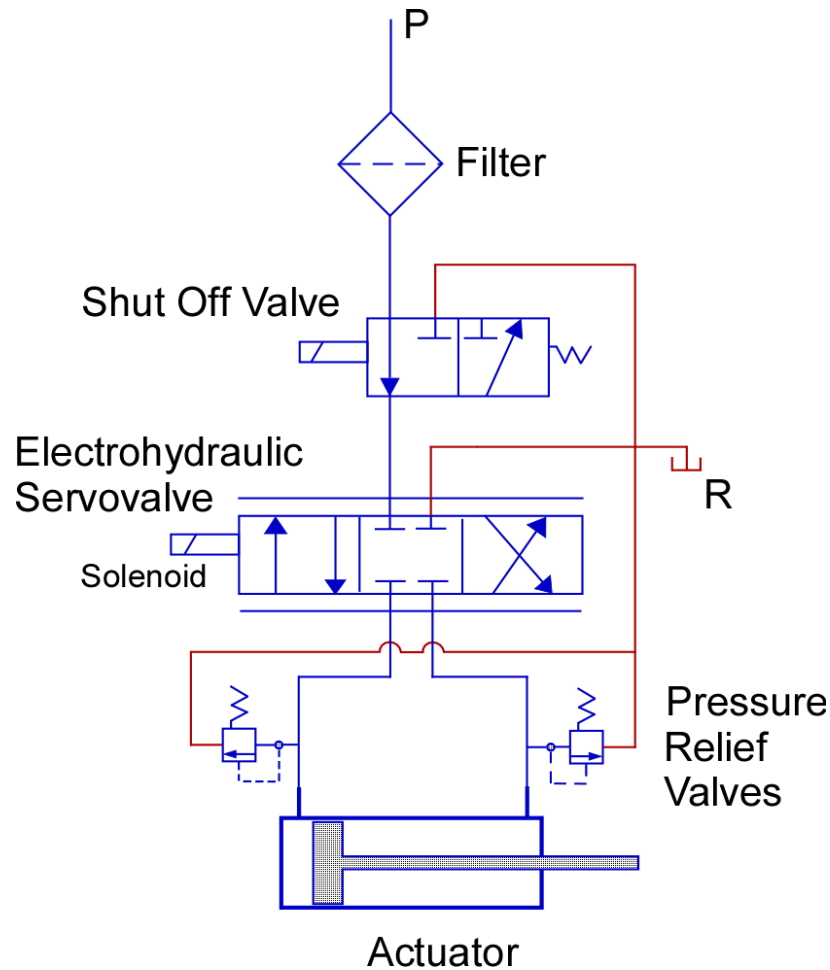


Fig 5.17: A simple PCU

This PCU shows the pressure input going through a filter to a shut off valve. If the shut off valve is open (as shown), then pressure is applied to a solenoid operated servo valve. When closed, the SOV ports pressure to return. The servo valve controls actuator position. (Typically, actuator position is measured by a LVDT on the actuator piston and fed back to a controller that provides closed loop position feedback – see position control system.) The pressure relief valves will bleed off pressure if the pressure in the actuator chamber exceeds a certain level. Pressure can increase above acceptable limits due to external loads or thermal expansion of the fluid. As shown in the Figure, PCUs are built from other hydraulic components, which are packaged into an assembly. An understanding of PCU behavior and characteristics can be ascertained by understanding each component in the system and how it interacts with other components. An analysis or simulation model can be built using models for the individual components to better understand behavior and performance characteristics. Actuator transfer function is a simple first-order lag ($K / (1+Ts)$). Typical values for a PCU time constant are around 0.1 second. This correspond to a bandwidth (-3 dB down) of 1.6 Hz approximately.(10 rad/s). The phase lag at 1 Hz is often used as a measure of the actuator performance and would be 32° in the above case.

5.8 Auto-stabilization systems: It is important to have improved damping and stability about three axes of a military/civil aircraft. This can be achieved by an auto-stabilization system, or, as it is sometimes referred to, a stability augmentation system (SAS). Yaw stability augmentation systems are required in most jet aircraft to suppress the lightly damped short period yawing motion and the accompanying oscillatory roll motion due to yaw/roll cross-coupling known as Dutch roll motion which can occur over parts of the flight envelope. In the case of military aircraft, the yaw damper system may be essential to give a steady weapon aiming platform as the pilot is generally unable to control the short period yawing motion and in fact get out of phase and make the situation worse. A yaw damper system is an essential system in most civil jet aircraft as the un-damped short period motion could cause considerable passenger discomfort. A yaw damper may be insufficient with some aircraft with large wing sweepback to suppress the effects of the yaw/roll cross-coupling and a roll damper system may be also necessary. The possible low damping of the short period response can also require the installation of a pitch damper (or pitch stability augmentation) System. Hence, three-axis stability augmentation systems are installed in most high-performance military jet aircraft and many civil jet aircraft. A single channel, limited authority stability augmentation system is used in many aircraft which have an acceptable though degraded and somewhat lightly damped response, over parts of the flight envelope without stability augmentation. 'Single channel' means that there is no back-up or parallel system to give a failure survival capability. The degree of control, or authority, exerted by the stability augmentation system is limited so that in the event of a failure in SAS, the pilot can over-ride and disengage it. Typical authority of the SAS is limited to control surface deflection corresponding to $\pm 0.5 g$. A simple SAS is shown schematically in fig 5.18. It comprises a rate gyroscope which senses the angular rate of rotation of the aircraft about the auto-stabilized axis and which is coupled to an electronic unit which controls the stability augmentation actuator. The stability augmentation actuator controls the main servo actuator (driving the control surface) in parallel with the pilot's control by means of a differential mechanism-typically a lever linkage differential. The control surface angular movement is thus sum the sum of the pilot's stick and the stability augmentation output. The SAS produces a control surface movement which is proportional to the aircraft's rate of rotation about the axis being stabilized and hence a damping moment proportional to the angular rate of rotation of the aircraft about that axis. In effect a synthetic $N_r r$ or $L_p p$ or $M_q q$ term. In practice, the stability augmentation damping term is more complicated than a simple (constant) \times (aircraft rate of rotation) term because of factors such as stability augmentation servo performance and the need to avoid exciting structural resonance, i.e. 'tail wagging the dog' effect. This latter effect is due to the force exerted by the control surface actuator reacting back on the aircraft structure which has a finite structural stiffness. The resulting bending of the aircraft structure may be sensed by the stability augmentation rate gyro sensor and fed back to the actuator and so could excite a structural mode of oscillation, if the gain at the structural mode frequencies was sufficiently high. In the case of SAS with a relatively low stability augmentation gearing, it is generally sufficient to attenuate the high frequency response of the stability augmentation with a high frequency cut-off filter to avoid exciting the structural modes. The term stability augmentation gearing is defined as the control surface angle/degree per second rate of rotation of the aircraft. With higher stability augmentation gearings, it may be necessary to incorporate 'notch filters' which provide high attenuation at the specific body mode flexural frequencies. Most simple, limited authority yaw dampers feed the angular rate sensor signal to the stability augmentation actuator through a 'band pass filter' with a high frequency cut-off (see fig 5.19). The band pass filter attenuation increases as the frequency decreases and becomes infinite at zero frequency

(i.e. DC) and so prevents the stability augmentation actuator from opposing the pilot's rudder commands during a steady rate of turn. The yawing motion frequency is in the center of the band pass range of frequencies. The angular rate sensor output signal resulting from the short period yawing motion thus passes through the filter without attenuation or phase shift and so provides the required signal to the stability augmentation actuator to damp the oscillator yawing motion. (such type of filter is also called 'wash-out filter').

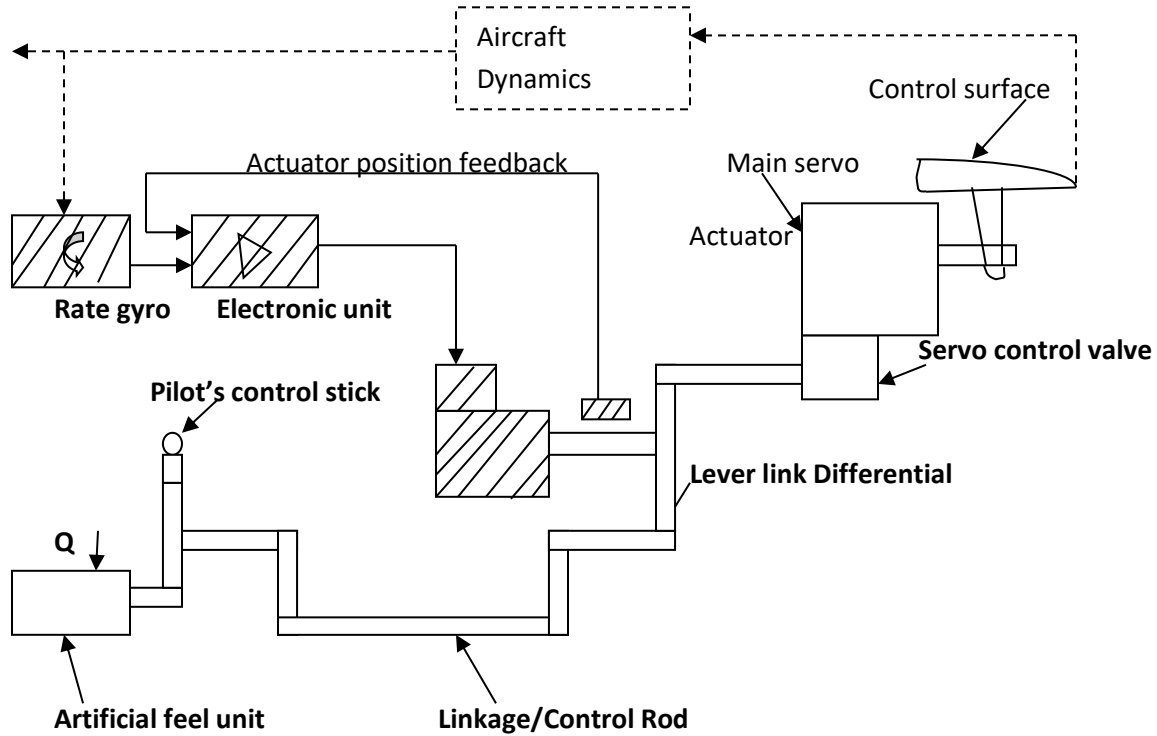


Fig 5.18 Simple stability augmentation system

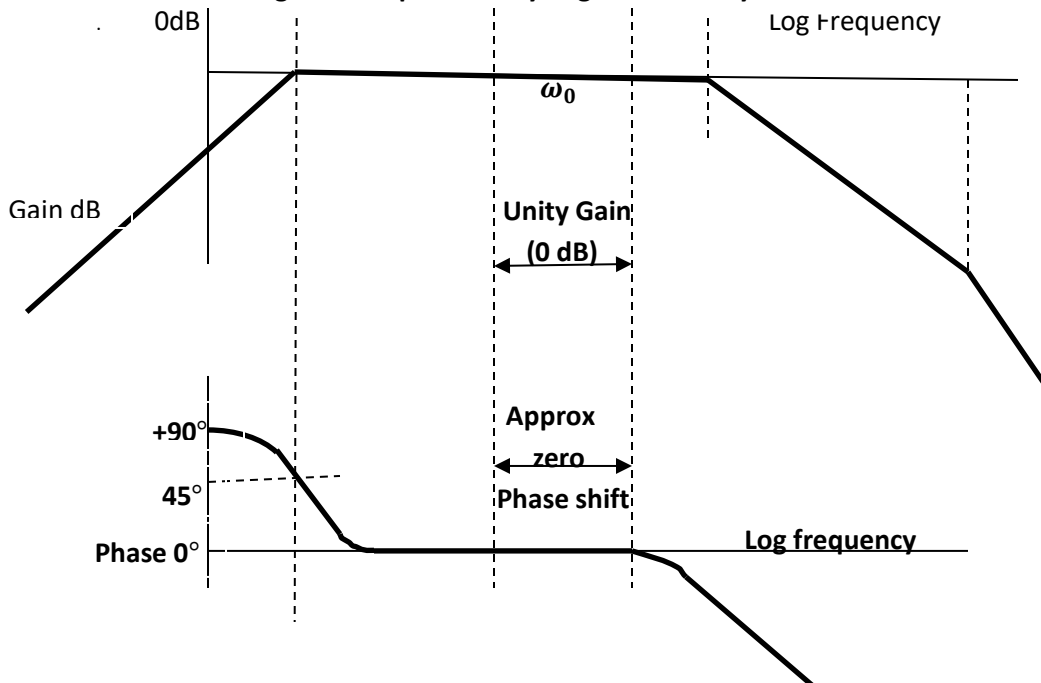
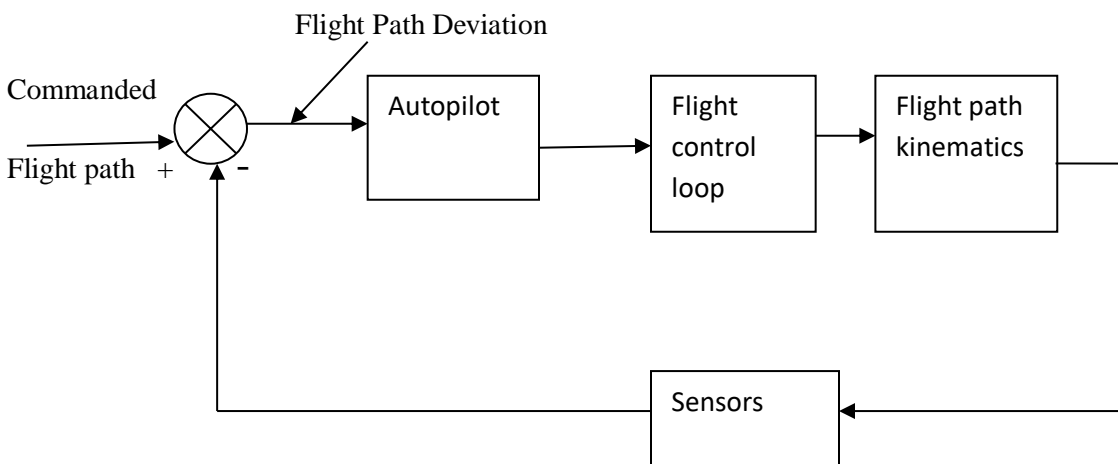


Fig 5.19 DC blocking or ‘wash-out’ filter with high frequency cut-off

5.9 Autopilots

5.9.1 Basic principles: Autopilots are used to reduce the pilot work load. The basic loop through which the autopilot controls the aircraft’s flight path is shown in fig 5.20. The autopilot exercises a guidance function in the outer loop and generates commands to the inner flight control loop. These commands are attitude commands which operate the aircraft’s control surfaces through a closed-loop control system so that the aircraft rotates about the pitch and roll axes until the measured pitch and bank angles are equal to the commanded angles. The changes in the aircraft’s pitch and bank angles then cause the aircraft flight path to change through the flight path kinematics. For example, to correct a vertical deviation from the desired flight path, the aircraft’s pitch attitude is controlled to increase or decrease the angular inclination of the flight path vector to the horizontal. The resulting vertical velocity component thus causes the aircraft to climb or dive so as to correct the vertical displacement from the desired flight path.

To correct a lateral displacement from the desired flight path requires the aircraft to bank in order to turn and produce a controlled change in the heading so as to correct the error. The pitch attitude control loop and heading control loop, with its inner loop commanding the aircraft bank angle, are thus fundamental inner loops in most autopilot control modes. The outer autopilot loop is thus essentially a slower; longer period control loop compared with the inner flight control loops which are faster, shorter period loops.

**Fig 5.20: Autopilot loop.**

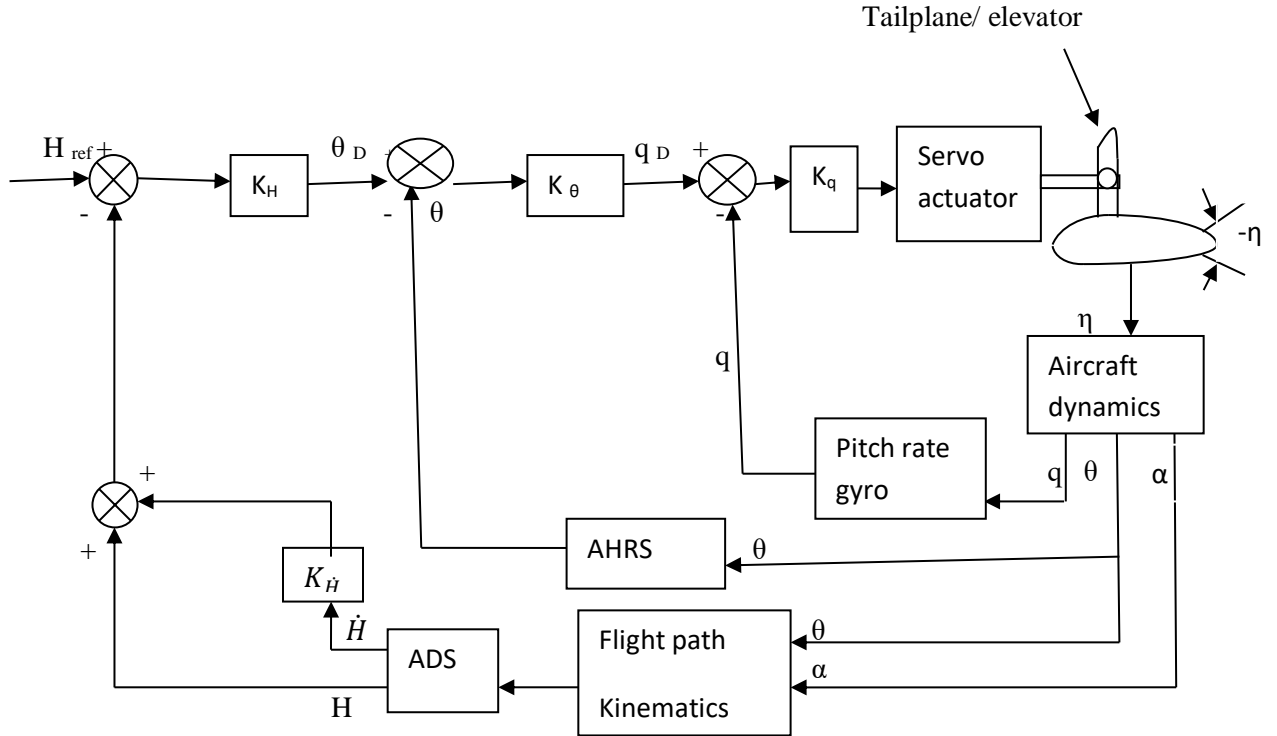


Fig: 5.21 Height control autopilot: ADS (air data system), AHRS (Attitude heading & reference system)

5.9.2 Height control autopilot: Height is controlled by altering the pitch attitude of the aircraft. The basic height control autopilot loop is shown in fig 5.21. The pitch rate command inner loop provided by the pitch rate gyro feedback enables a fast and well damped response to be achieved by the pitch attitude command autopilot loop. The pitch attitude command loop response is much faster than the height control loop response-fraction of a second compared with several seconds. The open-loop transfer function of the height control loop in fact approaches that of a simple integrator at frequencies appreciably below the bandwidth of the pitch attitude command loop. The height error gain, K_H (or gearing) is chosen so that the frequency where the open-loop gain is equal to unity (0 dB) is well below the bandwidth of the pitch attitude loop to ensure a stable and well damped height loop response.

The pitch attitude loop bandwidth thus determines the bandwidth of the height loop so that the importance of achieving a fast pitch attitude response can be seen. The transfer function of the flight path kinematics is derived as follows. Vertical component of the aircraft's velocity vector is

$$V_T \sin \theta_F = \dot{H}$$

where θ_F is the flight path angle, that is the inclination of the velocity vector V_T to the horizontal.

$\theta_F = \theta - \alpha$; where θ is the aircraft pitch angle and α is the angle of incidence, $V_T \approx U$, aircraft forward velocity and θ_F is assumed to be small angle. Hence

$$\dot{H} \approx U(\theta - \alpha)$$

Thus

$$H = \int U(\theta - \alpha) dt$$

5.9.3 Heading control autopilot: The function of the heading control autopilot is to automatically steer the aircraft along a particular set direction. In a perfectly coordinated turn centripetal acceleration is $g \tan \phi = U \dot{\psi}$, where ϕ is the aircraft bank angle, U is the aircraft forward velocity and $\dot{\psi}$ is the rate of change of heading. Hence, for small bank angles

$$\dot{\psi} = \frac{g}{U} \phi$$

The basic control law used to control the aircraft heading is thus to demand a bank angle, ϕ_D , which is proportional to the heading error, $\psi_E = (\psi_{COM} - \psi)$, where ψ_{COM} is the commanded heading angle and ψ the heading angle.

$$\phi_D = K_\psi \cdot \psi_E; \text{ where } K_\psi \text{ is the heading error gain.}$$

The heading control loop is shown in more detail in the block diagram in fig 5.22. The inner bank angle command loop should have as high a bandwidth as practical as well as being well damped in order to achieve a 'tight' heading control with good stability margin. The dynamic behavior of the lateral control system of an aircraft is complicated by the inherent cross-coupling of rolling and yawing rate and sideslip velocity on motion about the roll and yaw axes. However, a good approximation of the aircraft and autopilot behavior can be obtained by assuming pure rolling motion and neglecting the effects of cross-coupling between the roll and yaw axes. Considering the bank angle demand loop, the aerodynamic transfer function relating roll rate, to aileron angle, ξ is

$$\frac{p}{\xi} = \frac{L_\xi}{L_p} \cdot \frac{1}{1 + T_R D}$$

Where T_R is the roll rate response time constant ($= \frac{I_x}{L_p}$) and L_ξ is the rolling moment derivative due to aileron angle, ξ and L_p is the rolling moment derivative due to roll rate, p and I_x is the moment of inertia about the roll axis.

$$\dot{\phi} = p + q \sin \phi \tan \theta + r \cos \phi \tan \theta; \quad \text{If } \phi \text{ and } \theta \text{ are small angles}$$

$$\dot{\phi} = p; \text{ i.e.}$$

$$\phi = \int p dt$$

It is assumed that there is no loss of height when the aircraft banks to correct heading, appropriate changes to the pitch attitude and hence incidence being affected by the height control hold autopilot control.

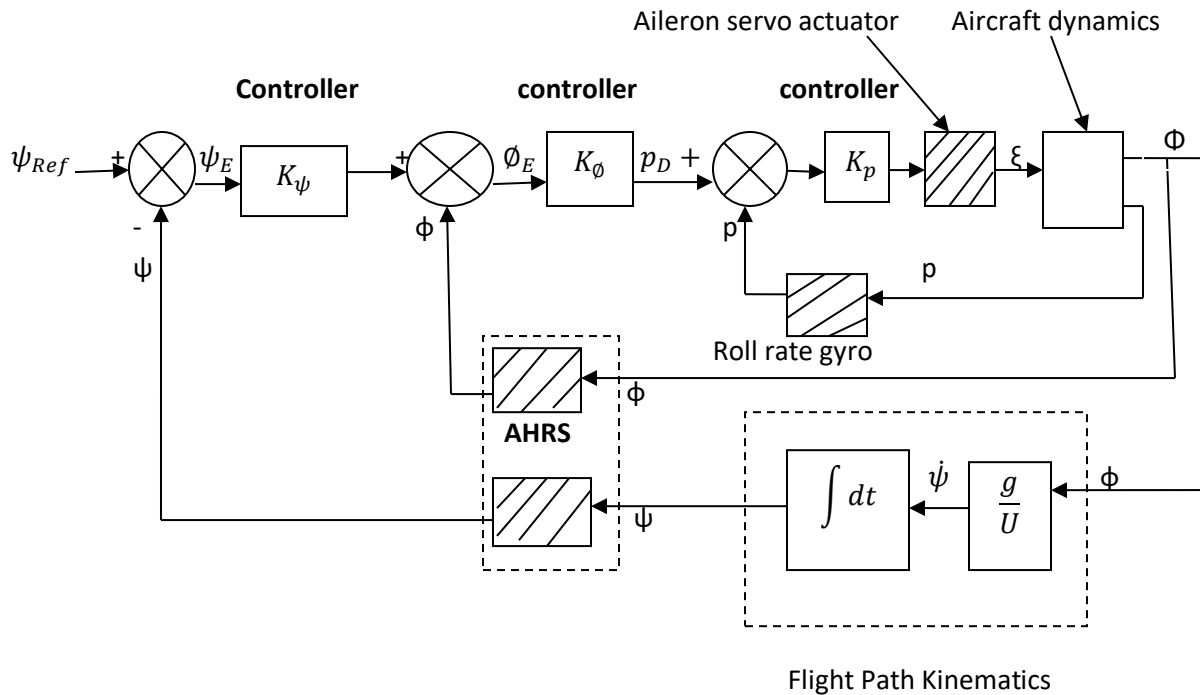


Fig 5.22 Heading control loop

5.9.4 ILS coupled autopilot control:

5.9.4.1 Approach guidance systems: ILS is a radio- based approach guidance system installed at major airports and where the runway length exceeds 1800 m which provides guidance in poor visibility conditions during the approach to the runway. The runway approach guidance signals from the ILS receivers in the aircraft can be coupled into the autopilot which then automatically steers the aircraft during the approach so that it is positioned along the center line of the runway and on the descent path defined by the ILS beams. As explained in Unit-IV, the ILS system basically comprises a localizer transmitter and a glide slope transmitter located by the airport runway together with two or three radio marker beacons located at set distances along the approach to the runway. The airborne equipment in the aircraft comprises receivers and antennas for the localizer, glide slope and marker transmissions. The guidance geometry of the localizer and glide slope beams is shown in Fig 5.23. The localizer transmission, at VHF frequencies (108-122 MHz), provides information to the aircraft as to whether it is flying to the left or right of the centre line of the runway it is approaching. The localizer receiver output is proportional to the angular deviation γ_L of the aircraft from the localizer beam centre line which in turn corresponds with the centre line of the runway.

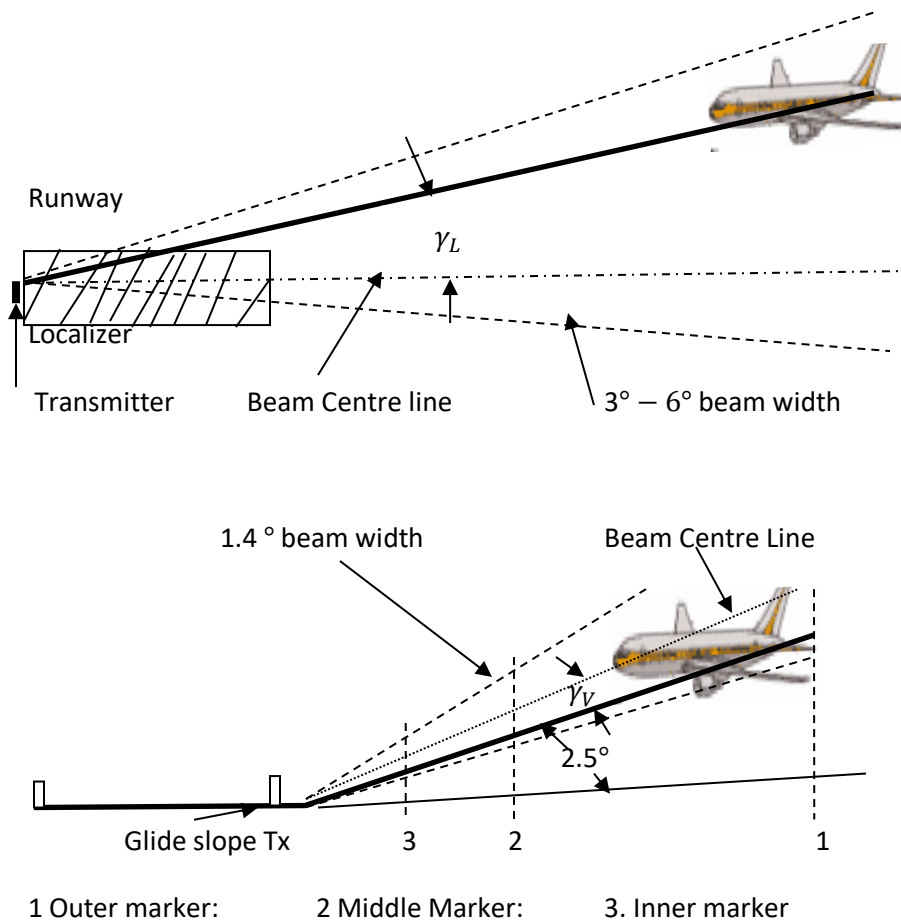


Fig 5.23 ILS Localizer and glide slope geometry

The glide slope (or glide path) transmission is at UHF frequencies (329.3-335 MHz) and provides information to the aircraft as to whether it is flying above or below the defined descent path of nominally 2.5°, for the airport concerned. The glide slope receiver output is proportional to the angular deviation γ_V of the aircraft from the centre of the glide slope beam which in turn corresponds with the preferred descent path. (The sign of the γ_L and γ_V signals is dependent on whether the aircraft is to the left or right of the runway centre line, or above or below the defined glide slope.) The marker beacon transmissions are at 75 MHz. The middle marker beacon is located at a distance of between 1,000 and 2,000 m from the runway threshold and the outer marker beacon is situated at a distance of between 4,500 and 7,500 m from the middle marker. The inner marker beacon is only installed with an airport ILS system which is certified to category III landing information standards and is located at a distance of 305 m (1,000 ft) from the runway threshold. It should be noted that ILS does not provide sufficiently accurate vertical guidance information down to touch down. The height limits and visibility conditions in which the autopilot can be used carry out a glide slope coupled approach to the runway depends on the visibility category to which the autopilot system is certified for operation, the ILS ground installation standard, the runway lighting installation and the airport's runway traffic control capabilities. Visibility conditions are divided into three categories, namely Category I, category II and category III, depending on the vertical visibility ceiling and the runway visual range (RVR). The visibility

conditions deteriorate as the category number increases; 'Cat-III' includes zero visibility conditions. This is shown in Table-1 below. An automatic glide slope coupled approach is permitted to a height of 30 m (100 ft) above the ground, but only if the following conditions are met:

1. There is sufficient vertical visibility at a height of 100 ft with runway visual range of at least 400 m for the pilot to carry out a safe landing under manual control (category II visibility conditions). This minimum permitted ceiling for vertical visibility for the landing to proceed is known as the decision height (DH).
2. The autopilot system is certified for Cat. II operation. Hence, when the decision height is reached the pilot carries out the landing under manual or automatic control. Alternately, the pilot may execute a go-around maneuver to either attempt to land a second time or divert to an alternative airport/airfield.

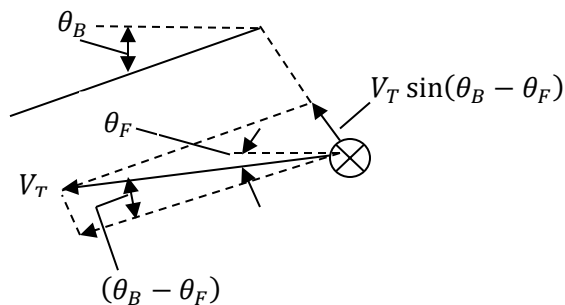
A very high integrity autopilot system is required for fully automatic landing below a DH of 100 ft- (Cat- III conditions).

5.9.4.2 Flight Path Kinematics: The mathematical relationship between the flight path velocity vector and the angular deviation of the aircraft from the guidance beam, or 'beam errors' (γ_L and γ_V) are basically the same for the lateral and vertical planes. These relationships are derived below as they are fundamental to both the localizer and glide slope control loops.

Table 1 Visibility categories

Category	Minimum Visibility Ceiling	Runway Visual Range
I	200 ft	800 m
II	100 ft	400 m
III a	12-35 ft	100-300 m
Depending on aircraft type and size		
III b	12 ft	< 100 m
III c	0 ft	0 m

The particular parameters for each loop can be readily substituted in the general case which is shown in fig 5.24. θ_F is the angle between the flight path velocity vector V_T and a chosen spatial reference axis.



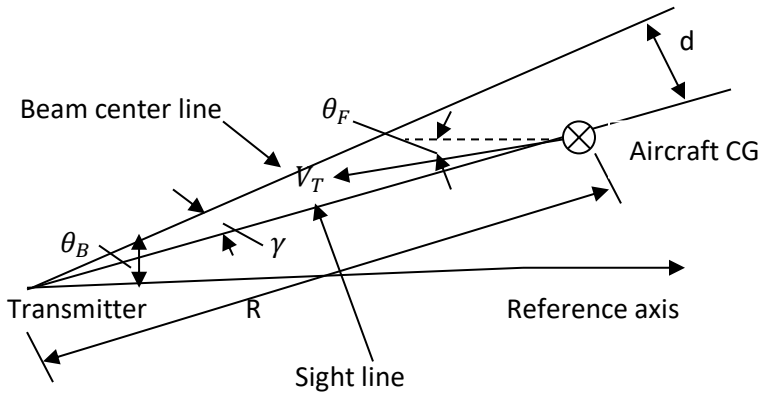


Fig 5.24 Guidance geometry

In vertical guidance case, the reference axis is the horizontal axis. In the lateral case, the reference axis is the runway center line. θ_B is the angle between the centre line of guidance beam and the chosen reference axis. In the vertical case $\theta_B = 2.5^\circ$ nominally and in the lateral case $\theta_B = 0$. From fig 5.24, it can be seen that the component of the flight path velocity vector normal to the sight line is equal to $V_T \sin(\theta_B - \theta_F)$, that is $U(\theta_B - \theta_F)$ as $V_T \approx U$ and $(\theta_B - \theta_F)$ is small angle. The rate of rotation of the sight line is thus equal to $U(\theta_B - \theta_F)/R$ where R is the slant range of the aircraft from the transmitter. θ_B is fixed, so that $\dot{\theta}_B = 0$. Hence

$$\dot{\gamma} = U(\theta_B - \theta_F)/R \quad (1) \quad ; \text{ and}$$

$$\gamma = \int \frac{U}{R}(\theta_B - \theta_F) dt \quad (2)$$

The beam error $\gamma = d/R$, where d is the displacement of the aircraft's centre of gravity (CG) from the beam centre line. Hence as R decreases, a given displacement produces an increasing beam error. For example, a displacement of 5 m at a range of 1,500 m gives a beam error of 3.3 milliradians that is 0.2° . At a range of 300 m, the same offset produces a beam error of 1° . The guidance sensitivity thus increases as the range decreases, as can also be seen from the equation (2) above.

5.9.4.3 ILS localizer Coupling Loop: The ILS localizer coupling loop of the autopilot is shown in the block diagram at fig 5.25. Referring to equation (1) and substituting the appropriate values of θ_B and θ_F , that is $\theta_B = 0$ and $\theta_F = \psi$

$$\dot{\gamma}_L = U \psi / R$$

$$\gamma_L = \int \frac{U}{R} \psi dt$$

The relationship is shown in the block diagram in fig 5.25. It can be seen that the loop gain decreases as R decreases and will reach a point where the loop becomes unstable. Gain scheduling with range is thus required. The localizer controller in the autopilot provides a proportional plus

integral of error control and generally a phase advance term. It should be noted that some filtering of the beam error signal, γ_L , is required to remove the 90 Hz and 150 Hz modulation components inherent in the ILS system and specially to attenuate the noise present. This filtering inevitably introduces some lags.

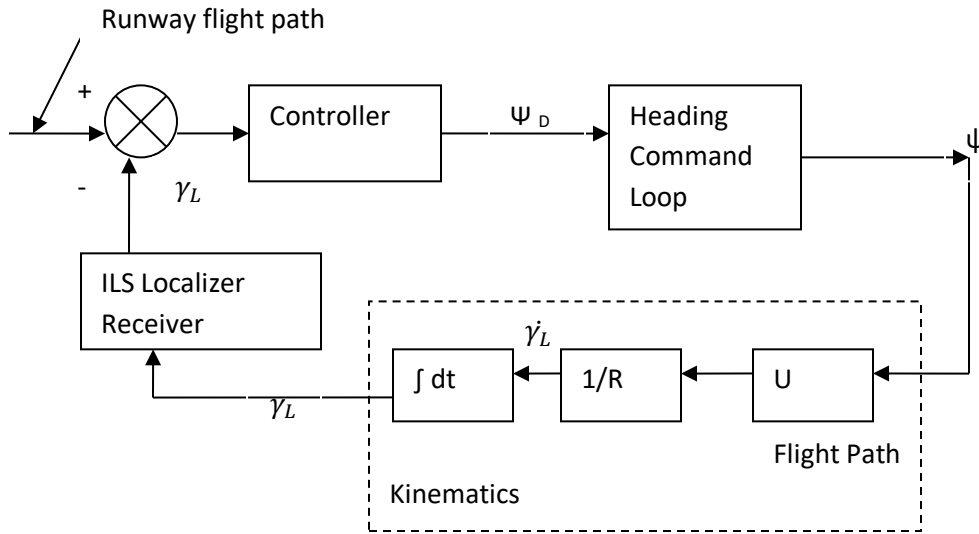


Fig 5.25 Localizer coupling loop (ψ is a/c heading relative to runway centre line bearing)

5.9.4.4 ILS Glide Slope Coupling Loop: The ILS glide slope coupling loop is shown in Fig 5.26. The pitch attitude command loop which controls the inclination of the flight path velocity vector is the same as that described in ‘height control autopilot’. The flight path kinematics has been described in paragraph 5.6.2 above. $\theta_F = (\theta - \alpha)$ where θ is the aircraft pitch angle and α is the angle of incidence. Substituting the appropriate values, $\theta_B = 0.044$ radians (2.5°) and $\theta_F = (\theta - \alpha)$ in equation (1) in paragraph 5.6.2 yields

$$\dot{\gamma}_V = U (0.044 - \theta + \alpha) / R \quad ; \text{Hence}$$

$$\gamma_V = \int \frac{U}{R} (0.044 - \theta + \alpha) dt$$

As in the localizer coupling loop, the loop gain increases as the range decreases and will ultimately cause instability. Gain scheduling with range is required. The airspeed, U , is controlled by an auto-throttle system, and is progressively reduced during the approach according to a defined speed schedule. The glide slope controller generally comprises a proportional plus integral and phase advance control terms with a transfer function of the form

$$K_C \left(1 + \frac{1}{T_1 D} \right) \left(\frac{1 + T_2 D}{1 + \frac{T_2 D}{n}} \right)$$

Where K_C is the controller scalar gain, T_1 is the integral term time constant, T_2 is the phase advance time constant and n is the phase advance gain.

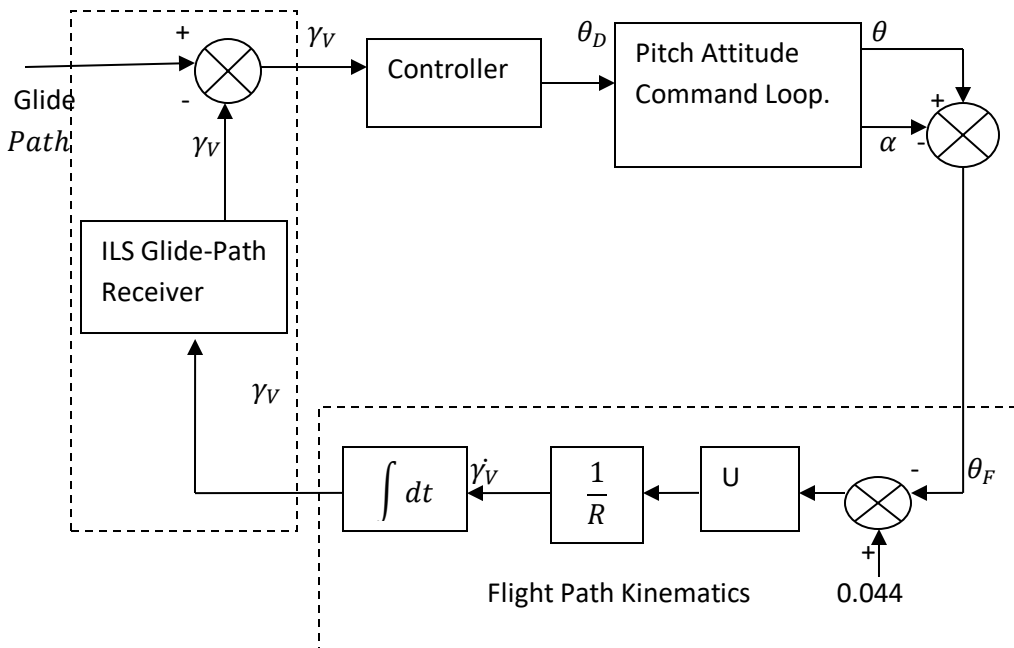


Fig 5.26 Glide Path Coupling Loop.

5.10 Automatic Landing System:

5.10.1 Introduction: The previous sections 5.9 have described the automatic coupled approach phase of an automatic landing using the guidance signals from the ILS system in Cat-II or Cat-I visibility conditions. The pilot, however, takes control from the autopilot when the decision height is reached and lands the aircraft under manual control. Attempting to land an aircraft under manual control with decision height of less than 100 ft, as in Cat-III conditions, is very demanding because of the lack of adequate visual cues and the resulting disorientation which can be experienced. There are only two alternatives for affecting a safe landing in such conditions:

1. A fully automatic landing system with the autopilot controlling the landing to touchdown. A very high integrity autopilot system is required with failure survival capability provided by redundancy such that the probability of a catastrophic failure is less than 10^{-7} /hour. High integrity autopilot systems capable of carrying out fully automatic landing in cat-III conditions are now at a mature stage of development and large number of civil jet aircraft operated by major airlines worldwide are now equipped with such systems.
2. The use of an enhanced vision system with HUD using millimetric wavelength radar sensor in the aircraft to derive a synthetic runway image. This is presented on the HUD together with the primary flight data, including the flight path velocity vector, and provides sufficient information for the pilot to land the aircraft safely under manual control.

It is appropriate at this point to describe the visibility categories and the autopilot capabilities for operation in these categories. There are two basic parameters used to define the visibility category (1) decision height, which is the minimum vertical visibility for the landing to proceed, and (2) the runway visual range. Table -1 shows the various visibility categories. The safety and integrity requirements for the autopilot system to be qualified for operation in the various visibility categories and the limits on its operation are shown in Table-2. The flight path guidance system must also meet the appropriate category standards and accuracy. For example, a Cat-II ILS system must provide accurate glide path guidance down to a height of 100 ft above the ground.

5.10.2 A typical Automatic Landing System: An automatic landing system (made by the Blind Landing Experimental Unit (BLEU) part of the UK Defense Research Agency) is shown in fig 5.27 and is divided into four phases from the time the outer marker beacon is reached, about 8000 m from the threshold. These phases are briefly described below.

1. **Final approach.** This phase covers the approach from the outer marker beacon to the inner marker beacon. At the inner marker beacon the aircraft flight path should be aligned with the defined glide path at a height of 100 ft above the ground and also aligned with the centre line of runway. During this phase, the autopilot controls the aircraft flight path using the guidance signals from the ILS system. The aircraft height above ground is measured very accurate radio altimeter.
2. **Constant attitude.** The guidance signals from the ILS are disconnected from the autopilot when the aircraft reaches a height of 100 ft above the ground. The autopilot then controls the aircraft to maintain the pitch attitude and heading at the values set during the approach until the height is reached at which the flare-out is initiated.
3. **Flare.** The aircraft pitch attitude is controlled by the feedback of the radio altimeter derived height to produce an exponential flare trajectory. The flare is initiated at a height around 50 ft where the aircraft is over or very near the runway threshold. The aircraft is progressively rotated in pitch during the flare so that the flight path angle changes from the -2.5° to -3° value at the start of the flare to the positive value specified for touchdown.

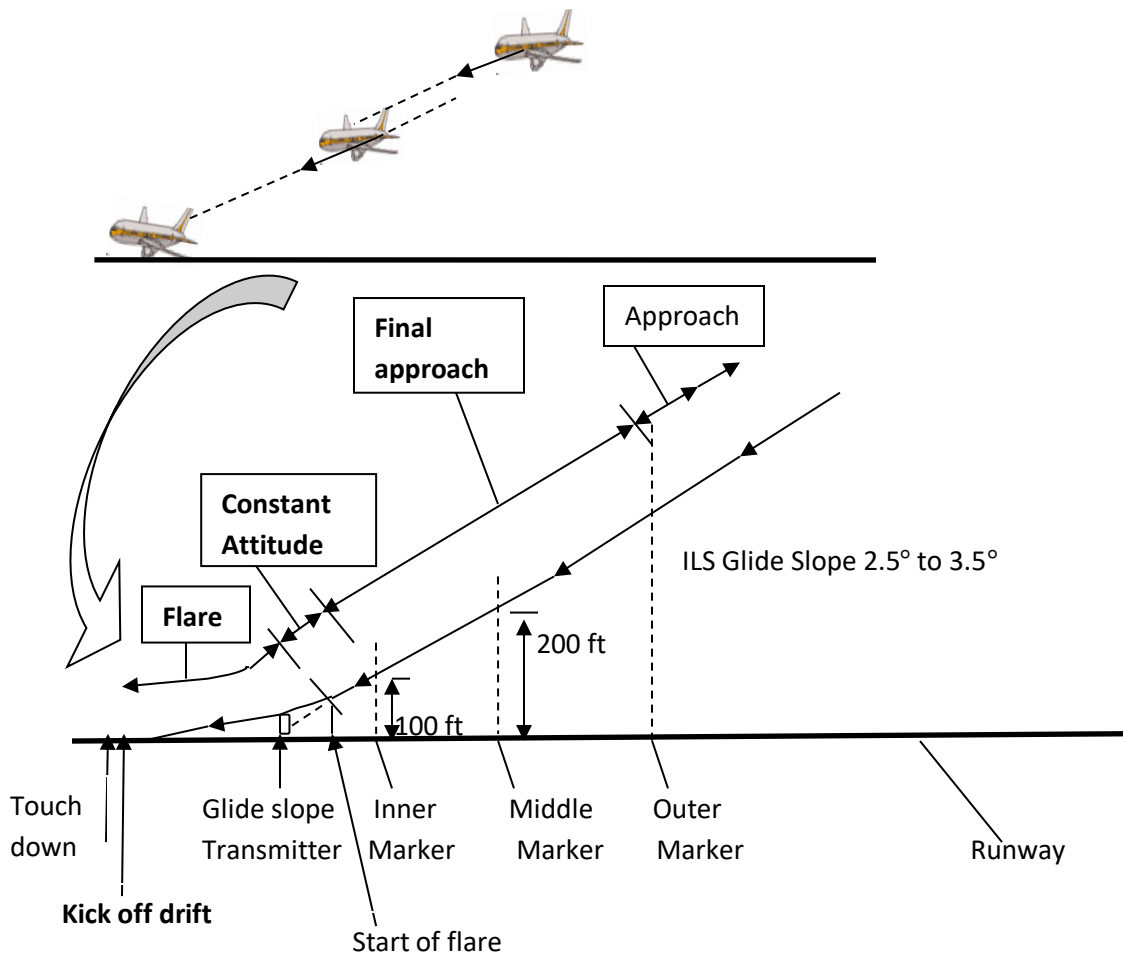


Fig 5.27 BLEU automatic landing system

4. **Kick off drift.** Just prior to touchdown a 'kick off drift' maneuver is initiated through the rudder control so that the aircraft is rotated about the yaw axis to align it with the runway. This ensures the undercarriage wheels are parallel to the runway centre line so that no sideways velocity is experienced by the wheels when they make contact with the runway.

Table-2: Safety and integrity requirements.

Category	Autopilot requirements and operational limits
I	Simplex autopilot system acceptable. Pilot takes over the landing at a DH of 200 ft
II	Fail passive autopilot system required. Pilot takes over the landing at DH of 100 ft.
III a	Full automatic landing system with automatic flare. Failure survival autopilot system with a probability of catastrophic failure of less than 10^{-7} per hour required.
III b	Same as III a as regards autopilot system capability and safety and integrity requirements, but with automatic roll out control after touchdown incorporated. Runway guidance system required. Pilot assumes control at some distance along the runway.
III c	Same as III b as regards autopilot system capability and safety and integrity requirements, but with automatic taxiing control incorporated. Runway guidance required to taxi point.

5.10.3 Automatic Flare control: The phases of the automatic landing have just been described in the above paragraphs. The automatic control loops for pitch attitude and heading control during the 'constant attitude' phase have also been covered. The automatic flare control system needs further explanation. The mathematical law describing the exponential flare maneuver is:

$$\dot{H} = -KH \quad (1)$$

Where H is the aircraft height above the ground and K is a constant.

The solution of equation (1) is

$$H = H_0 e^{-t/T}$$

Where H_0 is the aircraft height above the ground at the start of the flare maneuver, T is the time constant = 1/K. (Time, t, is measured from the start of the maneuver.) The horizontal velocity of the aircraft is effectively equal to U as the flight path angle is small angle. Assuming U is constant, the trajectory will thus be exponential.

The control law used for the auto flare is

$$H + T \dot{H} = H_{REF}$$

H_{REF} is a small negative height, or, bias, which ensures there is still a small downwards velocity at touchdown. This avoids the long exponential 'tail' to reach zero velocity and enables a reasonably precise touchdown to be achieved. The auto flare is initiated at a height of 50 ft where the aircraft is over or very near the runway threshold so that the radio altimeter is measuring the height of the aircraft above the runway. Low range radio altimeters are used to ensure accuracy. Safety and integrity considerations generally dictate a triplex or even quadruplex configuration of totally independent radio altimeters.

The block diagram for the automatic flare control loop is shown in Fig 5.28 which also indicates the redundancy necessary to meet the safety and integrity requirements in the automatic landing system. The required control law response can be obtained by feeding back the rate of change of height suitably scaled by the required time constant, that is $T\dot{H}$, together with the height measured by the rad.alt. This is because the response of a closed loop system approaches the inverse of the feedback path transfer function if the gain in forward loop is sufficiently high. The aircraft height response thus approaches that of a simple first-order system with a transfer function of $1/(1 + T D)$ at low frequencies where the forward loop gain is high. The \dot{H} feedback term can be derived by differentiating the suitably smoothed rad.alt output. A filter is required to smooth the noise present on the rad.alt out-put and the differentiation process amplifies any high frequency noise components which are present. The H signal so obtained thus has lags present in its response because of the smoothing filters required.

An alternative and superior source of \dot{H} can be derived from inertial mixing of the INS derived vertical velocity. This is assuming there is adequate redundancy, for example a triplex INS

installation. The internal mixing enables an \dot{H} output to be obtained with an excellent dynamic response and low noise content.

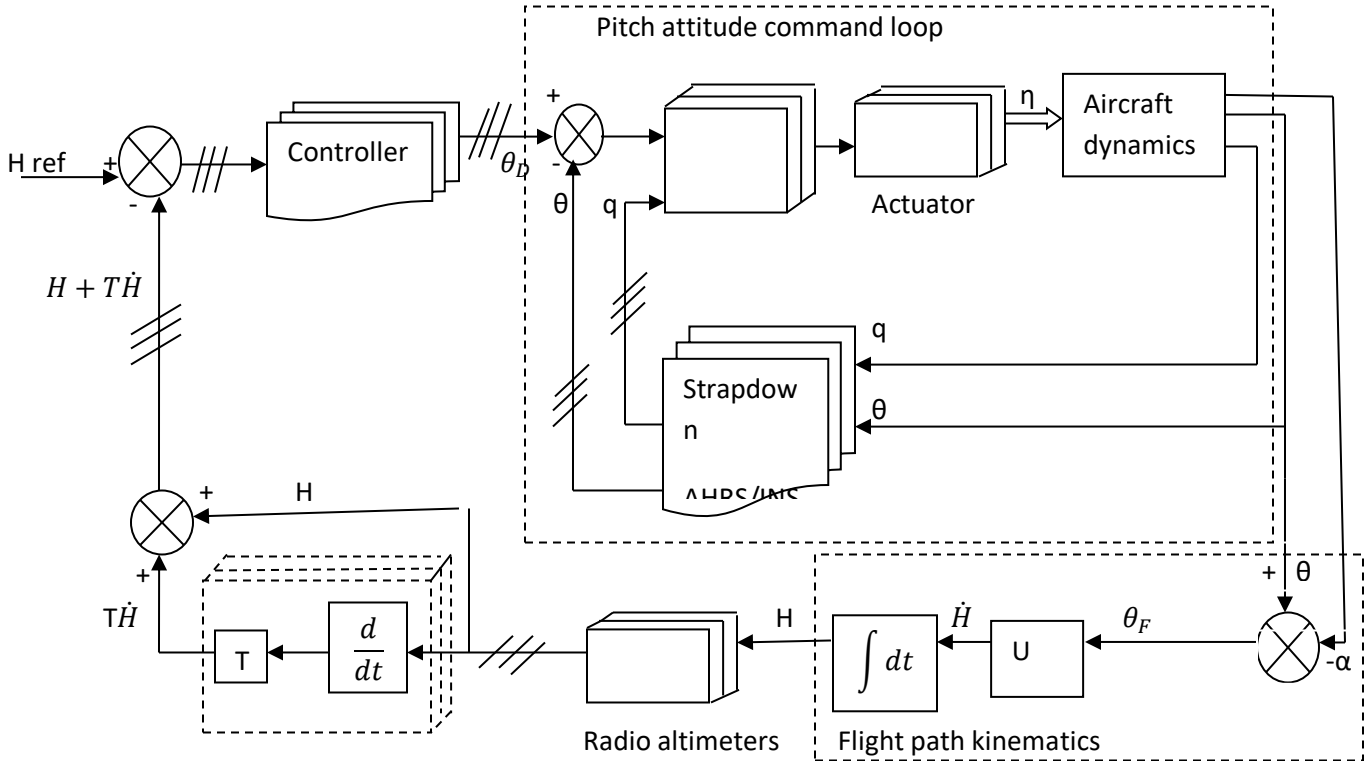


Fig 5.28 Automatic flare control loop

The auto flare is a high order system; apart from the lags present in the filtered rad.alt. signals there are also the lags present in the response of the pitch attitude command loop. This loop controls \dot{H} and its response is significantly slower at low speeds during the approach.

A proportional plus integral control term is used in the auto-flare controller to ensure accuracy and some phase advance is generally provided to compensate for the lags in the loop and hence improve the loop stability and damping.

The approach speed is typically around 65 m/s (130 knots) so that vertical velocity at the start of the flare is around $65 \sin 2.5^\circ$ that is 2.84 m/s or 9.3 ft/s. The flare time constant is typically around 5 seconds so that the vertical velocity is reduced exponentially from around 2.84 m/s at the start of the flare to about 0.6 m/s at touchdown. The corresponding time to touchdown is around 7.7 seconds. Hence, assuming the approach speed stays constant; the touchdown point would be around 500 m from the runway threshold.

5.11 Satellite Landing Guidance Systems: The navigation position accuracy of 1 m which can be achieved with the differential GPS technique is being exploited in the US for landing guidance with a system called the Ground Based Augmentation System, GBAS. The GBAS, when installed at an airport, will be able to provide the high integrity and accurate guidance necessary for landing in Cat-III visibility conditions. The equipment is simpler and less expensive to install and maintain than an Instrument Landing System (ILS), so the GBAS life-cycle operation costs are a fraction of the other systems. It is therefore an attractive proposition for the many smaller airports which are not equipped with ILS (Instrument Landing System).

It is also a more flexible system. For example, the final approach path need not be limited to straight line approaches, but can be curved or stepped, horizontally or vertically.

The GBAS is shown schematically in Fig 5.29. It consists basically of several GPS receivers connected to a base station in an equipment room. The base station processes the measurements from the GPS receivers, determines the differential corrections, estimates their quality and broadcasts this information to nearby aircraft. In addition, the co-ordinates of the final approach paths are transmitted to the aircraft.

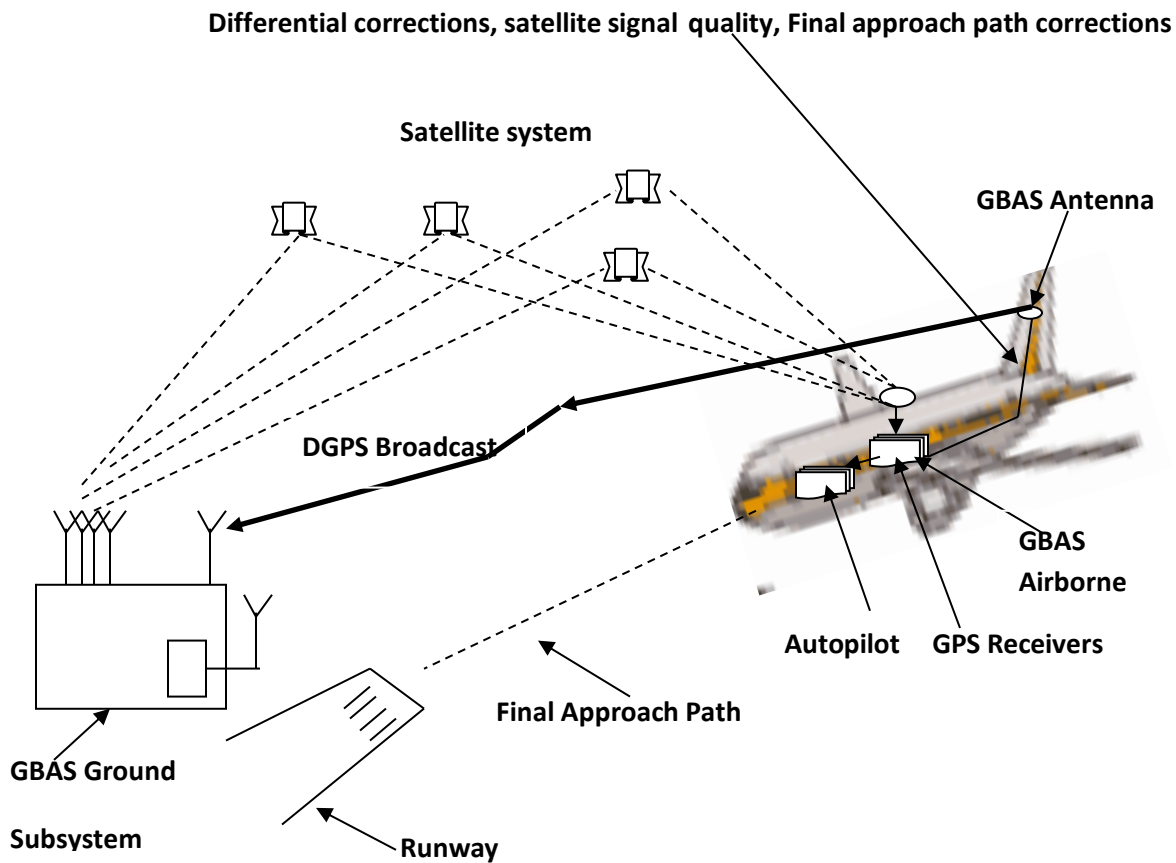


Fig 5.29: GBAS landing guidance system

The control laws exercised by the autopilot during the automatic landing are basically similar whether the guidance is provided by an ILS or the GBAS. The flight path kinematics to align the aircraft's flight path with the commanded flight path is the same whether this is defined by the radio or the GBAS.

The signals from the GBAS are tailored to provide 'ILS look alike' guidance for the pilot's display in terms of their sensitivity. This is to maximize pilot and operator acceptability.

An optional provision is made in the GBAS for additional ranging signals to be provided by ground based transmitters called 'pseudolites' which can be installed to meet high availability requirements.

5.12 Speed Control and Auto-Throttle Systems: Control of the aircraft speed is essential for many tasks related to the control of the aircraft flight path, for example the position of the aircraft relative to some reference point.

The aircraft speed is controlled by changing the engine thrust by altering the quantity of fuel flowing to the engines by operating the engine throttles. Automatic control of the aircraft's speed can be achieved by a closed-loop control system whereby the measured airspeed error is used to control throttle servo actuators which operate the engine throttles. The engine thrust is thus automatically increased or decreased to bring the airspeed error to near zero and minimize the error excursions resulting from disturbances. A typical airspeed control system is shown in the block diagram in fig 5.30.

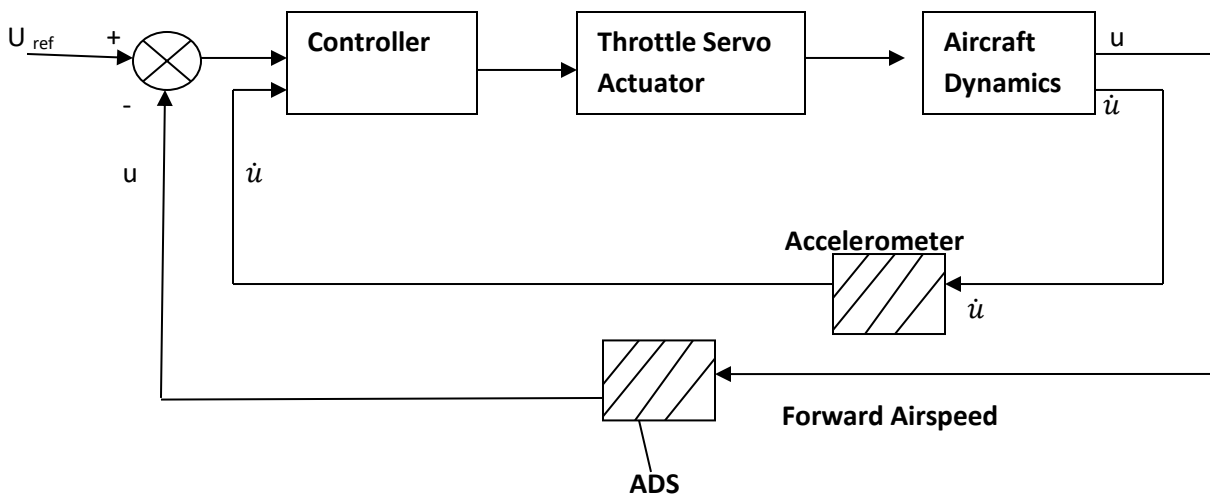


Fig 5.30: Airspeed control system

In any closed loop system, the lags in the individual elements in the loop resulting from energy storage processes (e.g. accelerating inertias) exert a destabilizing effect and limit the loop gain

and hence the performance of the automatic control system. The dynamic behavior of the engines over the range of flight conditions, the throttle actuator response and the aircraft dynamics must thus be taken into account in the design of the speed control system. The response of the jet engine thrust to throttle angle movement is not instantaneous and approximates to that of a simple first order filter with a time constant which is typically in the range of 0.3 to 1.5 seconds, depending on the thrust setting and flight condition. Clearly, the lag in the throttle servo actuator response should be small compared with the jet engine response. The aircraft dynamics introduces further lags as a change in thrust produces an acceleration (or deceleration) so that integration is inherent in the process of changing the airspeed. The derivation of airspeed from the air data system can also involve lag.

The rate of change of forward speed, \dot{U} , derived from a body mounted accelerometer with its input axis aligned with the aircraft's forward axis, can provide a suitable stabilizing term for the control loop. (The \dot{U} term could also be provided by a strap-down AHRS/INS.) A proportional plus integral of error control is usually provided to eliminate steady-state airspeed errors.

A duplicate configuration is generally used so that the system fails passive. The throttle actuator is de-clutched in the event of a failure and the pilot then assumes control of the engine throttle.

5.13 Flight Management Systems:

5.13.1 Principles: The FMS has become one of the key avionics systems because of the major reduction in pilot work load which is achieved by its use. In case of military aircraft, they have enabled single crew operation of advanced strike aircraft. Fig 5.31 is a block diagram of a typical flight management system. The **benefits** they offer are as follows:

- *Quantifiable economic benefits-* provision of automatic navigation and flight path guidance to optimize the aircraft's performance and hence minimize flight costs.
- *Air traffic-* growth of air traffic density and consequently more stringent ATC requirements, particularly the importance of 4D navigation.
- *Accurate navigation sources-* availability of accurate navigation sources. For example, INS/IRS, GPS, VOR, DME and ILS.
- *Computing power-* availability of very powerful, reliable, affordable computers.
- *Data bus system-* ability to interconnect the various sub-systems.

The FMS carries out the following **tasks**:

- Flight guidance and lateral and vertical control of the aircraft flight path.
- Monitoring the aircraft flight envelopes and ensuring safe margins are maintained with respect to the minimum and maximum speeds over the flight envelop.
- Automatic control of the engine thrust to control the aircraft speed.

In addition the FMS plays a major role in the flight planning task, provides a computerized flight planning aid to the pilot and enables major revision to the flight plan to be made in flight, if necessary, to cope with changes in circumstances.

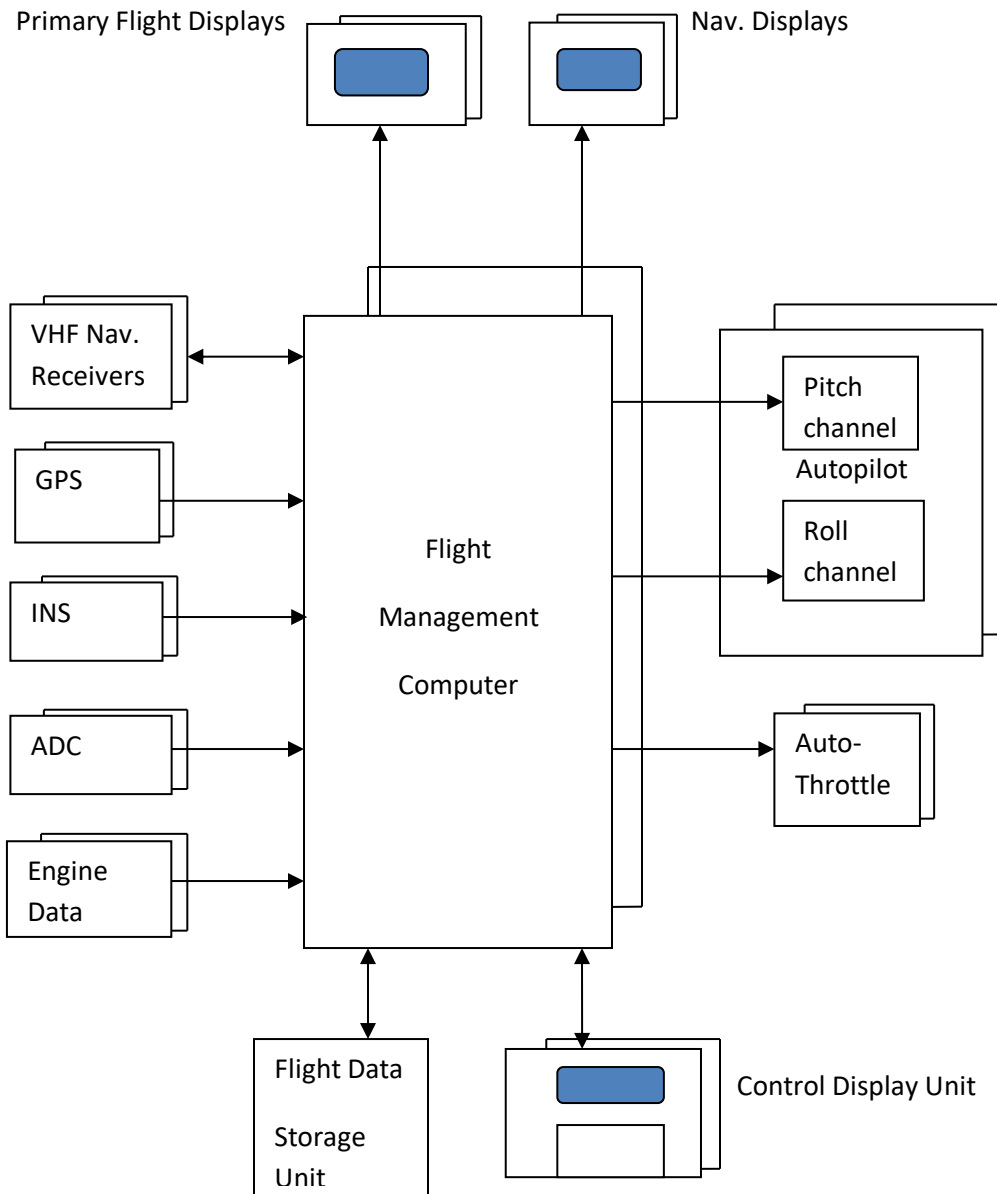


Fig 5.31: Flight management system block diagram

Fig 5.32 shows the flight management system architecture of a modern airliner, in this case Airbus A380. Two independent Flight Management Systems; FMS-1 on the Captain’s side and FMS-2 on

the First Officer's side carry out the flight management function. The cockpit interfaces to the flight crew provided by each FMS comprise a Navigation Display (ND), a Primary Flight Display (PFD), a multi function display (MFD), a Keyboard and Cursor Control Unit (KCCU) and an Electronic Flight Instrument System (EFIS) Control Panel (EFIS CP).

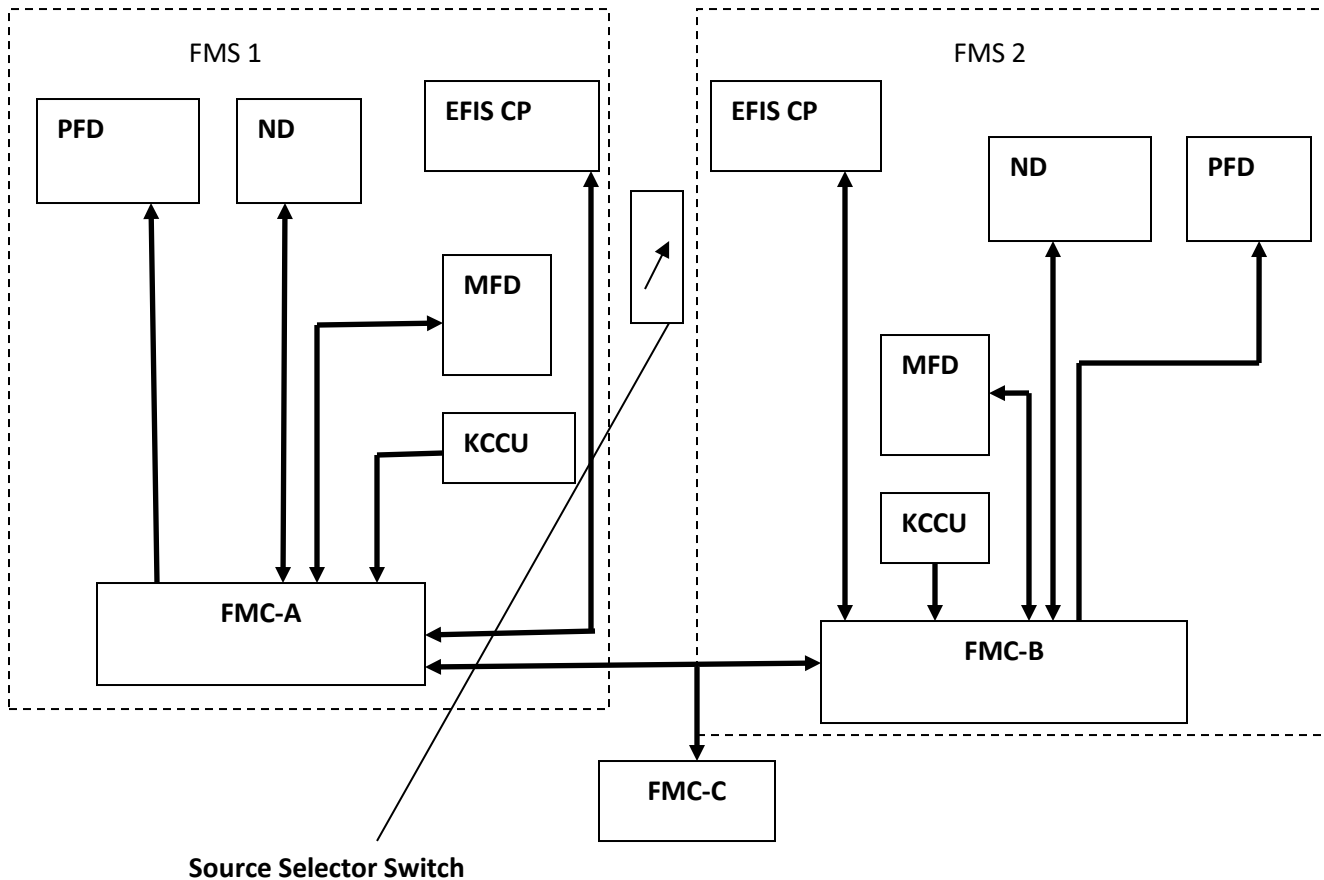


Fig 5.32 FMS Architecture (Airbus A380)

The *Multi-Function Display* (MFD) displays textual data; over 50 FMS pages provide information on the flight plan, aircraft position and flight performance. The MFD is interactive; the flight crew can navigate through the pages and can consult, enter or modify the data via the Keyboard and Cursor Control Unit (KCCU).

Keyboard and Cursor Control Unit (KCCU) enables the flight crew to navigate through the FMS pages on the MFD and enter and modify data on the MFD, as mentioned above, and can also perform some flight plan revisions on the lateral Navigation Display (ND).

The *EFIS Control Panel* (EFIS CP) provides the means for the flight crew to control the graphical and textual FMS data that appear on the ND and PFD.

There are three *Flight Management Computers*; FMC-A, FMC-B and FMC-C to carry out the functional computations, which can be reconfigured to maintain the system operation in the event of failures. There are three different FMS operating modes; Dual Mode, Independent Mode and Single Mode dependent on the system status.

Dual Mode:

Both flight management systems, FMS-1 and FMS-2, are healthy. Fig 5.33 shows the configuration in normal operation in the left side illustration and the configuration after a single flight management computer failure in the right side illustration. In normal operation, FMC-A provide data to FMS-1, FMC-B provide data to FMS-2 and FMC-C is the standby computer. Of the two active computers, one FMC is the 'master' and the other is the 'slave' depending on which autopilot is active and the selected position of the FMS Source Select Switch.

The two active FMCs independently calculate data, and exchange, compare and synchronize these data. The standby computer does not perform any calculations, but is regularly updated by the master FMC. In the case of a single FMC failure, for example FMC-A, FMC-C provides data to FMS-1, as shown in the right side illustration in Figure 5.33.

Independent Mode

In the Independent Mode, FMS-1 and FMS-2 are both operative, but there is no data exchange between them because they disagree on one or more items such as aircraft position, gross weight, etc. this case is shown in the left side illustration in figure 5.34.

Single Mode

The loss of two FMC's causes the loss of either FMS-1 or FMS-2. The data from the operative FMS is displayed to the flight crew by operating the Source Select Switch. This case is shown in the right side illustration in Figure 5.34.

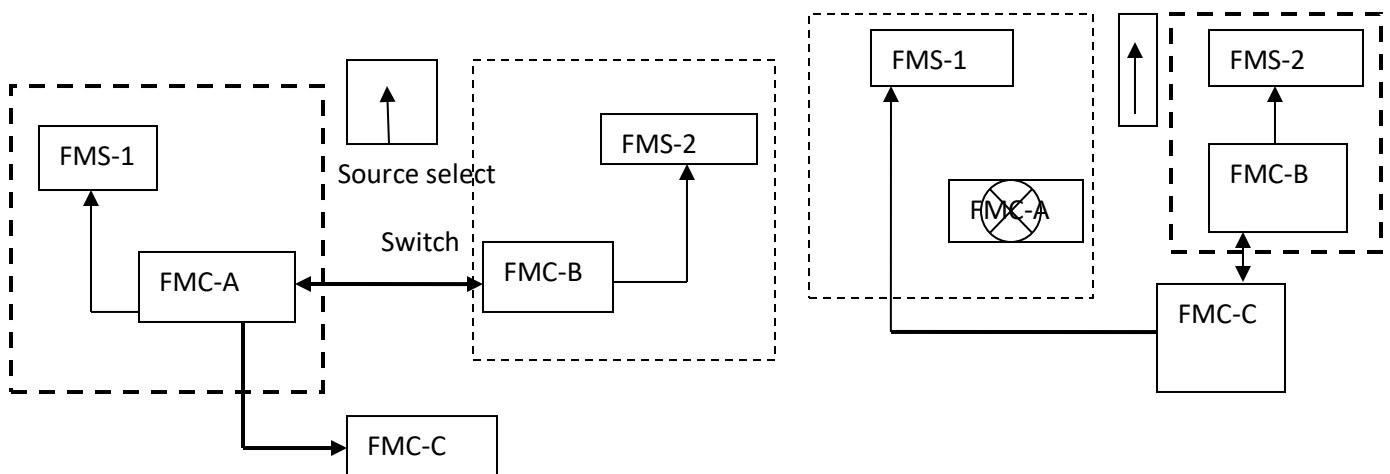


Fig 5.33 Dual Mode Operation

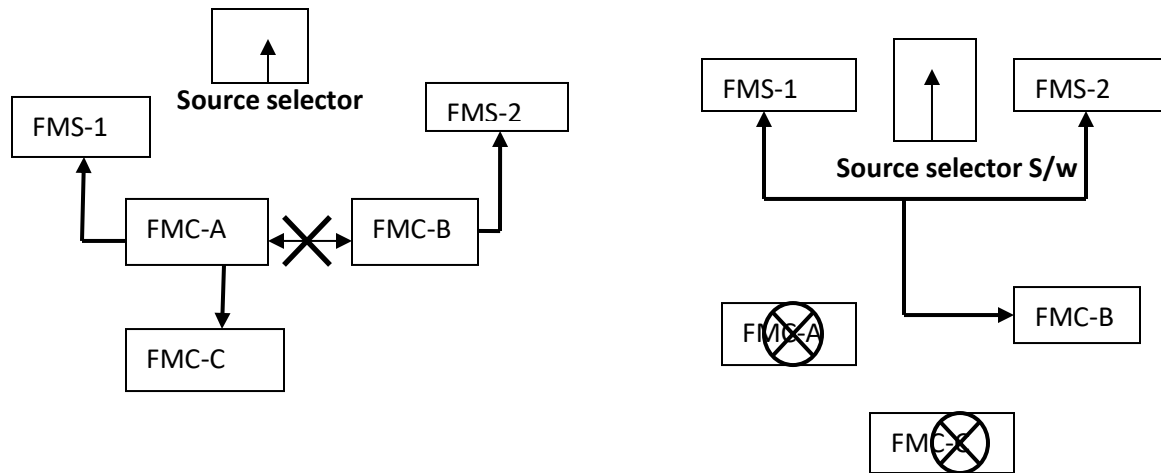


Fig 5.34 Independent Mode and Single Mode configurations

5.13.2. Navigation and Guidance: The FMS combines the data from the navigation sources, comprising the inertial systems, GPS and the radio navigation systems, in a Kalman filter to derive the best estimate of the aircraft position. The accuracy of the estimate is also evaluated. Figure 5.35 is a block diagram of the Kalman filtering of the navigational sources. Each FMS computes the aircraft position and the position accuracy. The FMS computed position is an optimum combination of the inertial position and the GPS or radio position, depending on which equipment provides the most accurate data. This results in four navigation modes in decreasing order of priority:

- Inertial (IRS)-GPS
- Inertial (IRS) – DME/DME.
- Inertial (IRS) – VOR/DME.
- Inertial (IRS) only.

The FMS aircraft position always uses the inertial position. This combination is not possible if the inertial position is not valid, and in this case all the FMS navigation and flight planning functions are no longer available. The FMS continually computes the Estimated Position Uncertainty (EPU), and the EPU is used, together with the Required Navigation Performance (RNP) to define the aircraft navigation accuracy. The FMS continuously compares the actual EPU with the current RNP, and defines the navigation class as:

- HIGH, if the EPU is less than, or equal to the RNP.
- LOW, if the EPU is greater than the RNP.

The navigation class has to satisfy the airworthiness Authorities Accuracy requirements (AAAR).

The FMS computes ground speed, track, wind direction and velocity. (It should be noted that the air data system provides the height information for vertical navigation.) As stated earlier, the FMS provides both lateral and vertical guidance signals to the autopilot to control the aircraft flight path. In the lateral case, the FMS computes the aircraft position relative to the flight plan and the lateral guidance signals to capture and track the flight path specified by the flight plan. Three –dimensional vertical guidance is provided to control the vertical flight path profile including the time dimensions. This is of particular benefit during the descent and approach.

5.13.3 Flight Planning: A major function of an FMS is to help the flight crew with flight planning and it contains a database of:

- *Radio NAVAIDS*- VOR, DME, TACAN, NDB, comprising identification, latitude/longitude, altitude, frequency, and magnetic variation.
- *Waypoints*-usually beacons.
- *Airways*- identifier, sequence number, waypoints.
- *Runways*- length, heading, elevation, latitude, longitude.
- *Airport Procedure*- ICAO code, SID, STAR, ILS, profile descent.
- *Company routes*- original airport, destination airport, route number, cruise altitude, cost index.

The navigation data base is updated every 28 days, according to ICAO and is held in non-volatile memory. It is clearly essential to maintain the recency and quality of the data base and the operator is responsible for the detail contents of the data base which is to ARINC 424 format.

The flight crew can enter the flight plan in the FMS including all the necessary data for the intended lateral and vertical trajectory. When all the necessary data is entered, the FMS computes and displays the speed, altitude, time, and fuel predictions that are associated with the flight plan.

The flight crew can change the flight plan at any time; a change to the lateral plan is called a 'lateral revision' and a change to the vertical plan a 'vertical revision'. The FMS can simultaneously memorize four flights plans:

- One active flight plan for lateral and vertical long term guidance and for radio navigation auto-tuning.
- Three secondary flight plans with drafts to compare predictions, to anticipate a diversion or to store company, ATC and Onboard Information System flight plans.

The lateral flight plan includes the departure, cruise and arrival and is composed of waypoints that are linked with flight plan legs and transition between legs.

A flight plan can be created in three ways:

1. By inserting an origin/destination pair and then manually selecting the departure, waypoints, airways and arrival.
2. By inserting a company route stored in the database.

3. By sending a company request to the ground for an active Flight Plan (F-PLN) uplink.

The flight crew can perform the following lateral revisions:

- Delete and insert waypoints.
- Departure procedures: Take-off runway, Standard Instrument Departure (SID) and transition.
- Arrival procedure: runway, type of approach, Standard Terminal arrival Route (STAR), via, transition.
- Airways segments.

The flight crew can also perform the following vertical revisions:

- Time constraints.
- Speed constraints
- Constant Mach segments.
- Altitude constraints.
- Step altitude.
- Wind

5.13.4 Performance Prediction and Flight Path Optimization : The FMS is able to optimize specific aspects of the flight plan from a knowledge of the aircraft type, weight, engines and performance characteristics, information on the wind and air temperature and the aircraft state-airspeed, Mach number, height, etc.

The FMS continually monitors the aircraft envelope and ensures that the speed envelope restrictions are not breached. It also computes the optimum speeds for the various phases of the flight profile. This is carried out taking into account factors such as:

- Aircraft weight- computed from knowledge of the take-off weight and the fuel consumed (measured by the engine flow meters). It should be noted that fuel can account for over 50% of the aircraft weight at take-off.
- CG position- computed from known aircraft loading and fuel consumed.
- Flight level and flight plan constraints.
- Wind and temperature models.
- Company route cost index.

The recommended cruise altitude and the maximum altitude are also computed from the above information.

The flight crew enters the following data to enable the performance computations and flight plan predictions to be made.

- Zero Fuel Weight (ZFW) and Zero Fuel Centre of Gravity (ZFCG).

- Block fuel.
- Airline Cost Index.
- Flight Conditions (Cruise Flight Level (CRZ FL), temperature, wind).

The FMS computes the following predictions from the flight plan and the flight crew data entries:

- Wind and temperature
- Speed changes
- Pseudo waypoints computation: T/C, T/D, LVL OFF.
- For each waypoint or pseudo waypoint:
 - Distance
 - Estimated time of arrival (ETA)
 - Speed
 - Altitude
 - Estimated Fuel on Board (EFOB).
 - Wind for each waypoint or pseudo waypoint.
- For primary and alternate destination
 - ETA
 - Distance to destination
 - EFOB at destination

These predictions are continually updated depending on:

- Revisions to the lateral and vertical flight plans.
- Current winds and temperature.
- Actual position versus lateral and vertical flight plans.
- Current guidance modes.

The predictions and the lateral flight plan combine to form a vertical profile that has six flight phases. Flight envelope protection is achieved by computing maximum and minimum selectable speed, stall warning, low energy threshold, alpha floor and reactive wind shear detection. The FMS also computes maneuvering speed and flap and slat retraction speed.

5.14 Cost Index (CI):

5.14.1 Introduction: The cost index (CI) is a number used in the Flight Management System (FMS) to optimize the aircraft's speed. It gives the ratio between the unit cost of time and the unit cost

of fuel. With this number, and knowledge about the aircraft's performance, it is possible to calculate the optimal speed for the aircraft, which results in the lowest total cost. Speeds slower than the optimal speed will result in less fuel burn, but also in more flying time. The cost of the extra flying time outweighs the fuel savings at speeds below the optimum speed. Speeds faster than the optimal speed will result in more fuel burn, but also in less flying time. The saving of less flight time does not outweigh the fuel burn at speeds above the optimum speed. A low cost index means that the cost of time is low or that fuel is expensive. It will result in a low speed. High cost index means high cost of time (e.g. passengers about to miss their flight connection) or low fuel price (rare these days). At the minimum cost index (0) only fuel counts. This will result in the aircraft flying at Maximum Range Cruise. At the maximum cost index only time counts. This will result in the aircraft flying at Maximum Cruise Speed (V_{ma} / M_{ma} with a buffer). Airlines generally have a standard cost index they use for planning and adjust them on a flight by flight basis.

The idea behind the CI concept is to balance both fuel and time related costs. With surge in fuel prices in the early 1970s both airlines & aircraft manufacturers started concentrating on systems of reducing the fuel consumption. In some airlines, fuel cost at one point represented no less than 45%, but gradually decreased to a mere 20% effectively emphasizing the other aspects of the cost equation. The wide spread use of Flight Management Systems (FMS) since the early 1980s enabled airlines to take into account the other cost and time-related aspects as well.

In addition to navigation functions, the Flight Management Computer (FMC) carries out real-time performance optimization aimed at providing best economics, not necessarily in terms of fuel consumption but rather in terms of direct operating cost:

- Climb, cruise & descent speeds a function of selectable constraints (altitude, arrival time...)
- Minimum fuel, time or cost.

5.14.2 Definition & Determination: The fundamental rationale of the CI is to achieve minimum trip cost by means of a trade-off between operating costs per hour and incremental fuel burn. In essence, the CI is used to take into account the relationship between fuel- and time-related costs. CI is defined as:

$$\text{Cost Index (CI)} = \frac{C_T}{C_F}$$

Where C_T = Time-related cost per minute of flight;

C_F = Cost of fuel per Kg.

Trip Cost.

Total cost of a specific trip is the sum of a fixed cost and variable costs:

$$C = C_F \times \Delta F + C_T \times \Delta T + C_c$$

with C_F = cost of fuel per kg
 C_T = time-related cost per minute of flight
 C_c = fixed costs independent of time
 ΔF = trip fuel
 ΔT = trip time

In order to minimize C or the total trip cost we therefore need to minimize the variable cost :

$$C_F \times \Delta F + C_T \times \Delta T$$

For a given sector and period, the fuel price may be assumed to be a fixed value.

Let us consider a cost function $\tau = C/C_F = \Delta F + C_T/C_F \times \Delta T$ with $C_T/C_F = CI$
 (defined as the cost index)

Over a certain stage length ΔS this means :

$$\tau (1 \text{ nautical mile}) = 1/SR + CI \times 1/V$$

with SR being the specific range at weight, altitude and other conditions
 $SR = \Delta S/\Delta F$ (nautical miles per kg)

with V being the ground speed to cover ΔS stage nautical miles including winds
 $V = aM + V_c$ (V_c as the average head or tail wind component)

For a given sector, minimum trip cost is therefore achieved by adopting an operational speed that properly proportions both fuel- and time-related costs.

5.14.3 Time-Related Costs: Time related costs contain the sum of several components:

- Hourly maintenance cost
- Flight crew and cabin crew cost per flight hour:
 - * Even for crew with fixed salaries, flight time has an influence on crew cost. On a yearly basis, reduced flight times can indeed lead to:
 - Normal flight crews instead of reinforced ones.
 - Lower crew rest times below a certain flight time
 - Better and more efficient use of crews.
- Marginal depreciation or leasing costs (i.e. the cost of ownership or aircraft rental) for extra flying per hour.

In addition to the above time-related costs, extra cost may arise from overtime, passenger dissatisfaction, and missed connection. These costs are airline specific. If an airline can establish good cost estimates, it is possible to draw a cost Vs arrival time function and hence to derive a cost index.

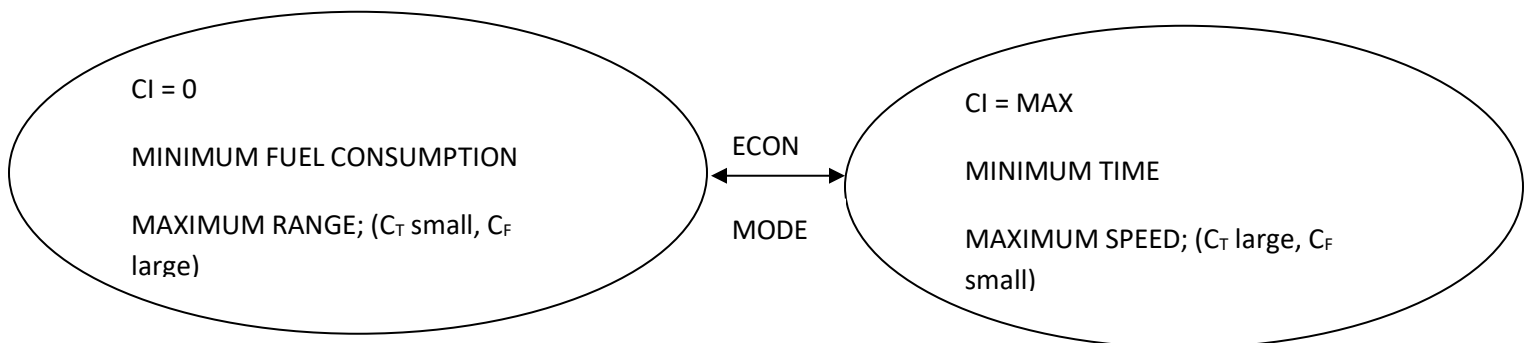
With time-related costs, the faster the aircraft is flown, the more money is saved. This is because the faster the aircraft is flown, the more miles time-related components can be used and the more miles can be flown and produced between inspections when just considering maintenance cost. However, if the aircraft is flown faster to reduce time-related costs, fuel burn increases and money will be lost in turn.

On the other hand, to avoid over-consumption of fuel, the aircraft should be flown more slowly. To solve this dilemma, the FMS uses both ingredients, and is therefore able to counterbalance these costs factors and to help select the best speed to fly, therefore called ECON (i.e. minimum cost) speed.

5.14.4 Cost index Calculation:

$$CI = \frac{C_{Time}}{C_{Fuel}}$$

This mathematical expression is to be found in many Flight management Systems (Of Smiths or Sperry/Honeywell). This could be from 0 to 99. Units are given in kg/min.



Scaled 0 to 99 or 999(Depending on FMS Vendor)

Extreme cases :

- 1) $C_I = 0$ or practically, when C_T small, C_F large or
MINIMUM FUEL MODE for Maximum Range (MRC).

This is the case of greatest influence of fuel cost in the operating bill.

- 2) $C_I = \text{MAX}$ or practically, when C_T large, C_F small or
MINIMUM TIME MODE for Maximum Speed (MMO - 0.02 = M 0.82 for A300-600, A310, M 0.80 for A320 Family, M 0.84 for A330/A340).

The cost index effectively provides a flexible tool to control fuel burn and trip time between these two extremes. Knowledge of the airline cost structure and operating priorities is essential when aiming to optimize cost by trading increased trip fuel for reduced trip time or vice-versa.

The mere fact that fuel costs can significantly vary from one sector to another and throughout the year should prompt airlines to consider adopting different cost indices for their various routes, seasonally readjusted to account for recurring fluctuations.